



Olson, Erin D. (2014) Characterization of the GSTM1 transgenic SHRSP rat. PhD thesis.

<http://theses.gla.ac.uk/5272/>

Copyright and moral rights for this thesis are retained by the author

A copy can be downloaded for personal non-commercial research or study, without prior permission or charge

This thesis cannot be reproduced or quoted extensively from without first obtaining permission in writing from the Author

The content must not be changed in any way or sold commercially in any format or medium without the formal permission of the Author

When referring to this work, full bibliographic details including the author, title, awarding institution and date of the thesis must be given.

Characterization of the *GSTM1* Transgenic SHRSP Rat

Erin D. Olson BSc, MRES, MSc

**Submitted in fulfilment of the requirements for the
degree of doctor of philosophy**

**University of Glasgow
Institute of Cardiovascular & Medical Sciences,
College of Medicine, Veterinary and Life
Sciences**

March 2014

Declaration

I declare that the work presented in this thesis is to the best of my knowledge original, and my own work. This thesis is a record of research performed by myself with the exception of some myography experiments of mesenteric arteries (Mrs. Elisabeth C. Beattie) and some sacrifice of animals (Dr. Delyth Graham, Dr. Caline Koh-Tan, and Elisabeth Beattie). This work has not been submitted previously for a higher degree and was carried out under the supervision of Dr. Delyth Graham, Dr. Martin McBride and Professor Anna F. Dominiczak.

A handwritten signature in black ink, appearing to read "Erin Olson". The signature is written in a cursive style with a horizontal line underneath it.

(Erin Olson)

Acknowledgements

First of all, I would like to thank my supervisors Prof. Anna F. Dominiczak, Dr. Delyth Graham and Dr. Martin McBride for their support and advice. I am extremely grateful for all of their time and guidance they have invested in me along with all of the wonderful opportunities afforded to me over the last four years.

I would like to extend my gratitude to Professors Andrew Baker and Godfrey Smith for encouraging me to apply to the BHF program and for all the direction and leadership they provided during the past four years.

I would like to thank Dr. Caline Koh-Tan, Mrs. Elisabeth Beattie and Mrs. Wendy Beattie for their assistance and expertise in all things molecular/*Gstm*/ and rat related for my transgenic animals. I would like to extend a special thanks to Prof. John D. Hayes for his kind donation of antisera against rat *Gstm1*, and to Drs. Pravanec and Landa, for their help in developing both lines of the *Gstm1* transgenic SHRSP. Furthermore, I must say a huge thank you to all the lovely people at the BHF GCRC who have helped me achieve this goal. There are far too many of you to mention, but it has been a pleasure working with you all and I take away many happy memories from the BHF.

To the BHF girls and our many add-ons through the years, you have been my closest friends and will always hold a special place in my heart. Thank you for all of the Glaswegian subtitles and putting up with my Americanisms. I hope we will always stay in touch and stay socially well.

Finally, very special thanks to my husband, who has been my rock these past five years, for all of the encouragement and support when I needed it most. I could not have done this without you. I love you and can't wait to start our next adventure.

Table of Contents

Title Page	1
Declaration	2
Acknowledgements	3
List of Publications	11
Abstracts	11
Papers	12
List of Abbreviations and Acronyms.....	13
Summary	16
1 Introduction.....	20
1.1 Cardiovascular Disease.....	21
1.2 Blood Pressure.....	22
1.2.1 Blood Pressure Control and Regulation	23
1.3 Animal Studies	34
1.3.1 SHRSP	35
1.3.2 Oxidative Stress in Cardiovascular studies	45
1.3.3 Identification of <i>Gstm1</i> as a candidate gene for oxidative stress and its role in the development of hypertension in the SHRSP	55
1.4 Hypothesis	62
2 Materials and Methods.....	63
2.1 In vivo experimental procedures	64
2.1.1 Experimental Animals	64
2.1.2 Hemodynamic Profile	66
2.1.3 Echocardiography	68
2.1.4 Metabolic Cages.....	68
2.2 Ex vivo Experimental Procedure.....	69
2.2.1 Tissue Preparation	69
2.2.2 Organ Mass index	69
2.2.3 Histology	70
2.2.4 GFR.....	72
2.2.5 Oxidative Stress Measurements	72
2.2.6 Wire Myography	75
2.2.7 Pressure Myography	76
2.3 General Molecular Biology.....	77
2.4 RNA Extraction	77
2.4.2 DNase Treatment of Extracted Total RNA.....	77
2.4.3 Reverse Transcription (RT)-PCR	78
2.4.4 Real-Time Polymerase Chain Reaction	78
2.5 Genomic DNA Preparation	79

2.5.1	DNA Extraction	79
2.5.2	Sequencing.....	79
2.5.3	Copy Number Variation	81
2.6	Protein Extraction	82
2.6.1	Protein Extraction	82
2.6.2	Protein Quantification	82
2.6.3	Gel Electrophoresis.....	83
2.6.4	Western Immunoblotting	84
2.7	Statistical Analysis.....	84
3	<i>In vivo</i> Phenotypic Characterization of the <i>Gstm1</i> transgenic SHRSP rat	86
3.1	Introduction	87
3.2	Materials and Methods	89
3.2.1	Hemodynamic Measurements	89
3.2.2	Echocardiography	90
3.2.3	Tissue Collection.....	90
3.2.4	Statistics	90
3.3	Results.....	91
3.3.1	Hemodynamic Measurements	91
3.3.2	Echocardiography - Baseline	107
3.3.3	Cardiac and Left ventricular Hypertrophy assessed at sacrifice... ..	115
3.4	Discussion	118
4	Molecular Characterization of the Effects of <i>Gstm1</i> Over Expression in the Transgenic SHRSP	123
4.1	Introduction	124
4.2	Materials and Methods	127
4.2.1	Animal Strains	127
4.2.2	mRNA Expression.....	127
4.2.3	Protein Expression and Localization (IHC)	128
4.2.4	Localization of the Transgene Insertion Site.....	130
4.2.5	Copy Number Variation	133
4.2.6	Statistics	133
4.3	Results.....	134
4.3.1	<i>Gstm1</i> Expression in Cardiovascular Relevant Tissues.....	134
4.3.2	Location of the Transgene Insertion Site	143
4.3.3	Copy Number Variation	147
4.4	Discussion	152
5	<i>Ex vivo</i> Effects of <i>Gstm1</i> Expression.....	157
5.1	Introduction	158
5.1.1	Renal Function	158

5.1.2	Vascular Function.....	159
5.1.3	Aims.....	160
5.2	Materials and Methods	161
5.2.1	Metabolic Cages.....	161
5.2.2	Estimated Glomerular Filtration Rate	161
5.2.3	Tissue Collection.....	161
5.2.4	Wire myography.....	162
5.2.5	Pressure Myography	162
5.2.6	Oxidative stress	163
5.2.7	Histology - Gross Pathology Analysis	163
5.2.8	Statistical Analysis.....	163
5.3	Results.....	164
5.3.1	Effects of <i>Gstm1</i> expression on oxidative stress	164
5.3.2	Effects of <i>Gstm1</i> on Renal Function.....	168
5.3.3	Effects of <i>Gstm1</i> expression on the Vasculature	174
5.4	Discussion	186
6	Characterization of the <i>GSTM</i> family in a human cohort.....	193
6.1	Introduction	194
6.2	Materials and Methods	197
6.2.1	Ethics and Demographics	197
6.2.2	RNA Extraction	197
6.2.3	Reverse Transcriptase.....	198
6.2.4	Relative real-time PCR.....	199
6.2.5	DNA Extraction	199
6.2.6	Genotyping.....	200
6.2.7	Statistical Analysis.....	201
6.3	Results.....	203
6.4	Discussion	209
7	General Discussion	212
	Appendices	250
	Microsatellite Markers.....	250
	Transgene Sequence.....	251

LIST OF TABLES

TABLE 1-1: CLASSIFICATION OF HYPERTENSION	23
TABLE 3-1: SYSTOLIC BLOOD PRESSURE MEASURED BY TAIL CUFF PLETHSMOGRAPHY MEASUREMENTS FROM 5-12 WEEKS	93
TABLE 3-2: BASELINE VS. SALT LOADING STRAIN COMPARISON	101
TABLE 4-1: TAQMAN REAGENT LIST.....	127
TABLE4-2: TEMPERATURE CYCLING FOR TAQMAN	128
TABLE 6-1.....	197

LIST OF FIGURES

FIGURE 1-1: THE COMPLEXITY OF BP REGULATION AND THE ROLE OF THE KIDNEYS AND RAAS.....	25
FIGURE 1-2: GENELOGICAL BACKGROUND OF THE STROKE PRONE SPONTANEOUSLY HYPERTENSIVE RAT (SHRSP)	37
FIGURE 1-3: OXIDATIVE STRESS ENZYMES AND THEIR ROLES IN MAINTAINING THE BALANCE BETWEEN O ₂ ⁻ AND NO.....	49
FIGURE 1-4: ORGANISATION OF THE GLUTATHIONE S-TRANSFERASE MU GENES IN HUMAN AND	56
FIGURE 1-5: CHROMOSOME 2 CONGENIC STRAIN SP.WKYGLA2c*	58
FIGURE 1-6: DAY-TIME AND NIGHT-TIME AVERAGE SYSTOLIC AND DIASTOLIC BLOOD PRESSURE	59
FIGURE 3-1: SYSTOLIC BLOOD PRESSURE IN TRANS1, TRANS2 AND PARENTAL STRAINS.	94
FIGURE3-2: DIASTOLIC BLOOD PRESSURE IN TRANS1, TRANS2 AND PARENTAL STRAINS.	95
FIGURE3-3: PULSE PRESSURE IN TRANS1, TRANS2 AND PARENTAL STRAINS.	96
FIGURE3-4: HEART RATE IN TRANS1, TRANS2 AND PARENTAL STRAINS.	97
FIGURE 3-5: LOCOMOTOR ACTIVITY IN TRANS1, TRANS2 AND PARENTAL STRAINS.....	98
FIGURE 3-6: SYSTOLIC BLOOD PRESSURE FOR SALT-LOADED SHRSP, WKY AND TRANS1 RATS.....	102
FIGURE 3-7: DIASTOLIC BLOOD PRESSURE FOR SALT-LOADED SHRSP, WKY AND TRANS1 RATS.	103
FIGURE 3-8: PULSE PRESSURE FOR SALT-LOADED SHRSP, WKY AND TRANS1 RATS.....	104
FIGURE 3-9: LOCOMOTOR ACTIVITY FOR SALT-LOADED SHRSP, WKY AND TRANS1 RATS.	105
FIGURE 3-10: HEART RATE FOR SALT-LOADED SHRSP, WKY AND TRANS1 RATS.....	106
FIGURE 3-11: LEFT VENTRICULAR MASS INDEX FOR SHRSP, WKY TRANS1 AND TRANS2 RATS	109
FIGURE 3-12: RELATIVE WALL THICKNESS IN SHRSP, WKY, TRANS1 AND TRANS2 RATS.....	110
FIGURE 3-13: FRACTIONAL SHORTENING IN SHRSP, WKY, TRANS1 AND TRANS2 RATS	111
FIGURE 3-14: STROKE VOLUME IN SHRSP, WKY, TRANS1 AND TRANS2 RATS	112
FIGURE 3-15: CARDIAC OUTPUT IN SHRSP, WKY, TRANS1 AND TRANS2 RATS	113
FIGURE 3-16: EJECTION FRACTION IN SHRSP, WKY, TRANS1 AND TRANS2 RATS	114
FIGURE 3-17: LVMI IN SHRSP, WKY TRANS1 AND TRANS2 RATS.....	116
FIGURE 3-18: CARDIAC MASS INDEX IN SHRSP, WKY TRANS1 AND TRANS2 RATS	117
FIGURE 4-1: SCHEMATIC OF THE INVERSE PCR (IPCR) PROCEDURE WITH RESULTS	132
FIGURE 4-2: CHANGES IN RENAL <i>GSTM1</i> EXPRESSION BETWEEN TRANS1, TRANS2 AND PARENTAL STRAINS AT 5 WEEKS.	136
FIGURE 4-3: CHANGES IN RENAL <i>GSTM1</i> EXPRESSION BETWEEN TRANS1, TRANS2 AND PARENTAL STRAINS AT 21 WEEKS.	137

FIGURE 4-4: EXPRESSION OF TOTAL <i>GSTM1</i> IN CARDIOVASCULAR RELEVANT TISSUES FOR TRANS1, TRANS2 AND PARENTAL STRAINS AT 5 WKS OF AGE.....	138
FIGURE 4-5: TOTAL <i>GSTM1</i> EXPRESSION FOR TRANS1, TRANS1 AND PARENTAL STRAINS AT 21 WKS OF AGE IN CARDIOVASCULAR RELEVANT TISSUES	139
FIGURE 4-6: TRANSGENE (WKY SPECIFIC) <i>GSTM1</i> EXPRESSION IN TRANS1, TRANS2 AND PARENTAL STRAINS AT 5 WEEKS OF AGE.....	141
FIGURE 4-7: TRANSGENE (WKY SPECIFIC) <i>GSTM1</i> EXPRESSION IN TRANS1, TRANS2 AND PARENTAL STRAINS AT 21 WEEKS OF AGE.....	142
FIGURE 4-8: <i>GSTM2</i> EXPRESSION IN TRANS1, TRANS2 AND PARENTAL STRAINS AT 21 WEEKS OF AGE.	145
FIGURE 4-9: <i>GSTM3</i> EXPRESSION IN TRANS1, TRANS2 AND PARENTAL STRAINS AT 21 WEEKS OF AGE.	146
FIGURE 4-10: LOCALIZATION OF <i>GSTM1</i> IN THE AORTA AT 21 WEEKS OF AGE.	148
FIGURE 4-11: SCHEMATIC OF THE INVERSE PCR PROCEDURE WITH RESULTS.....	149
FIGURE 4-12: MAPPING THE TRANSGENE INSERTION SITE BY INVERSE PCR FOR TRANS1 RATS.	150
FIGURE 4-13: COPY NUMBER VARIATION BETWEEN PARENTAL STRAINS AND TRANS1 RATS	151
FIGURE 5-1: RENAL OXIDATIVE STRESS MEASUREMENTS IN SHRSP, WKY AND TRANSGENIC LINES AT 21 WEEKS OF AGE.....	165
FIGURE 5-2: RENAL OXIDATIVE STRESS MEASUREMENTS IN SHRSP, WKY AND TRANSGENIC LINES AT 21 WEEKS OF AGE FOR SALT LOADED ANIMALS.....	167
FIGURE 5-3: VASCULAR OXIDATIVE STRESS MEASUREMENTS IN SHRSP, WKY AND TRANSGENIC LINES AT 21 WEEKS OF AGE.....	169
FIGURE 5-4: OXIDATIVE STRESS MEASUREMENTS IN SHRSP, WKY AND TRANSGENIC LINES AT 21 WEEKS OF AGE IN CARDIOVASCULAR TISSUES.....	170
FIGURE 5-5: PROTEINURIA MEASUREMENT IN URINE IN 21 WEEK OLD ANIMALS.....	173
FIGURE 5-6: ASSESSMENT OF RENAL FIBROSIS BY PICROSIRIUS RED IN 21 WEEK OLD ANIMALS	176
FIGURE 5-7: HAEMATOXYLIN AND EOSIN STAINING IN KIDNEY SECTIONS FROM TRANSGENIC AND PARENTAL STRAINS AT 21 WEEKS OF AGE.	177
FIGURE 5-8: CONCENTRATION RESPONSE CURVES IN THE PRESENCE AND ABSENCE OF THE NOS INHIBITOR L-NAME IN AORTA	178
FIGURE 5-9: NITRIC OXIDE BIOAVAILABILITY IN 21 WEEK AORTA.....	179
FIGURE 5-10: EFFECTS ON CARBACHOL-INDUCED VASORELAXATION OF AORTAE	180
FIGURE 5-11: MESENTARIC RESISTANCE ARTERIES CONTRACTILE RESPONSE TO NORADRENALIN.....	182
FIGURE 5-12: MESENTARIC RESISTANCE ARTERY FUNCTION IN RESPONSE TO CARBACHOL-STIMULATED NITRIC OXIDE RELEASE.	183

FIGURE 5-13: COMPARISON OF STRUCTURAL PARAMETERS OF MESENTERIC RESISTANCE ARTERIES OVER A RANGE OF INTRALUMINAL PRESSURES.....	184
FIGURE 5-14: COMPARISON OF MECHANICAL PARAMETERS OF MESENTERIC RESISTANCE ARTERIES	185
FIGURE 6-1: ALLELIC DISCRIMINATION OF SNPs.....	202
FIGURE 6-2: CLUSTER PLOT OF THE RS11807 GENE	205
FIGURE 6-3: HUMAN GLUTATHIONE S-TRANSFERASE AND GLUTATHIONE PEROXIDISE EXPRESSION.....	206
FIGURE 6-4: GENOTYPE-PHENOTYPE ASSOCIATION BETWEEN <i>GSTM5</i> AND RS11807.	207
FIGURE 6-5: GENE EXPRESSION CORRELATION AS DEPICTED BY SCATTER PLOTS.....	208

List of Publications

Abstracts

Erin Olson, Martin McBride, Caline Koh-Tan, Elizabeth Beatty, Delyth Graham
Transgenic Rescue of *Gstm1* in the SHRSP Rat, Scottish Society of Experimental Medicine, February 2011, (Oral Communication)

Erin Olson, Martin W McBride, Michal Pravenec, Vladimir Landa, HH Caline Koh-Tan, Elisabeth Beattie, Anna Dominiczak, Delyth Graham *Gstm1 Transgenic Rescue Improves Hemodynamic Profile in the SHRSP Rat, Eurotools, Stresa (Italy) June 2011 (Poster Communication)*

Erin Olson, Martin W McBride, Michal Pravenec, Vladimir Landa, HH Caline Koh-Tan, Elisabeth Beattie, Anna Dominiczak, Delyth Graham *Gstm1 Transgenic Rescue Improves Hemodynamic Profile in the SHRSP Rat, Scottish Cardiovascular Forum, 2012 (Poster Communication)*

Erin Olson, Martin W McBride, Michal Pravenec, Vladimir Landa, HH Caline Koh-Tan, Anna Dominiczak, Delyth Graham *Hemodynamic Profile Improved by Transgenic Insertion of *Gstm1*, Integrative Mammalian Biology Symposium, March 2012 (Poster Communication)*

Erin Olson, Martin W McBride, Michal Pravenec, Vladimir Landa, HH Caline Koh-Tan, Elisabeth Beattie, Anna Dominiczak, Delyth Graham *Transgenic Rescue of Glutathione-S-Transferase Mu-Type 1 Improves Hemodynamic Profile in the Stroke Prone Hypertensive Rat, European Society of Hypertension, London (England), April 2012 (Poster Communication)*

Erin Olson, Martin W McBride, Michal Pravenec, Vladimir Landa, HH Caline Koh-Tan, Elisabeth Beattie, Anna Dominiczak, Delyth Graham *Improved Hemodynamic Profile by Transgenic Rescue of Glutathione-S-Transferase Mu-Type 1 in the Stroke Prone Hypertensive Rat, Rat Genomics Meeting, Oxford (England), December 2012 (Poster Communication)*

Erin Olson, Martin W McBride, Michal Pravenec, Vladimir Landa, HH Caline Koh-Tan, Anna Dominiczak, Delyth Graham *Transgenic Rescue of Glutathione-S-Transferase Mu-Type 1 in the Stroke Prone Hypertensive Rat Improves Hemodynamic Profile and Oxidative Stress, European Society of Hypertension, Milan (Italy), June 2013 (Oral Communication)*

Book Chapters/Original Papers/Manuscripts in preparation

Olson E, Graham D. Animal Models in Pharmacogenomic Research. Padmanabhan S (ed). Handbook of Pharmacogenomics and Stratified Medicine. Elsevier, 2014 (in press).

McLaughlin J, Beattie E, Murphy MP, Koh-Tan HH, **Olson E**, Beattie W, Dominiczak AF, Nicklin SA, Graham D. Combined therapeutic benefit of mitochondria-targeted antioxidant, MitoQ₁₀, and angiotensin receptor blocker, losartan on cardiovascular function. *J Hypertension*. 2013 Dec 4 (in press)

List of Abbreviations and Acronyms

•	hydroxyl free radical
2D-DIGE	2 Dimensional difference in gel electrophoresis
ACE	angiotensin converting enzyme
ACE	angiotensin-converting enzyme
ADH	anti-diuretic hormone
ADP	adenosine diphosphate
AGT	angiotensinogen
Ang	angiotensin
Ang II	angiotensin II
ANOVA	analysis of variance
Anp	atrial natriuretic peptide
ARE	antioxidant response element
AT1	angiotensin II type 1 receptor
AT1R	AngII type 1 receptor
AT2	angiotensin II type 2 receptor
ATP	adenosine triphosphate
AU	arbitrary units
AUC	area under the curve
BAC	bacterial artificial chromosome
BCA	bicinchoninic acid
BGH	bovine growth hormone
BH ₄	tetrahydrobiopterin
BN	Brown Norway rat
BP	blood pressure
Bpm	beats per minute
BSA	bovine serum albumin
Ca2+	calcium
CAD	coronary artery disease
CHD	coronary heart disease
CMI	cardiac mass index
CNV	copy number variation
CO ₂	carbon dioxide
Cpm	counts per minute
CTMP	carboxy-terminal modulator protein
Cu/Zn-sod	copper/zinc sod
CVD	cardiovascular disease
DT	day-time
DBP	diastolic blood pressure
De	external diameter
dH ₂ O	distilled water
Di	internal diameter
DTT	dithiothreitol
Edg1	endothelial differentiation gene receptor 1

EDTA	ethylenediamine tetra-acetic acid
EF1 α	elongation factor 1 α subunit
eGFR	estimated glomerular filtration rate
eNOS	endothelial nitric oxide synthase
GFP	green fluorescent protein
GPx	glutathione peroxidase
GRA	glucocorticoid-remidiable aldosteronism
GSH	reduced glutathione
GSS	glutathione synthase
GSSG	glutathione disulfide
GSSH	oxidized glutathione
GST	glutathione-S-transferase
<i>Gstm1</i>	glutathione s-transferase mu type 1 .
H ₂ O	water
H ₂ O ₂	hydrogen peroxide
HCl	hydrogen chloride
HPLC	high-performance liquid chromatography
i.p.	intraperitoneal
i.v.	intravenous
ICC	Immunocytochemistry
IPA	Ingenuity Pathway Analysis
IPTG	Isopropyl-beta-D-thiogalactopyranoside
K ⁺	potassium
KCl	potassium chloride
LB	Luria broth
L-NAME	NG-nitro-L-arginine methyl ester
LV	left ventricular
LVMI	left ventricular mass index
M	molar
MAP	mean arterial pressure
MAPK	mitogen-activated protein kinase
mg	milligrams
MI	myocardial infarction
miRNA	microRNA
mL	millilitre
mM	millimolar
mmHg	millimetre of mercury
MRA	mesenteric resistance arteries
NT	night-time
NaCl	sodium chloride (salt)
NADH	nicotinamide adenine dinucleotide
NADPH	nicotinamide adenine dinucleotide phosphate
nM	nanomolar
NO	nitric oxide
NOS	nitric oxide synthase

NRK52E	normal rat kidney epithelial cells
O ₂	molecular oxygen
O ₂ •-	superoxide anion
OH•	hydroxyl radical
ONOO•	peroxynitrite
PBS	phosphate-buffered saline
PCR	polymerase chain reaction
PE	phenylephrine
PKC	protein kinase C
PP	pulse pressure
qRT-PCR	quantitative real-time PCR
QTL	quantitative trait locus
RAAS	renin angiotensin aldosterone system
RNA	ribonucleic acid
RNS	reactive nitrogen species
ROS	reactive oxygen species
rRNA	ribosomal RNA
SBP	systolic blood pressure
SEM	standard error of the mean
SHR	Spontaneously hypertensive rat
shRNA	short-hairpin RNA
SHRSP	Stroke-prone spontaneously hypertensive rat
siRNAs	short interfering RNA
SOD	superoxide dismutase
TBE	tris-borate EDTA
TF	transcription factor
TGF	tubuloglomerular feedback
UTR	untranslated region
VSMC	vascular smooth muscle cell
WHO	World Health Organization
WKY	Wistar Kyoto rat
X-gal	5-Bromo-4-chloro-3-indolyl β-D-galactopyranoside
YAC	yeast artificial chromosome
µL	Microlitre
Mm	micrometre (micron)
µM	Micromolar

Summary

Essential or primary hypertension is a complex polygenic disease with genetic heritability averaging approximately 30% and with strong influence of environmental factors and gene-environment interaction. Heterogeneity in the general population and the polygenic complexities of the disease has meant that identification and functional validation of candidate genes has proved extremely difficult in humans. Several strategies have been developed to dissect genetic determinants of hypertension, one of which is the use of rodent models (1;2). Animal models of heritable hypertension offer more favourable investigative opportunities because of reduced genetic heterogeneity, the capacity for controlled breeding and environmental conditions, and the ability to produce genetic crosses and analyse large numbers of progeny. The stroke-prone spontaneously hypertensive rat (SHRSP) is a commonly used model of human essential hypertension. Previous studies conducted in our laboratory utilizing a combination of congenic strain construction and genome-wide microarray expression profiling in the SHRSP have allowed us to identify the positional candidate gene, glutathione S-transferase μ -type 1 (*Gstm1*), which is involved in the defence against oxidative stress and is significantly down-regulated in the SHRSP (3;4). Genomic DNA sequencing of *Gstm1* in SHRSP and WKY identified 13 single nucleotide polymorphisms (SNPs), an insertion and a deletion (5). Luciferase reporter gene assays implicated five SNPs to be responsible for significant reduction in luciferase activity measurements (6). In consideration of these previous studies, it is hypothesized that *Gstm1* deficiency in the SHRSP plays a causative role in the development of oxidative stress and hypertension.

To establish definitive proof that reduced *Gstm1* expression affects blood pressure regulation and oxidative stress, two independent transgenic lines (referred to as Trans1 and Trans2) of SHRSP were created with the aim of rescuing *Gstm1* deficiency by incorporation of a normal *Gstm1* gene into the SHRSP genome. Generation of these transgenic SHRSP rats involved microinjection with a 2.7 kb linear construct encoding wild type (WKY) *Gstm1* under the control of the universal EF-1 α promoter. They were generated using the same expression platform and microinjection fragment purification protocol employed in the successful production of the CD-36 transgenic, rat as previously described (7). The transgenic protocol was carried out in collaboration with Dr

Michal Pravenec (Prague), who is an expert in transgenic rat production, using male and female SHRSP rats from the University of Glasgow colony.

Oxidative stress is an important pathogenic factor in the development of cardiovascular disease. Glutathione S-transferases protect against oxidative stress-induced injury through the detoxification of reactive oxygen species. It is hypothesised that *Gstm1* deficiency in the SHRSP plays a causative role in the development of oxidative stress and hypertension. Thus the aims of this study were to establish definitive proof that reduced *Gstm1* expression in the SHRSP plays a causative role in the development of hypertension and oxidative stress through utilizing a combinational approach of *in vivo* and *ex vivo* studies alongside molecular analysis to fully characterize the *Gstm1* transgenic SHRSP rat. Additionally, information and insights gained from this investigation from the *Gstm1* transgenic SHRSP will be applied to a translation aspect for the investigation of GSTM family in humans.

Functional validation through hemodynamic and cardiac analysis included measurement of systolic, diastolic and mean arterial blood pressures, pulse pressure and heart rate using the Dataquest IV telemetry system (Data Sciences International) and transthoracic echocardiography was used to assess cardiac geometry and contractility. Telemetry data show that there is a significant reduction in systolic blood pressure, diastolic blood pressures, and pulse pressure in both of the transgenic lines when compared to the SHRSP suggesting that incorporation of a WKY type *Gstm1* gene into the SHRSP genome does indeed reduce the hypertensive phenotype. Moreover, the observed reduction in systolic blood pressure is remarkably similar in magnitude to that demonstrated in the Chromosome 2 congenic strain, SP.WKYGla2c*, in which *Gstm1* was identified as a candidate gene for hypertension. In order to investigate the potential role of *Gstm1* deficiency in the salt-sensitivity phenotype in SHRSP rats, parental strain rats and Trans1 animals underwent 1% salt loading starting at 18 weeks of age. This resulted in Trans1 displaying a trend towards salt-sensitivity (i.e. exaggerated night-time daytime blood pressure variation) similar to that of the SHRSP, however, the Trans1 line still maintained a significant decrease in systolic and diastolic blood pressure compared to the SHRSP during salt loading.

In parallel with the significantly lower SBP, DBP and PP we also observe significantly improved cardiac function and reduced cardiac hypertrophy in the two independently generated transgenic lines. While there was no significant changes in both fractional shortening (FS) and ejection fraction (EF), between the four strains, relative wall thickness was significantly reduced in WKY, Trans1, and Trans2 rats when compared to the SHRSP with Trans1 and Trans2 rats showing an intermediate phenotype between the parental strains.

Analysis of genetic and molecular changes resulting from the random insertion of *Gstm1* into the SHRSP genome included assessment of transgene (WKY form) and total *Gstm1* gene expression, protein quantification, immunohistochemistry (IHC), transgene insertion and copy number. Both transgenic lines demonstrated an increase in total and transgene specific expression of *Gstm1* in kidneys at 5 weeks of age as well as increased transgene expression in several other cardiovascular tissues. Protein expression was also similarly increased in the kidney at 5 weeks of age and showed a similar expression pattern to that of the WKY. Additionally, we saw increased total *Gstm1* expression in a range of cardiovascular tissues at 21 weeks of age without changes of other *Gstm* family members (*Gstm2* and *Gstm3*). Although it was not possible to identify the exact location of the transgene insertion site in both transgenic lines, data presented indicate that they are not identically inserted. Furthermore, sequencing data shows that each transgenic line contains multiple copies of the transgene across a number of generations.

To assess renal function in the *Gstm1* transgenic lines, rats from each line that were implanted with telemetry probes were assessed by 24-hr metabolic cage measurements which allowed for analysis of indirect glomerular filtration rate along with proteinuria and urinary electrolyte measurements. Histological analysis was used to assess renal morphology by examining haematoxylin and eosin (H&E) stained sections. Fibrosis was examined by staining with picrosirius red. At 21 weeks, we saw evidence of reduced renal pathology as indicated by the absence of renal vessel hyperplasia and reduced proteinuria in the WKY, Trans1, and Trans2 rats. H&E staining showed a more similar morphology to the WKY in the transgenic lines with no signs of accelerated hypertension. These improvements in renal pathology were also apparent in salt-loaded Trans1 rats.

Oxidative stress and myography measurements were also carried out in order to ascertain the impact of increased *Gstm1* expression on the SHRSP genetic background. The data presented in this study clearly shows a reduction in renal oxidative stress in both transgenic lines. Furthermore, these improvements in oxidative stress were also apparent in salt-loaded Trans1 rats. Aortic and mesenteric artery wire myography data showed that there was no significant difference between SHRSP and transgenic lines for vascular function. Pressure myography in the mesenteric arteries, demonstrated that the transgenic lines were only significantly different from the SHRSP in terms of increased vessel cross sectional area (CSA), but did show trends of improved structure and mechanical alterations of these vessels.

Additionally, we investigated the rodent *GSTM* family and applied them to a human cohort in order to assess translational aspects and expanded the study previously conducted by Delles *et al.* (8). The investigation included a larger number of subjects than that studied previously by Delles *et al.* and allowed for the elucidation of the relationship between other members of the *GSTM* family and human essential hypertension. While there was no significant difference in renal expression in *GSTM5*, *GSTM3*, *GPx-1* and *GPx-3* between normotensive and hypertensive patient, we found that *GSTM2* expression was significantly increased in hypertensive patients when compared to normotensive patients. Moreover, we found there to be a borderline significance ($p=0.054$) between the rs11802 SNP genotype and *GSTM5* expression. Further investigation between gene expression correlations showed there was a significant linear correlation between *GSTM5* and *GPx-1*.

In summary, multiple phenotypic and molecular techniques were applied in the analysis of the *GSTM1* transgenic SHRSP. Transgenic SHRSP rats expressing the WKY form of the *GSTM1* gene demonstrate significantly reduced blood pressure, oxidative stress and improved levels of renal *GSTM1* expression. This data supports the hypothesis that significantly reduced renal *GSTM1* plays a causative role in the development of hypertension in the SHRSP rat.

1 Introduction

1.1 Cardiovascular Disease

Approximately one third of adults in westernized countries have at least one form of cardiovascular disease (CVD) (9) and a substantial proportion (60%) of these adults are under 60 years old (9;10). This shift in demographics from the traditional 65+ years of age to that of 44+ years of age is a significant increase in premature CVD diagnosis. The early onset of CVD has been estimated to kill an average of 17.3 million people each year which represents 30% of all global deaths (11). Of these deaths an estimate 7.3 million were due to coronary heart disease and 6.2 million were due to stroke (10). By 2030 it is expected that 23.6 million deaths will be caused by CVD (10). Consequentially, these statistics result in CVD being considered as the single largest risk for mortality in industrialized and more specifically in developing countries (12). The percentage of premature deaths from CVDs ranges from 4% in high-income countries to 42% in low-income countries (10). A major factor that contributes to this mortality rate is high blood pressure, or hypertension, which accounts for nearly two-thirds of all strokes and a half of all ischemic heart disease (13). The most recent estimate indicates that globally 7.6 million premature deaths (13.5% of total global mortality) and 92 million disability-adjusted life years (6.0% of the global total) were attributable to high blood pressure (1). In addition to this, high blood pressure is a major risk for dementia, chronic kidney disease and heart failure (2;14). These statistics are similar in the UK where over 150,000 people died from cardiovascular disease in 2008, 300,000 people are living with moderate to severe disability as a result of stroke, and 10% of the population have significant kidney impairment. In 2006, the resulting health care cost of these diseases added up to approximately 14 billion, of which 80.4% was spent on patient care and 19.6% spent on medication (15). Moreover, total economic costs for of CVD reached 30.6 billion in 2006 (15). For these reasons, the pressing need for increased awareness and for a comprehensive, more focused international research basis is needed to fully understand the complications and genetic aspects related to CVD.

Cardiovascular disease is an umbrella classification of disease that includes all heart and circulation disorders. These classifications encompass ailments that directly affect the heart (i.e. arrhythmias, cardiomyopathies and congenital heart disease), from conditions that arise as a consequence of vascular disease (i.e. coronary heart disease, stroke, transient ischemic attack), as well as

conditions that can lead to, or result from, vascular disease including diabetes and chronic kidney disease (15). There are nine main risk factors for CVD, many of which are linked to each other. The major modifiable risk factors are; smoking, poor diet, high blood cholesterol, high blood pressure, lack of exercise, obesity, and diabetes (9). Other minor risk factors include medication, excess alcohol consumption, and psychosomatic stress. Additionally, there are non-modifiable risk factors that include ageing, family history, gender and ethnicity (9). Unfortunately, all or most of these risk factors affect health in Scotland, with hypertension being most prevalent, which illustrates a need for further research in CVD (16).

1.2 Blood Pressure

Blood pressure is considered one of the principal vital signs and is measured as the arterial pressure exerted by the systemic circulation of blood upon the walls of vessels. It is determined primarily by three factors: renal sodium excretion and resultant blood volume, cardiac performance, and vascular tone (17). With each beat of the heart blood pressure varies between maximum (systolic) and minimum (diastolic) pressure. Systolic blood pressure is the pressure that is exerted when the ventricles of the heart are contracting (beating); while diastolic blood pressure is the relaxed blood pressure where the heart refills with blood. Classification of blood pressure as adopted by the American Heart Association is generally, Hypotension, Desired, Pre-hypertensive, Stage 1 Hypertension, Stage 2 Hypertension and Hypertensive Crisis (Table 1.1). In the UK blood pressure is usually categorized in to three groups; low, high and normal. While there are varying categories of blood pressure classifications, most authorities have defined elevated blood pressure (hypertension) as either a systolic blood pressure ≥ 140 mmHg or a diastolic blood pressure ≥ 90 mmHg. The hypertension cut off of 140/90 mmHg was selected in the early 20th century based on the fact that only 5–10% of the US population had blood pressures in that range (18).

Table 1-1: Classification of Hypertension

Blood Pressure (BP) Category	Systolic BP (mmHg)	Diastolic BP (mmHg)
Normal	<120	<80
High Normal	135-139	85-59
Mild Hypertension (Grade 1)	140-159	90-99
Moderate Hypertension (Grade 2)	160-179	100-109
Severe Hypertension (Grade 3)	≥180	≥110

Values taken from (19)

Both systolic and diastolic blood pressures increases progressively with age. While diastolic blood pressure is understood to continue increasing until approximately 50 years of age, systolic blood pressure has been known to increase with age until approximately 80 years old. Mean systolic blood pressure increases with age in both men and women, rising from 127 mmHg in men aged 16-24 to 145 mmHg in men aged 75 and over, and from 119 mmHg to 149 mmHg in women (10). Adolescent blood pressure (15-19 yrs old) generally averages 117/77 mmHg. According to the Scottish Health Survey, 33% of Scottish men and 33% of Scottish women are hypertensive or are treated for hypertension (20).

Epidemiological studies have documented multiple contributing factors, such as age, gender, body mass index, to the onset of essential hypertension (21). However, the specific underlying mechanisms involved in the development of hypertension are still not completely understood. A wide variety of physiological systems that have pleiotropic effects and interact in a complex manner have been found to influence BP (*Figure 1.1*). Sodium and fluid balance, and vasomotor tone are important in BP regulation. Both of these mechanisms are affected by numerous genetic and environmental factors, controlled by hormonal, non-sympathetic, paracrine and intracellular feedback loops.

1.2.1 Blood Pressure Control and Regulation

Blood pressure homeostasis is one of the most important and finely regulated systems of the body. Through this system, the body relies on the delivery of oxygen, nutrients and hormones at specific times and precise concentrations and to ensure the removal of metabolic waste products such as carbon dioxide. Many physiological mechanisms exist to ensure that both acute and long-term local and global blood flow is maintained at an appropriate level to supply individual organs in response to metabolic demands. Blood pressure, or mean arterial

pressure, is regulated through a complex physiological system involving the endocrine and nervous systems, in addition to the kidney heart and blood vessels. The definition of blood pressure is the rate of blood flow produced by the heart (cardiac output) multiplied by the resistance of the blood vessels to blood flow (vascular resistance). The resistance is produced mainly in the arterioles and is known as systemic (or peripheral) vascular resistance.

There are various homeostatic mechanisms involved in blood pressure control that interact with one another in order to maintain appropriate feedback responses to environmental factors such as diet, exercise and stress that impact on blood pressure level. Both the nervous system and the renin angiotensin-aldosterone system (RAAS) are intimately involved in regulating these parameters (22). The main organ involved in long-term regulation of blood pressure is the kidney, as it regulates blood volume by controlling salt and water levels within the body. Studies conducted by Guyton *et al.* showed that whenever blood pressure increases above an equilibrium level, the kidneys will excrete more sodium and water and thus decreases blood volume and cardiac output which then restores arterial pressure to normal (17). Bianchi *et al.* in 1974 then confirmed the importance of the role that the kidney plays in blood pressure regulation during his experiments where renal transplants between hypertensive and normotensive rats demonstrated a reduction of BP in hypertensive rats receiving normotensive kidneys and an increase in BP with normotensive rats receiving hypertensive kidneys, concluding that hypertension travels with the kidney (23).

1.2.1.1 *Renin Angiotensin System*

Arterial pressure is regulated by a variety of endogenous factors, in particular the Renin-Angiotensin System (RAS) system (24). The renin-angiotensin system, is known as a physiological regulator and has been the subject of study for over a century (new insights RAS). The RAS is a hormonal cascade where the protein substrate angiotensinogen is successively metabolized by renin and angiotensin converting enzyme (ACE) to form

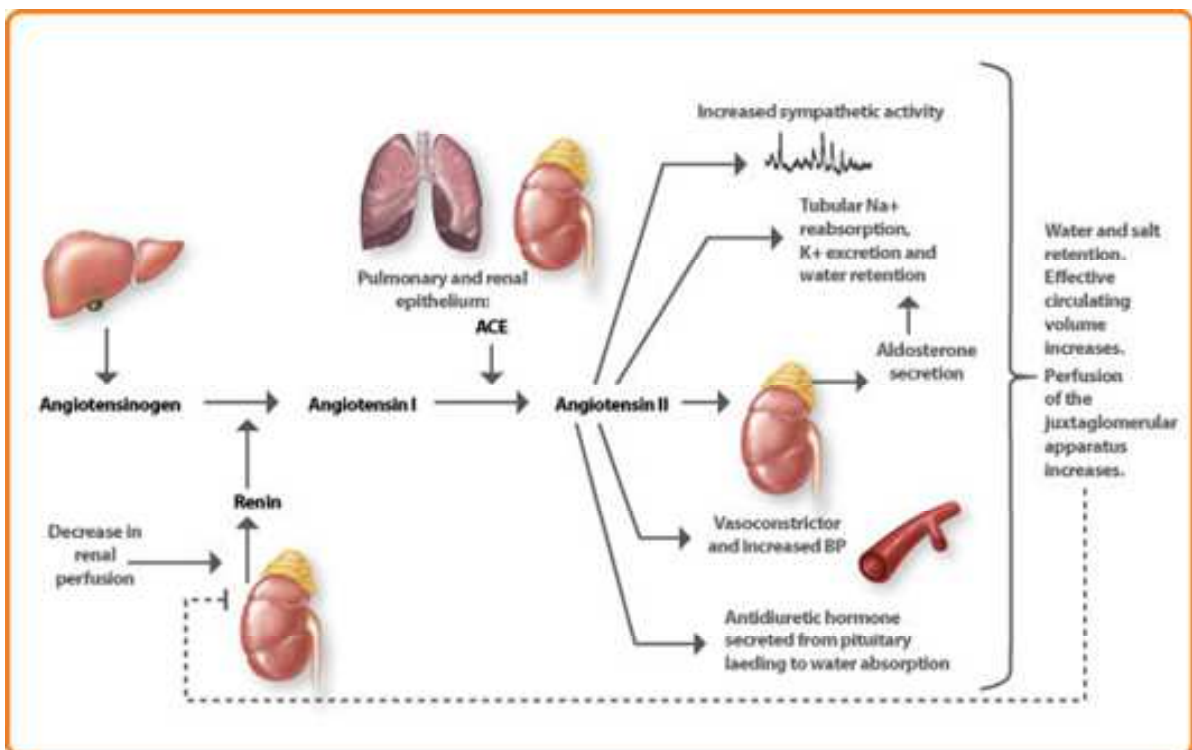


Figure 1-1: The complexity of BP regulation and the role of the kidneys and RAAS

Angiotensinogen is released from the liver and cleaved by renin (released from the glanular cells of the juxtaglomerular complex) forming AngI. AngI is cleaved by ACE expressed on endothelial cells in the lung and is transformed into AngII. AngII is the main active peptide of the RAS and acts through binding to the AT₁R or the AT₂R. AngiotensinII stimulates the hypertrophy of renal tubule cells, leading to further sodium reabsorption. In the adrenal cortex, it acts to cause the release of aldosteron. Aldosterone acts on the tubules (e.g., the distal convoluted tubules and the cortical collecting ducts) in the kidneys, causing them to reabsorb more sodium and water from the urine. This increases blood volume and, therefore, increases blood pressure. In exchange for the reabsorbing of sodium to blood, potassium is secreted into the tubules, becomes part of urine and is excreted. Figure adapted from Schrier RW, ed. Renal and Electrolyte Disorders 5th ed. 1997.

angiotensin (Ang) II, its major biologically-active peptide (24). Ang II interacts with multiple different vascular beds and organ systems that ultimately lead to elevated extra-cellular fluid (EFC) volume and thus resulting in raised arterial blood pressure (17). Ang II also causes vasoconstriction of the renal and systemic arterioles, which then increases total peripheral resistance and blood pressure. Furthermore, activation of Ang II receptors in the brain elevates blood pressure by increasing sympathetic output to the heart and vasculature, which increases cardiac output and total peripheral resistance. Ang II causes increase release of arginine vasopressin from the posterior pituitary gland which increases fluid retention in the renal collection duct in the kidneys (25). Additionally, Ang II stimulates thirst and the increased fluid ingestion expands blood volume thus elevating blood pressure through aldosterone secretion. Plasma Ang II increases aldosterone release from the adrenal gland and acts directly on the tubular receptors, which increases sodium chloride and fluid re-absorption in the distal nephron to increase ECF volume (26). Moreover, it stimulates sympathetic nervous activity which causes increased heart rate and blood vessel constriction (27).

The classical actions of RAS, particularly its cardiovascular effects, are induced by activation of the angiotensin II type 1 (AT_1) receptor. The efficacy of specific AT_1 blockers (ARBs) in treating hypertension and reducing cardiovascular risk reflects the important role of this receptor in a variety of disorders (28). Similarly, targeted deletion of the major murine AT_1 (AT_{1A}) receptor cause a marked reduction of blood pressure and salt sensitivity in mice, confirming its importance in cardiovascular control (28).

1.2.1.2 Other Mechanisms of Blood Pressure Regulation

1.2.1.2.1 Autonomic Nervous Control

In addition to the RAAS system, there are many other factors involved in blood pressure control. The most rapid in responding to the fall or rise in blood pressure is the autonomic nervous system as it receives information from the baroreceptors which relays to the vasomotor centre. The activation of the

baroreceptors in turn activates the sympathetic and parasympathetic nervous systems (29).

The role of the arterial baroreflex is to maintain blood pressure homeostasis. This reflex mechanism counteracts deviations of blood pressure from a reference set point by modulating heart rate, peripheral vascular tone and other cardiovascular variables through autonomic paths. Blood pressure information is sensed by stretch receptors (baro receptors) located on the wall of the carotid arteries and aorta. When a change in blood pressure occurs, a modification in the dilation of arterial walls is sensed by these receptors and information is sent to control centers located in the brain stem through afferent neural fibres. These centres process the baroreceptor inputs and modulate autonomic outflow so as to produce changes in the cardiovascular variables, i.e. heart rate, and vasoconstriction. Since the primary role of the baro-receptor is blood pressure regulation, an impairment of the baro-reflex will likely result in a significant deregulation of blood pressure. This is inclusive of sudden pressure drops on shifting positions as well as aberrant pressure rises with major risks of fatal events such as myocardial infarction and stroke.

The sympathetic arm of the autonomic nervous system acts to stimulate the heart, constrict blood vessels, and stimulate the adrenal gland. Stimulation of the adrenal glands from increased impulses of the sympathetic system results in a release of norepinephrine and epinephrine that increases heart rate and contractility. The parasympathetic system acts to depress cardiac function and dilatation of selected vascular beds.

1.2.1.2.2 *Endothelin*

ET has been shown to affect almost every blood pressure regulating system associated with sodium homeostasis (ET). The two primary receptors responsible for this are ET_A and ET_B . In general, activation of ET_B reduces blood pressure and promotes urinary Na secretion through multiple cascades such as endothelial cell NO production with resultant vasodilation, inhibition of NA transport to the proximal tubule, reduced water re-absorption, and inhibition of renin release.

1.2.1.3 Hypertension

Raised blood pressure or hypertension is estimated to cause approximately 7.5 million deaths, ~12.8% of all annual deaths (30). According to the Global Health Risks Report by the World Health Organization, arterial hypertension remains the leading cause of morbidity and mortality world-wide (30). Hypertension is considered a major risk factor for coronary heart disease and cerebrovascular disease (31). Blood pressure levels have been shown to be positively and progressively related to the risk of stroke and coronary heart disease. In some age groups, the risk of CVD doubles for each incremental increase of 20/10 mmHg of blood pressure. In addition to coronary heart disease and cerebrovascular disease, uncontrolled blood pressure causes heart failure, renal impairment, peripheral vascular disease and damage to retinal blood vessels and visual impairment (31). Moreover, studies have shown that by achieving the target blood pressure of 140 mmHg there would be a 28-44% reduction in ischaemic heart disease, depending on the age (32).

Hypertension is a multifactorial disorder that is most likely a result from the combination of various environmental determinants and genetic inheritance, and can be classified as either essential (primary) or secondary (33;34). Essential hypertension is described as a rise in blood pressure where there is no evident medical cause, and is the most prevalent type of hypertension that affects 90-95% of hypertensive patients(33;34). Although no direct cause has been identified, there are many factors such as sedentary lifestyle (35), stress, hypokalemia (36), salt sensitivity (37), and obesity (38) with more than 85% of cases occur in those with a body mass index greater than 25 (39) that increase the risk of hypertension. Additionally, the risk of high blood pressure can also increase with age (40), by inherited genetic mutation, and/or family history (41). Existing evidence suggests that the genetic contribution for blood pressure variation in essential hypertension is about 30-50% (42). Secondary hypertension indicates that the increase in blood pressure is a result of (i.e. secondary to) another condition, such as renovascular hypertension caused by renal arterial stenosis as a result of hormonal changes, chronic renal failure, hyperthyroidism, neorogenic disorders that cause increased expression of adrenaline, or tumours (33;34).

1.2.1.4 Environmental Influences

Hypertension is a disease of modern civilization and is greatly influenced by environmental factors and lifestyle choices. Blood pressure studies carried out on a population wide basis have shown that hypertension rates can differ greatly among population groups of similar genetic background due to environmental differences. For instance, the prevalence of hypertension differs between non westernized and westernized populations such as African and African-Americans (43;44). Furthermore, these rates can quickly increase within the same ethnic groups and when populations migrate from low to high-risk environment (I.e. dietary or exercise changes) (43;44). To contextualize environmental influences, mean placebo-subtracted SBP reduction for drug monotherapy is in the range of 6.9-9.3 mmHg for four of the most common BP drug classes (45). Estimated SBP reductions for some of the major lifestyle modifications are in or near this range (46). Major components such as smoking/tobacco use, obesity, poor diet, physical inactivity, and heavy alcohol consumption, as well as many of the minor components such as pollutants, have been extensively investigated in order to determine the cardiovascular risk level they present in today society (46).

Risk factors such as alcohol and smoking are some of the more easily managed risk factors. Alcohol is considered a threshold risk factor where low to moderate alcohol consumptions results in only a low cardiovascular risk level, but high alcohol consumption, like that which is culturally present in the west of Scotland, results in a high CVD risk level (47). Consequently, reduction to moderate or complete alcoholic abstinence significantly reduces hypertension (15). Smoking, on the other hand, is considered one of the main avoidable risk factors contributing to hypertension and CVD. The immediate noxious effects of smoking are related to over-activity of the sympathetic nervous system, which increases myocardial oxygen consumption through a rise in blood pressure, heart rate and myocardial contractility (48). Chronic cigarette smoking induces arterial stiffness, a well known contributor to CVD, which can persist for up to a decade after smoking cessation. Additionally, the incidence of hypertension is increased with those who smoke more than 15 cigarettes per day (48).

Another medical complication that is associated with hypertension that is heavily prevalent in today's society is obesity. It is well known that there is an increase

of 3 mmHg (for systolic) and 2 mmHg (for diastolic) in blood pressure respectively, with every 10 kg increase in body weight (49). Studies have also shown that cerebrovascular disease, ischemic heart disease and congestive heart disease are also cardiovascular complications of obesity (49).

Abundance or lack of vitamins and minerals, such sodium, and potassium, due to diet choices has also been shown to play a role in blood pressure regulation. Increased sodium consumption through processed foods has been shown to increase water retention. Conversely, too little potassium intake effects cell sodium levels which effects systemic sodium levels resulting in water retention and elevated blood pressure (50).

Traditionally, studies investigating the correlation between hypertension and the environment have been based upon lifestyle choices such as diet, smoking and/or exercise. However, recent studies have elucidated that environmental exposure to pollutants and other harmful chemical also contribute to CVD risk (51;52).

1.2.1.5 Genetic Influences

Cardiovascular disease is a result of a complex interaction between genes and environment. In the past half century, impressive progress has been made in understanding its varied causes and manifestations (53); however, complete understanding of the initiating factors of essential hypertension are still elusive. Essential hypertension has been shown to run in families and evidence for genetic influence comes from multiple sources. Twin studies document a greater concordance of blood pressures in both maternal and fraternal twins (54), and population studies show a greater similarity of blood pressures within families than between families (55). Adoption studies confirm the latter observation because they demonstrate greater concordance of blood pressure among biological siblings than adoptive siblings living in the same household (56). Moreover, Lifton *et al.* demonstrates that single genes can impart large variance of blood pressure is demonstrated by rare the rare Mendelian forms of hyper- and hypo-tension (57).

The investigation of rare forms of Mendelian forms of blood pressure variation where mutations in single genes produce large effects of blood pressure has

resulted in several genes being identified and characterized (58). The pathological variants in Mendelian or monogenic hypertension are known to follow the classic rules of Mendelian genetics and are often distinguishable specific genotype features (i.e. electrolyte and hormonal abnormalities) (59). Monogenic investigations have lead to the identification of mutations in 12 genes that lead to 8 different distinguishable Mendelian syndromes of hypertension and 9 genes associated with Mendelian forms of hypotension. Furthermore, 8 of these genes are associated with the alteration of salt re-absorption in the kidney (58;60). However the overall contribution of these conditions to blood pressure regulation in the general population is small.

What is known as the candidate gene approach typically compares the prevalence of hypertension or the level of blood pressure among individuals of contrasting genotypes at candidate gene/loci in pathways known to be involved in blood pressure regulation. An example of this relates to genes of the renin-angiotensin-aldosterone system, such as the *M235T* variant in the angiotensinogen gene (61). The *M235T* gene has been associated with increased circulating angiotensinogen levels and blood pressure in many distinct populations (61-63). A second example involves a common variant in the angiotensin-converting enzyme (ACE) gene that has been associated in some studies with blood pressure variation in men (64;65). However, most monogenetic variants only modestly affect blood pressure, and other candidate genes have not shown consistent and reproducible associations with blood pressure or hypertension in larger populations (58;66). Generally, monogenetic variants mutations account for only a small percentage of hypertension. A primary reason for this lies in the fact that numerous interacting genetic loci can influence the same phenotype, and studies have shown that multiple loci are involved in overall blood pressure variation (33).

Large-scale meta-analyses of genome-wide association studies (GWAS) from the Global Blood Pressure Genetics (Global BPgen) and Cohorts for Heart and Aging Research in Genome Epidemiology (CHARGE) consortia identified a total of 43 independent loci significantly associated with systolic blood pressure, diastolic blood pressure and hypertension (59;67;68). These genetic variations include single nucleotide polymorphisms (SNPs), variable number tandem repeats (VNTR), insertions, deletions and duplications. Many of these variants were found

to alter various systems, such as the renin-angiotensin system, renal sodium handling system, cholesterol metabolism pathways, inflammation, and oxidative stress (33).

While identifying and understanding monogenic and polygenic forms of hypertension improve our comprehension of the genetic architecture of blood pressure and provide new biological insights in to blood pressure control, common genetic causes of hypertension in the general population remains elusive (63;69;70).

1.2.1.6 Current prevention strategies

Prevention of hypertension, although relatively unfashionable when compared to new drug and surgery related technologies, is the cheapest and simplest way to reduce the prevalence of hypertension. Primordial prevention, which refers to a lifestyle that does not permit risk factor to appear, is used by the American Heart Association (AHA) to promote “ideal cardiovascular health” by incorporating Life’s simple 7 (www.mylifecheck.org). This ideal cardiovascular health incorporates sufficient exercise, a superior diet score, absence of smoking, a BMI less than 25 kg/m^2 , and ideal health factors, i.e. normal blood pressure, cholesterol, and fasting glucose. In addition to healthy life style choice, clinical prevention using drugs such as aspirin and statins are well known protectors of cardiovascular health. In general, primary prevention of both hypertension and cardiovascular events denotes delaying or limiting a first event in individuals who have not yet been formally diagnosed. This also includes individuals with risk factors where the risks themselves are often regarded as diseases and are targets for therapy.

1.2.1.7 Current treatment strategies

Considering that hypertension is a major public health concern and a primary cardiovascular risk that contributes significantly to cardiovascular mortality (71;72), its treatment is therefore important as a primary and secondary prevention strategy. Initial management of hypertension uses a multipronged approach, with emphasis lifestyle measures (non-pharmacological) and add-on

drug management (73). With recent studies providing increasing evidence that non-pharmacological therapies play important roles in both the prevention and reduction of hypertension, lifestyle medication can serve as an initial treatment to hypertension before the start of drug therapies (74). Furthermore, with hypertensive patients these therapies can facilitate a reduction of medication reliance for the hypertensive individual, provided that sustain in lifestyle change. Major lifestyle environmental factors which influence hypertension are dietary excess of sodium and fat Harp (75), a deficiency of fibre and potassium (76), lack of physical activity, psychosocial stress, and alcohol intake (77) Numerous short-term trials have documented that individuals can make these lifestyle changes which lower blood pressure (73). For example, the American Heart Association has originated the dietary approaches to stop hypertension program (DASH) as a crucial step to hypertension management. The DASH study showed that a diet full of fruits, vegetables and calcium while being low in sodium was beneficial to treating hypertension (77). The study also concludes that exercise is a critically important component, especially in children and young adults with hypertension from heightened sympathetic nervous system activity (77).

When lifestyle changes need to be supplemented in order to obtain more ideal blood pressure levels, drug therapies are often prescribed. The main classes of blood-pressure-lowering drugs can be grouped into two categories. The first category consists of drugs that inhibit or block the renin-angiotensin-aldosterone system, namely angiotensin-converting enzyme (ACE) inhibitors and angiotensin receptor blockers, beta-blockers and aldosterone antagonists. The second category consists of drugs that lower blood pressure independently of the renin-angiotensin system, and cause reflex activation of this system such as calcium antagonists and diuretics. Because of the variety of choice for drug mediated blood pressure reduction, deciding upon an initial drug management approach is a contentious issue. The JNC-1 report emphasized beta-blockers and thiazide diuretics as suitable drugs for first line management (74). On the other hand, recent studies that have evaluated newer drugs such as ACE inhibitors and CCB molecules report better outcomes as compared to the beta-blockers and thiazides. The British National Institute of Clinical Excellence (NICE) guidelines utilize ABCD algorithm for initial pharmacological management of hypertension

but has modified these to ACD algorithm in view of changing evidence (16). Current thinking is to start with an ACE inhibitor in young individuals and CCB in older individuals and step-up the drug therapy until blood pressure targets are reached (74).

1.3 Animal Studies

Given that hypertension is under polygenic control, and is due to a culmination of multiple gene-gene and gene-environment interactions, genetic studies involving genetic modification or dissection are not feasible in humans due to ethical implications. For this reason, an array of experimental models have been developed as a reductionist paradigm in order to study the determinants of essential hypertension (78). The most widely used experimental models are rodents models, specifically rats. Since rats have long been a favoured species for the study of hypertension, a variety of genetically hypertensive strains and non-genetic models have been developed and well characterized over the past 35 years (79-82). The range of available models addresses both essential and secondary hypertension. Examples of non-genetic models include surgically induced hypertension (2 kidney 1 clip) where hypertension is induced by unilateral restriction of the renal artery, the deoxycorticosterone acetate (DOCA) -salt rat where hypertension is induced through the use of a mineralocorticoid, (DOCA), and diet-induced hypertension through increased salt intake (81).

Genotype-driven genetic models, typically transgenic or knock-in/knock-out, have been extremely important in the study of Mendelian hypertension. Phenotypic-driven genetic models such as the spontaneously hypertensive rat (SHR) are used to identify underlying genes or mechanisms contributing to development of hypertension. Among these strains is the stroke-prone spontaneously hypertensive rat (SHRSP) (83;84) which is a model for essential hypertension, endothelial dysfunction and oxidative stress (79;80). The SHRSP develops a number of vascular complications, such as cardiac hypertrophy, cardiac failure and stroke (80;85;86). These animal models provide favourable investigative opportunities because of reduced genetic heterogeneity, controlled breeding, the ability to produce genetic crosses and analyse large numbers of

progeny (87). Although no species or model can consistently fulfil all the needs each study requires, it is important to work with the most appropriate model which most fully addresses the research question under investigation.

1.3.1 SHRSP

Spontaneously-hypertensive, stroke-prone rats are a unique genetic model of severe hypertension and cerebral stroke. They are of particular interest because their pathophysiology is very similar to that of stroke patients in the clinical setting (88). They were first developed in 1974 by Yamori *et al.* (89) as a substrain of the spontaneously hypertensive rat and were used as a genetic model for severe hypertension with alterations in their endocrine signaling systems (90). According to the National BioResource Project for the Rat database, the SHRSP is the strain showing the highest blood pressure among 179 stains (91), indicating that the SHRSP has a distinct set of hypertension genes that make the SHRSP unique among the various rat strains. While there is likely to be significant overlap of disease related genes between the SHRSP and other hypertensive strains, the gene-gene interaction within the SHRSR is necessary for a full-blown effect on blood pressure. When compared with the SHR, the SHRSP has a high incidence of stroke (80 vs 10%) and severe hypertension (220-240 mmHg vs 180-220 mmHg) (92). Furthermore, the incidence of stroke reaches 100% in SHRSP rats with a high salt diet (89). The cerebral stroke observed in SHRSP rats is reported to be similar to brain oedema due to malignant hypertension or hyalinosis of small arteries due to severe hypertension rather than atherosclerosis based (91).

1.3.1.1 *Identifying QTL's*

A major challenge in hypertension research is to identify the underlying causative factors responsible for the disease phenotype. One approach that has been used extensively is the genome wide scan and quantitative trait loci (QTL) mapping. QTL mapping is a phenotype driven approach that does not require a prior knowledge of either causative genes or their function, and can lead to the identification of novel genes involved in disease. QTL analysis involves at least two strains (generally rats or mice) that differ genetically with regard to the trait of interest and a genetic marker that distinguish between these parental

lines. Molecular markers, such as SNPs, simple sequence repeats (SSRs or microsatellites), restriction fragment lengths polymorphism (RFLPs) and transposable element positions are preferred because these markers are unlikely to affect the trait of interest (93). The parental strains are then crossed, resulting in heterozygous (F1) individuals. The F1 individuals are then crossed again using giving rise to F2 individuals where the phenotypes and genotypes are scored. Markers that are genetically linked to a QTL influencing the trait of interest will segregate more frequently with trait values whereas unlinked markers will not show a significant correlation.

The principal goal of QTL analysis has been to answer the question of whether phenotypic differences are primarily due to a few loci with fairly large effects, or too many loci, each with small effects. It appears that a substantial proportion of the phenotypic variation in many quantitative traits can be explained with few loci of large effect, with the remainder due to numerous loci of small effect (94;95). Once QTL have been identified, molecular techniques can be employed to narrow the QTL down and to identify candidate genes. Indeed, the Rat Genome Database (<http://rgd.mcw.edu/>) has compiled more than 300 QTLs influencing rat blood pressure (91) with a considerable number of these QTLs being identified through experimental SHR/ SHRSP crosses with normotensive rat strains. Unfortunately, few causative genes have been identified thus far despite the large numbers of QTLs identified. This is primarily due to the fact that function analysis of candidate genes to confirm causality is extremely complex and requires a series of multiple investigations.

1.3.1.1.1 QTL interaction in Complex diseases

Genome-wide linkage studies performed on several rat crosses have been successful in identifying large chromosomal regions containing quantitative trait loci (QTLs) which are involved in blood pressure regulation (42;96).

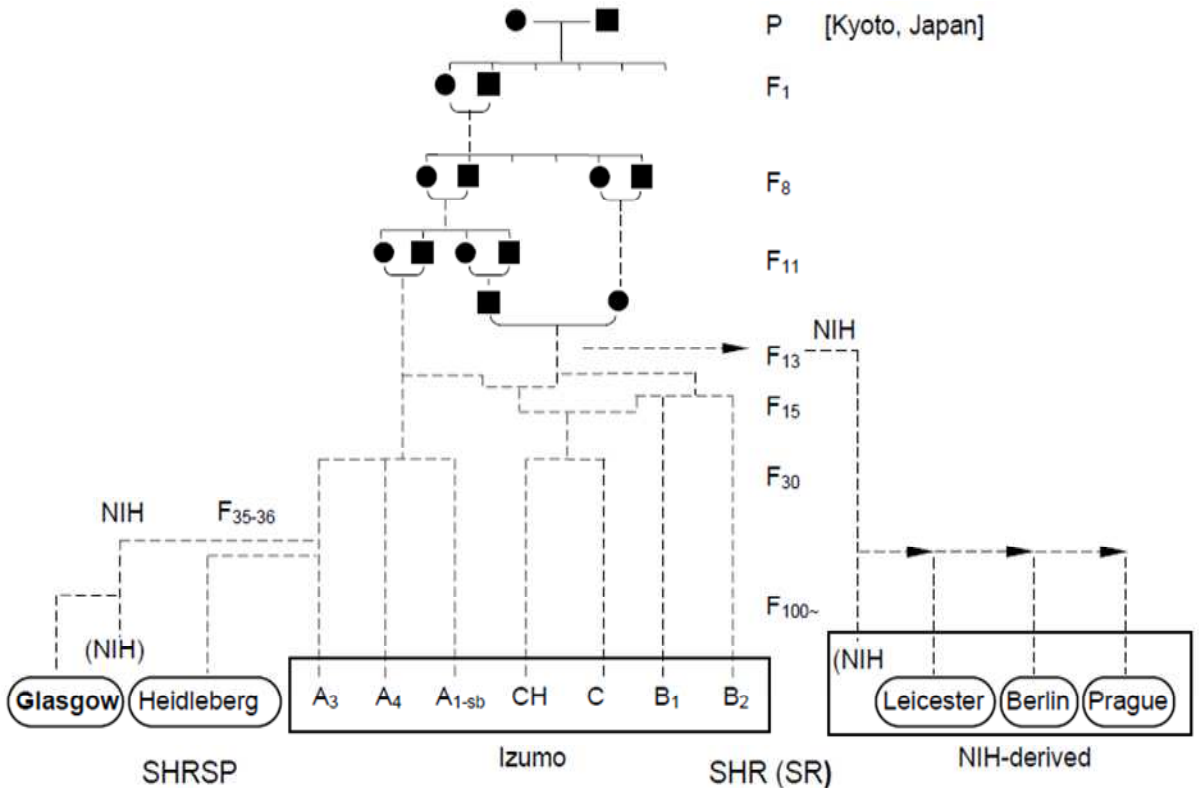


Figure 1-2: Geneological background of the Stroke Prone Spontaneously Hypertensive Rat (SHRSP)

The SHRSP strain, maintained at Glasgow University (Gla), was obtained after filial generation 35-36. Personal communication & Ref. (89)

There have been numerous studies where the production of novel designer strains such as recombinant inbred strains or congenic strains, has allowed confirmation and genetic dissection of blood pressure QTLs (79;96-98).

1.3.1.2 Recombinant inbred strains

Recombinant inbred strains are derived from F2 individuals obtained by crossing of two highly inbred stains. Randomly chosen F2 pairs are brother-sister mated for more than 20 generations to become genetically fixed. Individual recombinant strains have unique combinations of loci derived by segregation and recombination of alleles present in the progenitor strains. An important feature of these strains is that because they are inbred, repeated assay can be carried out in order to precisely classify the phenotype of each strain from the average results obtained from the measurement of multiple rats from each strain. This precise estimation of phenotype-genotype relationship is extremely important when studying highly variable traits such as blood pressure. Moreover, since data are cumulative across studies, accumulated data can be analyzed and trait relationships studied in a manner not possible with conventional, genetically segregated populations. This is a major advantage for the analysis of complex patho-physiological traits.

1.3.1.3 Congenic Strains

Congenic strains have been produced in order to confirm the existence of a QTL and to begin narrowing down the chromosomal region of interest for gene identification. A congenic strain is one in which the chromosomal region of interest has been selectively replaced by the homologous region from another stain. These strains are generated by mating two inbred strains and backcrossing the descendent to the original strains (known as the recipient strains) for at least 5-10 generations.

Typically selection for the desired phenotype or genotype drives the strain's generation. Through this either a desired phenotype, or a desired chromosomal region (assayed by genotype) is passed from the donor stain to the recipient strain. The congenic stain is then compared to a pure recipient strains to determine whether they are phenotypically different. If the quantitative trait of the congenic strain is significantly different from the former strain, it can be

concluded that a QTL that contributes to a phenotypic difference resides within this chromosome region. Upon completion of the congenic stain, brother-sister mating is ensures homozygosity for the congenic chromosome. Furthermore, construction of congenic sub-strains help to enable genetic dissection

Since the early 1990's, congenic stains have been an integral part in blood pressure and QTL-QTL interaction studies. However there are several limitations or difficulties that are involved when using congenic strains. Namely, that a single congenic strains does not necessarily resolve closely linked QTLs that act in the same direction, especially in the case of polygenic traits (99;100).

Furthermore, there is also the chance that there is a lack of polymorphisms between the inbred strains used thus making it difficult to identify causative genes between the two strains (101;102). However, advances in technology mean that traditional genetic mapping techniques can now be complemented by high-throughput methods, such as high-density arrays of synthetic oligonucleotides (103-105), cDNAs (106) for studying gene function and regulation, or identifying the genetic basis from an observed phenotype and deciphering the gene networks that contributed to increased susceptibility to metabolic disease processes in humans (68;107). Moreover these methods allow gene expression monitoring on a genome-wide scale and offer an opportunity to establish functional links between genotype and phenotype for complex diseases (68;108). Methods, such as microarray expression analysis have consistently been used as complimentary methods in order to generate genome-wide expression profiles in rodents (102) Flint (109) and has been routinely used in combination with traditional quantitative trait locus (QTL) mapping techniques (109).

1.3.1.3.1 Microarray analysis

Microarray profiling involves the hybridization of nucleic acid samples (or targets) to oligonucleotide probes that allow for the determination of a sequence or to detect variation in gene sequence or expression. Microarray has led to gene profiling that has played a key role in understanding drug side effects at the molecular level, and especially, novel molecular profiles for endocrine linked diseases such as hypertension (110). Since the premise of microarray profiling is that steady-state mRNA levels are altered in diseased samples, examining the

changes in mRNAs expressed in tissues and/or cells can elucidate unique expression patterns identifiable to a specific disease (110).

1.3.1.4 Transgenic Strategies

The first transgenic animals were generated around thirty years ago by injection of naked DNA into the pronuclei of mouse zygotes. This method of transgenic generation only allowed for random insertion into the genome (111). Even until recently, gene targeting involving homologous recombination (HR) in embryonic stem (ES) cells or cloning through nuclear transfer was limited to species where appropriate cells were available. While these techniques have been used for the generation of useful mutants in many different species (i.e. mouse, cow, pig), they are cumbersome and expensive and do not allow targeted modification of specific genes. Furthermore, while several of these strategies have been readily available for a number of years in the mouse, the same cannot be said of the rat because of the lack of appropriate technologies. Rat ES cells and induced pluripotent stems cells (iPS) have been available but the culture conditions for these cells and methodology for inducing HR were imperfect (112-114). Furthermore, *in vitro* cultivation of rat spermatogonial stem cells and their ability to undergo HR has proven to be unsatisfactory (115;116). However, other methods based on the *in vitro* genetic engineering of pluripotent stem cells, transposon-mediated mutagenesis (117) and Nethyl- N-nitrosourea (ENU) mutagenesis (118;119) have been used with some success for producing mutations in the rat genome.

Traditionally, the rat has been an important biomedical research model whose utility has led to significant advancements in modern medicine for humans. However, due to the difficulties mentioned above, the rat has been significantly hampered by a lack of technologies for targeted genome modification (120). An early example of successful transgenic rat production, which allowed confirmation of the importance of a gene for fatty acid metabolism and insulin resistance in the SHR model, is the transgenic rescue of *Cd36* (121). *Cd36* was first identified as a candidate gene by QTL analysis and confirmed by congenic strain production. The SHR rat was found to lack a functional *Cd36* gene therefore; this gene was transgenically rescued by random insertion of the wild-type version of the gene into the SHR genome. Two independent transgenic lines

were generated, and these lines were investigated in terms of insulin action in isolated muscle and glucose intolerance in order to measure insulin sensitivity. In both lines expression of wild-type *Cd36* on the SHR genetic background induced improvements in glucose tolerance, insulin-stimulated glucose incorporation into muscle glycogen, and serum fatty-acid levels. Other factors, such as body weight, were not significantly different in the transgenic lines compared with the SHR progenitor strain (121). Further research into each of the independent lines identified differential expression patterns of *Cd36* when the transgenic lines were compared showing unique characteristics for each line. However, in both lines, the *Cd36* transgene substantially corrected (>70%) the SHR muscle defect in insulin action compared with normotensive control rats which supports their concept that primary genetic defects in fatty-acid metabolism contributes to the pathogenesis of insulin resistance (121).

Despite over 195 transgenic or mutant rats that have been produced using either chemicals (118), transposons (117), nuclear transfer (122), rat ES cells (112;113), induced pluripotent stem cells (iPS) (114), or spermatogonial stem cells (SSC) (116), none, of these methods until very recently were amenable to any form of targeted gene modification.

However, several new approaches have enabled precise genome engineering in order to generate modifications, such as point mutations, accurate insertions and deletions, and conditional knockouts and knock-ins.

1.3.1.4.1 Embryonic Stem cells

Embryonic stem cells are pluripotent cells derived from the inner cells mass in very early stage embryos which can differentiate to any cell type in the embryo. When foreign DNA is introduced directly into ES cells, it may integrate randomly within the genome. However, if the introduced DNA is similar in sequence to part of the host genome, it may undergo “homologous recombination” and integrate as a single copy at a specific (123). Additionally, ES cells colonize the host embryo and often contribute to the germ line, resulting in the production of transgenic offspring with the same newly introduced DNA. Thus providing a powerful developmental tool to generate experimental animals. Since stem cells

are easily accessible for genetic modification, they can be used to test transgene expression in both *in vivo* and *in vitro* environments (123).

The strong activity in most cell lines and permissibility in most tissues make the cytomegalovirus (CMV) promoter, human polypeptide chain elongation factor 1 α promoter (the EF-1 α promoter) and mouse class I promoter (H-2K) some of the more popular choices for promoters (124;125). Unfortunately, *in vivo* the CMV promoter has shown to be silenced at the mRNA level in liver (126) and within several weeks in multiple organ systems as well (127;128). Other choices, like the EF-1 α promoter have shown to be consistent in their gene expression *in vivo* (124).

1.3.1.4.2 Zinc fingers nucleases

Another method for creating knock-in and knock-out models is the use of zinc finger nucleases (ZFNs). ZFN allows for a directly targeted mutagenesis at the 1-cell-stage embryo and thus making ES obsolete in this process. Without ES generation to consider, the ZFN process makes model generation much faster and avoids background strain limitations and is directly applicable to the rat. ZFNs have been used in recent years to successfully create numerous transgenic rat models on a variety of genetic backgrounds (129).

Zinc fingers were first discovered and used in 1985. They originated from biochemical studies arising from the interpretation of the interaction of the Xenopus protein transcription factor IIIA (TFIIIA) with 5S RNA (130). Subsequent studies investigating the structure revealed that zinc-fingers consisted of a three-dimensional structure that readily interacted with DNA (130), where each finger constitutes a self-contained domain stabilized by a zinc (Zn) ion ligated to a pair of cysteines and a pair of histidines and also by an inner structural hydrophobic core (130). Because of this three dimensional structure, zinc fingers can be linked linearly in tandem to recognize nucleic acid sequences of varying lengths. This modular design offers a large number of combinatorial possibilities for the specific recognition of DNA (or RNA).

Application of this specific recognition lead to the use of zinc fingers being used to construct DNA-binding proteins for specific intervention in gene expression.

By fusing zinc fingers to nucleases to create hybrid molecules composed of tandem zinc finger-binding motifs to a non-specific cleavage domain of the restriction endonuclease, such as FokI, genes can be selectively altered by targeting the peptide to the desired gene target. One of the first examples of the power of the method was published in 1994 when a three-finger protein was constructed to block the expression of a human oncogene transformed into a mouse cell line (131). More specifically, zinc finger nucleases (ZFNs) have the ability to create site-specific double-stranded breaks which are repaired via non-homologous end joining (NHEJ) which then results in the arbitrary addition or deletion of base pairs. The first successful example of ZFN technology in rats was by Geurts *et al.* (2009), where a single injection of DNA or messenger RNA that encodes specific ZFNs into one-cell transgenic rat embryos that express GFP lead to a high frequency of animals that do not express the transgenic marker as a consequence of homologous recombination at the GFP site (129). Specifically, ZFN reagents targeted a single-copy Green Fluorescent Protein (GFP) transgene inserted in a rat chromosome. Full knockout of the GFP transgene was achieved, as mutant animals lacked both GFP expression and wild-type GFP sequence. Animals were then bred to wild-type animals with 1 out of 1 GFP offspring.

There are two major platforms for generating polymeric zinc fingers with defined specificities. The first is a proprietary platform developed by Sangamo Biosciences and has partnered with Sigma to sell pre-assembled ZFN's via the Compozr program (<http://www.compozrzfn.com/>). The second platform, an OPEN platform, was developed by the Zinc Finger Consortium (<http://www.addgene.org/zfc>; www.zincfingers.org/software-tools.htm) makes their modular assembly zinc finger pools and reagents freely available. Both platforms are available for transgenic animal research purposes.

1.3.1.4.3 TALENs

A more recent advancement in the production of knock-in or knock-out rats is the development of Transcription activator-like (TAL) effectors. TALs are a newly described class of specific DNA binding protein, so far unique in the simplicity and manipulability of their targeting mechanism. Produced by plant pathogenic bacteria in the genus *Xanthomonas*, the native function of these proteins is to directly modulate host gene expression (132). Upon delivery into host cells via

the bacterial type III secretion system, TAL effectors enter the nucleus, bind to effector-specific sequences in host gene promoters and activate transcription (132). Their targeting specificity is determined by a central domain of tandem, 33-35 amino acid repeats, followed by a single truncated repeat of 20 amino acids. Of the naturally occurring TAL effectors that have been investigated, most have between 12 and 27 full repeats (133). Within the DNA binding domain, positions 12 and 13 of each repeat species the target nucleotide sequence and is referred to as the ‘repeat-variable di-residue’ (RVD). Furthermore, for TAL-effector activity, all naturally occurring recognition sites are preceded by a T (134;135). Because of the straight forward sequence relationships and ease of designations through simple ‘protein=DNA code’ that relates modular DNA binding, Transcription activator-like effector nucleases (TALENs) have rapidly emerged as an alternative to ZFNs for genome editing.

TALENs are similar to ZFNs and comprise a non-specific FokI nuclease domain fused to a customizable DNA-binding domain. Early investigations using TALENs were based on natural TALE scaffolds where FokI cleavage domain replaced the natural C-terminal activation domain, and resulted in modest targeted cleavage properties (136). Research done by Mussolino *et al.* showed that TALENS with higher activity can be made by truncating the natural TALE scaffold on either side of the repeat units, retaining a minimum of 150 residues at the N-terminus and 20 amino acids at the C-terminus (136-138). These investigations resulted in tailored TALENs improving genome modification of up to 20% of target *al.ileles* in transfected cells and having a comparable success rate of that of ZFNs (136-138). Additionally, the new optimized TALEN architecture has shown to be successful in the modification of human induced pluripotent stem cells (iPSCs) as well as in zebrafish and rat zygotes with similar knockout efficiencies as ZFNs (137-140). Furthermore, recent studies by SO and SO *et al.* using the CCR5 and the IL2RD loci in cultured human cells have shown that TALENs have significantly less cytotoxicity when compared to ZFNs (137). Furthermore, *in vivo* studies in the rat have not only showed less toxicity, but TALEN generated knockout animals resulted in an higher percentage of newborn animals compared to data obtained previously with ZFNs (129;141). A second advantage to using TALENs, is the increased specificity. Mussolino *et al.* showed that unlike the ZFN, the CCR5-

specific TALEN was able to discriminate between the CCR5 target locus and a highly similar site in CCR2(137).

1.3.2 **Oxidative Stress in Cardiovascular studies**

Oxidative stress is thought to result from an imbalance between the generation of reactive oxygen and nitrogen /species and the antioxidants that scavenge them. Under physiological conditions, several tightly controlled oxidative stress pathways contribute towards the production of reactive oxygen species (ROS), while several intra- and extra-cellular antioxidant enzymatic systems account for the reduction of ROS. In the past two decades, our concept of how oxidative stress contributes to chronic diseases has undergone considerable evolution. Traditionally, reactive oxygen species and their resultant oxidative stress have been examined in the context of damage to biologically important targets such as proteins, lipids, and DNA. Recently, these studies have led to clinical investigations implicating oxidative stress in human disease, including atherosclerosis and cardiovascular disease. For instance, oxidative stress in atherosclerotic cardiovascular disease is highlighted by the increase of biomarkers indicative of risk factors for coronary artery disease which have shown to have predicative values for cardiovascular risk in both primary and secondary prevention (142). End products such as serum lipid hydroperoxides (LOOH) which is generated from polyunsaturated fatty acids, Malondialdehyde (MDA) an end product of lipid peroxidation can be easily measured and have been shown to be elevated in association with cardiovascular risk factors (143;144).

Although the mechanisms underlying cardiovascular disease are complex and multifactorial, there is growing evidence to suggest that an increased production of ROS, or oxidative stress, plays a critical role in the development of CVD (145).

1.3.2.1 ***Reactive oxygen species and nitric oxide***

Reactive oxygen species (ROS) play a crucial role in human physiological and pathophysiological processes. They are ubiquitous reactive derivatives of O₂ metabolism found in the environment and in all biological systems. Reactive oxygen species (ROS) include free radicals, such as superoxide anion (O₂⁻),

hydroxyl radical (OH^-), nitric oxide (NO) and lipid radicals (LOO^-), which possess unpaired electrons, or include molecules that possess oxidizing actions, such as hydrogen peroxide (H_2O_2), hypochlorous acid (HOCl) and peroxynitrite (ONOO^-) (146).

Physiologically, ROS are produced in a controlled manner at low concentrations intracellularly that can act as intracellular second messengers that modulate the function of biochemical pathways and regulation (147-149). An example of this cell signalling function is the role that ROS play in maintaining vascular integrity through regulating endothelial function and vascular contraction and relaxation (148;150). Under pathological conditions, increased ROS bioactivity leads to endothelial dysfunction, increase contractility, vascular smooth muscle cell growth, lipid peroxidation (increase MDA), and inflammation which are all important factors of vascular damage (148;150).

Clinical studies have indicated that the inhibition of the RAAS is beneficial for hypertensive patients (151). Research by Matsuno *et al.* have shown that inhibition of the RAAS reduces up regulation of several NADPH oxidase isoforms which results in a reduction of oxidative stress. For instance, animals without the Nox1 protein develop less hypertension with angiotensin II infusion (or an increase in the RAAS) than animals with the Nox1 protein (152). Other ROS sources have been investigated in animal models with salt-induced hypertension where the up regulation of mitochondrial *SOD2* demonstrated an antihypertensive effect (153). Furthermore, antioxidants either targeted to the mitochondria (eg, mitoTEMPO and MitoQ) or endogenously expressed in the mitochondria (*SOD2* and thioredoxin 2) have all been shown to attenuate angiotensin II-induced hypertension (154;155).

Reactive nitrogen species, such as nitric oxide (NO) and peroxynitrite (ONOO^-), are biologically important O_2 derivatives that are recognized to be important in vascular biology through their oxidation/ reduction (redox) potential (147). Nitric oxide, also known as endothelium-derived relaxing factor (EDRF), is biosynthized endogenously from L-arginine, oxygen and NAPDH by various nitric oxide synthases (NOS) enzymes and is responsible for vasorelaxation by its effect on the vascular smooth muscle cells (VSMCs) (156;157). Vascular NO relaxes blood vessels, prevents platelet aggregation and adhesion, limits oxidation of low

density lipoprotein (LDL) cholesterol, inhibits proliferation of vascular smooth muscle cells, and decreases the expression of pro-inflammatory genes that advance atherogenesis (157-159). An increased production and/or impaired inactivation of ROS (i.e. oxidative stress) leads to reduced bioactivity of NO. A dominant mechanism reducing bioavailability of vascular NO is rapid oxidative inactivation by the ROS superoxide (O_2^-).

1.3.2.2 *Oxidative stress*

Under normal physiological conditions, reactive oxygen species (ROS) produced in the course of normal metabolism are fully inactivated by an elaborate defensive cascade of cellular and extracellular antioxidants (160). However, certain pathological conditions increase the generation of ROS and/or the depletion of antioxidant capacity which leads to enhanced ROS activity and oxidative stress. Oxidative stress is often defined as an abnormal level of reactive oxygen species (ROS), such as free radical (e.g. nitric acid, hydroxyl group, superoxide) or non-free radicals (e.g. hydrogen peroxide, lipid peroxide) that lead to oxidative damage and a biological system's inability to readily detoxify the reactive intermediates (Figure 1-3). This imbalance often leads to consequential injury to cells or tissue.

Compelling evidence has shown the oxidative stress to be associated with diverse physiological events, including cancer, the development of vasculopathies (hypertension, artherosclerosis), renal disease and neuro-degeneration (148). Furthermore, increased production of ROS generally occurs as a result of inflammation, ageing, UV radiation, excessive alcohol consumption, cigarette smoking, and many other factors (161).

1.3.2.3 *The antioxidant system*

In order to protect against increased ROS levels, several different oxidases exist within vascular tissue, including superoxide dismutase (*SOD*), catalase, thioredoxin peroxidase, peroxiredoxin and glutathione peroxidase (*GPx*), which convert ROS into less noxious compounds. Superoxide dismutase (*SOD*) dismutates O_2^- at a rate of 2.4×10^9 mol.L $^{-1}$.s $^{-1}$ to the more stable hydrogen peroxide (H_2O_2), which is then converted to water by catalase or glutathione

peroxidase (*GPx*) (149;162;163). Collectively, these enzymes provide a first line of defence against superoxide and H₂O₂. Whilst such enzymes are of enormous importance in limiting ROS-mediated damage to intracellular macromolecules, there are additional anti-oxidants such as ascorbate which scavenges superoxide in order help maintain a normal homeostatic balance of ROS.

However, in the case of the diseased states many of these antioxidant molecules may not be present at sufficient levels (164). Moreover, the expression of ROS-producing enzymes have been shown to be altered by hormones such as angiotensin II (Ang II) or cytokines such as tumour necrosis factor (TNF) - α and interleukin (IL) -1B (149).

1.3.2.3.1 Glutathione

Glutathione (GSH) is found in the cytosol of cells where concentration ranges from 1-10 mM, with the majority of cells ranging between 1-2 mM and around 10 mM in hepatocytes (165). GSH plays major roles in the different cellular compartments. In the mitochondria GSH regulates the balance between apoptosis versus necrosis (166), and in the nucleus, is found to be a key modulator of cellular division (167). GHS is considered a unique γ -glutamyl-lcysteinylglycine. This is largely due to the fact that it contains an unusual peptide linkage between the γ -carboxyl group of the Glu side-chain and the amino group of the cysteine (1,2). GSH synthesis involves the combination of cysteine with glutamate to produce c-glutamylcysteine. This reaction is catalyzed by the enzyme glutamate cysteine ligase (GCL), which is also called γ -glutamylcysteine synthetase. This enzyme requires coupled ATP hydrolysis to form an amide bond between the c-carboxyl group of glutamate and the amino group of cysteine (168). A secondary step involves the enzyme glutathione synthetase, responsible for adding glycine to the dipeptide to produce GSH (γ -glutamylcysteinylglycine) and also requires coupled ATP hydrolysis (169). GSH when reduced results in the formation of glutathione disulfide (GSSG).

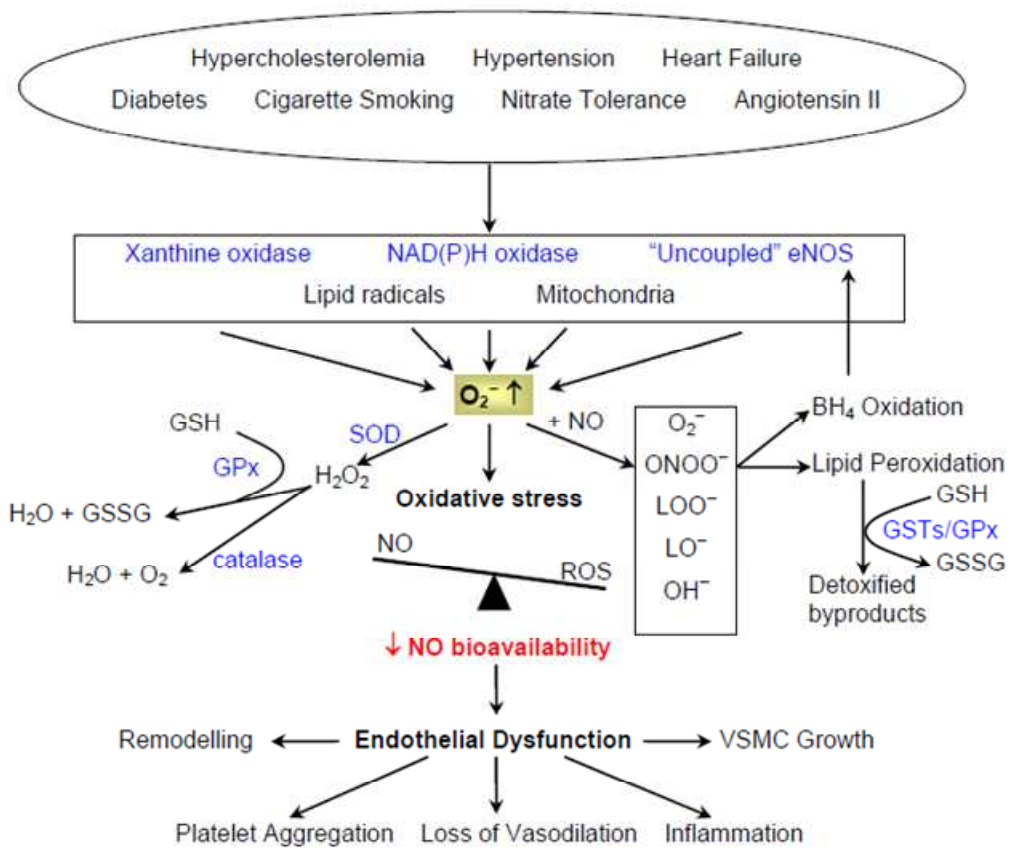


Figure 1-3: Oxidative stress enzymes and their roles in maintaining the balance between O₂⁻ and NO.

BH_4 = tetrahydrobiopterin; eNOS = endothelial nitric oxide synthase; H_2O = water; H_2O_2 = hydrogen peroxide; GPx = glutathione peroxidase; GSH = glutathione; GSSG = oxidized glutathione; GSTs = glutathione s-transferases; LO $^\cdot$ or LOO $^\cdot$ = lipid radicals; NAD(P)H = nicotinamide adenine dinucleotide (phosphate); NO = nitric oxide; O_2 = molecular oxygen; O_2^- = superoxide anion; ONOO^- = peroxynitrite; ROS = reactive oxygen species; SOD = superoxide dismutase; VSMC = vascular smooth muscle cell. Adapted from Ref (146).

The GSH-glutathione disulfide system is considered the most abundant redox system in eukaryotic cells (170). Qualitative and quantitative alterations of the GSH-GSSG redox system induced by reactive oxygen and nitrogen species has been implicated in the pathogenesis of certain chronic illnesses (such as sickle cell disease, asthma, and preeclampsia) are comprehensively reviewed by Dalle-Donne *et al.* (171).

The biologically active site of GSH is represented by the thiol group of the Cys residue. The high nucleophilicity of the thiol functionality facilitates the role of GSH as a free radical scavenger both under physiological conditions and in xenobiotic toxicity (172-174). GSH also helps in the regeneration of other antioxidants, e.g. vitamin E and ascorbic acid (ASC) (175-177). GSH is a cofactor for glutathione peroxidase in the decomposition of hydrogen peroxide or organic peroxides; for glyoxalase 1 in the detoxification of methylglyoxal and other α -oxo-aldehydes; and for maleylacetoacetate isomerase in the conversion of maleylacetoacetate and maleylpyruvate to the corresponding fumaryl derivatives. GSH can also react with a number of endogenous moieties, resulting in the generation of bioactive endogenous GSH adducts. Although some adducts can be formed directly, glutathione- S-transferase (GST)-mediated reactions generally predominate (175).

1.3.2.3.2 Glutathione peroxidises

Glutathione peroxidises were the first selenoproteins to be identified in higher organisms (178). First discovered in 1973, over the past four decades they have been found in all higher organisms. The GPx family have been shown to play a role in the first line of defence for oxidative stress, by reducing H₂O₂ to water and second line of defence, by reducing organic peroxides such as lipid hydroperoxide to water and lipid alcohol, via conjugation of glutathione, forming GSSG (179;180). Moreover, the term “glutathione peroxidise” has been used to describe enzymes that may similarly catalyze the reduction of hydroperoxides by GSH, but are neither structurally nor phylogenetically related to the family, such as GSH-S-transferases (24), selenoprotein P (181) or human peroxiredoxin VI

(182). The *GPx*, now known as *GPx-1*, that gave its name to the entire glutathione peroxidise family catalyzes the reduction of H₂O₂ and soluble organic hydroperoxides at the expense of GSH (183). *GPx-1* is the most abundant *GPx* in mammals. It appears to be predominantly localized in the cytosol and the matrix space of mitochondria (184), and also protects the organism against oxidative damage (185). Its affinity for GSH comes from its structure of a lysine and four arginine residues which surrounds the active site selenium and serve to direct the two GSH molecules into an orientation that allows for the GSH sulphur to react with the selenium.

Out of the 8 *GPxs* which are found in mammals, only half of them are known to contain selenocysteine, where selenocysteine (Sec) is at the catalytic centre and is a key component to the of the catalytic activity(180;186). *GPx-1* and *GPx-2* are homotetrameric proteins, *GPx-3* is a homotetrameric glycoprotein while *GPx-4* is a monomeric enzyme (180). *GPx-1*, also known as cytosolic *GPx*, can metabolize H₂O₂ and a variety of organic peroxides, including cholesterol and long-chain fatty acid peroxides with the aid of phospholipase A₂ activity. *GPx-2* found mainly in the epithelium of gastrointestinal tract (GSHPx-GI), displays a substrate specificity that appears largely identical to that of *GPx-1* (187). *GPx-3*, a typical extracellular glycolated protein with a largely unknown function, and was first purified from plasma (188). *GPx-3* mRNA is found to be expressed predominantly in kidney with the primary biosynthesis site in the proximal tubules (189). *GPx-3* is also expressed in adipose tissue and lung epithelial cells (190;191). Its hydroperoxide specificity resembles that of *GPx-1* (192), and can also reduce complex lipid hydroperoxides at a low rate (193). *GPx-4* can react with phospholipid hydroperoxide (PHGPx).

A *GPx-1*^{-/-} knockout mouse shows increased susceptibility to ROS-induced oxidative stress (194). Studies focusing on the induction of *GPx-1* have shown the *GPx-1* to protect endothelial cells against oxidative stress, and transgenic studies with *GPx-1* expression improved endothelial dysfunction (195). The cellular and tissue location of each of the *GPxs* have been shown to be critical for their biological functions (186). As mentioned earlier, *GPx-3* has activity against phospholipid hydroperoxides (190). While *GPx-4* is responsible for protection of membranes against oxidative damage and also control of cell function. While

GPxs are important, there are also other enzymes that have peroxidase activity, most notably the GSTs.

1.3.2.3.3 Glutathione S-Transferases

The glutathione S-transferases (GST) are a supergene family of soluble dimeric enzymes that catalyse the conjugation of glutathione (GSH) to a variety of electrophiles including arene oxides, unsaturated carbonyls, organic halides and other substrates (196). They play a key role in phase II of enzyme digestion (197), have a primary function of metabolizing a broad range of reactive oxygen species (ROS), and have been implicated in a number of diseases, including childhood asthma (198) and lung cancer (199). They also detoxify noxious electrophilic metabolites of xenobiotics which are produced intracellularly following exposure to air-borne products of combustion, from consumption of either over-cooked or mycotoxin-contaminated food, or from drinking polluted water (200). GSTs play a particular role in the protection against oxidative stress through their ability to catalyse the conjugation of GS with 4-hydroxynonenal (201;202), a major genotoxic and cytotoxic α,β -unsaturated aldehyde formed from n-6 polyunsaturated fatty acids during lipid peroxidation (203). Furthermore, GSTs can also conjugate GSH with adenine and thymine propenals, reactive purine and pyrimidine bases formed during DNA damage from oxidative stress (204). GST expression has been shown to be under the control of glucocorticoid response element (GRE), xenobiotics response element (XRE) or antioxidant response element (ARE) (197;200).

There are two distinct, evolutionary separate multigene families with GST activities. The first superfamily consists of cytosolic proteins and the second consists of membrane-bound proteins (205;206). The cytosolic protein family is highly complex and in mammals at least 7 classes of transferase, designated Alpha, Mu, Pi, Sigma, Theta, Zeta and Kappa, have been characterized. While these enzymes are referred to as cytosolic GST, the Kappa class is located in the mitochondrion and are best referred to collectively as soluble GST (207). The cytosolic proteins are also considered the genuine GSTs, having both STs_N and GSTs_C domains (208). The second family, or the microsomal transferases family - recently called the MAPEG, Membrane Associated Proteins involved in Eicosanoid and Glutathione metabolism (206) has not been as thoroughly studied

as the soluble GST family. However, recent advances in molecular cloning have revealed that it contains significantly more members than was thought even just a couple of years ago (209;210). In addition to the structural differences between the two superfamilies, each family is functionally unique. The soluble transferases act primarily as detoxication enzymes to prevent cytotoxic and genotoxic damage cause by electrophiles generated as breakdown products of macromolecules. The MAPEG family serve to inhibit lipid peroxidation during oxidative stress (211).

The soluble GSTs are dimeric proteins where each subunit is about 26 kDa and formed only from subunits within the same class (212). These GSTs are known as 2-domain structures with the first structure made of structurally conserved nucleophilic glutathione binding sites (g-sites), and the second domain the diverse hydrophobic binding sites (H-sites) that determines the substrate specificities (213), with substrates being electrophilic compounds that react with the thiol moiety of glutathione (197). The G-sites mainly consist of interaction with N-terminal residues while the H-sites involve C-terminal residues and other parts of the protein. Through catalysis, GSTs bind a variety of electrophiles to the sulphhydryl group of glutathione which results in more water-soluble molecules (196). While GSTs are not unique in their function of protecting against phospholipid hydroperoxides and have been shown to have reduced activity towards phospholipid hydroperoxides than *GPx*-4, it should be recognized that their increased abundance in many tissues makes them physiologically important in reducing peroxidized lipids. Other roles that makes GST physiologically important are their ability to remove ROS, regenerate S-thiolated proteins, catalyze conjugations of endogenous ligands and catalysis of reactions in metabolic pathways not associated with detoxification (205). Furthermore, these biochemical data indicate the GSTs are not a first line of defence against free radicals. Generally, enzymes that are considered the first line of defence against oxidative stress are *SOD*, catalase and *GPx*. The GST family represents a second line of defence providers against oxidative stress that due to their broad range of substrate specificity are able to successfully reduce oxidative stress. While many studies on GSTs have focused mainly on the role of GST in cancer, new research has shown *Gstm1* to play a role in genetic models of hypertension (78;214;215)

1.3.2.3.3.1 Mu Family of S-transferases

As previously described, there are two distinct families of GST, the cytosolic proteins and the membrane-bound proteins (200;206). This thesis will focus only on the cytosolic (or soluble) enzymes. In mammals GSTs have eight cytosolic classes that have been identified—Alpha (A) located on chromosome 6, Mu (M) located on chromosome 1, Pi (P) located on chromosome 11, Theta (T) located on chromosome 22, Sigma (S) located on chromosome 4, Zeta (Z) located on chromosome 14, kappa (K) (chromosome location not known), and chi (O) (also called omega) on chromosome 10. Their classification was determined on the basis of a combination of criteria such as substrate inhibitor specificity, primary and tertiary structure similarities and immunological identity (216;216). Within these major classes, there are subclasses with different gene codes. For example, five different genes code for Mu class GSTs (*GSTM1-M5*) (198). The Mu class genes are situated in tandem (5-*GSTM4-GSTM2-GSTM1-GSTM5-GSTM3-3'*) in a 20 kb cluster on chromosome 1p13.3 (217). Each *GSTM* gene consists of 8 exons and 7 introns. The sequences of these genes and their encoded amino acid sequences are highly homologous, suggesting gene duplication in the evolution of the *GSTM* genes. Early investigative work with the *GSTM*s reported polymorphisms in the *GSTM1* gene where single base changes gave rise to the functionally identical *GSTM1*A* and the *GSTM1*B* alleles (204), a duplication of the *GSTM1* gene (218), and the deletion of *GSTM1* gene resulting in the null allele *GSTM1*0* (219;220). The significance of the null *GSTM1* genetic variation in human was first recognized in cancer studies demonstrating that patients carrying the *GSTM1*0* allele were at increased risks for colon and lung cancers (199). Allelism has also been identified in the *GSTM3* with *GSTM3*A* and *GSTM3*B* where *GSTM3*B* differs from *GSTM3*A* by a 3bp deletion on intron 6. Furthermore, this difference creates a recognition motif for the YY1 transcription factor in *GSTM3*B* and thus the possibility of differently regulated expression between alleles. Recent studies have shown many more polymorphisms in the *GSTM* family (221) however, the human polymorphism of *GSTM* and their pathological connections are not the main focus of this thesis.

In the rat, a 155kb *GSTM* cluster locus is located on chromosome 2q34 in the order of M7-M1-M2-M4-M6b-M3-M6a, followed by M5 in an inverted orientation (Figure 1-4). In regards to the GST family in rodents, there is

extensive research on the biochemistry of GSTs as well as their roles as phase II detoxification enzymes during the early literature of rodent GSTs. However, new and recent studies have shown the GSTs, specifically *GSTM1*, to be correlated with the development of hypertension. Our group has indentified *GSTM1* to be a positional and functional candidate gene for hypertension (96). There is also data on differential expression of this gene in other hypertensive rat strains as compared to normotensive reference strains (214;215). Further studies have shown that the difference in mRNA expression was reflected at the protein level in the kidney and was inversely correlated with renal ROS levels, suggesting that the pathophysiological roles of *GSTM1* in hypertension involve the defence against oxidative stress (96).

1.3.3 Identification of *Gstm1* as a candidate gene for oxidative stress and its role in the development of hypertension in the SHRSP

A genome-wide scan previously performed in the Glasgow laboratory by cross-breeding the SHRSP and WKY inbred strains identified a QTL on rat chromosome 2 encoding genes involved in blood pressure regulation (78). This QTL was confirmed and further refined by congenic breeding where genomic regions from the WKY were introgressed onto the background of the SHRSP. This strategy generated rats with significantly reduced blood pressure compared to the SHRSP (SP.WKYGla2c* congenic strain) (Figure 1-6) (78). Microarray expression profiling in the kidney at 16 weeks of age in the SHRSP, WKY and the SP.WKYGla2c*strain identified *Gstm1* as a functional candidate gene. Additional studies were carried out in order to examine *Gstm1* expression differences between SHRSP and WKY rats prior to the onset of hypertension. Microarray analysis assessed renal gene expression at 5 wks of age in the WKY, SHRSP, and the SP.WKYGla2c* rats. Results showed a significant reduction in the expression of *Gstm1* in the SHRSP at this early time point (96).

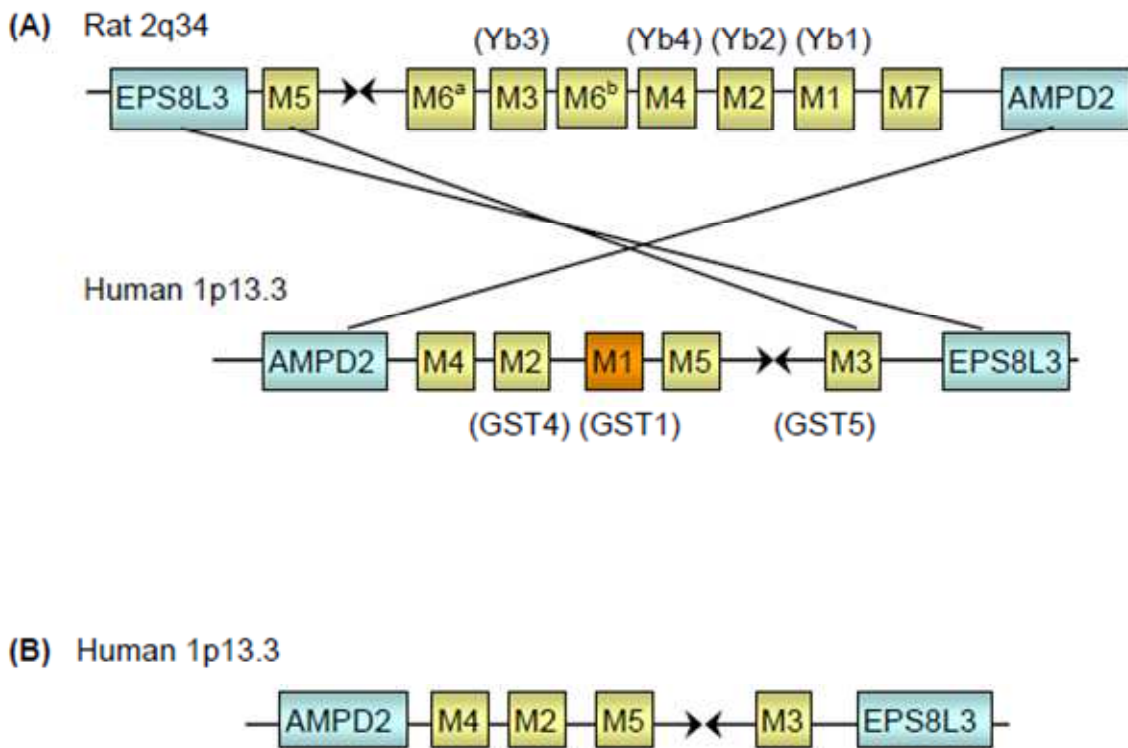


Figure 1-4: Organisation of the glutathione s-transferase mu genes in human and rat

(A) Synteny between rat *Gstm* gene cluster on chromosome 2 and human *GSTM* gene cluster on chromosome 1. The names in brackets are the alternate names for the respective genes in earlier literature. AMPD2, adenosine monophosphate deaminase 2; EPS8L3, epidermal growth factor receptor pathway substrate 8-like protein 3; GSTs, glutathione S-transferase; (B) Organisation *GSTM* genes in individuals missing *GSTM1* gene. Figure taken from (222)

In addition, it was shown that antihypertensive treatment was unable to impact on expression levels of *Gstm1* in SHRSP rats (i.e. was unable to improve expression levels) indicating that this deficiency in *Gstm1* expression appears to be a primary cause, rather than secondary to increase in blood pressure levels (87).

Further investigation of this differential *Gstm1* expression showed that the SHR and SHRSP genome contains 13 single-nucleotide polymorphisms (SNPs) within the promoter, a missense mutation and a 3' untranslated region (UTR) polymorphism that was not found in the WKY or BN strains. Luciferase reporter constructs compared the transcriptional activities of *Gstm1* between the SHRSP and WKY in addition to subcloning experiments were able to identify and isolate two SNP clusters that were responsible for the reduced expression in the SHRSP. Additional luciferase experiments suggested that an interaction between one or more SNP in each cluster contributed to reduced transcription. Other novel constructs were generated by site-directed mutagenesis in order to more fully investigate this interaction, however no consistent effects on expression were observed. The Transfac database was used to identify several potential transcription factor binding sites affected by the SHRSP mutations, the strongest candidate being peroxisome proliferator-activated receptor gamma (PPAR γ), with binding sites affected in both implicated clusters.

In order to investigate the physiological effects of reduced renal *Gstm1* expression in the SHRSP, renal GSH levels were measured at 5 and 16 weeks. Results showed lower expression levels in the SHRSP at both time points when compared to the WKY. Interestingly, GSH expression in the SP.WKY2GlaC* congenic strain was similar to that of the SHRSP at 5 weeks of age and similar to the WKY at 16 weeks of age. This data, when combined with the significant reduction of SBP in the SP.WKYGla2c* congenic strain leads to the hypothesis that renal oxidative stress caused by impaired GSH metabolism (reduced *Gstm1* expression) may contribute to the hypertensive profile of the SHRSP.

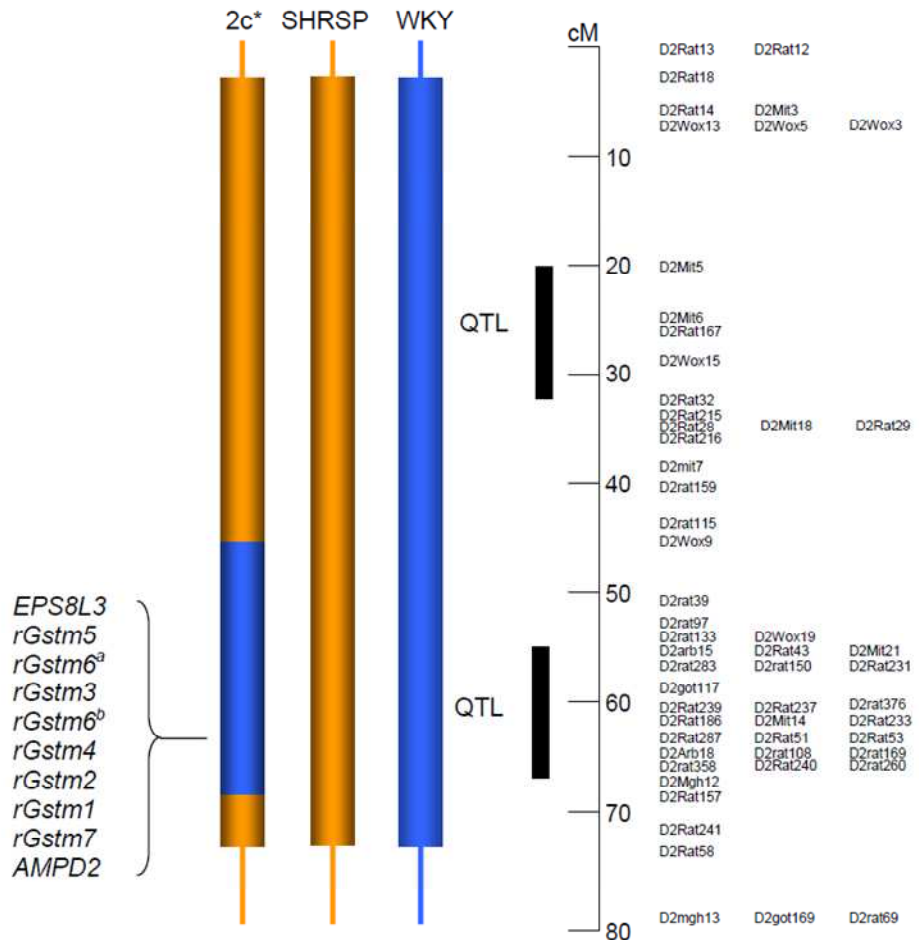


Figure 1-5: Chromosome 2 congenic strain SP.WKYGla2c*

A: The congenic strain contains a 22-cM segment, encompassing a quantitative trait locus (QTL), transferred from WKY (donor strain; blue) to the genetic background of SHRSP (recipient strain; orange) between the markers D2Wox9 and D2Mgh12. The congenic strain described is the SP.WKYGla2 (D2Wox9 - D2Mgh12) and is abbreviated to SP.WKYGla2c* and 2c* in figures. The *Gstm* family gene locus is encompassed within the congenic region, under the quantitative trait locus (QTL). Adapted from (78).

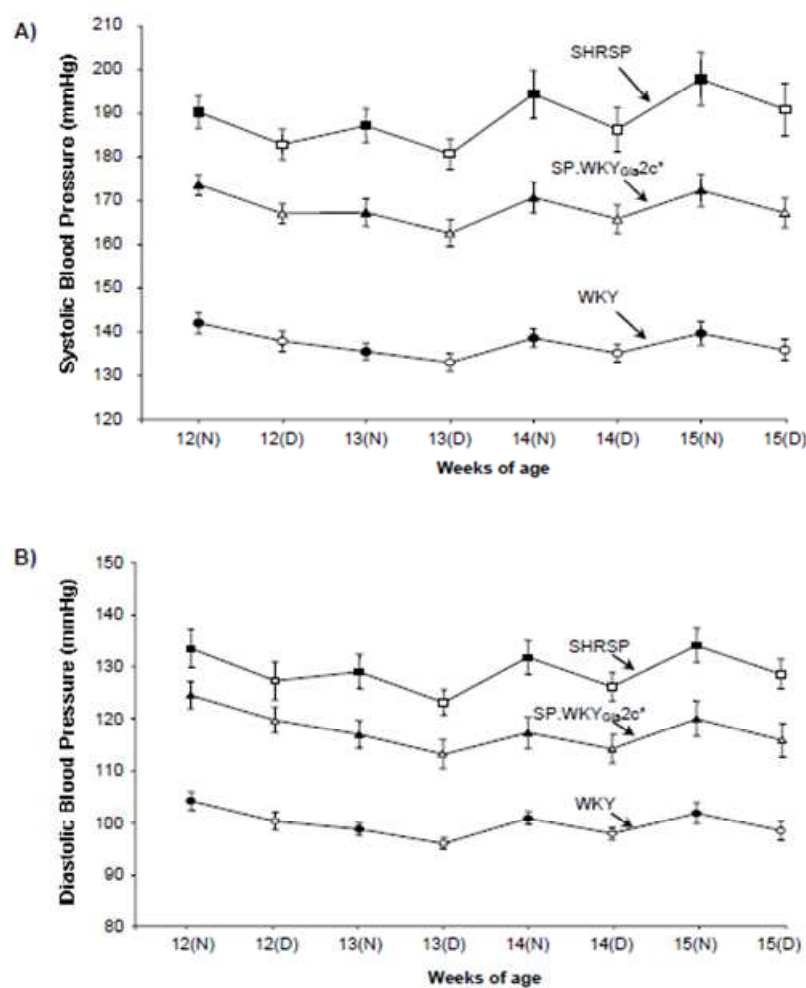


Figure 1-6: Day-time and night-time average systolic and diastolic blood pressure
 Systolic (A) and Diastolic (B) blood pressure, measured by radio-telemetry over a three-week period for SHRSP, WKY and congenic strain SP.WKY_{Gla2c*}. n = 8-11 per group. Adapted from (78).

Following on from these *in vivo* and *ex vivo* investigations, more specific *in vitro* and *in vivo* studies were conducted to examine the role of *Gstm1* in the kidney. In order to elucidate the role of *Gstm1* in rat kidney tubule epithelial cells (NRK-52E), RNA interference (RNAi) was used to knockdown *Gstm1* expression. Three different short interfering RNA (siRNA) sequences, targeted to *Gstm1*, were used and each significantly reduced expression of *Gstm1* in both protein and mRNA levels. Off target effects were prevented through reduction of siRNA concentration. To assess the effect of *Gstm1* knockdown in an *in vivo* setting, local delivery to the kidney via the renal artery was attempted. However, the delivery was shown to cause significantly renal damage. As an alternative route, plasmid vectors were generated that expressed *Gstm1* specific short-hairpin RNA (shRNA) molecules based on the sequences that successfully knocked down *Gstm1* expression *in vitro*. Unfortunately, transfection into the NRK-52E cells was poor and knock-down was not confirmed.

The role of *Gstm1* in the protection against cellular oxidative stress was evaluated in NRK-52E cells through *Gstm1* knockdown and subsequent measurements of oxidative stress markers. Total GST activity was not reduced in cells transfected with *Gstm1* specific siRNA, however, activity was increased following over expression of *Gstm1*. Additionally, knock down of *Gstm1* did not show any change in glutathione levels. Oxidative stress was determined by measuring 8-isoprostan e (a marker of lipid peroxidation), 8-hydroxy-2-deoxyguanosine (8-OH-dG) (a marker of oxidative DNA damage) and by the comet assay (DNA damage). No significant difference in the levels of 8-isoprostan e or 8-OH-dG was observed in cells treated with *Gstm1* specific siRNA compared to control siRNA, however significant DNA damage was demonstrated by comet assay.

While the functional studies discussed above evaluated the effects of modulating *Gstm1* expression *in-vitro*, the specific role for *Gstm1* in protection against oxidative stress and hypertension remained to be fully determined and thus provided the strong impetus to generate a transgenic model. In order to functionally validate *Gstm1* and provide definitive evidence of the direct role played by the *Gstm1* gene in hypertension, the transgenic strategy needed to be utilised. This is considered to be a gold standard method for functional validation of candidate genes. Therefore production of transgenic SHRSP rats in which the

Gstm1 had been ‘rescued’ was attempted. This involved the random insertion of wild-type *Gstm1* into the SHRSP genome. More advanced methods of genetic modification such as ZFN or TALEN technology were not available in the rat at this time, since the SHRSP rat transgenic production procedure was started prior to 2009. After several unsuccessful attempts in-house, SHRSP rats were transferred to the laboratory of our collaborator Dr Michal Pravenec (University of Prague) who successfully generated two novel transgenic lines incorporating the wild-type *Gsmt1* gene from the WKY into the SHRSP genome. The phenotypic and molecular analysis of these novel transgenic lines formed the basis of my PhD project.

1.4 Hypothesis

Oxidative stress is an important pathogenic factor in the development of cardiovascular disease. Glutathione S-transferases protect against oxidative stress-induced injury through the detoxification of reactive oxygen species. It is hypothesised that *Gstm1* deficiency in the SHRSP plays a causative role in the development of oxidative stress and hypertension.

1.4.1.1 Aims

A combination of congenic breeding and microarray analysis has identified *Gstm1* as a positional and functional candidate gene for hypertension in the strokeprone spontaneously hypertensive rat (SHRSP).

The aims of this study were to establish definitive proof that reduced *Gstm1* expression in the SHRSP plays a causative role in the development of hypertension and oxidative stress.

Specific aims:

1. To functionally validate *Gstm1* in an *in vivo* environment through assessment of hemodynamic and cardiac function
2. To assess genetic and molecular changes from the incorporation of *Gstm1* into the SHRSP genome
3. To assess renal function and oxidative stress parameters in the *Gstm1* transgenic lines.
4. To investigate translational aspects of the *GSTM* family from rodent and apply them to a human cohort

2 Materials and Methods

2.1 *In vivo* experimental procedures

2.1.1 Experimental Animals

2.1.1.1 Animal Strains

The animal strains used in this thesis were SHRSP_{Gla}, WKY_{Gla} and *Gstm1* transgenic SHRSP_{Gla}. Animal housing conditions consisted of controlled environmental conditions, where temperature was maintained at 21 °C with 12 hour light/dark cycles starting 7am to 7pm. Rats were fed a standard rat chow (rat and mouse No. 1 maintenance diet, Special Diet Services) and water provided *ad libidum*. Weaning of offspring took place at 3 weeks of age when they were sexed, ear-tagged (National Band and Tag. Co.) and caged, with a maximum of 3 animals per cage, according to sibling group and sex.

All work with experimental animals was in accordance to the Animals Scientific Procedures Act 1986 under the project license of Dr. Delyth Graham (60/4286) and Prof Anna F Dominiczak (60/3618). Inbred colonies of SHRSP and WKY have been maintained at the University of Glasgow since 1991 by brother-sister breeding. The colony started in 1991 when Dr. D.F. Bohr, from the Department of Physiology at the University of Michigan (USA), gifted 6 males and 7 females of each strain to the University of Glasgow. These colonies originated from the National Institute of Health, Bethesda, Maryland, USA, and were subsequently maintained at the University of Michigan as inbred colonies for 15 years. Integrity of the colonies was maintained, as well as the distinction between normotensive and hypertensive phenotypes, by selection of SHRSP adult breeders with blood pressures 170-190mmHg (males) and 140-170mmHg (females), and WKY adult breeders of 120-140mmHg (males) and 100-130mmHg (females). In order to confirm homozygosity of all loci, animals were selected at random and screened by microsatellite markers.

2.1.1.2 Transgenic Animals

Two independent transgenic lines of *Gstm1* SHRSP rats were created through incorporation, by microinjection, of a normal *Gstm1* gene into the SHRSP genome. The transgenic strains used in this study were derived by the same expression platform and microinjection fragment purification protocol as was employed in CD-36 rat transgenesis previously described by Pravenec *et al.* 2001

(7). In brief, the *Gstm1* cDNA sequence was cloned into pEF1/Myc-HisA (Invitrogen), an expression construct including the constitutive human elongation factor 1 α subunit (EF1 α) promoter and bovine growth hormone (BGH) polyadenylation signal separated by a multiple cloning site (223). The cloned cDNA ligation insertion was verified by direct sequencing with pEF1 T7F and BGH PolyAR primers. The resulting expression plasmid, named pEF1 WKY *Gstm1* was amplified and purified using the Qiagen Maxi kit (Qiagen, Hilden, Germany). The construct was linearized by digesting the pEF1 WKY *Gstm1* plasmid with the enzymes *Pvu*II and *Aat*II in order to have a final isolated fragment for transgene injection of 2.725kb fragment that encompassed the EF-1a promoter, *Gstm1* cDNA and BGH polyadenylation sequences. *Gstm1* protein expression from pEF1 WKY *Gstm1* was confirmed by transfection into HeLa cells and Western blotting as previously described (223). Generation of the transgenic rats was carried out in Prague (in collaboration with Dr Michal Pravenec) using male and female SHRSP from the University of Glasgow. The transgenic production process involved superovulation of female SHRSP which were then timed mated with SHRSP stud males to generate embryos. On day one embryos were harvested and microinjected with the DNA linear construct into the pronuclei. The embryos were then transferred into the oviducts of pseudopregnant female recipient rats, followed by natural pregnancy and pup rearing. This process was repeated a several times in order to generate an additional independent transgenic line in order to confirm assessment of phenotypic and genotypic changes.

To assess transgene expression, genomic DNA was isolated from 4-mm tail tips, and screened for transgene sequences by polymerase chain reaction (PCR) with primers amplifying across the EF1α promoter sequences (primers pEF1F + pEF1R), and with two primer pairs that spanned EF1α promoter and *Gstm1* cDNA sequence (pEF2F + pEF2R and pEF3F + pEF3R). Transgene positive pups from each of the independent transgenic lines were weaned and transported to the University of Glasgow for full phenotypic and molecular analysis. Additional PCR primers were created to confirm transgene insertion (pEF5F + pEF5R). Additionally, throughout the course of the study, genomic DNA was again isolated from the ear notch or tail tips of the transgenic animals to confirm the genetic background and to assure that the transgene was not lost in subsequent generations. Screening of polymorphic microsatellite markers located on

chromosome 2, 3, and 14, verified the SHRSP lineage of each of the transgenic animals. These markers are used for routine screening of SHRSP, WKY and congenic strains at the BHF GCRC (See appendix).

Due to mandatory quarantine period and health status issues (mycoplasma infection), transgenic founders were held within a Category III suite at the University of Glasgow and mated with SHRSP females from the Glasgow colony. All offspring were screened and transgenic positive males and females were mated to ‘fix’ the two independent transgenic lines (Trans1 and Trans2). Transgenic lines underwent caesarean re-derivation to ‘clean’ the health status (i.e. remove all mycoplasma infection) by fostering caesarean derived transgenic pups onto clean Sprague Dawley foster mothers who had just littered down. These ‘clean’ transgenic pups subsequently were interbred within each line for the establishment of the transgenic lines.

Trans2 animals, while showing a strong positive screening for the transgene, showed reduced fertility. This infertility led to difficulties with acquiring enough Trans2 animals to sustain the line, and generating enough stock animals to incorporate into the study. Because of this, it was not possible to include Trans2 animals into every experiment carried out within the project.

2.1.2 Hemodynamic Profile

2.1.2.1 *Blood Pressure measurements by Tail Cuff Plethysmography*

Measurement of systolic blood pressure was carried out using the well established method of tail cuff plethysmography as described previously (224). Rats were preheated at 30°C for 20 minutes in an insulated box to insure vasodilatation of the tail artery. Rats were then manually restrained by being wrapped in a soft cloth and an inflatable cuff placed on their tail along with a piezoceramic transducer (Hartmann & Braun type 2) for pulse detection. The pressure in the cuff is controlled in 1mmHg steps over a 300 mmHg range by pressure control unit (designed and built “in house” by DCBP Electronics, (Southern General Hospital, Glasgow). Multiple cuff inflation and deflation steps were carried out through the duration of each tail cuff session and the resulting pulsatile signal detected by the transducer was visualized as a function of

pressure and displayed on computer using Microsoft Windows compatible software. At least 8 of 10 readings were recorded, with the highest and lowest readings being discarded, and the remaining readings averaged for a single session value.

2.1.2.2 Blood Pressure measurements Telemetry

At 12 weeks of age, radiotelemetry probes were surgically implanted under sterile conditions into the abdominal aorta as previously described in (225;226) 7 days after implantation before baseline blood pressure measurements were recorded. Systolic blood pressure (SBP), Diastolic blood pressure (DPB), Mean arterial blood pressure (MAP), pulse pressure (PP), heart rate (HR) and motor activity were measured using The Dataquest IV telemetry system (Data Sciences International) as previously described in (227). Briefly, Heart rate, blood pressures, pulse pressure, and activity were recorded for 10 seconds every 5 min throughout the day and night. The results from each rat were averaged to weekly day and night averages using an excel spreadsheet macro. The telemetry recording equipment includes a transmitter (radio frequency transducer model TA11PA), receiver panel, consolidation matrix 4650, and a dedicated computer with accompanying software. All radio transmitter devices (probes) were calibrated and confirmed to be accurate within ± 3 mm Hg before being implanted.

Implantation of radio-telemetry probes was carried out while rats were anesthetized with 2.5% Isofluorane in 1.5 L/min O₂ for the duration of the surgical implantation process. After anesthetization, but before the start of the surgery, Carprofen (5 mg/kg) a non-steroidal anti-inflammatory analgesic was administered for pain control. The radio-telemetry probe was then inserted into the descending abdominal aorta pointing towards the proximal end of the animal (i.e. towards the heart), against the flow of blood, and was sutured to the abdominal wall in order to reduce movement of the probe while implanted. Following surgery, rats where housed in individual cages that were placed upon the receiver panel and monitored daily. The rats were free to roam about the cages and to feed and drink *ad libitum*.

2.1.3 Echocardiography

Transthoracic echocardiography was used to assess cardiac geometry and contractility, as previously described (228;229). Echocardiography was performed prior to sacrifice at 21 weeks of age. Animals were sedated and short axis 2-dimensional B-mode and M-mode images were taken through the left parasternal window at the papillary muscle levels using ACUSON Sequoia C512 Echocardiograph, which is capable of both 2-D and 3-D multiple frequency imaging. Averaged data from six consecutive cardiac cycles from each M-mode tracing were used in the following equation for the calculation of left ventricular mass (ASE-cube formula with Devereux correction factor) (LV mass = $0.8 [1.04[(EDD + PWT + AWT)^3 - EDD^3]] + 0.6$). Where PWT = Posterior wall thickness (mm), AWT = Anterior wall thickness (mm), EDD = End diastolic dimension (mm). LV end-systolic volume (ESV) and LV end-diastolic volume (EDV) can be calculated from two-dimensional images according to a modified Simpson's rule. LV ejection fraction (LVEF) is then determined from EDV and ESV. Cardiac index is estimated as cardiac output adjusted for tibia length

2.1.4 Metabolic Cages

Metabolic cages were used for housing individual rats for the collection of urine and the monitoring of water in-take for baseline and salt-loading studies. Telemetered rats were housed in metabolic cages at 16 (baseline) and 21 weeks for a 24 hour time period. For acclimation purposes, 15 week old rats were housed in metabolic cages for a 4 hour period prior to baseline measurements. Metabolic cages differ from standard cages by an upper chamber with a support grid that allows to rat to stand while allowing urine and feces to pass through the grid and into a funnel which separates and collects the feces and urine. A small feeder and marked water bottle on the outside of the cage allows access to standard rat chow and regular or salt-loaded water. Urine that was collected was kept on ice and stored at -80° C, until required for biochemical analysis.

2.2 *Ex vivo* Experimental Procedure

2.2.1 Tissue Preparation

At sacrifice animals were terminally anesthetized by isoflurane. The thoracic cavity was opened to expose the heart and blood samples were collected by cardiac puncture with a 23 gauge needle. Tissues, such as: kidneys, spleen, liver, aorta, heart, carotid arteries, fat, brain, adrenals and skeletal muscle, were harvested and snap-frozen in liquid nitrogen and stored at -70°C for RNA, DNA or protein extraction.

For histological assessment, tissues were blotted on tissue paper to remove excess blood and any additional surrounding connective tissues were separated from the vascular tissue immediately after harvest. Tissues were then fixed in a 10% formalin solution overnight at room temperature and subsequently transferred into PBS. The fixed samples were later embedded in paraffin blocks by trained technical staff in the laboratory. Paraffin section of 3-6 µm thickness were cut and baked onto silanized slides at 60°C for 3 hours followed by 40°C overnight. Both the paraffin blocks and sections were kept at room temperature and stored in appropriate boxes. Transverse cross sections of kidney and aorta were used.

Thoracic aortas and mesenteric resistance arteries were harvested and taken to determine endothelial function by wire and vessel morphology by pressure myography (see section 5.2.4-5.2.5). Blood samples collected in heparin and/or EDTA lined tubes during sacrifice were kept on ice until centrifugation at 2400 RPM for 20 mins at 4°C. Plasma was then extracted and stored at 80°C for renal function experiments.

2.2.2 Organ Mass index

Organ mass indices for whole heart, left ventricle plus septum, and kidneys were measured at time of tissue collection. At sacrifice organs were removed, blotted to remove excess blood and weighed. Organ weights were corrected for body weight or tibia length. After sacrifice a scalpel was used to expose the knee and ankle joint on an extended hind limb, the tibia length was determined using a

double-pointed drawing compass and was subsequently measured with a ruler. Both body weight and tibia length were used to assess organ mass indices, and both methods of measurements showed similar trends and significance for results.

2.2.3 Histology

2.2.3.1 *Histological Assessment of Gross Pathological Changes*

Histological analysis was used to assess cardiac and renal pathological changes by examining haematoxylin and eosin (H&E) stained sections. Fibrosis was examined by staining with picrosirius red where microscopic analysis and a colour threshold application were used to measure the average intensity of picrosirius red stain of fibrotic tissue.

2.2.3.2 *Immunohistochemistry*

Sections cut to 6 µm thickness were de-parafinised and hydrated by 2x7 minute washes in Histoclear before going down an ethanol gradient of 100%, 95% and 75% for 7 minutes at each stage. Sections were then washed in water for 7 minutes. Endogenous peroxide was then quenched by incubating slides for 30 minutes in 0.3% H₂O₂ (10ml 30% to 1L) in methanol at room temperature. Sections were then rinsed in 2 x 10 minute water washes. Sections were blocked for 60 minutes with 2% normal serum in PBS (2 drops of ABC kit blocking serum in 5ml PBS or 100µl appropriate serum in 5ml PBS). Slides were placed in humidified trays in order to prevent slides from drying out. Excess blocking reagent was removed and replaced with 1° Ab/antiserum or negative control diluted in blocking serum for overnight at room temperature. The following day, sections underwent 3x5 minutes washes in PBS. A biotinylated 2° Ab antibody, diluted in blocking reagent (ABC universal kit, 2 drops blocking serum + 2 drops supplied vectastain biotinylated antibody + 5ml PBS) was added for a 30 minute room temperature incubation. This was followed by 3x5 minute PBS washes. If the ABC 2° Ab antibody was used, and ABC complex was added to the sections and incubated for 30 minutes at room temperature. This was followed by 3x5 minute PBS washes. DAB chromogen (DAB substrate kit) for universal and peroxiase 2° Ab antibody was prepared following manufacturer's instructions. Sections were

incubated for 5 minutes at room temperature in a humidified chamber and then washed for 5 minutes in water. Sections were counterstained with Haematoxylin for 90-120 seconds and placed under a running tap for 5 minutes. Sections were then dehydrated through a reverse ethanol gradient of 70%, 95% and 100% for 7 minutes at each stage. Immediately following, sections then washed 2x's in HistoClear for 7 minutes and mounted using Histomount (National Diagnostics, GA, USA).

2.2.3.3 Heamatoxylin and Eosin Staining – cardiac and renal remodelling

Kidney sections from WKY, SHRSP, Trans1 and Trans2 were stained with Harris haematoxylin for 2 minutes, washed under a running tap for 5 minutes and transferred to eosin for 1 minute before final 5 minute water wash. Sections were then dehydrated through a reverse ethanol gradient of 70%, 95% and 100% for 7 minutes at each stage. Immediately following, sections then washed 2x's in HistoClear for 7 minutes and mounted using Histomount (National Diagnostics, GA, USA). Examination and analysis was performed under a microscope where nuclei appeared purple and cytoplasm pink.

2.2.3.4 Fibrosis staining and measurement

Fibrosis was assessed in renal sections from WKY, SHRSP, Trans1 and Trans2 rats using picrosirius red (Sigma-Aldrich, UK) which stains collagen type I and type III fibres bright red. After the removal of paraffin, sections were incubated under dark conditions in 0.1% picrosirius red solution for 90 minutes at room temperature, followed by 2 x 5 minutes washes in 0.01 N HCl and 1 x 5 minute wash under a running tap. Sections were then dehydrated through a reverse ethanol gradient of 70%, 95% and 100% for 7 minutes at each stage. Immediately following, sections then washed 2x's in HistoClear for 7 minutes and mounted using Histomount (National Diagnostics, GA, USA) and cured overnight on the bench top. Collagen was stained various shades of red, with the cytoplasm yellow.

2.2.4 GFR

Indirect glomerular filtration rates (GFR) were determined by measurement of urine and plasma creatinine concentrations. The equation (urinary creatinine concentration X urine flow rate) / plasma creatinine concentration was used to calculate GFR. All measurements were determined by a clinically validated automated analyzer (c311, Roche Diagnostics, Burgess Hill UK), using the manufacturers calibrators and quality control material for Isotope dilution-mass spectrometry (IDMS). All calculations were normalized to kidney weight.

2.2.5 Oxidative Stress Measurements

2.2.5.1 Lipid Peroxidation (Malondialdehyde) Assay

Samples were homogenized by polytron in 1ml of freshly prepared homogenisation buffer (10µl 0.5M BHT/acetonitrile per ml PBS) for every 100mg of tissue. Samples were immediately placed on ice until they were transferred into a 2ml Eppendorf tube and centrifuged at 3000g at 4°C for 10 minutes. If the samples were still turbid, supernatant was placed in a new eppendorf tube and centrifuged again. Standards and samples were transferred into a deep 96 well plate where 325µL of MDA cocktail was added to standards & samples. Plate was then sealed and placed in an oven for 1 hour at 45°C. Samples were then centrifuged at 2450g in 15 minutes at 4°C. 200µl of supernatant was transferred to a flat-bottom 96-well plate and absorbance was read at 586nm using a SpectraMax.

2.2.5.2 Glutathione Assay

Glutathione levels were measured according to Cayman Glutathione Assay Kit (#703002) manufacturer's instructions. Briefly, liver, heart, brain, kidney, and aorta tissue was homogenized in 1x MES buffer provided in kit in a bijou contain using a polytron (1ml for every 0.2g tissue). Homogenates were transferred to 2ml Eppendorf tubes and centrifuge at 10,000g for 15min at 4°C. Supernatant was transferred to a new 2ml Eppendorf and kept on ice. A 25 µL aliquot was reserved for protein measurement by BCA assay (see section 2.6.2). Fresh MPA reagent (5g MPA in 50ml H₂O) was prepared and used within 4hrs at 25°C. Equal

volumes of MPA were added to each sample. Samples were immediately vortexed, allowed to rest for 5 minutes at room temperature and then centrifuged at >2000g for 3 minutes. Supernatants were then transferred to a 2ml Eppendorf. 300 mls of each sample was transferred to a new 1.5 Eppendorf and 15 µL of 4M TEAM reagent (531µl triethanolamine + 469µl H₂O) was added to each sample and vortexed. Standards for measurements were set up according to manufacturer's instructions.

For measuring GSSG, a 100µL aliquot of standards and samples was removed to new tubes. 1µl of 1M 2-vinylpyridine solution (108µl 2-vinylpyridine + 892µl EtOH) was added to each of the 100µl aliquots. Samples were then vortexed and incubated at room temperature for 60 minutes.

Once GSSG samples were ready, 50µl of all samples (Total GSH and GSSG) were added to a clear 96-welled plate. Fresh Assay Cocktail was prepared (MES buffer, Cofactor Mixture, reconstituted Enzyme mixture, water, and reconstituted DTNB) according to protocol. The cocktail was added to the entire plate within 2 minutes using a multi-channel pipette. The plate was then covered and incubated in the dark on an orbital shaker for 25 minutes. Absorbance was read at 405nm on a SpectraMax.

2.2.5.3 Hydrogen Peroxide Assay

Hydrogen Peroxide levels were measured using Invitrogen's Amplex® Red Hydrogen Peroxide/Peroxidase Assay Kit Amplex Red (Invitrogen) according to manufactures instructions for tissues. The Amplex Red Assay uses 10-acetyl-3,7-dihydroxyphenoxazine (Amplex® Red Reagent) to detect hydrogen peroxide (H₂O₂) or peroxidase activity. In the presence of peroxidase, the Amplex® Red reagent reacts with H₂O₂ in a 1:1 stoichiometry to produce the red-fluorescent oxidation product, resorufin, where absorbance can be measured at 560 nm using a microplate reader.

2.2.5.4 Lucigenin Chemiluminescence

Protein was extracted from frozen tissue in a ROS protease inhibitor cocktail buffer (aprotinin, leupeptin, and pepstatin) using a pellet pestle in 1.5mL

Eppendorf on ice. Protein concentration was measured by BCA (see section 2.6.2) assay for analysis purposes. Basal levels of reactive oxygen species were measured using a luminometer by adding 175 µl of ROS buffer, 1.25µl of lucigenin and 50µl of sample. Immediately following basal activity, 25µl NADPH (1mM) was added to each sample and fluorescence was measured again. The average of 30 readings for each samples from both the basal and NAPDH recordings were used to calculate the change in lucigenin activity using the formula (NAPDH-BASAL) RLU/µg protein. RLU stands for relative lights unit in the Berthold Detection Systems MPL2 Luminometers. The intensity of the emitting light is proportional to the amount of enzyme present and is directly related to the amount of HGH antigen in the sample. By reference to a series of HGH standards assayed in the same way, the concentration of HGH in the unknown sample is quantified

2.2.5.5 Griess Assay

Total nitrate and nitrite concentrations were measured using the Cayman Biochemical Nitrate/Nitrite Colorimetric Assay Kit. All steps were followed using the manufacturer's instructions and recommendations. In short, the assay kit uses a simple two-step method for measuring the nitrite to nitrate ratio. The first step consists of converting nitrate to nitrite utilizing a nitrate reductase (Sulfanilamide/ Greiss Reagent 1). The second step is the addition of ethylenediamine/ Greiss Reagent 2 which turns nitrite into a deep purple azo compound. This azo chromophore conversion allows for a photometric measurement of the absorbance at 540 nm for an accurate quantification of NO₂-concentration. In order to measure nitrite alone (to attain the nitrite and nitrate ratio), the assay was performed a second time on the tissue samples without the addition of Griess reagents. Standards and samples for each assay were transferred into a flat bottom 96 well plate and absorbance was read at 540 nm. Determination of Nitrite and Nitrate samples was according to manufacturer's instructions.

2.2.6 Wire Myography

For examination of functional response and vascular reactivity, small (3rd order) mesenteric arteries (MRA) and thoracic aortas were harvested at 21 weeks of age. The vessels were dissected from connected tissue and stored in Krebs buffer overnight at 4 °C before use. For mesenteric arteries, a 2 mm (approximately) length of artery was mounted onto two stainless steel wires on a four channel small vessel myograph (Danish Myotechnology, Denmark). Changes in force were measured by connecting the force transducer to a myo-interface and were then recorded using a data acquisition package (ADI Instruments Powelab systems). The vessels were maintained in Krebs buffer (0.25 M NaCl; 0.001 M KCl; 2 mM MgSO₄; 50 mM NaHCO₃; 2 mM KH₂PO₄; 2 nM CaCl₂) warmed to 37 °C and bubbled with 95% O₂ and 5% CO₂ (pH 7.4). Following a 30 minute equilibrium period, vessels were set to a normalized internal diameter in order to achieve optimal contraction. Internal diameter was calculated using the following equation, $L_1 = 0.0^*L_{100}$. L₁₀₀ was determined using the LaPlace equation where effective pressure (P) equals wall tension (T) divided by the internal radius (P = T/r). After 1 hour, contractile response of the vessel was tested by a pre-treatment of KCl (10 μM) to determine the maximum active tension development that allowed for standardization of initial experimental conditions. Vessels were then washed 4 or more times with Krebs buffer and were allowed to rest for at least 30 minutes. A cumulative concentration curve of noradrenalin, 10 nM to 30 μM, was performed. Immediately following the noradrenalin addition, a carbachol dose response curve, 10 nM to 10 μM, was performed in order to ascertain the % relaxation in response to the stimulated contraction. The dose response curves were followed by a Krebs buffer wash out to baseline. The noradrenalin curve was then repeated in the presence of L-NAME (100 μM). The resulting increase of tension caused by L-NAME provided a measure for the effect of nitric oxide on basal tone. The percentage of maximum contraction was calculated in response to the noradrenalin without L-NAME.

For aortic measurements, a ring of 4 mm (approximately) length was mounted on a large wire myograph (Danish Myotechnology, Denmark). Aortic rings were stretched to 1.5 newtons over a period of 40 minutes in order to equilibrate. Changes in force were measured by connecting the force transducer to a myo-interface and were then recorded using a data acquisition package

(DanishMyoTech p100 pressure system, Denmark). All procedures steps are as explained in the previous paragraph with the exception that noradrenaline was replaced with phenylephrine.

2.2.7 Pressure Myography

In order to assess the pressure-diameter relationship differences between SHRSP, WKY and transgenic lines, pressure-diameter relationships were constructed to examine the structural and mechanical differences in mesenteric resistance arteries (DanishMyoTech p100 pressure system, Denmark)

Third order mesenteric arteries without side branches were dissected out of the surrounding connective tissues, cleaned, and placed in a calcium free Krebs (0.25 M NACl; 0.001 M KCL; 2 mM MgSO₄; 50 mM NaHCO₃; 2 mM KH₂PO₄; 1 mM EDTA) solution overnight at 4 °C. The following morning the MRA was attached to the glass canulae within the myograph with nylon threads. During the attachment process, MRA were maintained in 10 ml cold Ca²⁺ free Krebs solution while one end was attached and the vessel lumen was gently flushed to remove any remaining blood before the second end was attached to the canulae. Krebs solution temperature within the canulae was raised to 37 °C and was bubbled gently with 95% O₂ and 5% CO₂. To equilibrate the MRA, a prolonged intraluminal pressure at 70 mmHg for 60 minutes was maintained. Immediately following, the intraluminal pressure was reduced to 10 mmHg and incremental pressure increases of 20 mmHg until 120 mmHg over a period of 60 mins. Measurements of internal (D_i) and external (D_e) were measured and used to calculate structural parameters cross sectional areas (CSA) and wall to lumen ration using the following equations: CSA = (π/4) × (D_e²-D_i²). Wall/lumen = (D_e²-D_i²)/2D_i. The following mechanical parameters were calculated according to the method of (Baumbach and Heistad, 1989). Circumferential wall strain, where D₀ is the diameter at the lowest intraluminal pressure of 10 mmHg and D_i is the observed internal diameter for a given pressure, equals (D_i-D₀)/D₀. Circumferential wall stress = (PxD_i)/D_e-D_i where P is the intraluminal pressure.

2.3 General Molecular Biology

Any experiments involving RNA used autoclaved DEPC-treated dH₂O or RNase-free water (Qiagen). All plastic-ware used for RNA work was pre-treated and RNase-free (Life Technologies). Filtered RNase-free tips were used in all RNA work. Water used in any molecular was distilled water that was been autoclaved and referred to as sterile dH₂O.

2.4 RNA Extraction

2.4.1.1 Total RNA Extraction

Total RNA samples were extracted using Qiagen RNeasy kits (Qiagen, Hilden, Germany) according to manufactures recommended instructions for fibrous tissues (Appendix C of RNeasy Handbooks). The resulting elute was then quantified by measuring 1.5 µL of RNA sample using the NanoDop DN-1000 spectrophotometer spectrophotometer (NanoDrop Technologies LLC, Wilmington, Delaware USA) under the software program ND-1000 v3.2). Integrity of the extracted RNA was checked by Agilent. In brief, absorbance at 260 nm was used for quantification of nucleic acids with an optical density of 1 corresponding to 40ng/µL RNA. Ratios of absorbance (260 nm/280 nm) of approximately 2.0 for RNA indicated that the nucleic acid preparations were sufficiently free from protein contamination which could compromise downstream experiments. In order to determine the most accurate quantification, averages of duplicates or triplicates readings were taken.

2.4.2 DNase Treatment of Extracted Total RNA

The RNA samples were extracted on DNase treated columns by electing to take the optional DNase-treatment step in the RNeasy handbook. This was done by following manufacturer's recommended instructions where 80µL of DNase treatment (10µL DNase 1 stock +70µL RDD buffer) was added to each sample and incubated at room temperature for at least 15 mins.

2.4.3 Reverse Transcription (RT)-PCR

Reverse transcription was performed using the Applied Biosystems High Capacity cDNA Archive Kit (Applied Biosystems). All steps were performed according to manufacturer's instructions. 1 µg of DNase treated RNA samples were reverse transcribed into cDNA in a 100 µL reaction containing a final concentration of 1X RT buffer, 5mM MgCL₂, 1mM dNTP mixture, 1u/µL RNAsin (RNase inhibitor), 0.5 µg of random heximers, 15 u of AMV reverse transcriptase (Multiscribe) on a 96-well plate. For negative controls, additional reactions without reverse transcriptase were included. The reaction was then placed on a thermocycler and underwent the following two-step reaction conditions: 25 °C for 10 min, 37 °C for 120 mins. The samples were then stored at -20 °C until use.

2.4.4 Real-Time Polymerase Chain Reaction

Relative real-time RT-PCR quantitation of the samples was carried out in a two-step RT-PCR assay using the Taqman Gene Expression Assays from Applied Biosystems in a multiplex reaction (if the gene of interest and β-actin reacts with the same efficiency). Each reaction consisted of 2.5 µL Taqman Expression PCR Master Mix, 1x VIC labelled β-actin or GapDH probe (housekeeper), 1X FAM-labelled probe for the gene of interest, and 2 µL of cDNA in a final volume of 5 µL in a 384-well plate. The comparative ΔΔCT method was used for relative quantification of expression, normalized to β-actin or Gapdh (for heart tissue) in each sample and then expressed relative to SHRSP ABI PRISM 7700 Sequence Detection System User Bulletin #2).

In order to use the ΔΔCT, it was imperative to experimentally confirm that the amplification efficiencies of the target and control gene PCRs were the same (i.e. that E_X=E_R). Therefore the amplification efficiencies of each gene expression assay were measured in duplex PCRs with either GapDH or β-actin assays using a serial dilution of template. This process was performed for all gene expression assays and custom gene expression assays for each cDNA template (e.g. for cDNA from heart, kidney, aorta, liver and brain). Each assay was assessed according to the Applied Biosystems guidelines. Each gene expression assay for mRNA from each tissue that was used in this study amplified efficiently

2.4.4.1 Real-Time Polymerase Chain Reaction using SYBR Green:

Real-time RT-PCR quantitation of the samples was carried out in a two-step RT-PCR assay. The reactions were prepared using Applied Biosystems Power SYBR Green Master Mix. All reactions were completed in duplicate, including minus RT controls. Each reaction consisted of 2.5µL of cDNA sample (section 2.4.3), 3.65µL of RNase-free H₂O, 100µM sense primer, 100µM antisense primer, and 6.25 µL of master mix in a 12.5 µL reaction.

The following cycling parameters were used: 50°C for 10 minutes, then 95°C for 10 minutes. This was followed by 40 cycles of 95°C for 10 seconds and a combined annealing/extension temperature of 60°C for 2 minutes. During each cycle of the PCR the fluorescence emitted by the binding of SYBR-Green to the dsDNA produced in the reaction was measured. To confirm the specificity of the reactions dissociation curves were constructed for each primer pair at 0.1°C intervals between the temperatures of 60 °C and 95°C.

2.5 Genomic DNA Preparation

2.5.1 DNA Extraction

Genomic DNA from SHRSP, transgenic, and WKY animals was extracted using Qiagen DNeasy kits (Qiagen, Hilden Germany) according to manufacturer's instructions.

2.5.2 Sequencing

1-3 µg of genomic DNA, that was extracted as stated in 2.5.1, was digested separately with either *HindIII* or *PstI* restriction enzymes for 1.5 hours at 37° C in 0.5 µL epindorf tubes. Resulting fragments were then ligated overnight at 16 °C with T4 ligase. Primers designed specifically for *HindIII* (*GstmFragA*) and *PstI* (*GstmFragB*) restriction sites were used as primers with the ligated templates for the first round of PCR amplification. First round PCR was performed using the primer sets *GstmFragA* (1+2) and *GstmFragB* (1+2):

GstmFragA 1- ATT GCA TGA AGA ATC TGC TTA GG

GstmFragA 2- ACA AGC AGG GAG CAG ATA CTG GC

GstmFragB 1- AAA GGA GTG GGA ATT GGC TCC GG

GstmFragB 2- CAA CGC GTA TAT CTG GCC CGT AC

Product from the first round PCR was utilized as a template for a second nested PCR reaction using nested *Gstm1FragA* (3+4) and nested *Gstm1FragB* (3+4) primer sets:

GstmFragA 3- TGT ACG GGC CAG ATA TAC GCG TTG

GstmFragA 4- GAG CAG ATT GTA CTG AGA GTG CAC

GstmFragB 3- GGT AAA CTG GGA AAG TGA TGT CG

GstmFragB 4- GAG CAG ATT GTA CTG AGA GTG CAC

For a schematic view of this process pre refer to figure 4-11.

The PCR reactions were run on the Peltier Thermal Cycler (PTC-225) under the conditions 95 °C for 4 mins, 96 °C for 30s and 58 °C for 30s and 72 °C for 60s for 35 cycles, then held at 72 °C for 7 min. In order to separated the amplified fragments, 15-20 µL of PCR reaction was electrophoresed with 3µL of 6X loading dye in a 1% agarose gel at 100V for 1.5 hours, alongside a 1Kb DNA ladder. DNA fragments that were considered the correct sizes were then isolated from the aragose gels by Qiaquick gel desolving kt (Qiaquick handbook pg 25) according to handbook instructions (Qiagen). Extracted DNA eluate was then quantified by measuring 1.5 uL of RNA sample using the NanoDop DN-1000 spectrophotometer spectrophotometer (NanoDrop Technologies LLC, Wilmington, Delaware USA) under the software program ND-1000 v3.2, in which absorbance ratios of 260 nm/280 nm equalled approximately 1.8 for DNA. This indicated that the DNA preparations were sufficiently free from protein contamination. Like RNA samples, averages of either duplicate or triplicate measurements were taken for samples requiring precise quantification.

Eluted DNA was then placed into a plasmid cloning kit (Stratoclone) and cloned according to manufacturer's instructions (Stratoclone). Positive colonies were then screened and verified by 2% X-gal. Plasmid DNA was then prepped for DNA

sequencing using Qiagen Plasmid mini prep kit (Qiagen) according to manufacturer's instructions.

Plasmid DNA was sequenced by using Applied Biosystems BigDye Terminator n3.1 Cycle Sequencing kits. All reaction were performed on a 96 well plate and included included 3.5 μ l 5X sequencing buffer; 0.5 μ l Ready Reaction; 8 μ l template (100-200ng of plasmid DNA); ~3.2 μ l primer (2.0 μ M Final); ~4.8 μ l H₂O. The temperature program cycle was: 96 °C for 45 secs, 50 °C for 25 secs, 60 °C for 4 mins. Steps 1-2 repeated 25 times.

Sequencing was initially analyzed on Applied Biosystems SeqScape software version 2.1 to see if fragments aligned to the genome. Fragments that were aligned were then analyzed without the use of computer software and each nucleic acid was examined in order to verify that the connecting sequences were novel and not erroneous transgene fragments. Experimental sequences were then aligned with known sequences derived from bioinformatic databases such as UCSC genome browser or ENSEMBL.

2.5.3 Copy Number Variation

Identification of the *Gstm1* transgene across generations was determined in each transgenic line through Taq-man analysis. Copy number variation Taqman probes, SNP Genotyping Assay (Applied Biosystems) and SNP Gene Expression Assay (Applied Biosystems), were custom synthesized to a unique portion of the transgene construct. The SNP Genotyping Assay was analyzed by Taqman Genotyper, a specifically designed analysis package developed by Applied Biosystems for this assay. The SNP Gene Expression Assay was compared to a unique single copy gene (RNase P 30) that was custom designed for the genetic background of rats. Using the comparative ($\Delta\Delta CT$) method with additional steps as calculated by Applied Biosystems Copy Caller Software, copy number variation analysis was performed on the Taqman 7900.

2.6 Protein Extraction

2.6.1 Protein Extraction

Protein from tissues was extracted using a Hepes lysis buffer (50mM Hepes, 1mM DTT, 0.5% Tween, pH 7.4). On the night before extraction, one tablet of Roche EDTA-free protease inhibitor cocktail tablet was added for every 10 mls of Hepes lysis buffer used. The samples were homogenized in cold Hepes lysis buffer (1ml of Hepes buffer for up to 0.3g of tissue). The homogenates were kept on ice until centrifuged at 14,000 rmp for 10 mins at 4°C and the supernatant contain the protein was transferred to a new tube and kept on ice. 5µL of supernatant was removed to determine protein concentration by nanodrop. The rest of the protein was stored at -80 °C until needed.

2.6.2 Protein Quantification

The protein concentration of each sample was determined using a Peirce BCA (bicinchoninic acid) protein assay kit according to the manufacturer's instructions. The bovine serum albumin (BSA) standards were diluted to appropriate concentrations for the standard curve while the protein samples were diluted accordingly to fit within the standards spectrum. Briefly, a standard curve was generated using the following BSA dilutions: 2000 µg/mL, 1500 µg/mL, 1000 µg/mL, 750 µg/mL, 500 µg/mL, 250 µg/mL, 125 µg/mL and 25 µg/mL. 200 µL of working reagent was added to 25 µL of sample or standard in duplicate in a 96 well plate, and incubated for 30 minutes at 37°C in the dark. The plate was then analysed on a Wallac Victor² plate reader (Wallac, Turku, Finland) with absorbance at 570 nm. Results were then calculated according to the linear equation based on the standard curve generated.

For measurement of proteinuria in urine samples, the Peirce 660 Protein Assay from Thermo Scientific was used. Pre-diluted samples were used and purchased from Thermo Scientific. Urine samples were diluted with water in order to fall within the working range of the pre-dilute samples. 10µL of each replicate of standard, unknown sample and the appropriate blank sample were added into a microplate well. 150µL of the Protein Assay Reagent was added to each well. Plate was then covered and placed on a plate shaker at medium speed for 1

minute and then left to incubate for 5 minutes at room temperature. The plate was then analysed on a Wallac Victor² plate reader (Wallac, Turku, Finland) with absorbance at 570 nm. A standard curve was calculated by plotting the average Blank-corrected 660nm measurement for each BSA standard (see above for concentrations) vs. its concentration in µg/mL and then used to determine the protein concentration of each unknown sample.

2.6.3 Gel Electrophoresis

sodium dodecyl sulphate polyacrylamide gel electrophoresis (SDS-PAGE) and western immunoblotting was used to detect the *Gstm1* protein. First, samples were prepared at the appropriate concentration with 6x loading buffer containing: 10% weight/volume (w/v) SDS, 30% (v/v) glycerol, 10% (v/v) Tris-HCl pH 6.8, 0.01% (w/v) bromophenol blue and 2% (v/v) β-mercaptoethanol. Samples were heated at 95°C for 5 minutes to denature the protein, mildly cooled and loaded into the well.

The polyacrylamide (PA) gel consisted of a 4% stacking gel containing 13.3% (v/v) N,N'-methylene-bis-acrylamide (polyacrylamide 30%), 25% (v/v) Tris pH 6.8 (3.75 mM), 0.1% (v/v) SDS, 1% (v/v) ammonium persulphate (APS) and 0.1% (v/v) of N,N,N',N'-Tetramethylethylenediamine (TEMED). Since the molecular mass for *Gstm1* was 26 kDa, a 12% resolving gel which contained 40% (v/v) of PA (30%), 25% (v/v) of Tris pH 8.8 (11.25 mM), 0.1% (v/v) SDS, 1% (v/v) APS and 0.1% (v/v) TEMED was used.

Following sample loading, gels were electrophoresed at 100 V through the stacking gel, then switched to 200 V for electrophoresis through the resolving gel in running buffer (0.025 M Tris-HCl, 0.2 M glycine, 0.001 M SDS) for approximately 2 hours. Protein was then transferred to Hybond-P polyvinylidene difluoride membrane (Amersham Bioscience UK Limited, Buckingham, UK), to enable antibody binding and detection. Protein transfer was performed using an electric current which promotes protein migration from the gel to the membrane. Protein transfer was performed using the semi-dry method at 75 mV for 45 mins.

2.6.4 Western Immunoblotting

Once proteins were transferred to the membrane, antibody detection was performed. The membranes were first blocked in TBS-T [150 mM NaCl, 50 mM Tris, 0.1% (v/v) Tween-20] + 10% (w/v) fat-free milk powder (blocking buffer) for 8 hours at 4°C. Membranes were incubated with rabbit anti-rat *Gstm1* polyclonal antibody (gift from Prof. John Hayes, University of Dundee)diluted in blocking buffer at the 1:5000 dilution overnight at 4°C with shaking.

Following overnight incubation the membrane was washed twice in blocking solution for five minutes each at room temperature, followed by incubation with an 1:2000 dilution of the appropriate secondary antibody, goat anti-rabbit IgG secondary antibody conjugated to horseradish peroxidase (HRP) (Neomarkers, Fremont, CA, USA) for 1 hour at room temperature with shaking. The membrane was then washed six times for 15 minutes each at room temperature with shaking, four times with blocking solution and two times with tris buffered saline-tween (TBS-T). Proteins were visualized using Enhanced Chemiluminescent (ECL) Detection System (Amersham Biosciences UK Limited, Buckingham, UK) following the manufacturer's instructions. Films were exposed for various lengths of time, ranging from 10 seconds to 35 mins.

2.7 Statistical Analysis

In vivo phenotypic measurements were performed with 6 to 8 rats per group. Results are expressed as mean +/- standard error of the mean (SEM) unless otherwise stated. Repeated measures ANOVA was used to compare radiotelemetry data between groups, as described previously (Davidson *et al.*, 1995). Briefly this was a general linear model ANOVA using a Tukey pair-wise comparison. Statistical significance was considered with p values of < 0.05. Other comparisons between groups for the *in vivo* measurements were performed by one way ANOVA with Tukey's multiple comparison test, unless stated otherwise, and statistical significance was considered with p values of <0.05. Statistical analyses were performed using GraphPad Prism 4. *, **, *** represents p<0.05, p<0.01 and p<0.001 versus SHRSP, respectively.

Ex vivo experiments were performed with 4 to 8 rats per group as described in each figure's legend. Results are expressed as mean +/- standard error of the mean (SEM), unless otherwise stated. Statistical significance was considered with p values of < 0.05. Comparisons between groups were performed by one way ANOVA with Tukey's multiple comparison test, unless stated otherwise. Area under the curve was calculated from organ bath and myography response curves with one way ANOVA and Tukey's multiple comparison test used to determine significance between the 4 strains of animals. Statistical analyses were performed using GraphPad Prism 4. *, **, *** represents p<0.05, p<0.01 and p<0.001 versus control.

Molecular experiments were performed with 3 to 8 rats per group as described in each figure's legend. Results are expressed as mean +/- standard error of the mean (SEM), unless otherwise stated. Statistical significance was considered with p values of < 0.05. Comparisons between groups were performed by one way ANOVA with Tukey's multiple comparison test, unless stated otherwise. Tukey's multiple comparison test used to determine significance between the 4 strains of animals. Statistical analyses were performed using GraphPad Prism 4. *, **, *** represents p<0.05, p<0.01 and p<0.001 versus control.

Human translational experiments for gene expression were analyzed using Prism graph pad using student's t-test or 1-way ANOVA as appropriate. Initial SNP quality checking included estimation of allele frequencies using the Hardy-Weinberg equilibrium.

3 *In vivo* Phenotypic Characterization of the *Gstm1* transgenic SHRSP rat

3.1 Introduction

Studies in human and experimental medicine have shown that increased oxidative stress is associated with increased blood pressure (230;231). In 2000, Vaziri *et al.* reported that oxidative stress and arterial hypertension were produced in normal Sprague-Dawley rats through glutathione depletion by oral administration of buthione sulfoximine (BSO) (160). These findings are supported by other studies where the induction of chronic oxidative stress by glutathione depletion has been shown to cause severe hypertension in normotensive rats (230-232). Additionally, studies by McBride *et al.* have implicated that decreased renal *Gstm1* levels contribute to the development of oxidative stress and hypertension in the stroke-prone spontaneously hypertensive rat (SHRSP) rat via reduced antioxidant defences (96).

The SHRSP is a well characterized experimental model for human essential hypertension and stroke. Some of the characteristics in common between the SHRSP and human essential hypertension are; adult onset of hypertension and the continued increase of blood pressure with age, sexually dimorphic blood pressure levels, and proneness to stroke (227). The hypertensive phenotype in the SHRSP results in an increased cardiac workload and an impaired mechanical performance that contributes to cardiac hypertrophy (233). These similarities with human essential hypertension make the SHRSP one of the best existing models of human cardiovascular disease (36;37;84). The SHRSP model demonstrates an imbalance between nitric oxide (NO) and superoxide (O_2^-) levels leading to oxidative stress (78). This oxidative stress has been implicated in the development of vascular endothelial dysfunction and renal pathology (234;235).

Oxidative stress is an important pathogenic factor in the development of cardiovascular diseases and increased production of reactive oxygen species (ROS) and/or reduced defences against ROS not only leads to endothelial dysfunction, but also causes structural damage to tissue and organs, and is considered a major contributor to cardiac pathologies (231;236;237). Studies demonstrating that reduced *Gstm1* protein expression in the SHRSP is associated with increased oxidative stress (96) implicate *Gstm1* as an important functional candidate for development of endothelial dysfunction and hypertension. In

addition, pharmacological intervention studies and mRNA expression data in the SHRSP provide evidence to support a causal role for *Gstm1* in the development of hypertension (13). For example, significantly reduced renal *Gstm1* expression levels are already evident in 5-week old SHRSP before the onset of hypertension (238). Moreover, reduced expression of *Gstm1* in the SHRSP could not be improved by antihypertensive treatment (i.e. the angiotensin II type 1 receptor blocker, losartan) during either reversal studies (i.e. established hypertension) or prevention studies (i.e. development of hypertension). These data suggest that altered *Gstm1* expression may contribute directly to the pathogenesis of hypertension and is not an adaptive response caused by long-term differences in blood pressure.

It is generally accepted that the gold standard for proving causality of a functional candidate gene is to perform a transgenic knockdown or rescue experiment (Include a REF). Accordingly, in this project we aimed to 'rescue' the deficiency of *Gstm1* in the SHRSP by incorporation of a normal *Gstm1* gene from WKY into the SHRSP genome under the control of the universal EF-1 α promoter. As detailed in the Materials & Methods section (Chapter 2), two novel and independent SHRSP transgenic lines have been generated through a joint collaboration between Glasgow University and Prague's Academy of Sciences (Drs. Michal Pravenec and Vladimir Landa). SHRSP males and females were sent to Prague where the transgenic procedure was performed. This consisted of female SHRSP rats being super-ovulated and time-mated with male SHRSP rats. On day one of ovulation, embryos were harvested and injected with a linear construct that consisted of the EF-1 α promoter and *Gstm1* WKY gene. The embryos were then transferred into recipient females and normal gestation allowed to progress. Offspring were screened for insertion of the transgene and positive 'founder' animals were transferred to the University of Glasgow. This process generated two independent transgenic lines (Trans1 and Trans2).

The understanding of cardiovascular changes that are related to oxidative stress in the SHRSP rat will be important for the elucidation of mechanisms underlying human essential hypertension. The aim of this chapter was to phenotypically characterize the two independently generated transgenic rat lines, and establish definitive proof that defective *Gstm1* expression plays a functional role in blood pressure elevation and cardiovascular dysfunction. This was carried out though

examination of the effects of transgenic expression of wild type *Gstm1* on (1) hemodynamic parameters in the SHRSP, (2) examination of the cardiac function and mass through echocardiography.

3.2 Materials and Methods

3.2.1 Hemodynamic Measurements

3.2.1.1 *Tail cuff Plethysmography*

Measurement of systolic blood pressure was carried as described in the main methods section (Section 2.1.2.1). Male rats starting from the age of 5-8 weeks old, depending upon size, were tail cuffed every week in order to measure SBP until the implantation of telemetry probes at 12 weeks of age. Multiple cuff inflation/deflation values were obtained through the duration of each tail-cuff session and an average was taken for each animal. For SHRSP, WKY and Trans1, n=3 or more for each weekly reading; however, for Trans2 we n numbers were generally low (i.e. n=2) due to poor breeding performance.

3.2.1.2 *Telemetry*

3.2.1.2.1 Base line and salt loading

Baseline blood pressure characteristics were investigated by implantation of radio-telemetry probes (TA11PAC40) at 12 weeks of age and data was continuously recorded until 21 weeks of age in male WKY, SHRSP, Trans1, and Trans2 rats (n=7-8). In salt-loaded rats blood pressure characteristics were investigated in male WKY, SHRSP and Trans1 given 1% NaCl in the drinking water *ad libidum* for 3 weeks, starting at the beginning of week 18. Radiotelemetry measured systolic blood pressure (SBP, mmHg), diastolic blood pressure (DBP, mmHg), pulse pressure (PP, mmHg), heart rate (beats per minute, BPM) and motor activity (arbitrary units, AU). All hemodynamic measurements were carried out as described in section 2.1.2.2.

3.2.2 Echocardiography

Transthoracic echocardiography was performed on lightly anesthetized rats (1.25%-1.5 % isoflourane in 1.5 Liters/min O₂) placed in the left lateral decubitus position. Left ventricular motion mode (M-mode) measurements at the level of the papillary muscles were used to delineate wall thicknesses and internal diameters at systole (s) and diastole (d). Images were captured using an Acuson Sequoia C512 ultrasound system and then used to assess cardiac geometry and contractility, as previously described (228;239). Echocardiography was performed prior to sacrifice at 21 weeks. Cardiac index was estimated as cardiac output adjusted for tibia length. A typical echocardiogram examination lasts for approximately 5-10 minutes, from induction of anaesthesia. For further information please see section 2.1.3.

3.2.3 Tissue Collection

Animals were sacrificed at 21 weeks of aged. Tissues were excised and any excess blood removed before weighing kidneys, whole heart and left ventricular plus septum after dissection. This was corrected to tibia length. Further detail as described in section 2.2.2.

3.2.4 Statistics

Telemetry data was analyzed using a repeated measures ANOVA followed by a Tukey's post-hoc correction for multiple comparisons. Week one of the hemodynamic measurement period is a recovery period and has not been included in the statistical analysis. Pulse pressure diurnal variation and echocardiography data was analyzed using a one way ANOVA followed by a Tukey's corrections, unless stated otherwise. All data is displayed as mean with standard error of the mean.

3.3 Results

3.3.1 Hemodynamic Measurements

3.3.1.1 Tail Cuff data

Rats were tail cuffed starting between 5 and 8 weeks of age. The variable start date was dependent upon rat size since the tail cuff transducer has a lower size limit, and appropriate fit is necessary to ensure accuracy of BP measurement. Baseline systolic blood pressure was significantly reduced in both transgenic lines and WKY ($F = 8.35, p < 0.01$) when compared to SHRSP (Table 3-1).

3.3.1.2 Radio Telemetry Measurements – Baseline

3.3.1.2.1 Systolic blood pressure

At 12 weeks of age, rats underwent radio telemetry implantation and systolic blood pressure was measured by automated scheduled sampling every 5 mins. Raw data files were hourly averaged prior to exportation into an Excel spreadsheet where the data underwent analysis by a specifically designed Excel macro and were averaged into weekly daytime (7am-7pm) and night-time (7pm-7am) data sets (Figure 3-1). SBP rises continuously over the full hemodynamic measurement period (between 12 - 21 weeks of age) for both SHRSP and WKY parental strains and the two transgenic lines. However, the rate of increase is greater in the SHRSP strain. Baseline systolic blood pressure was significantly reduced in both transgenic lines ($F = 52.46, p < 0.001$) where SBP averaged 175.6 ± 6.22 mmHg for Trans1 rats and 174.2 ± 6.36 mmHg for Trans2 rats, when compared to SHRSP 198.1 ± 1.5 mmHg. While SBP in Trans1 and Trans2 rats was significantly higher than WKY (systolic 150 ± 4.7 mmHg, $F=56.24, p < 0.001$), they were not significantly different from one another ($F = 52.46, p > 0.05$).

3.3.1.2.2 Diastolic Blood Pressure

DBP also shows a continuous rise over the full measurement period for SHRSP, WKY and Trans1 rats. However, this trend was less pronounced in Trans2 rats. Baseline diastolic blood pressure for Trans1 and Trans2 rats averaged 124.3 ± 5.89 mmHg and 131.7 ± 1.33 mmHg, respectively, while DPB for the parental strains were 137.8 ± 9.3 mmHg and 107.1 ± 3.5 mmHg, for SHRSP and WKY

respectively. Repeated measure ANOVA determined that DBP for Trans1 and Trans2 lines were significantly different from both SHRSP and WKY (SHRSP: $F=107.1$, $p < 0.001$; WKY: $F=107.1$, $p < 0.001$) (Figure 3-2). Additionally, while diastolic blood pressure is not significantly different ($F=107.1$, $p > 0.05$), their slopes of lines are different.

3.3.1.2.3 Pulse Pressure

Pulse pressure between the parental strains, WKY (40.72 ± 0.65 mmHg) and SHRSP (59.68 ± 0.308 mmHg) was significantly different ($F=364.4$, $p < 0.001$). Pulse pressure in Trans 1 rats (51.79 ± 0.411 mmHg) was significantly reduced when compared to the SHRSP ($F=364.4$, $p < 0.001$) (Figure 3-3). While there is a large margin of error between animals for pulse pressure in Trans2 rats, the strain showed a significant reduction in pulse pressure (40.75 ± 0.53 mmHg) when compared to the SHRSP and Trans1 rats ($F=364.4$, $p < 0.01$). Additionally, pulse pressure in Trans2 was not significantly different to WKY rats ($F = 364.4$, $p > 0.05$) (Figure 3-3).

3.3.1.2.4 Heart rate and Locomotor Activity

Heart rate and activity are illustrated in Figures 3-4 and 3-5. There were no significant differences in heart rates across the measurement period between the four strains (WKY: 334.4 ± 6.0 BPM; SHRSP: 335.6 ± 4.39 BPM; Trans1: 324.7 ± 5.29 BPM; Trans2: 323.0 ± 5.59 BPM). Additionally, there was no significant difference in motor activity between the four strains (WKY: 2.965 ± 0.33 AU; SHRSP: 2.965 ± 0.30 AU; Trans1: 2.99 ± 0.31 AU; Trans2: 3.1 ± 0.27 AU).

Table 3-1: Systolic blood pressure measured by tail cuff plethsmography measurements from 5-12 weeks

	SHRSP	WKY	Trans1	Trans2
5 weeks	124 ±5.5	107.5 ± 5.38*	ND	ND
6 weeks	113.9 ± 5.18	127.5 ± 4.98*	ND	ND
7 weeks	152.8 ± 4.68	127.6 ±7.44*	126.5 ± 0.25*	100.3 ± 1.58*
8 weeks	164.9 ± 5.76	136.2 ±4.97*	135.5 ± 0.85*	124 ± 0.25*
9 weeks	188.2 ± 10.27	136.8 ±7.2*	142.3 ± 5.1*	ND
10 weeks	191.6 ± 8.3	139.7 ±8.38*	158.3 ±6.67*	88.93 ± 6.48*
11 weeks	205.9 ±3.87	134.7 ±8.03*	168.3 ± 0.399*	172.5*
12 weeks	197.9 ± 11.37	146.7 ± 5.74*	164.8 ± 7.23*	161.7 ± 5.55*

Systolic blood pressure is significantly reduced in both transgenic lines and WKY rats compared to SHRSP *(p<0.001). Statistical analysis was done by repeated measures ANOVA. Values are presented as mean ± SEM. ND = not determined

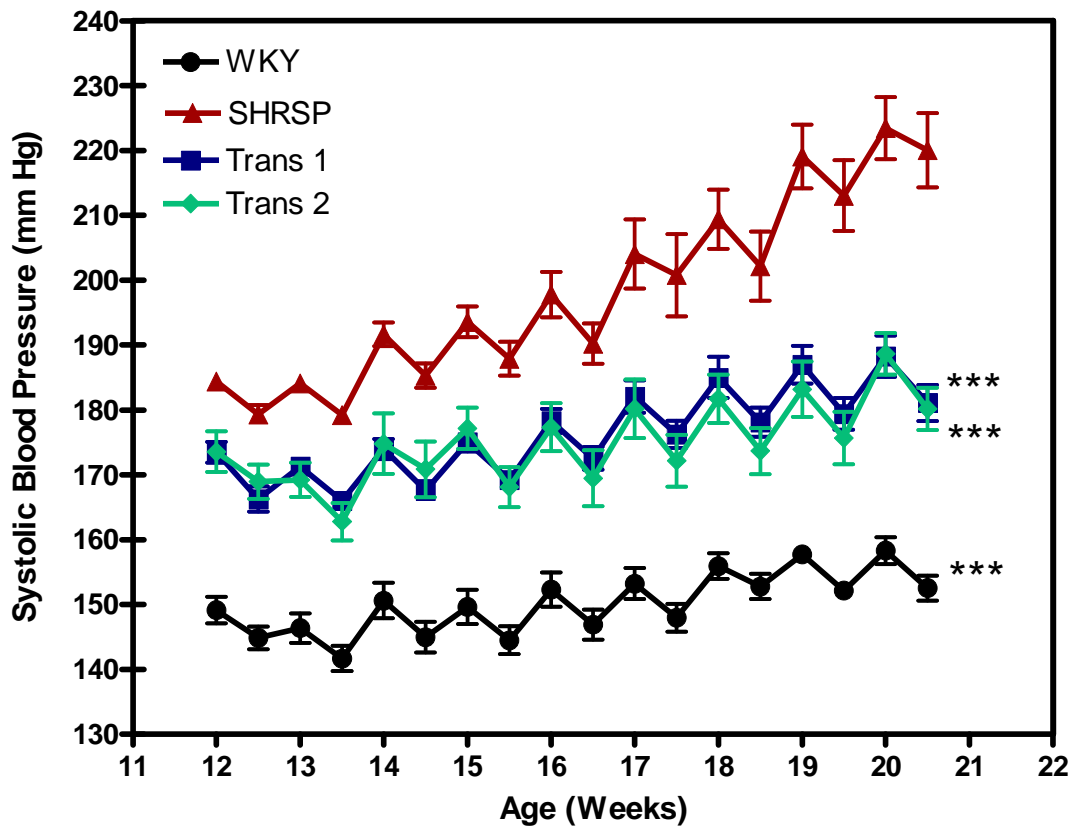


Figure 3-1: Systolic Blood Pressure in Trans1, Trans2 and Parental Strains.
Hemodynamic profile for Trans1 and Trans2 rats implanted at 12 weeks of age.

Weekly average daytime and night-time values for male WKY (n=6), SHRSP (n=6), transgenic 1 (n=8), and transgenic 2 (n=6) rats. Systolic blood pressure is significantly reduced in both transgenic lines and WKY rats compared to SHRSP ***($p<0.001$). Statistical analysis was done by repeated measures ANOVA. Values are presented as mean \pm SEM.

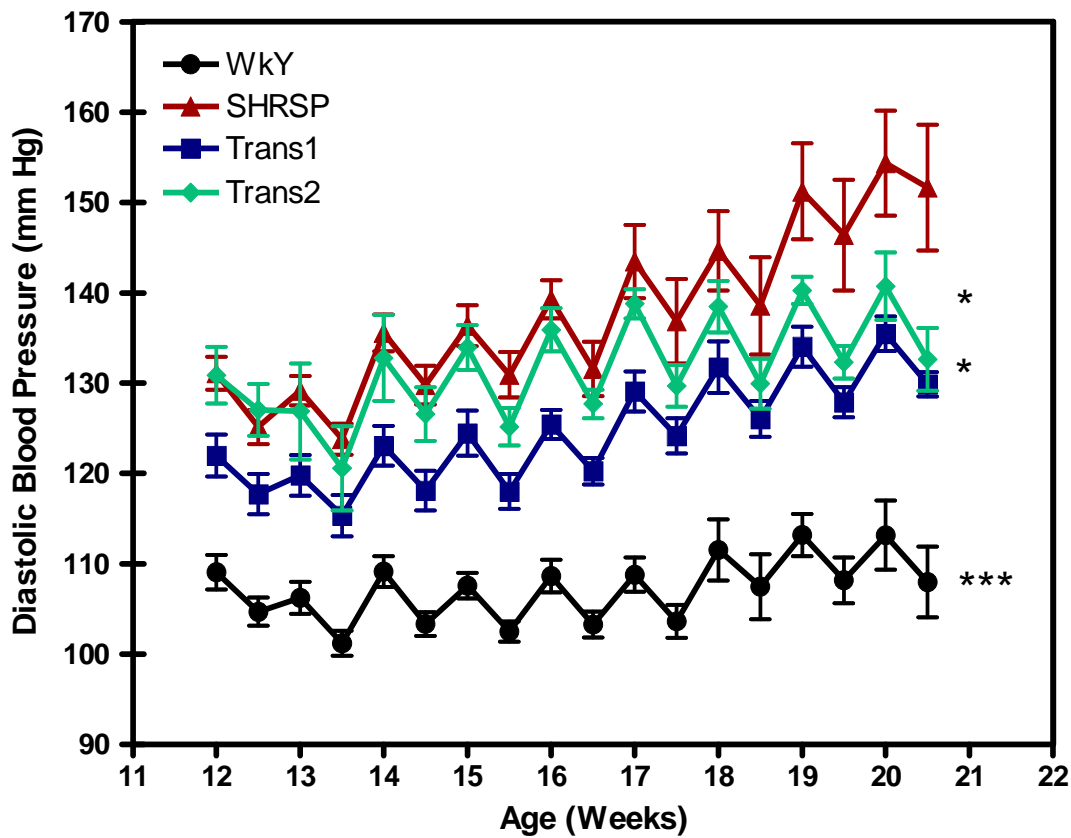


Figure3-2: Diastolic Blood Pressure in Trans1, Trans2 and Parental Strains.
 Hemodynamic profile for Trans1 and Trans2 rats implanted at 12 weeks of age.
 Weekly average daytime and night-time values for male WKY (n=6), SHRSP (n=6), transgenic 1 (n=8), and transgenic 2 (n=6) rats. Systolic blood pressure is significantly reduced in both transgenic lines and WKY rats compared to SHRSP ***($p<0.001$). *($p<0.05$). Statistical analysis was done by repeated measures ANOVA. Values are presented as mean \pm SEM.

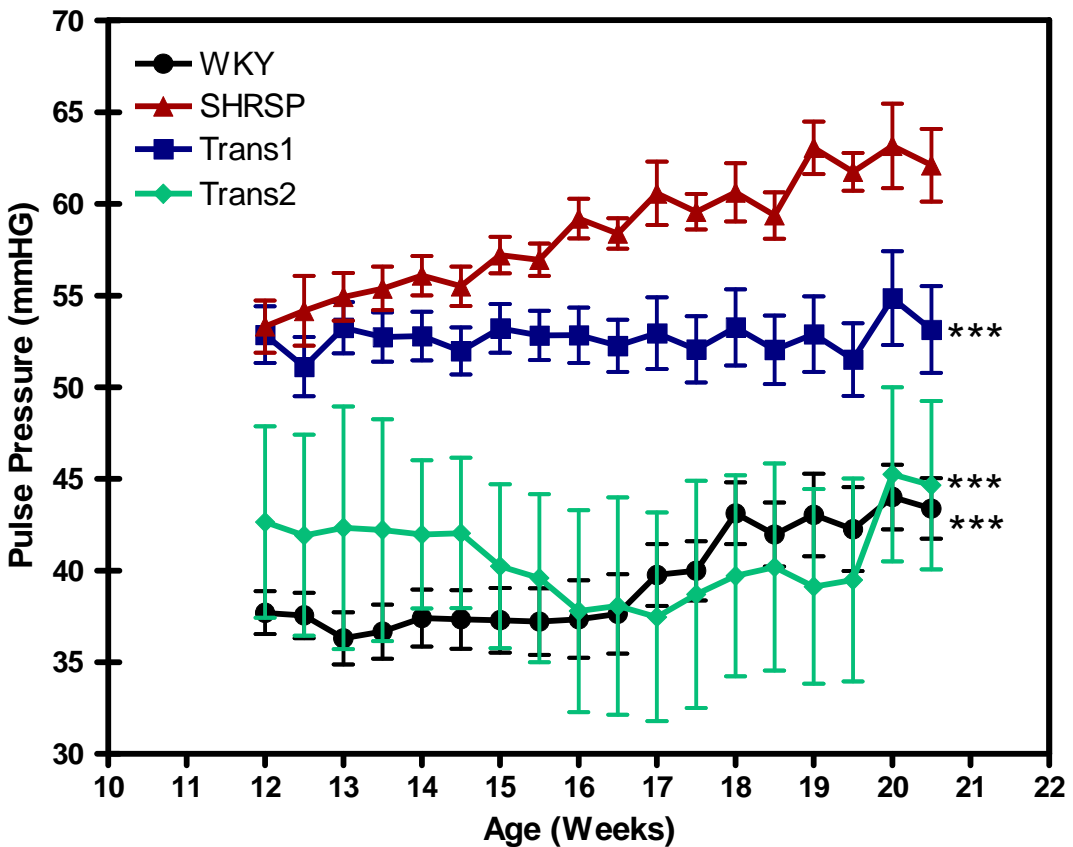


Figure3-3: Pulse Pressure in Trans1, Trans2 and Parental Strains.

Average weekly pulse pressure represented at night-time and day-time averages male WKY (n=6), SHRSP (n=6), Tran1 (n=8), and Trans2 (n=6) rats. Pulse pressure of transgenic animals was significantly lower than SHRSP. Pulse pressure in Trans1 rats was significantly increased from that of WKY; however, pulse pressure in Trans2 rats was not significantly different from WKY ***p<0.001 versus SHRSP. Statistical analysis was done by repeated measures ANOVA. Values are presented as mean \pm SEM

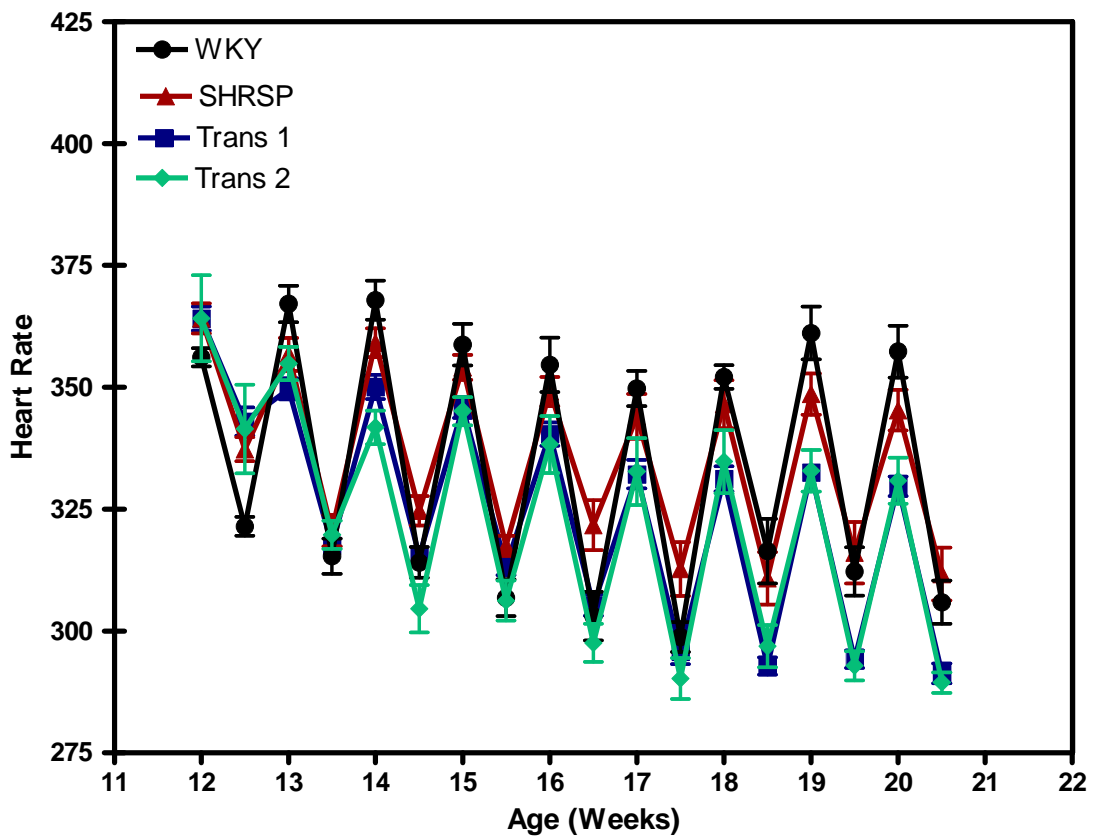


Figure3-4: Heart Rate in Trans1, Trans2 and Parental Strains.

Heart rate measured by radio telemetry, calculated as night-time and day-time averages, in male SHRSP ($n=6$), WKY ($n=6$), Trans1 ($n=8$) and Trans2 ($n=6$) rats from 12 to 21 weeks of age. There was no significant difference in heart rate between the different strains. Statistical analysis was done by repeated measures ANOVA. Values are presented as mean \pm SEM.

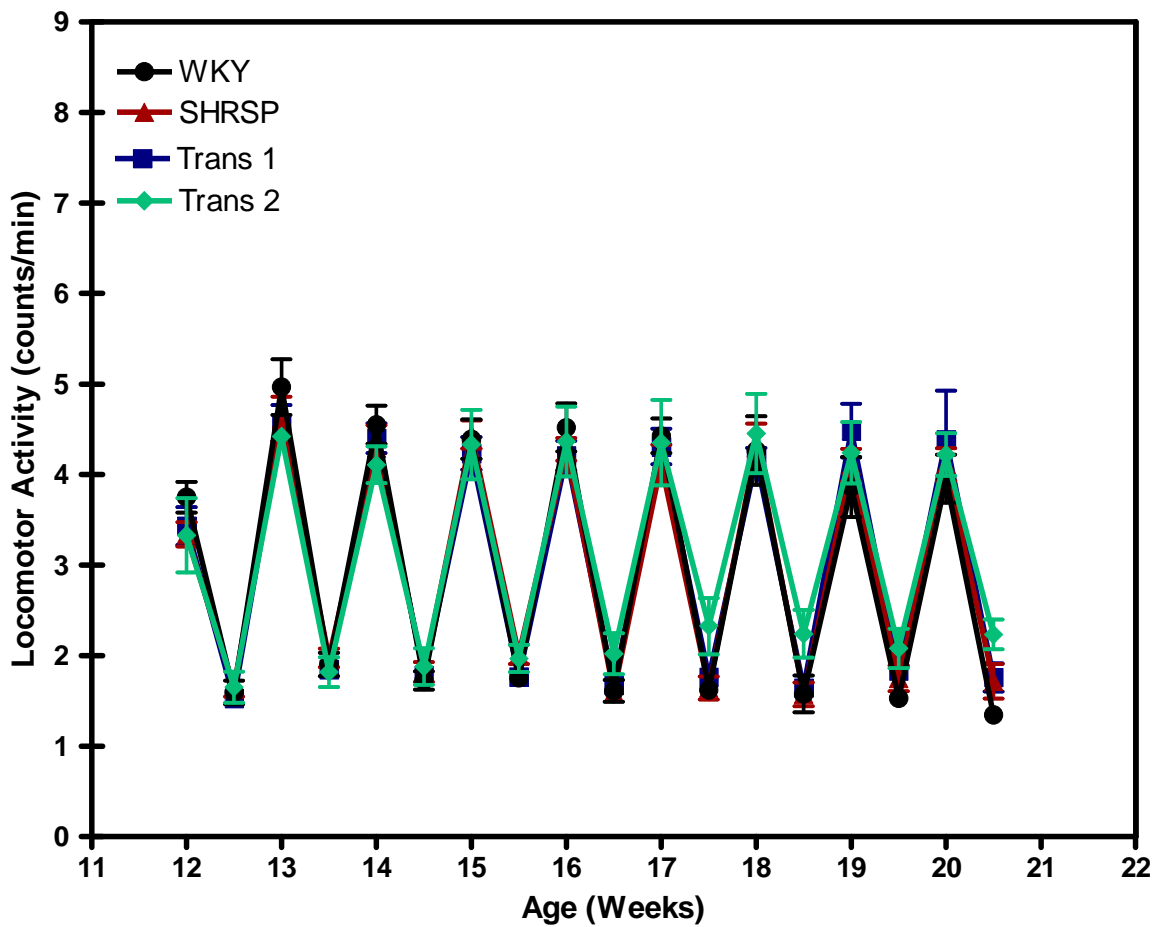


Figure 3-5: Locomotor Activity in Trans1, Trans2 and Parental Strains.
 Motor activity measured by radiotelemetry in SHRSP (n=6), WKY (n=6), Trans1 (n=8), and Trans2 (n=6) males rats from 12-21 weeks of age. Data calculated as day-time and night-time averages. There was no significant difference in motor activity between the different strains. Statistical analysis was done by repeated measures ANOVA. Values are presented as mean \pm SEM.

3.3.1.3 Radio Telemetry Measurements – 1% Salt Loading

3.3.1.3.1 Systolic blood pressure

Salt-loading with 1% NaCl from weeks 18-21 significantly elevated SBP in the SHRSP and Trans1 animals (SHRSP: Baseline 214.51 ± 5.12 vs. Salt 234.41 ± 5.79 ; Trans1: Baseline $183.13 \pm 2.79 \pm 5.12$ vs. Salt 205.91 ± 4.56 , $p<0.05$) as analyzed by t-test. There was no effect of salt loading on the WKY strain (Table 3-2).

Salt-loaded systolic blood pressure measured from 18-21 weeks of age (Figure 3-6) was significantly reduced in Trans1 rats (184.8 ± 4.14 mmHg) when compared to SHRSP (205.2 ± 5.58 mmHg) ($F = 14.6$, $p < 0.001$). Additionally, SBP in Trans1 rats and SHRSP was significantly higher than WKY (systolic 150.4 ± 1.39 mmHg, $F=4.41$, $p < 0.001$). Due to breeding limitations, Trans2 rats were not included in the salt-loading protocol.

3.3.1.3.2 Diastolic Blood Pressure

Diastolic blood pressure was significantly elevated in the SHRSP and Trans1 animals (SHRSP: Baseline 147.81 ± 5.66 vs. Salt 170.75 ± 5.21 ; Trans1: Baseline $130.85 \pm 2.79 \pm 1.99$ vs. Salt 150.49 ± 6.61 , $p < 0.05$) as analyzed by t-test. There was no effect of salt loading on the WKY strain (Table 3-2).

Salt-loaded diastolic blood pressure (Figure 3-7) for Trans1 averaged 124.3 ± 5.89 mmHg, while DBP for the parental strains SHRSP and WKY were 137.8 ± 9.3 mmHg and 107.1 ± 3.5 mmHg, respectively. Repeated measures ANOVA determined that DBP for Trans1 rats was significantly different from both SHRSP and WKY ($F = 20.21$, $p < 0.001$).

3.3.1.3.3 Pulse Pressure

Pulse pressure between salt-loaded WKY (39.45 ± 3.7 mmHg) was significantly reduced when compared to the SHRSP (58.41 ± 3.1 mmHg) (Figure 3-8). Previous studies that investigated pulse pressure differences between salt-loaded SHRSP and WKY and congenic rats have identified an exaggerated diurnal variation in the SHRSP (240). Pulse Pressure for Trans1 was significantly different from both SHRSP and WKY ($F = 11.80$, $p > 0.0005$). (Figure 3-8). Furthermore, diurnal

variation, the maximum difference between daytime and night-time pulse pressure, was significantly greater in the SHRSP ($p < 0.0001$) (Figure 3-8 Panel B) when compared to the WKY. Salt-loaded Trans1 rats displayed an intermediate phenotype where diurnal variation not significantly different from either the SHRSP or WKY ($p>0.05$). While there was an exaggerated diurnal difference in pulse pressure between the SHRSP and Trans1 strains during salt loading, there was no significant difference in pulse pressure between baseline and salt loading conditions for any of the strains (Table 3-2).

3.3.1.3.4 *Heart Rate and Locomotor Activity*

Salt loading conditions did not significantly change locomotor activity for any of the three strains when compared to baseline conditions. While there was no significant change in heart rate for parental strains during salt loading conditions when compared to baseline conditions, Trans1 HR was significantly increased (Baseline 311.96 ± 1.97 vs. Salt 327.35 ± 3.81 , $p<0.05$) as measured by t-test.

Heart rate and motor activity measured by radiotelemetry in salt-loaded rats are illustrated in Figures 3-9 and 3-10. Similar to baseline measurements, there was no significant difference in activity between WKY (3.14 ± 0.33 AU), SHRSP (3.21 ± 0.27 AU) and Trans1 rats (2.92 ± 0.29 AU) ($p>0.05$). However, after the addition of 1% NaCl at 18 weeks, a repeated measures ANOVA determined that day-time heart rate for SHRSP (340.4 ± 5.6 BPM) was significantly increased compared to the WKY (318.3 ± 10.23 BPM) and Trans1 rats (324.2 ± 8.2 BPM) ($F = 15.57$. $p<0.001$) (Figure 3-10).

Table 3-2: Baseline vs. Salt Loading Strain Comparison

		SHRSP	WKY	Trans1
SBP	Baseline	214.51 ± 5.12	154.49 ± 1.72**	183.13 ± 2.79*
SBP	1% Salt	234.41 ± 5.79*	156.72 ± 3.10**	205.91 ± 4.56*
DBP	Baseline	147.81 ± 5.66*	110.25 ± 3.25**	130.85 ± 1.99*
DBP	1% Salt	170.75 ± 5.21	109.72 ± 2.19**	150.49 ± 6.61*
PP	Baseline	61.67 ± 1.56	42.96 ± 1.89*	52.94 ± 2.15*
PP	1% Salt	62.89 ± 2.62	38.51 ± 2.33**	52.46 ± 4.51
Activity	Baseline	2.92 ± 0.18	2.75 ± 0.23	3.04 ± 0.211
Activity	1% Salt	3.19 ± 0.29	3.02 ± 0.12	2.91 ± 0.14
Heart Rate	Baseline	329.84 ± 5.08	334.18 ± 4.86	311.96 ± 1.97+
Heart Rate	1% Salt	340.15 ± 7.36	321.68 ± 3.58	327.35 ± 3.81

Baseline = averages of daytime + nighttime data over a 5 week baseline period. 1% salt = averages of daytime + nighttime data over a 3 week salt-loading period. Significantly different when compared to SHRSP *(p<0.05). Significantly different when compared to SHRSP and Trans1 **(p<0.05). Significantly different when compared to SHRSP and WKY +(p<0.05). Values are presented as mean ± SEM

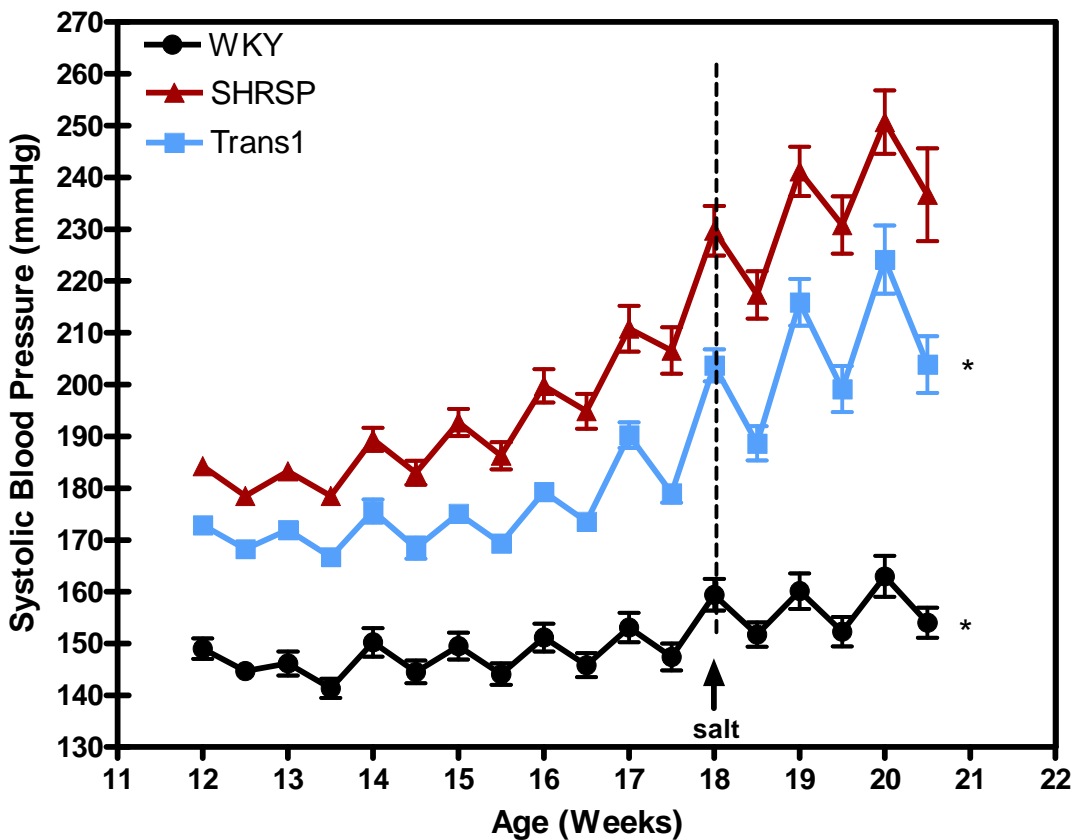


Figure 3-6: Systolic Blood Pressure for salt-loaded SHRSP, WKY and Trans1 rats.
 Hemodynamic profile for Trans1 rats implanted at 12 weeks of age and Salt loading at 18 weeks of age. Weekly average daytime and night-time values for WKY (n=8), SHRSP (n=8) and Trans1 (n=8) rats. Systolic blood pressure is significantly reduced in both Trans1 and WKY rats compared to SHRSP *(p<0.001), repeated measures ANOVA. Values are presented as mean \pm SEM

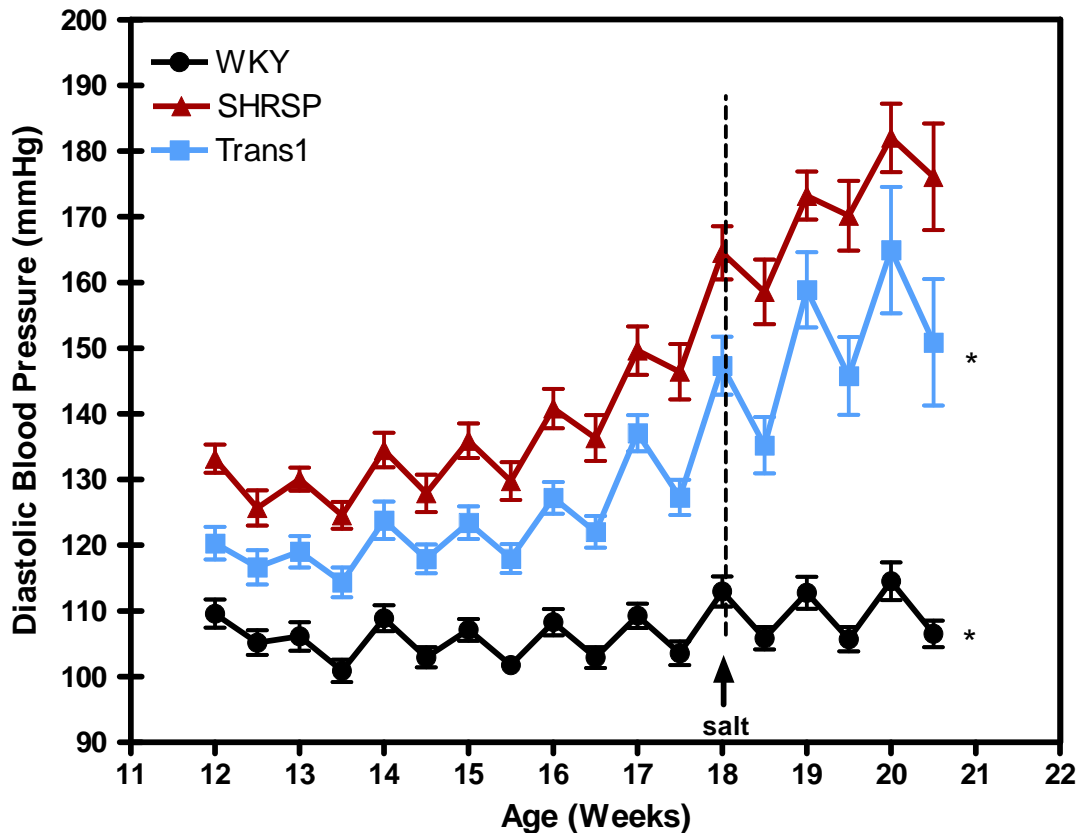


Figure 3-7: Diastolic Blood Pressure for salt-loaded SHRSP, WKY and Trans1 rats.
 Hemodynamic profile for Trans1 rats implanted at 12 weeks of age and Salt loading at 18 weeks of age. Weekly average daytime and night-time values for WKY (n=8), SHRSP (n=8) and Trans1 (n=8) rats. Diastolic blood pressure is significantly reduced in both Trans1 and WKY rats compared to SHRSP *(p<0.001), repeated measures ANOVA. Values are presented as mean \pm SEM

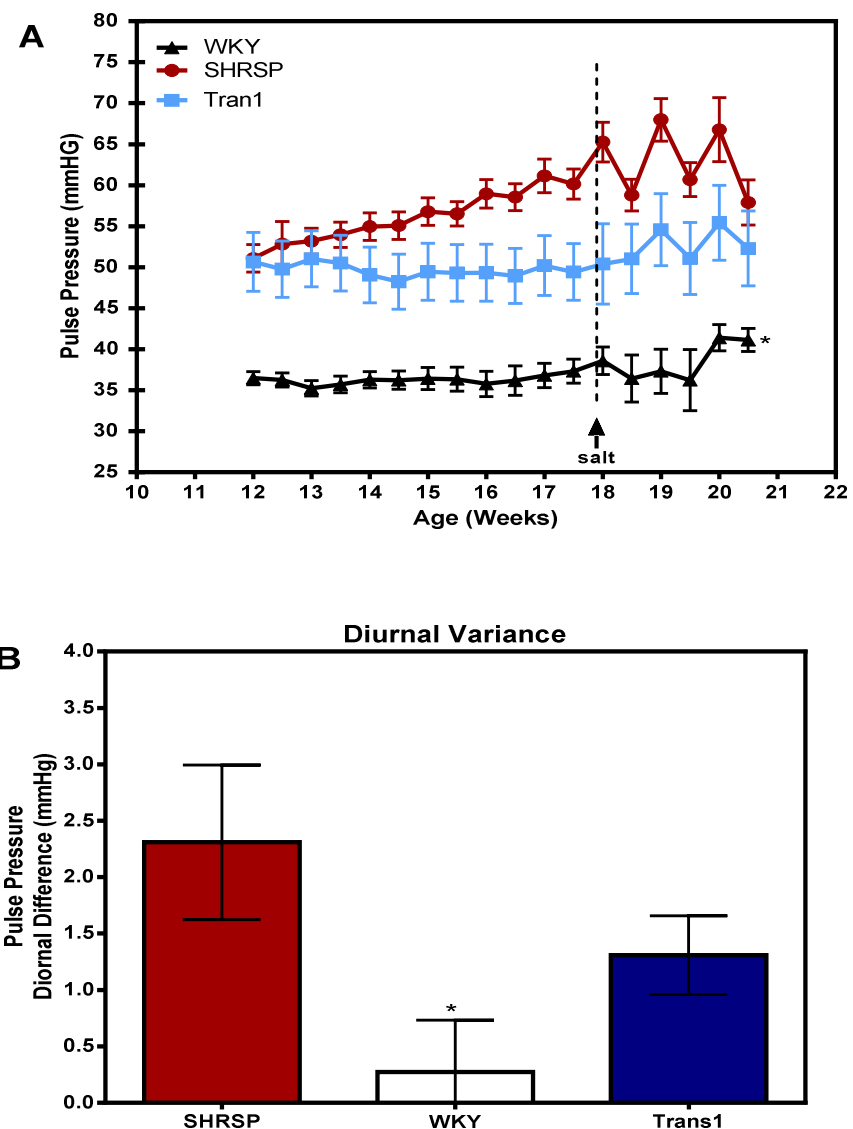


Figure 3-8: Pulse Pressure for salt-loaded SHRSP, WKY and Trans1 rats.
 Hemodynamic profile for Trans1 rats implanted at 12 weeks of age and salt-loaded at 18 weeks of age. Weekly average daytime and night-time values for WKY (n=8), SHRSP (n=8) and Trans1 (n=8) rats. (A) Pulse pressure is significantly reduced in both Trans1 and WKY rats compared to SHRSP *(p<0.001), repeated measures ANOVA. (B) WKY diurnal variation is significantly different from SHRSP ($p < 0.05$) as determined by one way ANOVA. Values are presented as mean \pm SEM.

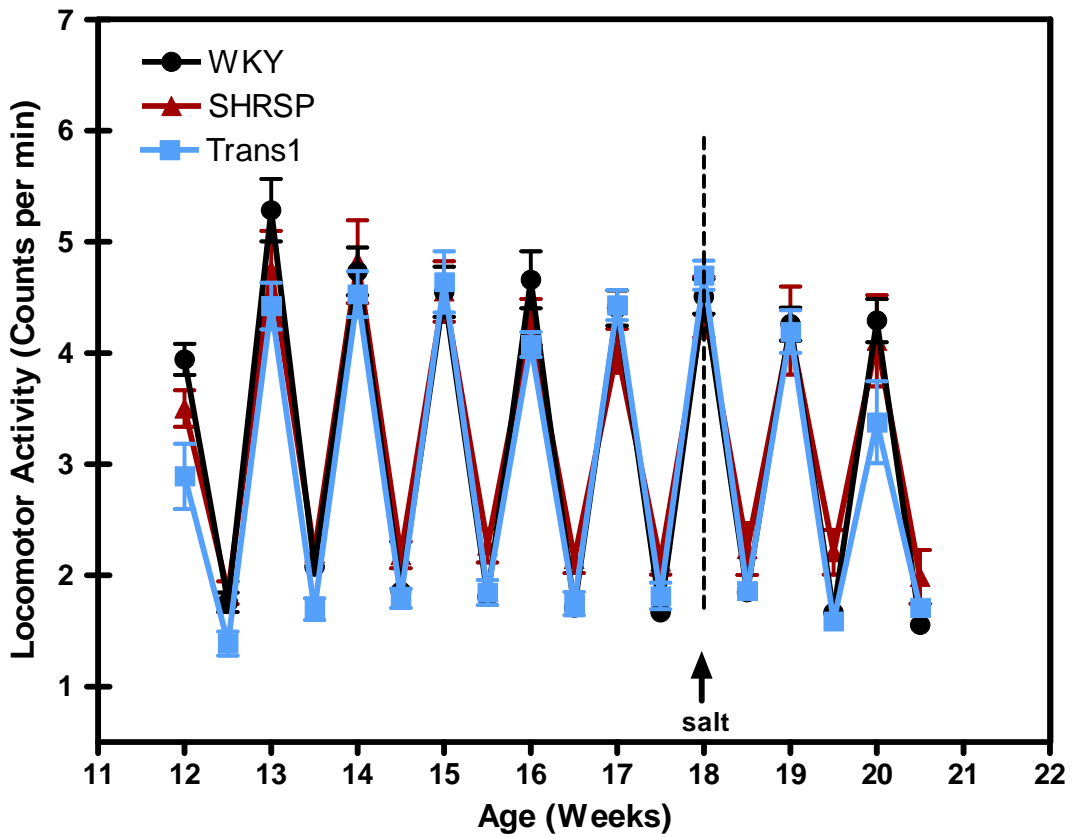


Figure 3-9: Locomotor Activity for salt-loaded SHRSP, WKY and Trans1 rats.
Telemetry measured data from 12 to 21 week olds. There was no significant difference in locomotor activity between the different strains as measured by telemetry and calculated as night-time and day-time averages. Values are presented as mean \pm SEM

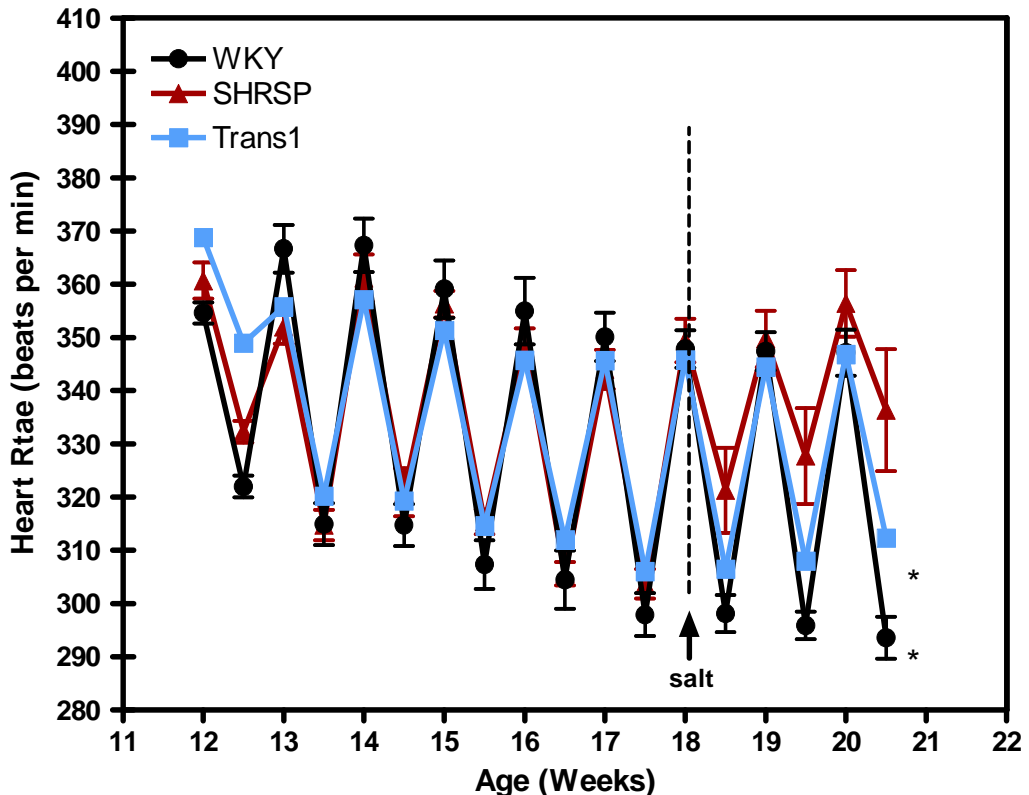


Figure 3-10: Heart Rate for salt-loaded SHRSP, WKY and Trans1 rats
 Telemetry measured data from 12 to 21 week olds. Average heart rate in beats per minute (bps) as measured by radiotelemetry and calculated as night-time and day-time averages. In WKY and Trans1 rats salt-loaded heart rate was significantly lower than SHRSP *($p<0.05$), repeated measures ANOVA. Values are presented as mean \pm SEM

3.3.2 Echocardiography - Baseline

3.3.2.1 LVMI mass assessed by Echocardiography

Left ventricular mass index (LVMI) were assessed in 21 week old WKY, SHSRP, Trans1 and Trans2 rats by echocardiography immediately prior to sacrifice. When compared to the normotensive WKY, SHRSP rats had a significantly increased LVMI at 21 weeks of age (SHRSP: 3.435 ± 0.29 mg/g; WKY: 2.41 ± 0.06 mg/g, $p < 0.05$). LVMI in Trans1 and Trans 2 rats was not significantly different from WKY at 21 weeks of age (Trans1: 2.61 ± 0.31 mg/g; Trans2: 2.75 ± 0.14 mg/g. $p > 0.05$). Additionally, LVMI in Trans2 rats was significantly reduced compared to that of the SHRSP ($p < 0.05$), however, the trend towards reduced LVMI in Trans1 rats did not reach statistical significance (Figure 3-12). Statistical analysis was performed by a student's t-test.

3.3.2.2 Relative Wall Thickness

Left ventricle wall thickness was measured by echocardiography. When compared to WKY rats, SHRSP had a significantly increased relative wall thickness (RWT) at 21 weeks of age (SHRSP: 0.8 ± 0.11 mm; WKY: 0.49 ± 0.12 mm, $F = 7.9$, $p < 0.001$). RWT in Trans1 and Trans 2 rats were not significantly different from WKY at (Trans1: 0.64 ± 0.07 mm; Trans2: 0.62 ± 0.11 mm, $p > 0.05$). Additionally, RWT in Trans1 and Trans2 rats was significantly reduced compared to that of the SHRSP ($F = 7.9$, $p < 0.05$) (Figure 3-12).

3.3.2.3 Fractional Shortening

Fractional shortening was measured by echocardiography in order to help ascertain myocardial contractility parameters. There were no significant differences in left ventricular ejection fraction between WKY, SHRSP, Trans1 and Trans2 rats (SHRSP: $42.15 \pm 10.14\%$; WKY: $36.5 \pm 7.53\%$; Tran1: $46.72 \pm 11.85\%$; Trans2: $42.72 \pm 6.99\%$, $F = 2.25$, $p > 0.05$) (Figure 3-13).

3.3.2.4 Stroke Volume

In order to determine blood/volume delivery by the heart per beat, stroke volume was measured by echocardiography. Stroke volume for SHRSP rats was significantly decreased when compared to WKY, Trans1 and Trans2 rats (SHRSP:

0.2282 ± 0.034 mL; WKY: 0.43 ± 0.032 mL; Trans1: 0.32 ± 0.086 ml; Trans2: 0.34 ± 0.045 mL, $F=8.87$, $p<0.05$, $p<0.001$) (Figure 3-14). Stroke volume in Trans1 and Trans2 rats was not significantly different from WKY (Figure 3-14)

3.3.2.5 Cardiac Output

Cardiac output was measured to assess the effectiveness of the heart to deliver blood to the rest of the body. Normotensive WKY cardiac output was measured at 126.2 ± 32.39 mls/min. Cardiac output for Trans1 and Tran2 rats was not significantly different from that of the WKY (Trans1: 100.5 ± 14.94 L/min; Trans2: 106.7 ± 16.28 L/min, $F=6.42$, $p>0.05$). However, SHRSP cardiac output was significantly decreased when compared to WKY, Trans1 and Trans2 rats (SHRSP: 72.86 ± 15.23 L/min, $F=6.42$, $p<0.05$) (Figure 3-15)

3.3.2.6 Ejection Fraction

Ejection fraction was also measured by echocardiography in order to determine heart function. There were no significant differences observed in left ventricular ejection fraction between WKY, SHRSP, Trans1 and Trans2 rats (SHRSP: $79.19 \pm 10.2\%$; WKY: $79.36 \pm 8.03\%$; Trans1; $84.95 \pm 6.55\%$; Trans2 $80.48 \pm 6.39\%$, $F = 2.25$, $p>0.05$) (Figure 3-16).

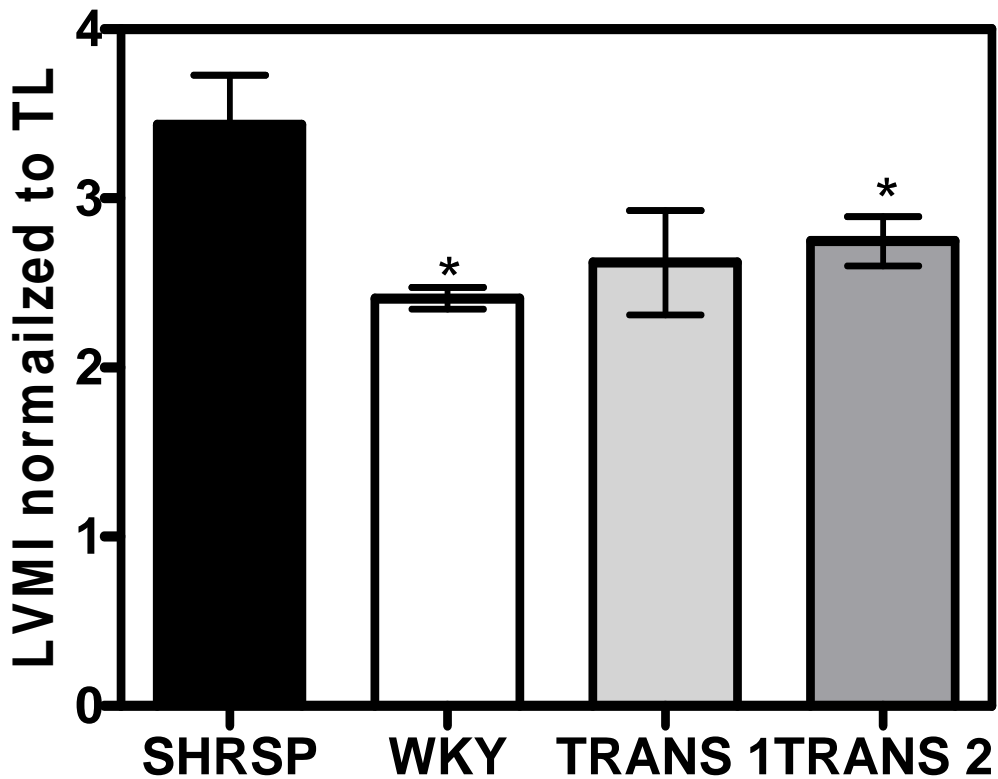


Figure 3-11: Left Ventricular Mass Index for SHRSP, WKY Trans1 and Trans2 rats
LVMI data as measured by echocardiography at 21 weeks of age, SHRSP (n=6),
WKY (n=6), Trans1 (n=8), Trans2 (n=8) rats. LVMI in WKY and Trans2 rats was
significantly less than that of the SHRSP *($p<0.05$), as compared by T-test. Values
are presented as mean \pm SEM.

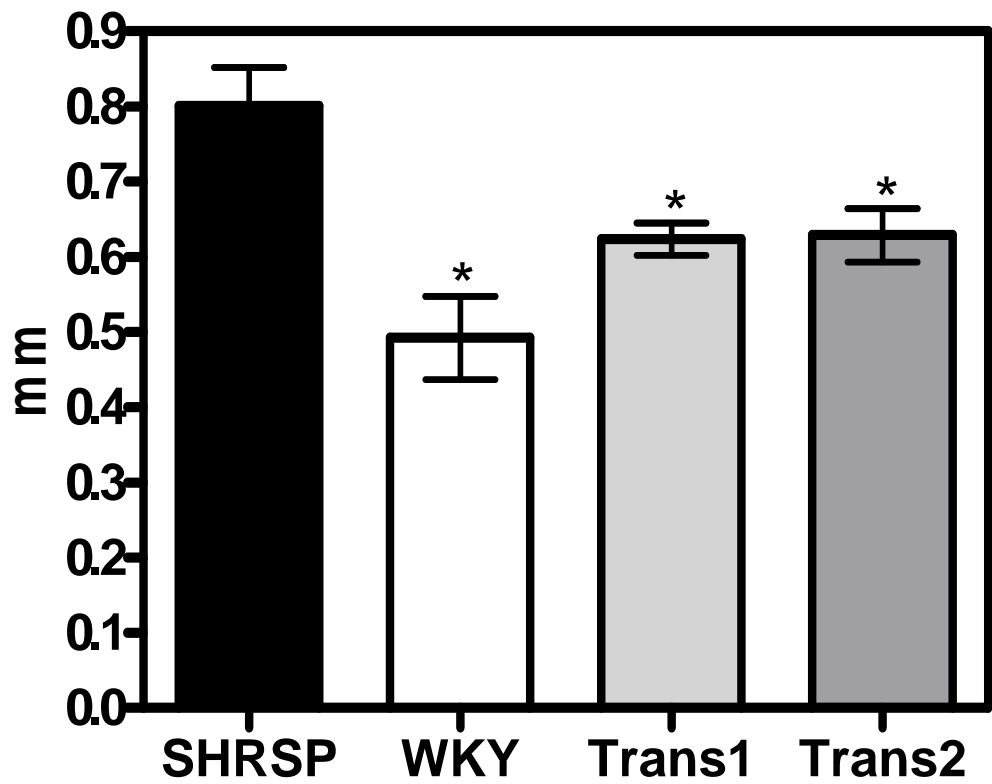


Figure 3-12: Relative wall thickness in SHRSP, WKY, Trans1 and Trans2 rats
Relative wall thickness as measured by echocardiography at 21 weeks of age, SHRSP (n=6), WKY (n=6), Trans1 (n=8), Trans2 (n=8) rats. RWT in WKY, Trans1 and Trans2 rats were significantly less than that of the SHRSP, $p<0.05$) Values are presented as mean \pm SEM.

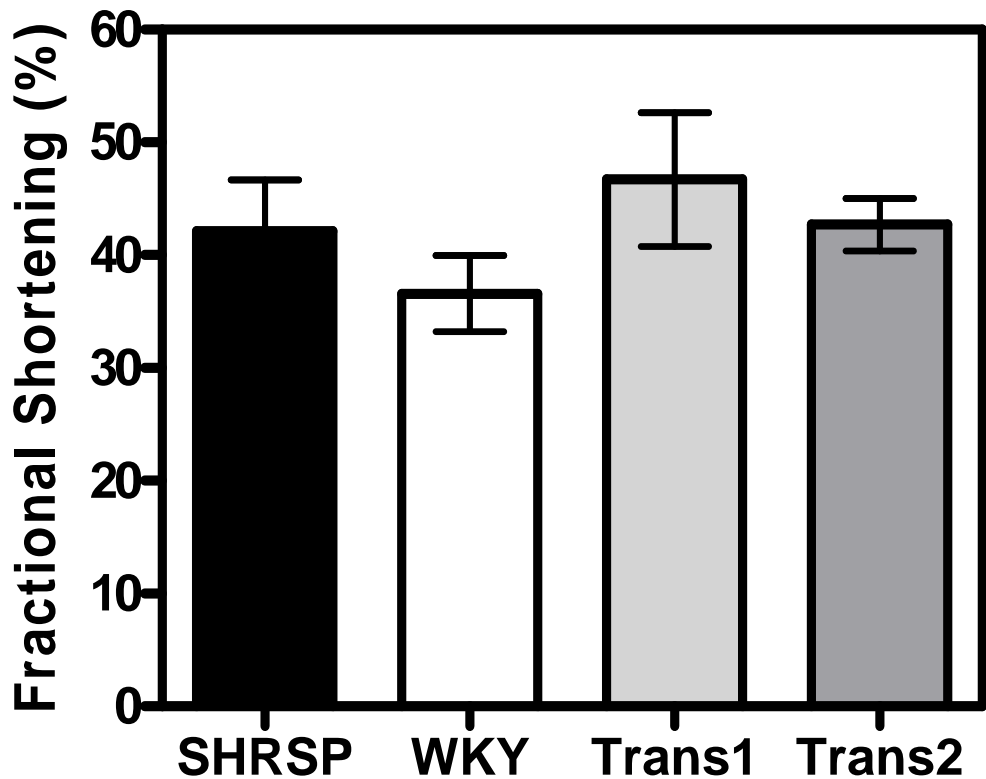


Figure 3-13: Fractional Shortening in SHRSP, WKY, Trans1 and Trans2 rats
Fractional Shortening as measured by echocardiography from 21 weeks of age,
SHRSP (n=6), WKY (n=6), Trans1 (n=8), Trans2 (n=8) rats. There were no
significantly differences between the four strains. Values are presented as mean
± SEM.

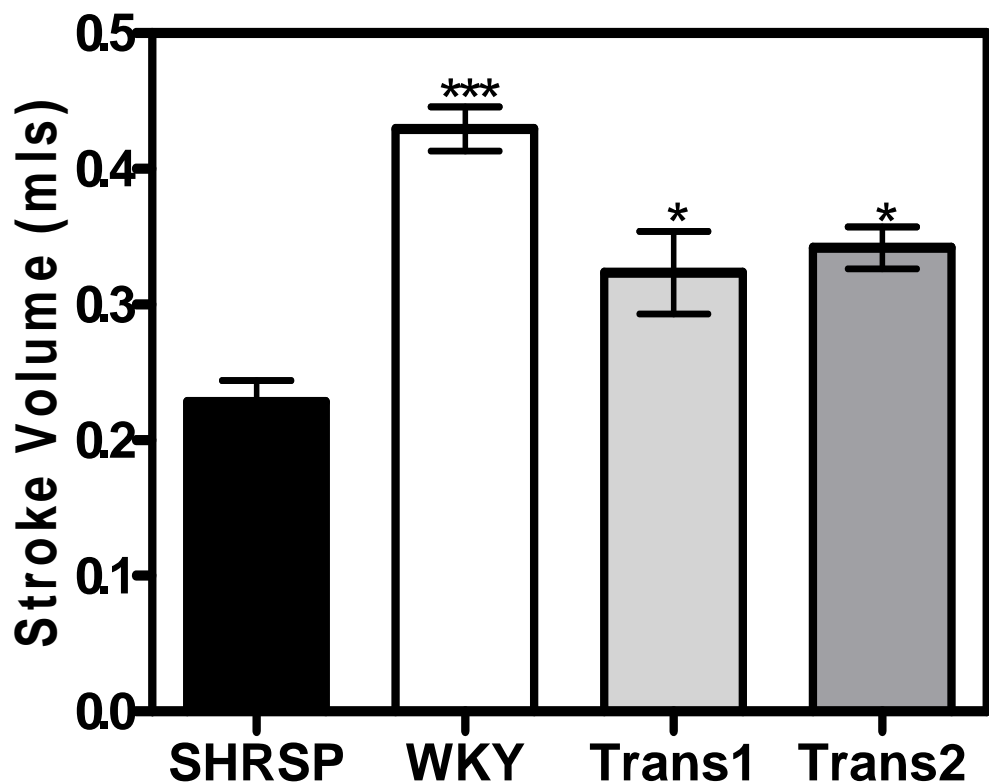


Figure 3-14: Stroke Volume in SHRSP, WKY, Trans1 and Trans2 rats
Stroke Volume as measured by echocardiography at 21 weeks of age, SHRSP (n=6), WKY (n=6), Trans1 (n=8), Trans2 (n=8) rats. Stroke volume in WKY, Trans1 and Trans2 rats was significantly greater compared to that of the SHRSP ***($p<0.001$) *($p<0.05$). Values are presented as mean \pm SEM.

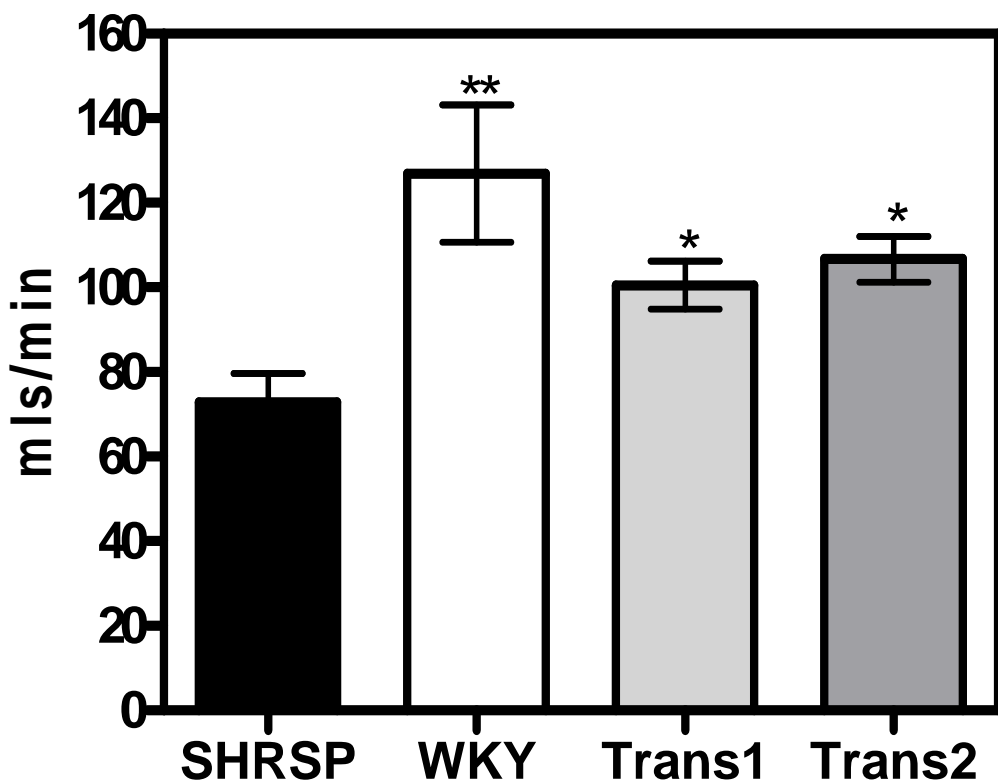


Figure 3-15: Cardiac Output in SHRSP, WKY, Trans1 and Trans2 rats
Cardiac Output as measured by echocardiography from 21 weeks of age, SHRSP (n=6), WKY (n=6), Trans1 (n=8), Trans2 (n=8) rats. Cardiac output in WKY, Trans1 and Trans2 rats was significantly different than that of the SHRSP **(p<0.001) *(p<0.05). Values are presented as mean \pm SEM.

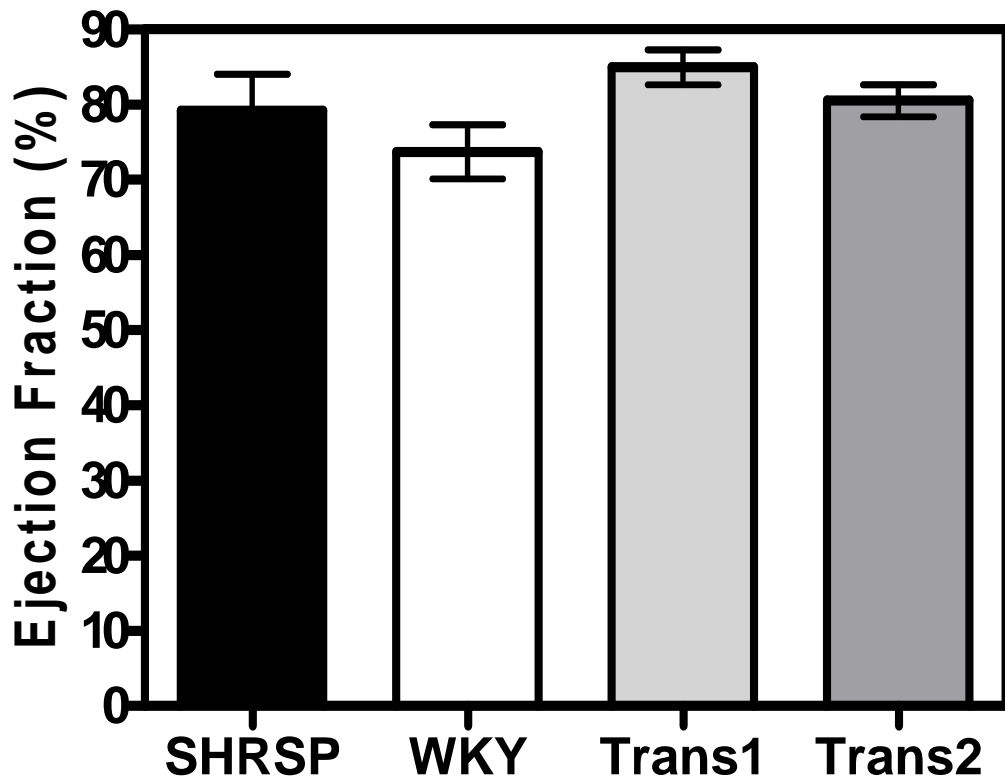


Figure 3-16: Ejection Fraction in SHRSP, WKY, Trans1 and Trans2 rats
Ejection Fraction as measured by echocardiography at 21 weeks of age, SHRSP (n=6), WKY (n=6), Trans1 (n=8), Trans2 (n=8) rats. There were no significantly differences between the four strains. Values are presented as mean \pm SEM.

3.3.3 Cardiac and Left ventricular Hypertrophy assessed at sacrifice.

Cardiac (whole heart) mass index and left ventricular (left ventricle + septum) mass index were measured to determine cardiac and left ventricular hypertrophy respectively at sacrifice (21 weeks of age). SHRSP (3.24 ± 0.04 mg/g), Trans1 (3.04 ± 0.11 mg/g) and Trans2 (3.16 ± 0.16 mg/g) rats demonstrated left ventricular hypertrophy when compared to the WKY (2.47 ± 0.06 mg/g) ($F = 32.13$; $p<0.001$) (Figure 3-17). There was no significant different between the two transgenic strains ($p>0.05$). For whole heart normalized to body weight, SHRSP (4.24 ± 0.04 mg/g), Trans1 (4.35 ± 0.36 mg/g) and Trans2 (4.12 ± 0.14 mg/g) rats demonstrated cardiac hypertrophy when compared to the WKY (3.34 ± 0.04 mg/g) ($F = 30.88$; $p<0.001$). There was no significant difference between the two transgenic lines ($p>0.05$) (Figure 3-18).

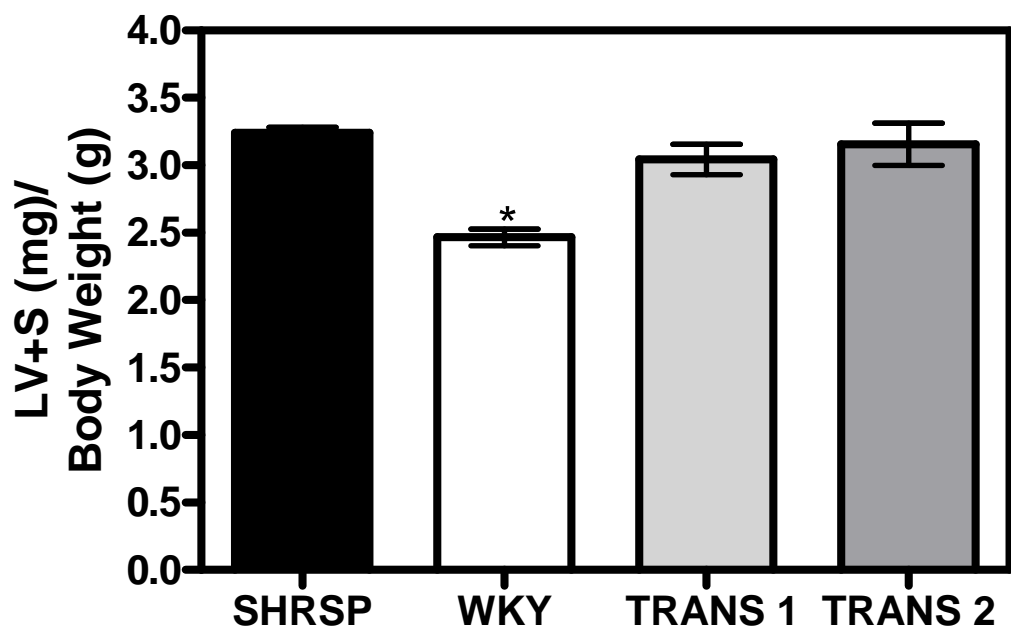


Figure 3-17: LVMI in SHRSP, WKY Trans1 and Trans2 rats

Left Ventricular mass index normalized to body weight at 21 weeks of age, SHRSP (n=6), WKY (n=6), Trans1 (n=8), Trans2 (n=8) rats at sacrifice. LVMI in WKY was significantly less than that of the SHRSP, Trans1 and Trans2 rats *($p<0.05$), one-way ANOVA. Values are presented as mean \pm SEM.

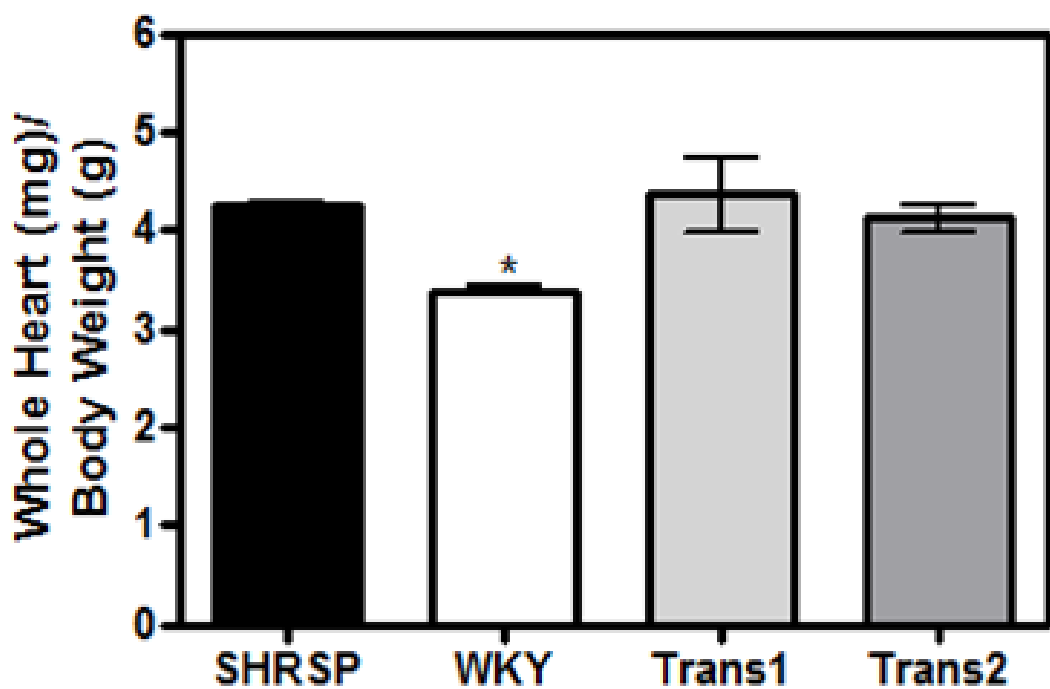


Figure 3-18: Cardiac mass index in SHRSP, WKY Trans1 and Trans2 rats
Whole heart weight normalized to body weight at 21 weeks of age, SHRSP (n=6),
WKY (n=6), Trans1 (n=8), Trans2 (n=8) rats at sacrifice. Cardiac mass index in
WKY rats was significantly less than that of the SHRSP, Trans1 and Trans2 rats
*(p<0.05). Values are presented as mean \pm SEM.

3.4 Discussion

In this Chapter significant reduction in hemodynamic parameters measured by radiotelemetry in *Gstm1* transgenic SHRSP rats provides convincing evidence that *Gstm1* plays an important role in blood pressure regulation in the SHRSP rat. In parallel with the significantly lower SBP, DBP and PP we also observe significantly improved cardiac function and reduced cardiac hypertrophy in the two independently generated transgenic lines. Moreover, the observed reduction in systolic blood pressure is remarkably similar in magnitude to that demonstrated in the Chromosome 2 congenic strain, SP.WKYGla2c*, in which *Gstm1* was identified as a candidate gene for hypertension (78). Importantly, these findings demonstrate that significant improvements in hemodynamic and cardiac parameters occur in two independently generated transgenic lines. These findings support the hypothesis that *Gstm1* plays a central role in blood pressure regulation, since random insertion of the transgene into two distinct genomic locations leads to similar levels of functional cardiovascular improvement.

Whilst the overall outcome of random *Gstm1* transgene insertion in the SHRSP is a significant reduction in the hypertensive phenotype, there are some subtle differences between the two independently generated transgenic lines. For example while diastolic blood pressure for both Trans1 and Trans2 rats is significantly lower than that of the SHRSP, the diastolic pressure profiles differ in the rate of increase over time between the two transgenic lines (Figure 3-2). Diastolic blood pressure in Trans1 rats originates lower than that of the SHRSP and remains significantly lower throughout the measurement period. On the other hand, diastolic blood pressure in Trans2 rats starts at a similar level to that of the SHRSP, but remains constant over time. These diastolic profile differences between the two independent transgenic lines could be a result of a number of factors. These factors include transgene insertion site effects, line specific mRNA or protein level differences, and/or variability due to small numbers in the Trans2 line resulting from breeding difficulties.

When transgenic lines are generated by microinjection of a transgene into a fertilized embryo there is the potential for the transgene to insert anywhere within the genome. Independently generated lines are highly unlikely to have the transgene inserted into the same genomic position, and thus have the same

effect. Furthermore, there is also a possibility that the transgene will insert into a region containing a gene that contributes to blood pressure regulation, and thereby, blood pressure control may be impacted by the insertion site. One example to illustrate the potential diversity in phenotypes between two independently generated transgenic rat lines with the same inserted transgene is the CD-36 transgenic SHR rat generated by Pravenec *et al.* (121). In this example, while two independent transgenic lines were produced using the same EF1- α promoter, there are unique differences between the transgenic lines. While incorporation of cd-36 ameliorated insulin resistance in both lines, one line had an additional effect of a modest decrease in blood pressure (121). Additionally, when developing transgenic lines, it is often difficult to ascertain what impact the insertion site will have on a particular phenotype. The generation of more than one transgenic line (using the same transgene and promoter) is therefore important in order to confirm that the phenotypic differences are the result of the transgene itself and not the insertion site. If the phenotypic changes are similar between two independently generated lines then this provides confidence that the phenotype differences are due to transgene functional effects (rather than insertion site effects).

Other factors that could contribute to line specific differences are mRNA or protein expression level differences within each independent line. Since each line was derived separately, Trans1 and Trans2 will most likely have a unique expression patterns with a distinct copy number profiles. Furthermore, transgene insertion by microinjection has the potential to insert multiple copies of the gene into the recipient genome (7;121). In other transgenic animals, studies have shown that gene expression is associated with copy number which resulted in varying effects on each transgenic line (241;242). Differences like copy number and expression patterns between Trans1 and Trans2 may be responsible for the line specific differences in diastolic BP profile. However without further investigation, it is difficult to reconcile the impact of copy number variation specifically on the rate of diastolic BP increase over time observed in the two rat lines.

An alternative explanation for the diastolic BP differences between the two transgenic lines could simply be due to breeding issues experienced with the Trans2 line. Trans2 rats were difficult to breed; showing low fertility throughout

the length of the project. Due to limited numbers of male stock animals, Trans2 rats underwent the radiotelemetry BP monitoring and echocardiography protocols at a later stage compared to Trans1 rats and parental strains. Some phenotypic drift is not uncommon in inbred rat colonies and may contribute in part to the DBP differences observed here.

In order to investigate the potential role of *Gstm1* deficiency in the salt-sensitivity phenotype in SHRSP rats, parental strain rats and Trans1 animals underwent 1% salt loading starting at 18 weeks of age, i.e. after the onset of adult hypertension. While some salt-sensitivity was evident in the Trans1 animals (i.e. exaggerated night-time daytime blood pressure variation) similar to the SHRSP, there was still a significant decrease in systolic and diastolic blood pressure compared to the SHRSP. This reduced hemodynamic profile during salt-loading is in contrast to the profile observed in the chromosome 2 congenic strain (SP.WKY_{Gla}2c*), which showed no significant difference in blood pressure profile compared to the SHRSP during salt-loading(78). However, there are many differences between the SP.WKY_{Gla}2c* strain and the *Gstm1* transgenic rats, such as the insertion of a single gene (in the transgenic) in contrast to a relatively large introgressed genomic region (in the congenic, approximately 59Mbp with boundary markers D2Wox9-D2Mgh12), that could potentially affect response to salt. The Trans1 line demonstrates similar blood pressure reduction during both baseline and salt-loading periods; therefore, we can conclude that the WKY-form of the *Gstm1* gene may play an important role in the preventative effects on salt-sensitivity in our transgenic animals.

Multiple publications suggest that pulse pressure is a better predictor of cardiovascular risk than isolated systolic or diastolic blood pressures (243;244). Figure 3-3 shows that pulse pressure is significantly reduced in both transgenic lines. While pulse pressure levels in Trans2 rats is more similar to that of the WKY than Trans1 rats, both lines show a reduction of cardiovascular risk when compared to the SHRSP. Elevated pulse pressures are thought to be associated with increased artery stiffness (245). Franklin *et al.* states that a high pulse pressure may reflect already diseased arterial walls in addition to several other adverse cardiac implications of potential prognostic value (245;246). Furthermore, several studies state that there is an association between pulse

pressure and a risk of morbid cardiovascular events which is independent of systolic and diastolic blood pressure (243).

When investigating the effects of salt loading on pressure, our data show that diurnal variation is exaggerated in SHRSP compared to WKY and Trans1 rats (Figure 3-7) which is in agreement with previously published data in salt-loaded parental strains (240). Koh-Tan *et al.* explains the importance of pulse pressure variability and its effects on end organ damage (240). In particular, the lack of blood pressure regulation has been shown to be correlated with the development and severity of renal damage (240;247;248). This damage is a result of altered microcirculation within the glomerular arterioles where a high pulsatile glomerular filtration rates may expose the glomerular capillaries to potentially damaging effects that lead to vascular damage in the kidneys (247). Measurement of vascular function and end organ damage are therefore pertinent considerations in this study and will be discussed in further chapters.

Echocardiography measurements allowed investigation of cardiac function and cardiac hypertrophy in the SHRSP, WKY and transgenic rats. Both fractional shortening (FS) and ejection fraction (EF), which are the most commonly used indexes of global left-ventricular systolic function, showed that there was no significant differences between the four strains. This data confirms previous findings at 16 weeks of age in the parental strains, and thus allows us to conclude that the insertion of the transgene did not have any adverse effects on cardiac function (239). Relative wall thickness, another commonly used parameter to describe the degree of left ventricular hypertrophy, was significantly reduced in WKY, Trans1, and Trans2 rats when compared to the SHRSP. While RWT in Trans1 and Trans2 rats was not reduced to WKY levels, they were not significantly different and thus showing an intermediate phenotype. Previous studies done in our lab have shown that in the SHRSP at 16 weeks of age, cardiac fibrosis (interstitial and perivascular) is observed (249;250). While cardiac fibrosis was not measured at 21 weeks in this study, we would hypothesize that there is a reduction of cardiac fibrosis in Trans1 and Trans2. However, while there is an improved cardiac function in the Tran1 and Trans2 lines, we cannot determine if this change is due to increased *Gstm1* expression or if this reduction is a secondary effect of the significantly lowered blood pressure in the transgenic animals. There is a lack of literature regarding a role

for *Gstm1* in cardiac disease. A fairly recent review by Conklin (251) on cardiovascular studies in humans states that little is known about how much *Gstm1* contributes to GST activity in cardiovascular tissues. These conclusions, in relationship to our findings, indicate that further investigation is required to determine the role that *Gstm1* plays in the healthy and diseased heart.

In conclusion, the production of two independent *Gstm1* transgenic lines generated on the SHRSP genetic background has provided a unique opportunity to investigate causality of *Gstm1* deficiency on the development of hypertension and cardiac hypertrophy. In this Chapter we have demonstrated a significant reduction in blood pressure in both transgenic rat lines, and improved cardiac function. This data supports the hypothesis that reduced renal *Gstm1* plays a causative role in oxidative stress mechanisms underlying the development of hypertension in the SHRSP.

**4 Molecular Characterization of the Effects of
Gstm1 Over Expression in the Transgenic
SHRSP**

4.1 Introduction

In the previous chapter it was demonstrated that *Gstm1* transgenic SHRSP rats have a significant decrease in systolic blood pressure and cardiovascular hypertrophy when compared to the parental SHRSP strain. The next stage of our study was designed to investigate the molecular changes occurring as a result of transgenic rescue of *Gstm1*. As previously mentioned, *Gstm1* was identified as a positional and functional candidate gene through a series of experiments involving the generation of chromosome 2 congenic rat strains and microarray expression profiling(78;87). These studies demonstrated that expression of *Gstm1* in the kidney was significantly reduced at 16 weeks of age in SHRSP compared to the chromosome 2 congenic strain (SP.WKY_{Gla}2c*) and normotensive WKY strains (40;85). Furthermore, additional microarray expression profiling and qRT-PCR validation demonstrated that *Gstm1* expression in 5 weeks old SHRSP rats was significantly reduced when compared to WKY and SP.WKY_{Gla}2c* rats (252). Taken together with the findings in the 2c* congenic strain, this reduction in expression prior to the onset of hypertension in this model is consistent with the hypothesis that reduced *Gstm1* expression is likely to be a causative factor in increased blood pressure and not a secondary event. In line with these early expression differences in the SHRSP, evidence in the literature also demonstrates that *Gstm1* expression in the SHR is reduced at 3 weeks of age when compared to the WKY (253).

In addition to the differences in *Gstm1* expression profile, previous DNA sequencing of the upstream regulatory region of *Gstm1* identified 13 single-nucleotide polymorphisms (SNPs), a missense mutation and a SNP in the 3' untranslated region (UTR) of the SHRSP and SHR that were not identified in the WKY or BN (254;255). Additionally, luciferase promoter assays implicated five SNPs to be responsible for significant reduction in *Gstm1* expression in the SHRSP (223). However, establishing definitive proof that a gene affects blood pressure requires evidence that changing the expression of the candidate gene in isolation, alters blood pressure. Depending on the direction of change of the implicated gene, this can be achieved by generating knockout, knock-in (targeted) or untargeted over-expression transgenic rat models. However, prior

to 2009 the ability to generate transgenic rats was severely limited due to the fact that, unlike the mouse, it was not possible to generate and maintain rat embryonic stem (ES) cells.

Despite these previous ES cell restrictions, technology did allow for 'transgenic rescue' in the rat, whereby normally functioning genes were microinjected into embryos of disease models in order to provide definitive proof of causality. An example of this gold standard method is the derivation of the CD-36 transgenic rat, whereby the CD-36 candidate gene was originally identified by QTL analysis and congenic strain construction and then confirmed by transgenic rescue (CD-36 overexpression) (121;256). Other examples included generation of transgenic animals expressing an antisense sequence to reduce expression of target genes (257), dominant negative mutants in order to induce dwarfism (258), or siRNA-expressing constructs (259). Since these early studies many transgenic rats, whether over-expression or knockout, have been produced for the advancement of cardiovascular studies (260-262). The generation of transgenic rats are fundamentally similar to that of a transgenic mouse where microinjection of the construct into the pronucleus of a single-cell embryo is followed by implantation into recipient females and resultant pups are screened for positive markers. However, these techniques are more successful in mice, typically generating 3%-5% transgene-positive offspring per injected embryo (263), compared to 0.2%-2% in rats (264;264).

Based on these successful transgenic investigations, and specifically the CD-36 study (121), the SHRSP *Gstm1* transgenic rat was produced using the WKY variant of *Gstm1* gene under the direction of the EF-1 α promoter. The EF-1 α promoter is a commonly used mammalian ubiquitous or "house-keeping" promoter. This gene has a housekeeping function in all cells and is expressed to high levels. Importantly, due to its indispensable housekeeping function in all cells, EF-1 α promoter expression is consistent from a temporal viewpoint, relatively insulated from changes in cell physiology and is cell type independent (265;266). There are several potential drawbacks associated with the production of transgenic lines using untargeted over-expression methods. These include random insertion sites, expression incompatibilities that could result in disrupted expression of vital genes, possible lethal transgene over-expression, insertion site discordance, and copy number variation (267-270).

It is hypothesized that incorporation of wild type *Gstm1* into the SHRSP genetic background will result in significantly increased *Gstm1* mRNA and protein expression in the kidney and other organs. Moreover, a better understanding of the transgene expression profile within the SHRSP *Gstm1* transgenic rat will help to elucidate whether the changes in both cardiac mass and cardiac function (as demonstrated in the previous Chapter) are simply secondary effects to the lower blood pressure or if *Gstm1* is having a direct effect on the heart.

The aims of the chapter were (1) to determine whether incorporation of WKY (wild-type) *Gstm1* within the SHRSP genome results in increased expression of *Gstm1* in cardiovascular relevant tissues (i.e. kidney, brain, heart, aorta, liver). (2) To determine if changes in mRNA expression leads to significant differences in protein expression and determine where expression is localized. (3) To identify the transgene insertion site in both transgenic lines and to determine if there are multiple copies.

4.2 Materials and Methods

4.2.1 Animal Strains

Male SHRSP, WKY, Trans1 and Trans2 rats (n=6-8) were sacrificed at 5 weeks of age (before onset of hypertension) and at 21 weeks of age (established hypertension). Kidney, heart, liver, thoracic aorta, and brain were taken during tissue harvest under deep terminal anaesthesia. Tissues were snap frozen in liquid nitrogen and stored at -80°C for analysis of DNA, mRNA or protein expression or fixed in 10% formalin for IHC.

4.2.2 mRNA Expression

4.2.2.1 qRT-PCR

RNA was extracted, quantified, DNase treated and reverse transcribed as described in section 2.4 in tissues from 5-week-old and 21-week-old male rats. Total mRNA expression of *Gstm1* and other *Gstm* family members were assessed by Applied Biosystems Gene Expression Assays and Custom Gene Expression Assays were used for all qRT-PCRs. The reaction constituents and temperature cycling parameters were as follows:

Table 4-1:Taqman Reagent List

Reaction Mixture	Volume
Master Mix	2.5
20x Gene Expression Assay	0.25
20X GapDH or β-Actin Assay	0.25
cDNA	2.0

Table4-2: Temperature Cycling for Taqman

Temperature	Time
50 °C	2 min
95 °C	10 Min
95 °C	15 sec
60 °C	1 min
Repeat steps 3 & 4 35x's	

All samples were amplified in triplicate with at least three treatment replicates included per experiment. Fluorescence of FAM and VIC dyes was measured for all reactions during temperature cycling. For all tissues, except heart, β-Actin was used as the housekeeping gene. For heart, GAPdH was used as the housekeeping gene. Data was analyzed as detailed in section 2.4.4.

4.2.2.2 SYBR Green

For transgene or WKY (wild-type) gene expression, Exiqon custom locked-nucleic acid SYBR Green probes were used, see section 2.4.4.1 for further details. The exact primer sequence for the LNA-SYBR green probes is copyrighted by Exiqon and is unknown outside of the company. However, it was assured that the primers overlap the SNPs specific to the WKY and transgene sequence of the *Gstm1* gene.

4.2.3 Protein Expression and Localization (IHC)

4.2.3.1 Protein expression

Protein was extracted from tissues using a Hepes lysis buffer (50mM Hepes, 1mM DTT, 0.5% Tween, ph 7.4). On the night before extraction, one tablet of Roche EDTA-free protease inhibitor cocktail tablet was added for every 10 mls of Hepes lysis buffer used. The samples were homogenized in cold Hepes lysis buffer (1ml of Hepes buffer for up to 0.3g of tissue). The homogenates were kept on ice until centrifuged at 14,000 rmp for 10 mins at 4 °C and the supernatant containing the protein was transferred to a new tube and kept on ice. 5µL of supernatant was

removed to determine protein concentration by nanodrop method. The rest of the protein was stored at -80 °C until required.

4.2.3.2 Western Blot

Protein samples were prepared and quantified as described in sections 2.6.1 and 2.6.2. Gel electrophoresis and blotting were carried out on these samples as described in section 2.6.3. Into each lane, 30µg of protein sample prepared in an equal volume of 2x sample reducing buffer was loaded and a low range rainbow marker was used to determine band size. For immunodetection the membrane was incubated at 4 °C overnight with a rabbit anti-rat *Gstm1* polyclonal antibody (gift from Prof. John Hayes, University of Dundee) used at a dilution of 1:5000 followed by a goat anti-rabbit IgG secondary antibody conjugated to horseradish peroxidase (Dako) at 1:2000 for one hour at room temperature. Bands were visualised using enhanced chemiluminescence, as described in section 2.6.4

4.2.3.3 Protein Expression and Quantification

The antisera used to assess the protein expression and localization of the *Gstm1* by immunohistochemistry were gifts from Prof. John D. Hayes. The protein concentration of each sample was determined using a Peirce BCA (bicinchoninic acid) protein assay kit according to the manufacturer's instructions. The bovine serum albumin (BSA) standards were diluted to appropriate concentrations for the standard curve while the protein samples were diluted accordingly to fit within the standards spectrum

4.2.3.3.1 IHC

Sections cut to 6 µm thickness were de-paraffinised and hydrated by 2x7 minute washes in Histoclear before going down an ethanol gradient of 100%, 95% and 75% for 7 minutes at each stage. Sections were then washed in water for 7 minutes. Endogenous peroxide was then quenched by incubating slides for 30 minutes in 0.3% H₂O₂ (10ml 30% to 1L) in methanol at room temperature. Sections were then rinsed in 2 x 10 minute water washes. Sections were blocked for 60 minutes with 2% normal serum in PBS (2 drops of ABC kit blocking serum in 5ml PBS or 100µl appropriate serum in 5ml PBS). Slides were placed in humidified trays in order to prevent slides from drying out. Excess blocking reagent was removed and

replaced with 1° Ab/antiserum or negative control diluted in blocking serum for overnight at room temperature. The following day, sections underwent 3x5 minutes washes in PBS. A biotinylated 2°Ab antibody, diluted in blocking reagent (ABC universal kit, 2 drops blocking serum + 2 drops supplied vectastain biotinylated antibody + 5ml PBS) was added for a 30 minute room temperature incubation. This was followed by 3x5 minute PBS washes. If the ABC 2°Ab antibody was used, and ABC complex was added to the sections and incubated for 30 minutes at room temperature. This was followed by 3x5 minute PBS washes. DAB chromogen (DAB substrate kit) for universal and peroxiase 2°Ab antibody was prepared following manufacturer's instructions. Sections were incubated for 5 minutes at room temperature in a humidified chamber and then washed for 5 minutes in water. Sections were counterstained with Haematoxylin for 90-120 seconds and placed under a running tap for 5 minutes. Sections were then dehydrated through a reverse ethanol gradient of 70%, 95% and 100% for 7 minutes at each stage. Immediately following, sections then washed 2x's in HistoClear for 7 minutes and mounted using Histomount (National Diagnostics, GA, USA).

4.2.4 Localization of the Transgene Insertion Site

1-3 µg of genomic DNA, that was extracted as stated in 2.5.1, was digested separately with either *HindIII* or *PstI* restriction enzymes for 1.5 hours at 37° C in 0.5 µL ependorf tubes. Resulting fragments were then ligated overnight at 16 °C with T4 ligase. Primers designed specifically for *HindIII* (*GstmFragA*) and *PstI* (*GstmFragB*) restriction sites were used as primers with the ligated templates for the first round of PCR amplification. First round PCR was performed using the primer sets *GstmFragA* (1+2) and *GstmFragB* (1+2):

GstmFragA 1- ATT GCA TGA AGA ATC TGC TTA GG
GstmFragA 2- ACA AGC AGG GAG CAG ATA CTG GC
GstmFragB 1- AAA GGA GTG GGA ATT GGC TCC GG
GstmFragB 2- CAA CGC GTA TAT CTG GCC CGT AC

Product from the first round PCR was utilized as a template for a second nested PCR reaction using nested *Gstm1FragA* (3+4) and nested *Gstm1FragB* (3+4) primer sets:

GstmFragA 3- TGT ACG GGC CAG ATA TAC GCG TTG
GstmFragA 4- GAG CAG ATT GTA CTG AGA GTG CAC
GstmFragB 3- GGT AAA CTG GGA AAG TGA TGT CG
GstmFragB 4- GAG CAG ATT GTA CTG AGA GTG CAC

For a schematic view of this process please refer to Figure 4-1.

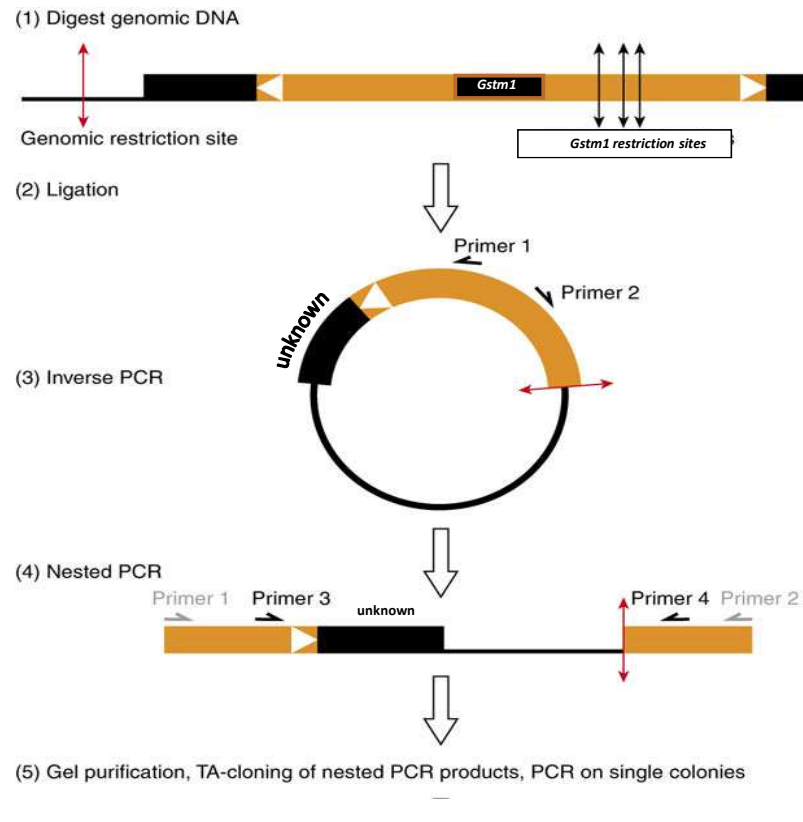
The PCR reactions were run on the Peltier Thermal Cycler (PTC-225) under the conditions 95 °C for 4 mins, 96 °C for 30s and 58 °C for 30s and 72 °C for 60s for 35 cycles, then held at 72 °C for 7 min. In order to separate the amplified fragments,

15-20 µL of PCR reaction was electrophoresed with 3µL of 6X loading dye in a 1% agarose gel at 100V for 1.5 hours, alongside a 1Kb DNA ladder.

DNA fragments that were considered the correct sizes were then isolated from the aragose gels by Qiaquick gel desolving kt (Qiaquick handbook) according to handbook instructions (Qiagen). Extracted DNA eluate was then quantified by measuring 1.5 uL of RNA sample using the NanoDop DN-1000 spectrophotometer spectrophotometer (NanoDrop Technologies LLC, Wilmington, Delaware USA) under the software program ND-1000 v3.2, in which absorbance ratios of 260 nm/280 nm equalled approximately 1.8 for DNA. This indicated that the DNA preparations were sufficiently free from protein contamination. Like RNA samples, averages of either duplicate or triplicate measurements were taken for samples requiring precise quantification.

Eluted DNA was then placed into a plasmid cloning kit (Stratoclone) and cloned according to manufacturer's instructions (Stratoclone). Positive colonies were then screened and verified by 2% X-gal. Plasmid DNA was then prepped for DNA sequencing using Qiagen Plasmid mini prep kit (Qiagen) according to manufacturer's instructions.

Plasmid DNA was sequenced by using Applied Biosystems BigDye Terminator n3.1 Cycle Sequencing kits. All reaction were performed on a 96 well plate and included included 3.5µl 5X sequencing buffer; 0.5µl Ready Reaction; 8µl template (100-200ng of plasmid DNA); ~3.2µl primer (2.0 µM Final); ~4.8µl H₂O.



IPCR amplifies the unknown DNA sequences that are immediately adjacent to the known sequence of our transgene

Figure 4-1: Schematic of the inverse PCR (IPCR) procedure with results
 Genomic DNA were digested with a restriction enzyme and ligated. Templates then underwent multiple PCR reactions in order to target specific products.
 Adapted from Bessereau (271).

The temperature program cycle was: 96 °C for 45 secs, 50 °C for 25 secs, 60 °C for 4 mins. Steps 1-2 repeated 25 times.

Sequencing was initially analyzed on Applied Biosystems SeqScape software version 2.1 to see if fragments aligned to the genome. Fragments that were aligned were then analyzed by hand and each nucleic acid was looked at in order to verify that the connecting sequences were novel and not erroneous transgene fragments. Experimental sequences were then aligned with known sequences derived from bioinformatic databases such as UCSC or ENSEMBL.

4.2.5 Copy Number Variation

Identification of the *Gstm1* transgene across generations was determined in both transgenic lines through Taq-man analysis. Copy number variation Taqman probes, SNP Genotyping Assay (Applied Biosystems) and SNP Gene Expression Assay (Applied Biosystems), were custom synthesized to a unique portion of the transgene construct. The SNP Genotyping Assay was analyzed by Taqman Genotyper, a specifically designed analysis package developed by Applied Biosystems for this assay. The SNP Gene Expression Assay was compared to a unique single copy gene (RNase P 30) that was custom designed for the genetic background of rats. Using the comparative ($\Delta\Delta CT$) method with additional steps as calculated by Applied Biosystems Copy Caller Software, copy number variation analysis was performed on the Taqman 7900.

4.2.6 Statistics

All results are displayed as mean \pm SEM and n represents the number of independent experiments performed. Data were analyzed using a one-way ANOVA followed by Tukey's post hoc test for all total gene and protein expression experiments. For Transgene expression, data were analyzed using a one-way ANOVA followed by Newman-Keuls' post hoc test.

4.3 Results

4.3.1 ***Gstm1*** Expression in Cardiovascular Relevant Tissues

4.3.1.1 Kidney

In order to fully assess changes in renal *Gstm1* expression in both transgenic lines, transgene (or WKY form) mRNA specific expression in addition to protein and IHC expression profiles were measured. At 5 weeks of age, total renal *Gstm1* expression was assessed by quantitative real time PCR (qRT-PCR) in male WKY, SHRSP, Tran1 and Trans2 rats. Total renal *Gstm1* mRNA at 5 weeks of age was significantly higher in Trans1, Trans2 and WKY rats compared to SHRSP ($p < 0.05$) (Figure 4-2). Furthermore, while renal expression of *Gstm1* in the Trans1 line was significantly less than that of the WKY, expression in the Trans2 line was not different from WKY expression. Transgene specific (or the WKY variant of *Gstm1*), renal *Gstm1* mRNA was assessed by SYBR quantitative real time PCR (qRT-PCR) in male WKY, SHRSP, Trans1 and Trans2 rats. Expression of transgene renal *Gstm1* mRNA at 5 weeks of age was significantly higher in Trans1, Trans2 and WKY rats when compared to with SHRSP ($p < 0.05$), (Figure 4-2). To further investigate the extent of the changes in *Gstm1* expression, total protein *Gstm1* levels in the kidney were measure by western blot and Immunohistochemistry (IHC). At 5 weeks of age, total *Gstm1* protein in Trans2 and WKY rat kidneys were significantly increased when compared to SHRSP levels. While protein levels in Trans1 rats were similar to that of Trans2, they were not significantly different from that of the WKY nor were they significantly different from that of the SHRSP (i.e. they were intermediate) (Figure 4-2). These expression levels were also confirmed with IHC where expression was found mainly in the distal tubules (Figure 4-2).

At 21 weeks of age, total renal *Gstm1* mRNA was significantly higher in Trans1 and WKY rats when compared to with SHRSP ($p < 0.05$), (Figure 4-3). Transgene renal *Gstm1* mRNA was significantly higher in Trans1 and WKY rats when compared to with SHRSP ($p < 0.05$), while Trans2 rats showed very little transgene expression (Figure 4-3). At 21 weeks of age, WKY *Gstm1* protein levels were significantly increased compared to that of the SHRSP (Figure 3-10) *($p < 0.01$). *Gstm1* protein levels in Trans1 and Trans2 rats were not significantly

different from that of the SHRSP ($p>0.05$). These expression levels were also confirmed with IHC, and similarly to 5 week kidneys, expression was found mainly in the distal tubules (Figure 4-3).

4.3.1.1.2 Total *Gstm1* expression in other cardiovascular relevant tissue

For other cardiovascular relevant tissues, both endogenous and transgene *Gstm1* expression (otherwise referred to as total *Gstm1* expression) was measured at both an early developmental stage (5 weeks) and after the full onset of hypertension (21 weeks). At 5 weeks of age, heart, brain and aorta total *Gstm1* mRNA levels were assessed by quantitative real time PCR (qRT-PCR) in male WKY, SHRSP, Trans1 and Trans 2 rats. Cardiac total *Gstm1* expression was significantly increased in SHRSP compared to WKY, Trans1 and Trans2 animals ($p<0.05$) (Figure 4-4 panel A). Levels of total *Gstm1* mRNA in brain showed no significant difference between all four strains (Figure 4-4 panel B). Vascular (aorta) total *Gstm1* expression was slightly increased in Trans1 and WKY rats, and significantly increased in Trans2 rats when compared to the SHRSP ($p<0.05$) (Figure 4-4 panel C).

At 21 weeks of age, brain, heart, aorta and liver total *Gstm1* mRNA levels were assessed by quantitative real time PCR (qRT-PCR) in male WKY, SHRSP, Trans1 and Trans2 rats. Cardiac total *Gstm1* expression was significantly increased in the Trans1 line when compared to WKY and SHRSP ($p < 0.05$) (Figure 4-5 panel A). Cardiac *Gstm1* expression in Trans2 rats showed a trend towards increase, but was not significantly different from WKY, Trans1 or SHRSP rats (Figure 4-5 panel A). Levels of total *Gstm1* mRNA in brain were significantly increased in Trans1 and Trans2 animals compared to SHRSP ($p<0.05$). There was no significant difference in neural *Gstm1* expression between SHRSP and WKY rats (Figure 4-5 panel B). Similar to findings in kidney, *Gstm1* expression in aorta was significantly increased in Trans1 and WKY rats when compared to and SHRSP ($p<0.005$) (Figure 4-5 panel C), however, aortic *Gstm1* expression in Trans2 rats showed an increased trend but was not significantly different from WKY, Trans1 or SHRSP rats (Figure 4-5 panel C). Total *Gstm1* expression in the liver was significantly increased in Trans1, Trans2 and WKY rats when compared to SHRSP ($p<0.05$) (Figure 4-5 panel D).

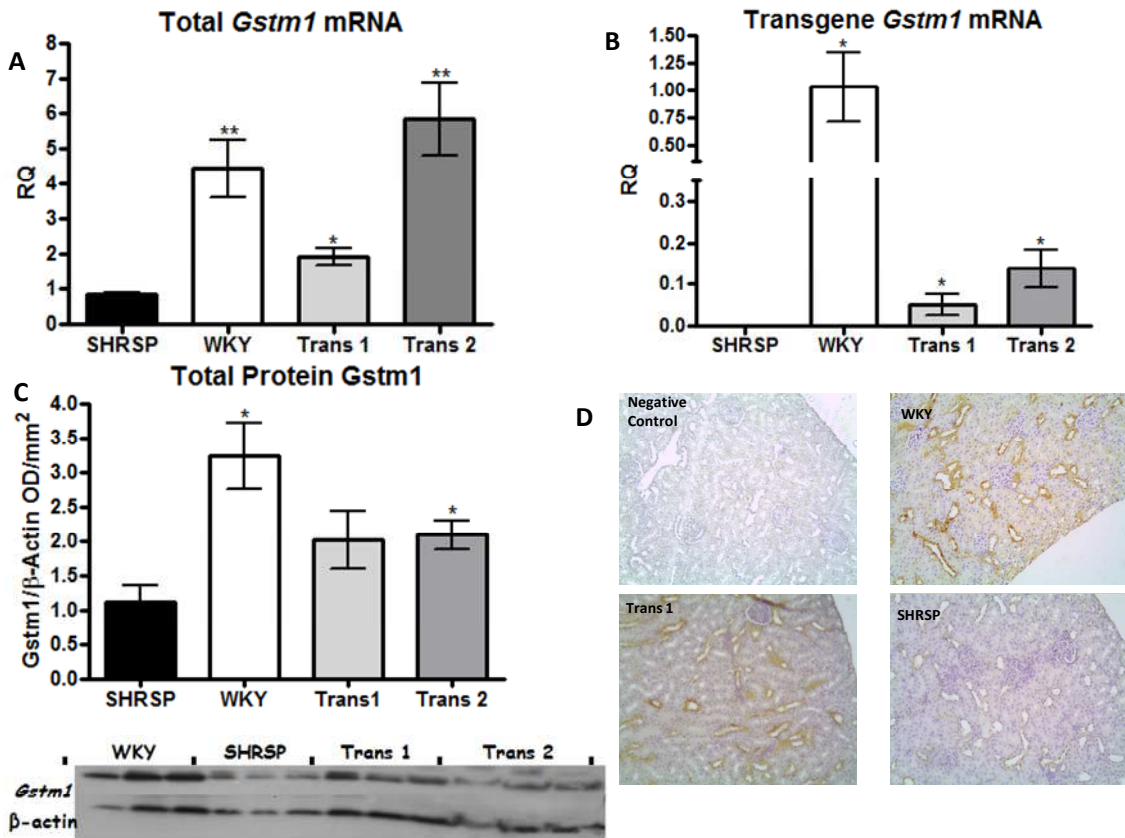


Figure 4-2: Changes in Renal *Gstm1* expression between Trans1, Trans2 and parental strains at 5 weeks.

Gstm1 expression in kidney at 5 wks of age in SHRSP (n=8), WKY (n=8), Trans1 (n=8), and Trans2 (n=3) rats. (A) Total *Gstm1* levels were significantly increased in WKY, Tran1 and Trans2 lines when compared to the SHRSP *(p<0.05) **(p<0.01). (B) WKY variant *Gstm1* levels were significantly increased in the WKY, Trans1 and Trans2 rats when compared to the SHRSP *(p<0.05). (C) Total protein was extracted from kidney tissue and resolved by gel electrophoresis. Western blot indicated an increased *Gstm1* expression in WKY, Trans1 and Trans2 rats when compared to SHRSP *(p<0.05). Increased *Gstm1* expression was confirmed by densitometry with each band normalized to *β*-Actin (n=3 for each strain). (D) IHC of *Gstm1* protein on whole kidney sections from WKY, SHRSP and Trans1 rats at 5 weeks of age. Magnification =10x. Values are presented as mean ± SEM.

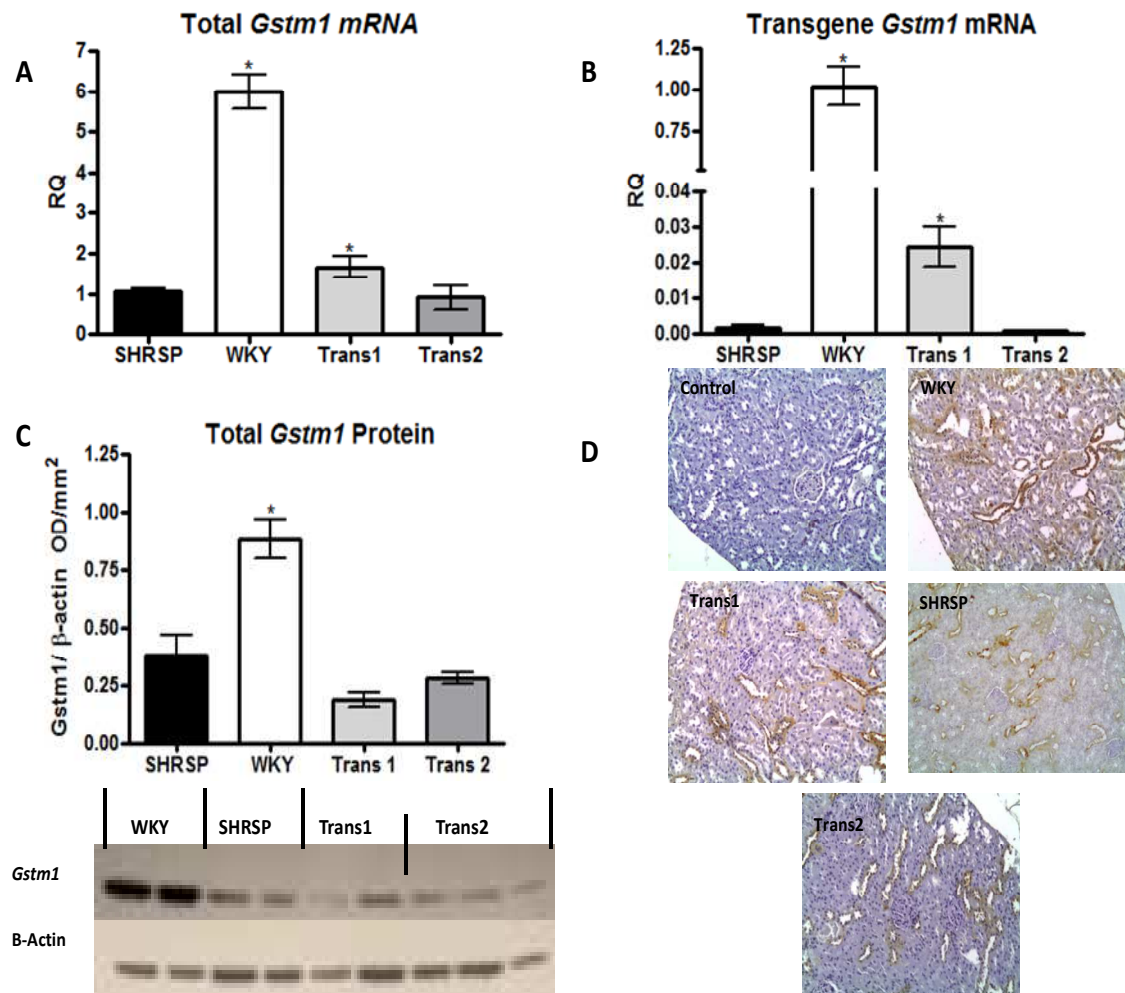


Figure 4-3: Changes in Renal *Gstm1* expression between Trans1, Trans2 and parental strains at 21 weeks.

(A) Total *Gstm1* expression in kidney at 21 weeks in SHRSP (n=8), WKY (n=8), Trans1 (n=8), and Trans2 (n=6) rats. Total *Gstm1* levels were significantly increased in WKY, Trans1 and Trans2 rats when compared to the SHRSP *(p<0.05) **(p<0.01). (B) WKY form *Gstm1* levels were significantly increased in WKY, Trans1 and Trans2 rats when compared to the SHRSP *(p<0.05). (C) Western blot indicated an increased *Gstm1* expression in WKY when compared to SHRSP *(p<0.05). Increased *Gstm1* expression was confirmed by densitometry with each band normalized to *β*-actin (n=3 for each strain). (D) IHC of *Gstm1* protein on whole kidney sections from WKY, SHRSP and Trans1 rats at 21 weeks of age. Magnification =10x. Values are presented as mean ± SEM

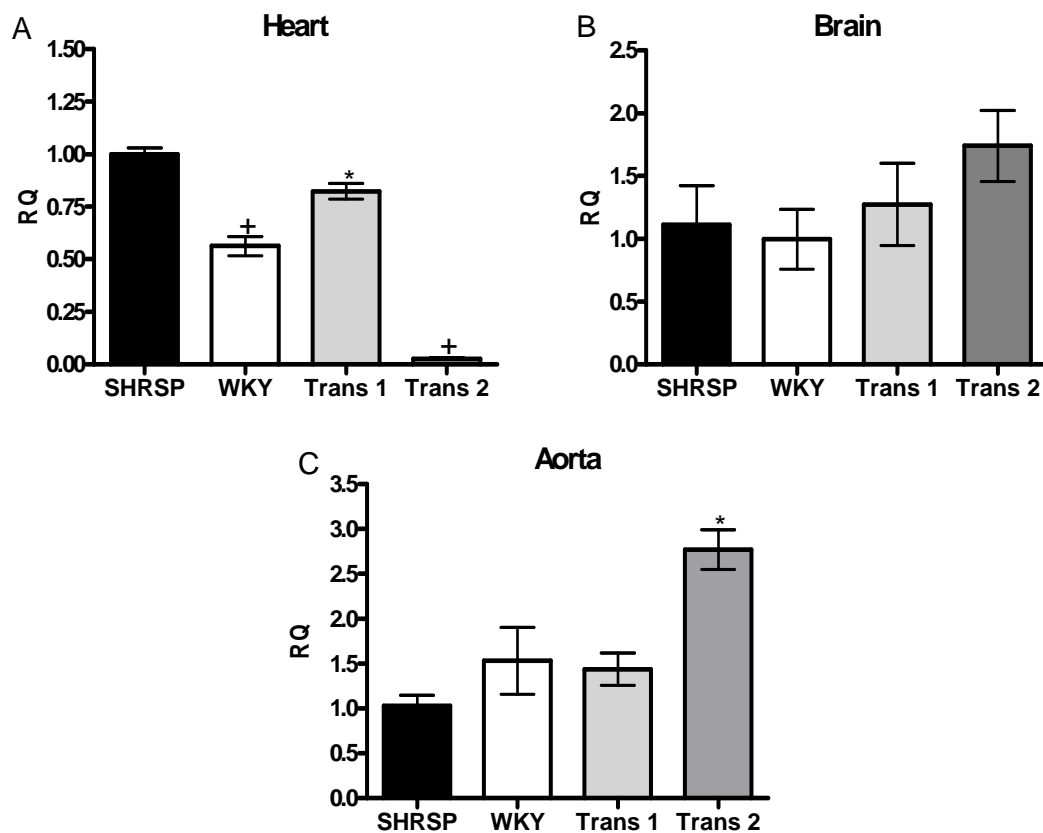


Figure 4-4: Expression of Total *Gstm1* in Cardiovascular Relevant Tissues for Trans1, Trans2 and Parental Strains at 5 wks of Age.
 Total *Gstm1* mRNA expression in (A) heart, (B) brain and (C) aorta at 5 wks of age in SHRSP (n=8), WKY (n=8), Trans1 (n=8), and Trans2 (n=3) rats. Cardiac *Gstm1* levels were significantly reduced in the animals when compared to SHRSP animals *($p<0.05$ vs. SHRSP), +($p<0.05$ vs. Trans1 rats). There were no significant differences in *Gstm1* expression levels in the brain between the four strains. Aortic *Gstm1* expression levels were significantly increased in Trans2 animals when compared to the SHRSP. Values are presented as mean \pm SEM

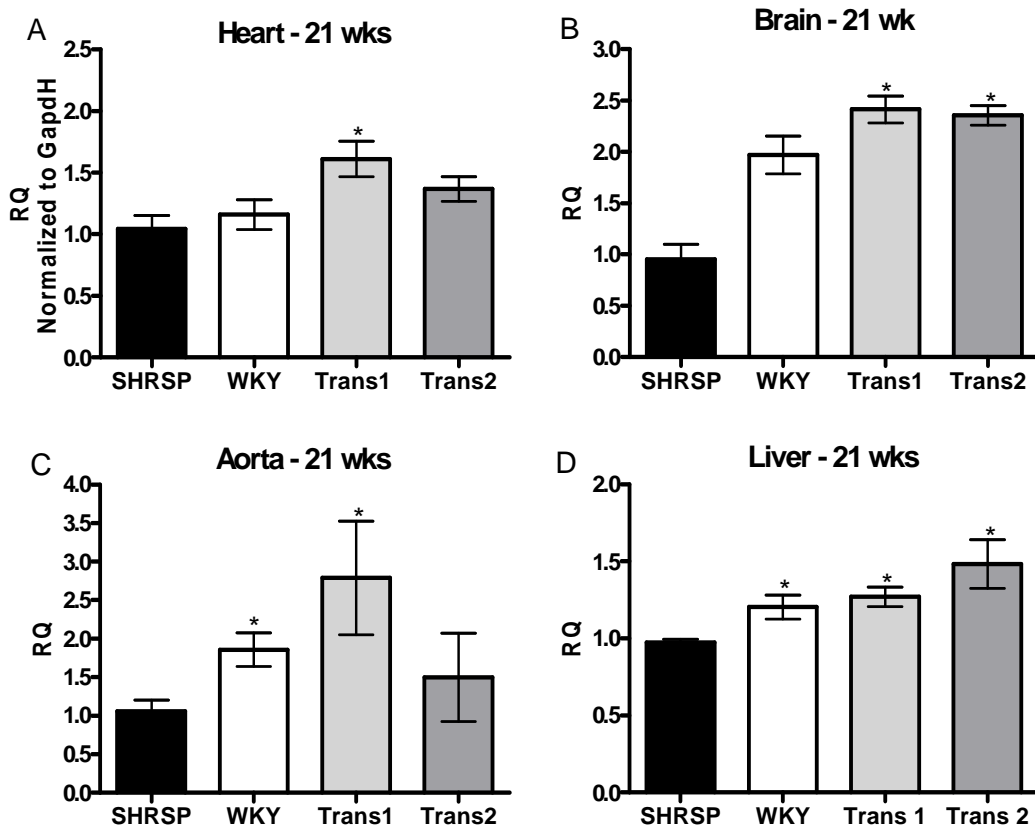


Figure 4-5: Total *Gstm1* Expression for Trans1, Trans1 and Parental Strains at 21 wks of Age in Cardiovascular Relevant Tissues

Total *Gstm1* mRNA expression in (A) heart, (B) brain, (C) aorta and (D) liver at 21 wks of age in SHRSP (n=8), WKY (n=8), Trans1 (n=8) and Trans2 (n=6) rats.

Cardiac *Gstm1* levels were significantly increased in Trans1 (n=8) animals when compared SHRSP (n=8) animals *($p<0.05$). Neural *Gstm1* levels were significantly increased in Trans1 (n=8) and Trans2 (n=6) rats when compared to SHRSP (n=8).

Aortic *Gstm1* expression levels were significantly increased in WKY (n=8) and Trans1 (n=8) animals when compared to the SHRSP (n=8) *($p<0.01$). Hepatic *Gstm1* levels were significantly increased in WKY (n=8), Trans1 (n=8) and Trans2 rats (n=6) when compared to the SHRSP *($p<0.01$). Values are presented as mean \pm SEM.

4.3.1.1.3 WKY Variant (Transgene specific) *Gstm1* expression in Cardiovascular Tissue

At 5 weeks of age, brain, heart and aortic transgene specific *Gstm1* mRNA levels were assessed by SYBR quantitative real time PCR (qRT-PCR) in male rats in the WKY, SHRSP, Trans1 and Trans 2 rats. Cardiac transgene *Gstm1* expression was significantly increased in the WKY when compared to the SHRSP ($p<0.05$) (Figure 4-6 panel A). Trans1 and Trans2 rats were not significantly difference from the SHRSP parental strain. The trend towards increased expression for the Trans2 line did not reach significance due to large variability probably due to low n numbers (Figure 4-6 panel A). Neural transgene *Gstm1* mRNA levels in WKY were significantly increased when compared to the SHRSP ($p<0.05$), however, while there was a similar increasing trend in transgene *Gstm1* expression in Trans1 and Trans2 rats, it did not reach significance ($p>0.05$) (Figure 4-6 panel B). Vascular transgene expression showed an increased trend in Trans1 and WKY rats and was significantly increased in Trans2 and ($p < 0.05$). Additionally, Trans2 vascular transgene expression was significantly increased to that of the WKY levels ($p < 0.05$) (Figure 4-6 panel C).

At 21 weeks of age, brain, heart, and liver transgene *Gstm1* mRNA levels were assessed in male rats in the WKY, SHRSP, Trans1 and Trans 2 rats. Cardiac transgene *Gstm1* expression was significantly increased in WKY when compared to SHRSP ($p<0.01$) (Figure 4-7 panel A). Cardiac *Gstm1* expression in Trans1 and Trans2 rats showed increased trends but was not significantly different from SHRSP rats (Figure 4-7 panel A). Levels of neural transgene *Gstm1* mRNA were significantly increased in WKY animals when compared to SHRSP ($p<0.01$). There was no significant difference in neural *Gstm1* expression between Trans1 and Trans2 and SHRSP animals ($p>0.01$) (Figure 4-7 panel B). Hepatic transgene *Gstm1* expression was significantly increased in WKY when compared to SHRSP ($p<0.01$) (Figure 4-7 panel C). Unfortunately, transgene expression in the aorta resulted in undefined errors where the experimentation appeared to proceed normally through all stages of testing but the instrument did not generate an analysis or provide final results at the end of the run. This lack of definite result was further investigated by Exiqon which could find no fault with the probe or

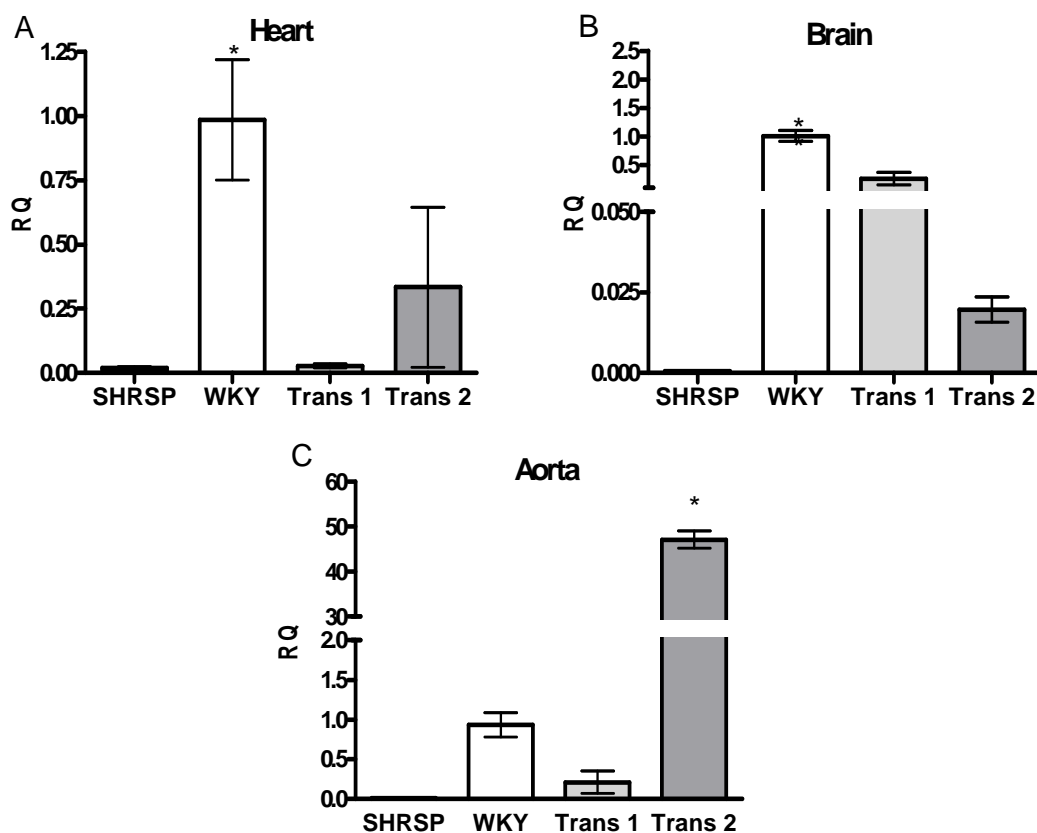


Figure 4-6: Transgene (WKY specific) *Gstm1* Expression in Trans1, Trans2 and Parental Strains at 5 Weeks of Age.

Transgene (WKY form) *Gstm1* expression in (A) heart, (B) brain and (C) aorta at 5 wks of age. Cardiac transgene *Gstm1* levels were significantly increased in the WKY (n=8) animals when compared to SHRSP (n=8) animals *($p<0.01$). Neural transgene *Gstm1* levels were significantly increased in the WKY (n=8) when compared to the SHRSP (n=8) *($p<0.01$). Aortic *Gstm1* transgene expression levels were significantly increased in Trans2 animals (n=3) when compared to the SHRSP (n=8) **($p<0.001$). Values are presented as mean \pm SEM.

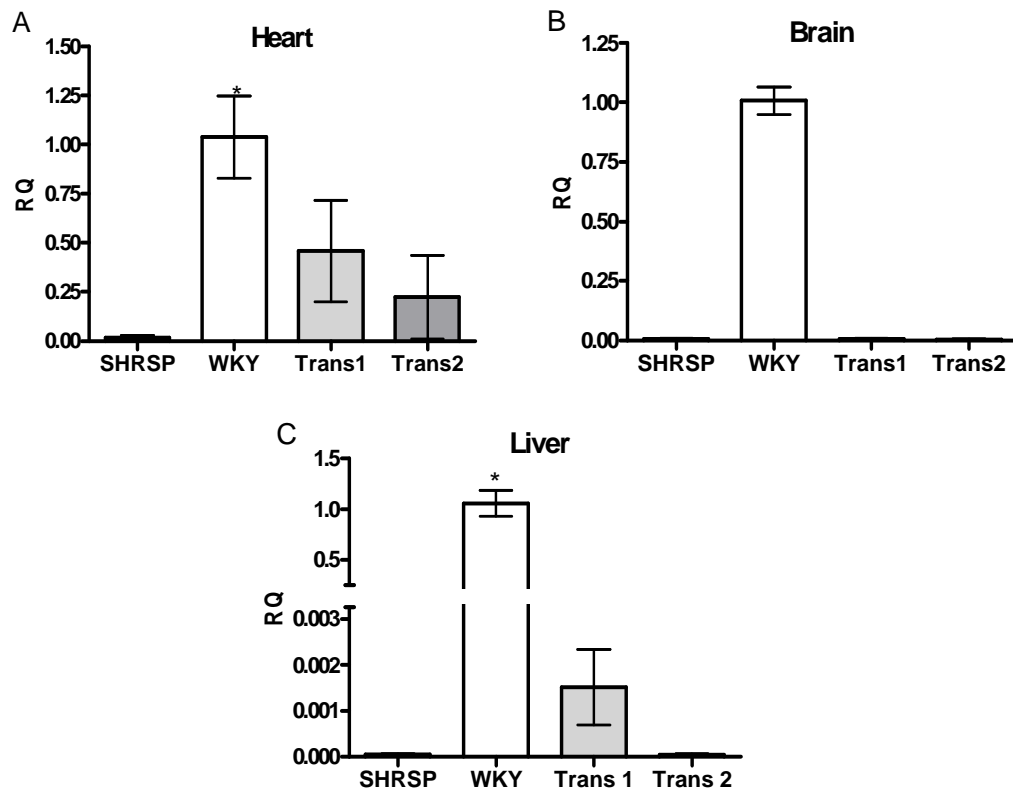


Figure 4-7: Transgene (WKY Specific) *Gstm1* Expression in Trans1, Trans2 and Parental Strains at 21 Weeks of Age.

Transgene (WKY form) *Gstm1* expression in (A) heart, (B) brain, (C) liver at 21 wks of age. Cardiac transgene *Gstm1* levels were significantly increased in WKY (n=8) when compared to SHRSP (n=8) *(p<0.01). Cardiac expression in Trans1 (n=8) and Trans2 (n=6) animals showed increased trends of expression when compared SHRSP animals. Neural transgene *Gstm1* levels were significantly increased in WKY (n=8) when compared to the SHRSP (n=8). Hepatic *Gstm1* levels were significantly increased in WKY (n=8) when compared to the SHRSP *(p<0.01) and Trans1 showed trends of increased expression. Values are presented as mean \pm SEM.

cDNA used and thus values for 21 week vascular expression data are not included.

4.3.1.1.4 Expression of Other *Gstm* Family Members

The mu family of glutathione tranfersases are highly homologous and in order to assess any changes to the mu family expression caused by the integration of the transgene, *Gstm2* and *Gstm3* mRNA expression was measured in a variety of tissues at 21 weeks of age. β -actin was used as a housekeeper for all experiments except for heart where GapdH was used. While brain *Gstm2* expression was significantly increased in the WKY compared to the SHRSP *($p<0.05$), there was no significant change in expression in neural, renal, cardiac, hepatic and vascular *Gstm2* expression in Trans1 and Trans2 rats was when compare to the SHRSP ($p>0.05$) (Figure 4-8). There was no significant change in *Gstm3* expression in the transgenic rats when compared to the SHRSP ($p>0.05$). The only significant differences in *Gstm2\3* expression occurred between WKY and Trans2 rats in renal *Gstm2* expression (Figure 4-8), and WKY and Trans1 rats in the liver (Figure 4-9).

4.3.1.2 Immunohistochemistry

To further investigate vascular *Gstm1* expression, IHC was performed on the aorta at 21 weeks of age. Measuring percent staining in the aorta demonstrated a significant increase of *Gstm1* in WKY (n=4) when compared to SHRSP (n=4) ($p<0.05$) (Figure 4-10). There was a an increased trend in protein expression for aortas in Trans1 (n=4) and Trans2 (n=4) rats which was not significantly different from either parental strain, conveying an intermediate expression (Figure 4-10)

4.3.2 Location of the Transgene Insertion Site

Inverse PCR was used to amplify regions of DNA adjacent to the transgene in order to determine the insertion site of the transgene in each of the transgenic lines. Liver genomic DNA from each transgenic line was restricted using the *HindIII* restriction enzyme, and inverse PCR was performed. Using transgene specific primers for the *HindIII* restriction site, we obtained positive PCR amplification for both transgenic lines (Figure 4-11). As shown in Figure 4-11, multiple unique bands were identified for each of the transgenic animals. These

bands were gel extracted, and the fragment was cloned into Strataclone vector. The clones were then screen and every band was sequenced. After being aligned to the transgene and IPCR sequence, results indicated that there was only one band from Trans2 rats to have unknown, or different from the transgene, sequence (Figure 4-11). This sequence was then blasted to the Brown Norway, including non-assembled trace sequences. This led to the sequence lining up to the trace sequence of rt71hp27.x. Recently, a new updated Brown Norway sequence has been made available on Ensembl with increased genome sequencing capabilities; however, unfortunately, these increases did not include the rt71hp27.x trace sequence.

After sequencing, none of the sequences for Trans1 rats using the *HindIII* restriction site were unique, and were generally inter-ligated transgene sequences, i.e. transgene fragments that were restricted and ligated onto other transgene fragments. In order to further investigate this, another restriction site, *PstI*, was used for identification of the insertion sequencing for Trans1 animals. As shown in Figure 3-14, where both *HindIII* and *PstI* restriction enzymes were used for restriction during inverse PCR, there are bands unique to the Trans1 rats when compared to the SHRSP. Unfortunately, similar to the *HindIII* restriction site, each of the *PstI* bands were either internal fragments or inter-ligated transgene fragments.

In order to ascertain that the transgene had not identically inserted itself into genome for both transgenic lines (which is highly unlikely), the primers used to verify the insertion site of the transgene into the rt71hp27.x trace sequence in the Trans2 line were used as sequencing primers for the insertion of the transgene into the Trans1 rat genomic DNA. For Trans1 line, there were no transgene sequences adjacent to the rt71hp27.x trace sequence. Allowing the conclusion, that while the exact insertion site within the genome for Trans1 rats is still unknown, it differs from that of the Trans2 line insertion site.

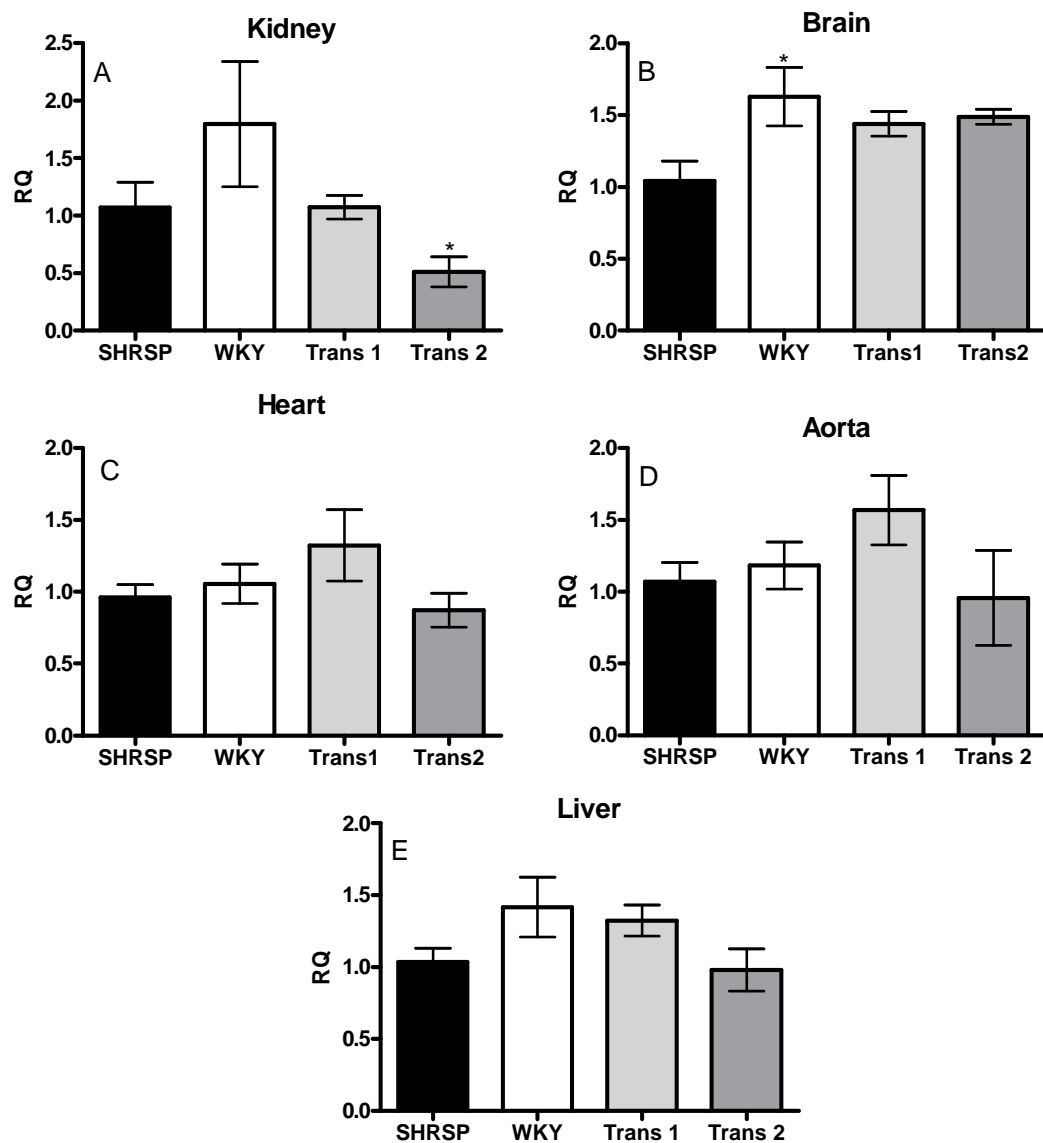


Figure 4-8: *Gstm2* expression in Trans1, Trans2 and parental strains at 21 weeks of age. Total *Gstm2* expression in (A) kidney, (B) brain, (C) heart, (D) aorta, (E) liver at 21 wks of age. Renal *Gstm2* levels of WKY, Trans1 and Trans2 animals were not significantly different from SHRSP ($p>0.05$). Renal *Gstm2* expression in Trans2 rats was significantly less than WKY (* $p<0.05$). Neural *Gstm2* levels were increased in WKY (n=8) when compared SHRSP (n=8) animals, but not in either Trans1 (n=8) or Trans2 (n=6) rats. Cardiac, aortic and hepatic *Gstm2* levels were not significantly different across all four strains. Values are presented as mean \pm SEM.

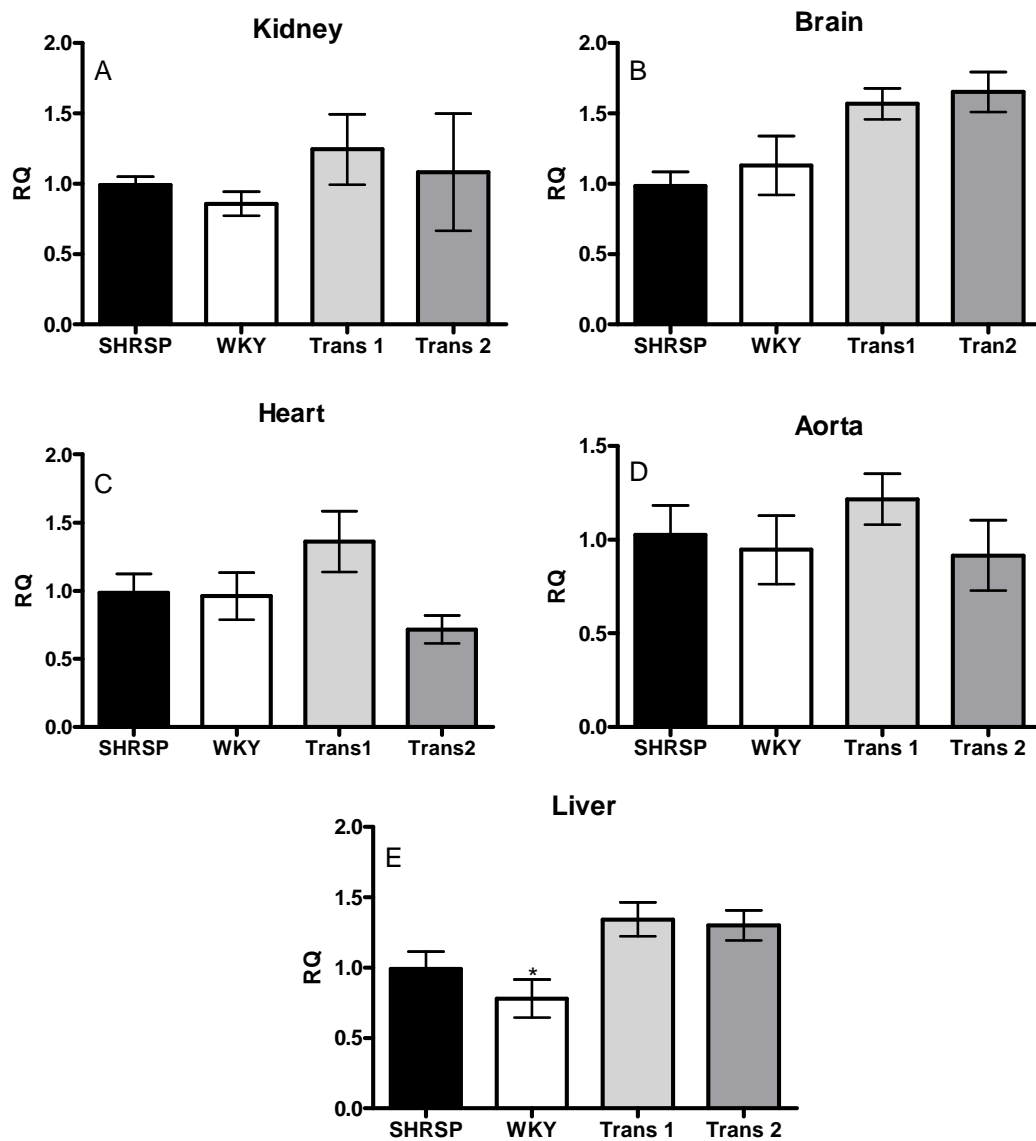


Figure 4-9: *Gstm3* expression in Trans1, Trans2 and parental strains at 21 weeks of age. Total *Gstm3* expression in (A) kidney, (B) brain (C) heart, (D) aorta, (E) liver at 21 wks of age. Renal, neural, cardiac, vascular and hepatic *Gstm3* levels in WKY (n=8), Trans1 (n=8) and Trans2 (n=6) animals were not significantly different from SHRSP (n=8) ($p>0.05$). The only significant difference in expression was hepatic *Gstm3* expression between the WKY and Trans1 animals (* $p<0.05$). Values are presented as mean \pm SEM.

4.3.3 Copy Number Variation

Data from the custom Taqman Copy Number Assay (Applied Biosystems) conveyed that there were multiple copies of the transgene in Trans1 rats across multiple generations (Figure 4-13). While this probe was custom designed and manufactured to anneal to SNP variations that were specific to the WKY variant of *Gstm1* there was, however, evidence of PCR amplification suggesting a mis-aligning of the probe within the SHRSP genome. Further investigation of this finding in conjunction with Applied Biosystems determined that mis-expression of the WKY *Gstm1* variant in the SHRSP genome was within their quality control parameters and was therefore an assay artefact. This caused difficulty analyzing transgene copy number with this probe. Because of these mis-alignment issues, and the delay in Trans2 rat breeding, these experiments were not repeated in Trans2 animals.

In order to further investigate transgene copy number in both transgenic lines, internal fragments from the inverse PCR sequencing were analyzed. When viewed, both transgenic lines included internal fragments that contained segments of the transgene that sequenced from the end of one copy into the beginning of the next, in a head-to-tail array.

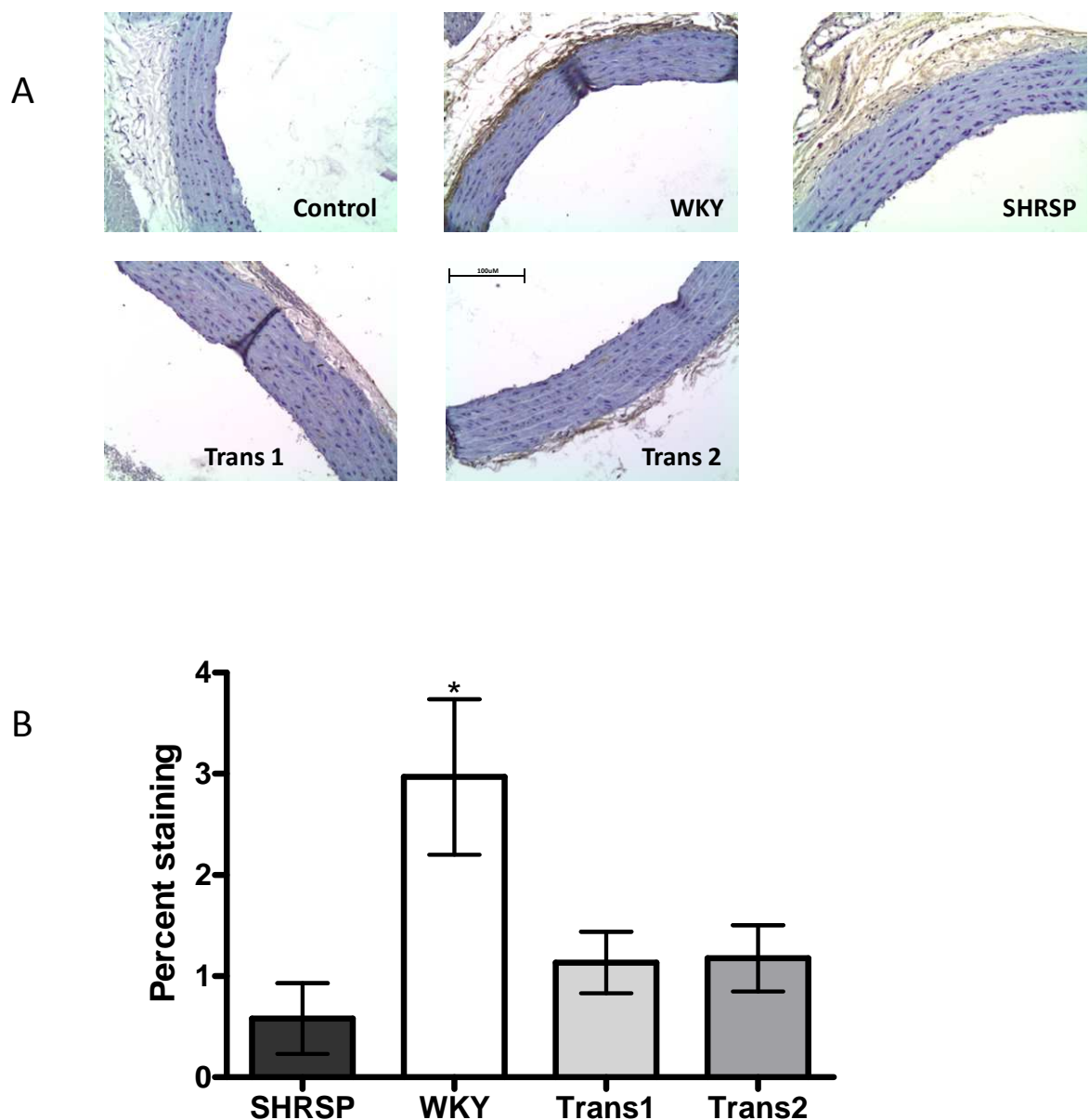
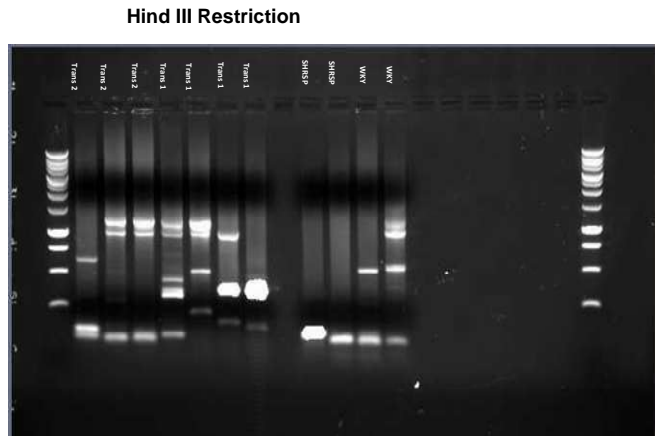
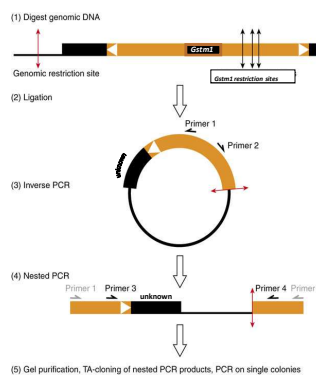


Figure 4-10: Localization of *Gstm1* in the Aorta at 21 weeks of age.
A: IHC of *Gstm1* protein in whole kidney sections from WKY, SHRSP, Trans1 and Trans2 rats at 21 weeks of age. Magnification =10x. **B:** quantitative measurement of *Gstm1* expression expressed as percentage staining (n=4 for all strains).

**B**

IPCR amplifies the unknown DNA sequences that are immediately adjacent to the known sequence of our transgene

Plasmid Vector towards PCR insert

CCGGCGAGCGCGCTAGACTAGTGGATCCCCGGCTGCAGCCCAATGTGAAATCGCCC
TT

Primer 3 and transgene end

TGTACGGGCCAGATAACCGCGTGCATTGATTATTGACTAGTAGGCTTGCAAACGTT

UNKNOWN

TTATAATAGTAATCAATTACGGGGTCATTAGTTCATAGCCCATATATGGAGTTCCGCGTTACATA
ACTTACGGTAATGGCCGCCCTGGCTGACGCCCAACGCCCGCCATTGACGTCATAATGGGAGGAGTATT
GACGTATGTCATAGTAACACCAATAGGGACTTTCCATTGACGTCATAATGGGAGGAGTATT
CGGTAACACTGCCCACTTGGCAGTACATCAAGTGTATCATGCCAAGTACGCCCTATTGACG
TCAATGACGGTAAATGGCCGCCCTGCATTATGCCAGTACATGCCATTATGGGACTTTCTAC
TTGGCAGTACATCTAGTATTAGTCATGCCTATTACATGGTGTGCGGTTTGGCAGTACATCA
ATGGGCGTGGATAGCGGTTGACTCACGGGGATTCCAAGTCTCACCCCCATTGACGTCATG
GGAGTTGGTGGCAACAAATCACGGGACTTCCAAGTGTGTAACAACCCCCCCCCAT
TGACGCAAATGGCGTAGGGCTGTACGGGGAGGTATATAAGCTATG

Primer 4

GTGCACTCTCAGTACAATCTGCTC

Plasmid Vector

AAGGGCGAATTCCACAGTGGATATCAAGCTTATCGATACCGTCGACCTCGAGGGGGCCGG
TACGGCAGCTTTGTCCTTGTAGGGTTAAATGCGCGCTTGACGTAATCATGGTCATAGCTG
TTGCTGTGAAATGTCCGCTCACATCCMMACACATACGAGGGGAGCATAAAGTGTAA
GCTGGGGTGTCTATGAKTGACTAACCTCMATAATTGCTGGCCCTATGACCGCTAGTCAGAAC
GTCTGCCACTCCAATAATTGATCGGCAG

Figure 4-11: Schematic of the inverse PCR procedure with results.

A: Liver genomic DNA from SHRSP ($n = 2$), WKY ($n=2$), Trans1 ($n=4$) and Trans2 ($n=3$) rats using restriction site *HindIII*. **B:** Templates underwent multiple PCR reactions in order to target specific products. Adapted from Bessereau (271). The text box is a representative sequence where the unknown/flanking region of DNA assembles to a trace archived sequence identified in the Trace Archives for Brown Norway (Trace Archive reference rt71hp27.x.)

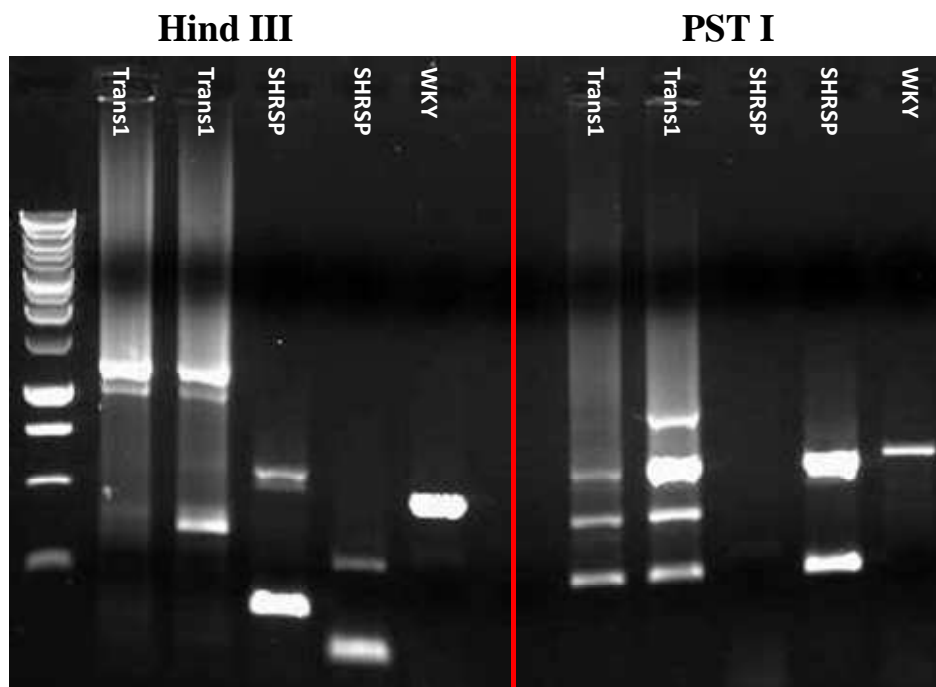


Figure 4-12: Mapping the transgene insertion site by inverse PCR for Trans1 rats.
Liver genomic DNA from SHRSP (n = 2), transgenic (n=2), WKY (n=1) rats was digested by *Hind*III and *Pst*I. Trans1 animals showed unique bands for both restriction sites

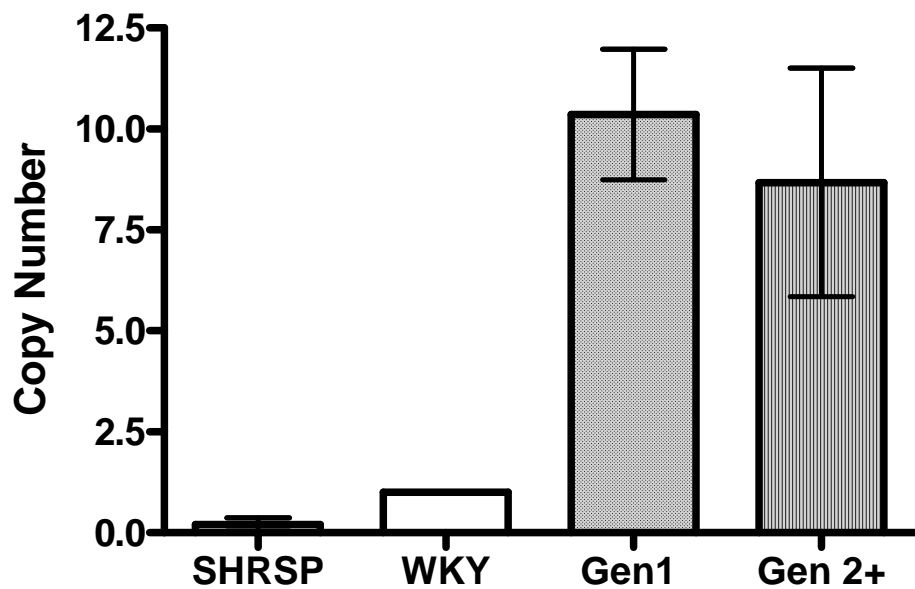


Figure 4-13: Copy number variation between parental strains and Trans1 rats
CNV as determined by Taq-man assay and Copy Caller analysis. Data show that Trans1 rats display a significant increase in wild type *Gstm1* copy number when compared to the SHRSP parental strain *($p<0.005$) across generations. Gen1 = 1st generation, Gen2+ = 2nd and subsequent generations. Values are presented as mean \pm SEM.

4.4 Discussion

In this chapter the molecular characterization of the *Gstm1* transgenic rat has been investigated before onset of hypertension (5 weeks) and at maturity (21 weeks). Both transgenic lines have demonstrated an increase in total and transgene specific expression of *Gstm1* in kidneys at 5 weeks of age (Figure 4-2) as well as increased transgene expression in several other cardiovascular tissues (Figure 3-4). Additionally, we saw increased total *Gstm1* expression in a range of cardiovascular tissues at 21 weeks of age (Figure 4-4) without potential changes of two other *Gstm* family members (*Gstm2* and *Gstm3*) that could be an artefact from the addition of the transgene (Figures 4-8 and 4-9). Although it was not possible to identify the exact location of the transgene insertion site in both transgenic lines, data presented indicate that they are not identically inserted and from this it can be inferred that the decrease in blood pressure is not due to the insertion site alone. Furthermore, sequencing data shows that each transgenic line contains multiple copies of the transgene across a number of generations.

Investigation at 5 wks of age, showed a significant increase in total and transgene (WKY) specific renal *Gstm1* mRNA expression in Trans1 and Trans2 rats (Figure 4-2) with a similar trend in renal *Gstm1* protein expression (Figure 4-2). While this was confirmed with IHC in whole kidney at 5 weeks of age for Trans1, IHC analysis for Trans2 was not feasible due to breeding difficulties which resulted in very low numbers of rats for this line. This general increase in renal *Gstm1* expression (Figures 4- 2) allows us to conclude that the increase in total *Gstm1* expression in the transgenic lines are a result of increased transgene specific *Gstm1* expression rather than changes in endogenous *Gstm1* (Figure 4-2). However, this increase of renal *Gstm1* mRNA expression is not sustained at the later time point investigated (i.e. 21 weeks of age) in the Trans2 line. This unsustained increase of expression, or return to SHRSP levels, at 21 weeks is also observed for protein levels in both Trans1 and Trans2 (Figure 4-3). However, an age related decline in transgene expression is not unique to these animals. Previous reports have shown that transgene expression levels can decline with time both *in vivo* and *in vitro* (Lit paper and references 6,9 of paper, Uneda *et al.*). For example, EGFP expression, under the control of the ef1- α promoter, was found to be progressively limited during the later stages of development

(272), and completely restricted in adult tissue of *X. laevis* (273), Medaka (274), and zebrafish (275). While these studies have reported a decrease in expression levels during later stages of life, each of these studies, in line with ours, demonstrated phenotypic differences at a later stage as a result of early developmental expression (272-275).

The over expression of *Gstm1* in the kidney before the onset of hypertension, appears to have a preventative effect on the progression of hypertension in the transgenic SHRSP rat (Figure 3-1 and Figure 4-2). While *Gstm1* mRNA is differentially expressed between the two transgenic lines (Figure 4-3) at 21 weeks of age, both lines continue to have almost identical reductions in systolic blood pressure. Indeed, increased mRNA and protein levels in the kidney at 5 weeks of age seem to be able to reduce the severity of disease in mature animals, at a time point when the SHRSP would have normally developed full hypertension. This reduced disease severity will be further examined in the subsequent chapter where renal and vascular pathology and function is investigated (*ex vivo*) in mature rats. Other studies have found similar results with early over expression of genes during development. Studies conducted by Perez *et al.* have shown the early increased expression of *Trx1* not only provided an increased resistance to oxidative stress in the mouse but elongated the life span of the animal as well (242).

While there seems to be very few phenotypic differences between the two transgenic lines, there are some expression differences that make each line unique. One factor that could potentially play a role in this variation of expression exhibited by the same transgene is the impact of the transgene insertion site (or positional effect). Often differences in expression are due to enhancers that regulate neighbouring genes (276). While these enhancers regulate their respective gene of interest, they can also affect the expression pattern of the transgene that is inserted near them. Identification of the exact transgene insertion site in our transgenic lines would have provided important information for the determination of these potential regulatory factors. However, despite concerted effort and utilization of both previous and new rat genome assemblies it was not possible to fully determine the exact location for either of the transgenic lines. The inverse PCR method used for the rapid *in vitro* amplification of unknown DNA sequences that flank a region of known sequence

proved to be problematic for our transgenic animals. While we did find many unique bands in the transgenic columns (Figures 4-11 and 4-12) that demonstrated additional fragments of DNA in the transgenic genomes unique to Trans1 and Trans2; ligation issues for both lines made it difficult to ascertain the insertion site. For Trans1, these ligation issues made it virtually impossible to determine the insertion site of the transgene. Each unique band was made up of various inter-ligated fragments of the transgene from internal copies. In order to accommodate for this, multiple restriction sites and corresponding primers were used. Nonetheless, there was no further insight to where the Trans1 integrated into the SHRSP genome.

We were able to establish the Trans2 insertion site to be within a region of the genome located in the trace archived sequenced area, rt71hp27.x. The rt71hp27.x. genome sequence has yet to be assembled to the rat genome which makes it impossible to know which chromosome this trace resides on, however, this is an ongoing process and hopefully future advancements by the EURATRANS collaborative Rat consortium will make this information available in the near future. Since there was additional rt71hp27.x sequence in Ensembl, the additional sequence was used to verify Trans2 insertion into this region by designing primers to the additional sequence. Because rt71hp27.x sequence has not yet been assembled to the Brown Norway genome, it is difficult to determine if Trans2 was indeed undergoing expression regulation from DNA-methylation or by any other regulating enhancers or genes (269). Further investigations will elucidate where this archived sequence is within the full rat genome.

An additional result arising from sequencing the unique bands from the transgenic rats has confirmed transgene integration and the incorporation of multiple copies numbers for both transgenic lines in a head to tail fashion. In addition to using sequencing as a method to confirm copy number across generations, copy number variation was assessed by CNV Taqman probes (Applied Biosystems) that were custom synthesized to a unique portion of the WKY form (transgene) construct (See Appendix). However, due to technical difficulties of unspecific primer annealing, this method was found not to be reliable (i.e. SHRSP animals were showing increased copy numbers when sequencing data confirm that no copy exists within this genome) (223). Moreover, Trans1 and Trans2 both had endogenous expression of *Gstm1* in their genome which increased the

possibility and occurrence of reduced primer specificity. Because of this, the copy number assessment was not reliable through this method. However, since genotyping was carried out on every Trans2 animal and on randomly selected Trans1 animals, we were assured that the transgene was present through multiple generations.

One of the reasons that the ef1-alpha promoter was chosen for this study was that the ef1- α promoter-driven transgenic animals have been widely used because of ubiquitous expression of the gene during development (277;278). However, as with all methods of genome manipulation there is always potential for unexpected effects in which makes each transgenic line produced unique (7). There are many factors that can be influenced when incorporating a new or different gene into the genome. Because of this, we investigated the effects of increased *Gstm1* on other members of the *Gstm* family. There are eight currently known members of the *Gstm* gene family in the rat and the entire family has a high sequence homology (211). In this study, we also examined two family members; *Gstm2* and *Gstm3*, in order assess any changes in expression of the *Gstm* family and to determine their potential to be altered as a result of increased *Gstm1* expression in the SHRSP. *Gstm2* expression was investigated because the sequence is the most similar to *Gstm1* and many IHC antibodies bind to both *Gstm1* and *Gstm2* (211). Measuring *Gstm2* expression allowed for a more in-depth assessment of the actual changes of *Gstm1* in the transgenic rats. *Gstm3* was then investigated in order to insure that other members of the *Gstm* family were not significantly altered with the incorporation of the transgene. Since there were no significant changes in *Gstm2* and *Gstm3* expression in the transgenic rats compared to the SHRSP in any of the tissues, we were able to conclude that increased *Gstm1* expression alone was having a functional affect on systolic blood pressure in the transgenic rat and not a combined effort of the *Gstm* family.

The current chapter has assessed the differences in expression levels of *Gstm1* in the two transgenic lines and has demonstrated that there is an increase in renal *Gstm1* prior to the onset of hypertension in both transgenic lines, which is maintained at 21 weeks of age in Trans1 rats. In the next chapter we follow up these findings by investigating whether the increased levels of *Gstm1* in kidney

and other cardiovascular tissues, has a functional impact on intermediate phenotypes including renal and vascular function and oxidative stress.

5 *Ex vivo Effects of Gstm1 Expression*

5.1 Introduction

In the previous chapters, it has been demonstrated that a significant increase in *Gstm1* expression in the kidney at an early stage of development resulted in a significant decrease in blood pressure and cardiac hypertrophy in the transgenic rat lines. To fully understand the effects of increased *Gstm1* expression in the SHRSP background, other functional aspects should be examined in order to determine if increased *Gstm1* expression results in improved intermediate phenotypes and reduced end organ damage (i.e. renal and vascular function and pathology).

It is well established that oxidative stress is an important pathogenic factor in the development of cardiovascular disease and increased production of reactive oxygen species (ROS) and/or reduced defences against ROS not only leads to endothelial dysfunction but also causes structural damage to tissue and organs (237;279;280). In particular, previous studies have shown that the oxidative stress pathways play important roles in the development of renal and vascular pathology (96;199). Considering the role of *Gstms* in the protection against reactive oxygen species it is anticipated that enhanced *Gstm1* expression will improve antioxidant defences in the tissues and organs where expression has been improved.

5.1.1 Renal Function

Hypertension is a multifactorial disease which affects many cardiovascular organs including the heart, blood vessels and kidneys (33). It is well established that hypertension is associated with renal injury and dysfunction which can result in poor fluid maintenance and electrolyte homeostasis. The SHRSP has a marked susceptibility to develop renal damage while the SHR, from which the SHRSP strain originated, is a relatively resistant strain (281). While both strains are considered hypertensive, and both have relatively similar genomes, the severity of renal injury is marked in the SHRSP, thus allowing us to conclude that SHRSP harbours genetic factors that contribute to renal injury susceptibility.

One of the main indications of renal impairment is the increased levels of proteinuria in the urine due to reduced glomerular filtrations or an insufficiency

of absorption due to the leakiness of the podocyte layer in the glomerulus (282). Furthermore, there is evidence for reduced renal function in SHRSP which is characterized by increased proteinuria, reduced glomerular filtration rate (GFR) and structural damage, such as glomerulosclerosis and tubulointerstitial damage after the onset of full hypertension and in salt-loading conditions (87;283). Additionally, there is increasing evidence in the literature that oxidative stress is central to this renal dysfunction (96;284-286).

5.1.2 Vascular Function

Endothelial dysfunction is also associated with hypertension. More specifically, increased blood pressure has been shown to decrease endothelium-mediated vasodilation and has been reported in both hypertensive patient and various animal models of hypertension (287;288). Vascular tone is normally regulated by a delicate balance between vasodilators and vasoconstrictors, whereas disturbance in the NO/O₂⁻ pathways can lead to hypertension which, if reaching malignant levels results in end-organ damage. However, mechanisms to explain the observed dysfunction are conflicting and vary depending upon the model examined. In the SHRSP, there is a decrease in endothelium-dependent relaxation despite increased eNOS activity (234;289;290). Data has shown that free radicals such as superoxide react with and inactivate the vasodilator nitric oxide, reducing NO bioavailability and impairing vascular function (237;290;291). Since *Gstm1* plays an important antioxidant role, we investigated the impact of increased *Gstm1* expression on vascular endothelial function through assessment of conduit (aorta) and resistance (mesenteric) artery function.

Additionally the mechanical properties of mesenteric resistance arteries (MRA) were investigated due to their fundamental importance in blood pressure regulation. Resistance arteries are the major site of resistance to blood flow and therefore play an important role in blood pressure regulation. Elevated peripheral resistance is a hallmark of essential hypertension; therefore, abnormalities in the morphology/mechanical function of resistance arteries can participate in mechanism that elevate blood pressure (292). It has been well established that vascular remodelling occurs in response to an increase in blood pressure. While the underlying mechanisms leading to vascular remodelling are

not well understood, it has been shown that the adaptive change in the structure and elasticity of the vessel is characterized by a change in vessel diameter and stress-strain relationship (293-295). Specifically, in the SHRSP, when compared to normotensive rates, lumen diameter is smaller and wall thickness to lumen ratio is increased (296).

5.1.3 Aims

In the previous chapters, we have shown that a significant increase in *Gstm1* expression at an early stage of development results in a significant decrease in blood pressure and cardiovascular risk in our transgenic lines. From this data, we hypothesized that this reduction in blood pressure and end organ damage are due to improved vascular and kidney function through reduced oxidative stress. The aim of this chapter was to investigate whether increased *Gstm1* gene expression plays a functional role in oxidative stress and end-organ damage. The functional properties of *Gstm1* in the transgenic SHRSP rats were examined through (1) oxidative stress measurements, (2) wire and pressure myography, (3) histological analysis and (4) renal function measurements.

5.2 Materials and Methods

5.2.1 Metabolic Cages

Telemetered animals were placed in metabolic cages for the collection of urine and the monitoring of water in-take for baseline and salt-loaded studies. At 16 weeks old, the rats were housed in the metabolic cages for 24 hours and baseline data was collected on water intake and urine volume for WKY, SHRSP, Trans1 and Trans2 animals. Additionally, at 21 weeks old, rats were housed in metabolic cages for 24 hours and additional baseline or salt-loading data (WKY, SHRSP, and Trans1 only) was collected on water intake and urine volume. Urine was kept on ice and stored at -80°C, until required for biochemical analysis for chloride, potassium and Sodium concentrations. The analysis was carried out using a Beckman CoulterAU640 clinical chemistry analyser (formally known as Olympus AU 640) using ion selective electrodes (ISE) utilising potentiometry. The urinary creatinine and total protein concentrations were assessed by creatinine clearance kit (Section 2.2.4) and Peirce proteinuria kits (Section 2.6.2), respectively.

5.2.2 Estimated Glomerular Filtration Rate

Kidney function was examined in rats at 21 weeks of age at baseline and after salt-loading. Blood samples were collected during sacrifice for WKY, SHRSP, and transgenic animals. To extract plasma, whole blood was collected into heparin lined tubes and was stored on ice for a maximum of 24 hours until centrifugation at 2240 g for 20 mins at 4°C. Plasma was removed without disturbing red and white blood cells and was stored at -80°C for future experiments. Urine was collected for 21 hours prior to sacrifice with water intake over 24 hours recorded. Indirect glomerular filtration rates (GFR) were determined by a clinically validated automated analyzer (c311, Roche Diagnostics, Burgess Hill UK), using the manufacturers calibrators and quality control material. All calculations were normalized to kidney weight.

5.2.3 Tissue Collection

Animals were sacrificed after 9 weeks of telemetry monitoring at 21 weeks of age. Blood samples were collected and plasma extracted for functional

measurements. A quarter of a kidney was fixed in 10% formalin for histological analysis (Section 2.2.3). Kidney, brain, heart, aorta, and liver tissues were snap frozen for further analysis. Thoracic aorta and mesenteric resistance arteries (MRA) were isolated for the investigation of endothelial function by wire myography and tested for mechanics by pressure myography. Oxidative stress measurements, as previously detailed, were investigated using snap frozen tissue. Oxidative stress details are contained in section 2.2.5.

5.2.4 Wire myography

For examination of functional response and vascular reactivity, small (3rd order) mesenteric arteries (MRA) and thoracic aortas were harvested from animals at 21 weeks of age. Full details of wire myography experiments are in Section 2.2.6. Mesenteric arteries and thoracic aortas were dissected from connected tissue, trimmed into sections approximately 2mm in length (4 mm for Aortas), and stored in overnight at 4° C before use. Contractile responses were tested by pre-treatment with KCL (10µM), noradrenalin (phenylephrine for aortas) and carbachol. Vessels were left to rest for 30 mins following two Krebs' buffer washes. A cumulative concentration response curve to noradrenalin for MRA and phenylephrine for aortas, 10 nM to 30 µM was performed first in the absence and again after two Krebs' washes, in the presence of L-NAME (100 µM). The increase in tension in the presence of L-NAME provided a measure of the effect of NO on basal tone and a measure of NO bioavailability. The percentage of maximal contraction was calculated compared to response at 30 µM noradrenalin/phenylephrine without L-NAME. Similarly for assessment of relaxation responses, carbachol curves from 10nM to 10 µM were performed to measure the percentage of relaxation from maximal contraction in response to stimulated NO release. AUC was calculated from the response curves.

5.2.5 Pressure Myography

In order to examine the structural and mechanical differences in mesenteric resistance arteries, the pressure-diameter relationship differences between SHRSP, WKY and transgenic lines, was assessed by pressure myography. Dissected MRA (approximately 2 mm in length) were subjected to increased intraluminal pressure from 10-110 mmHg at 10 and 20 mmHg intervals over a period of

approximately 30 mins. Measurements of internal (Di) and external (De) were measured and used to calculate structural parameters cross sectional areas (CSA) and wall to lumen ration using the equations listed in section 2.2.7.

5.2.6 Oxidative stress

For examination of the oxidative stress cascade, measurements on various steps of the oxidative stress pathway were performed in 5 week, 21 week and 21 week salt loaded animals (i.e. superoxide, hydrogen peroxide, nitric oxide, glutathione, and lipid peroxidation). Samples were homogenized using snap frozen tissues and all manufacturers' recommendations for each kit were used. All methods are fully described in Sections 2.2.5

5.2.7 Histology – Gross Pathology Analysis

Full details for the preparation of tissues and histological analysis is fully described in Section 2.2.3. To assess renal remodelling, 3 µm renal adjacent sections from WKY, SHRSP and transgenic animals were stained with Harris haematoxylin and eosin and structures of tissues were examined by microscopic analysis; nuclei appeared purple and cytoplasm pink. Fibrosis was examined by staining with picrosirius red. Microscopic analysis and a colour threshold application were used to measure the average intensity of picrosirius red stain of fibrotic tissue (ImageProPlus 4.1, Media Cybernetics, US).

5.2.8 Statistical Analysis

Animal work was carried out with 6-8 animals per group. All quantification of histological analyses was carried out blind. Statistical analysis was done using commercially available packages including Prism Graphpad®. Significance was set P<0.05 and calculated using a one way ANOVA. Tukey post-hoc analysis was performed if overall ANOVA at least one p<0.05.

5.3 Results

5.3.1 Effects of *Gstm1* expression on oxidative stress

5.3.1.1 Kidney

In order to assess the changes in oxidative stress as a result of increased *Gstm1* expression after the onset of hypertension, multiple stages of the oxidative stress cascade was measured (i.e. superoxide, hydrogen peroxide, glutathione and lipid peroxidation). At 21 weeks of age there was no significant difference between the strains for kidney levels of superoxide (O_2^-), as measured by lucigenin chemiluminescence, and hydrogen peroxide, as measured by Amplex Red Assay (Figure 5-1) ($p>0.05$). Intracellular GSSG: GSH ratio levels were measured in kidneys at 21 weeks age. GSSG: GSH ratios, which when elevated are indicative of oxidative stress; show a reduced trend in the WKY and both transgenic lines when compared to the SHRSP at 21 weeks of age (Figure 5-1). Measurement of lipid peroxidation using a malondialdehyde (MDA) assay showed a significant reduction in renal MDA production in the WKY (n=8), Trans1 (n=8) and Trans2 (n=6) when compared to the SHRSP (n=8) at 21 weeks of age ($p<0.05$) (Fig. 8 Panel A).

In order to further investigate renal oxidative stress levels during the early stages of development, and to determine if they correspond with the increase of *Gstm1* expression before the onset of hypertension, we measured GSSG: GSH ratio levels at 5 weeks of age. There were no significant differences in GSSG: GSH ratio levels between the four strains (Figure 5-2). Furthermore when GSSG: GSH ratio levels of 5 weeks are compared to that of 21 wks, ratio levels at 5 weeks of age were considerably reduced.

Additionally, glutathione measurements on salt-loaded kidneys were also performed at 21 weeks of age. GSSG:GSH ratios were significantly reduced in WKY and Trans1 animals when compared to the SHRSP (Figure 5-3) ($p<0.01$). Renal MDA production in salt loaded animals was significantly decreased in the WKY when compared to the SHRSP ($p<0.05$).

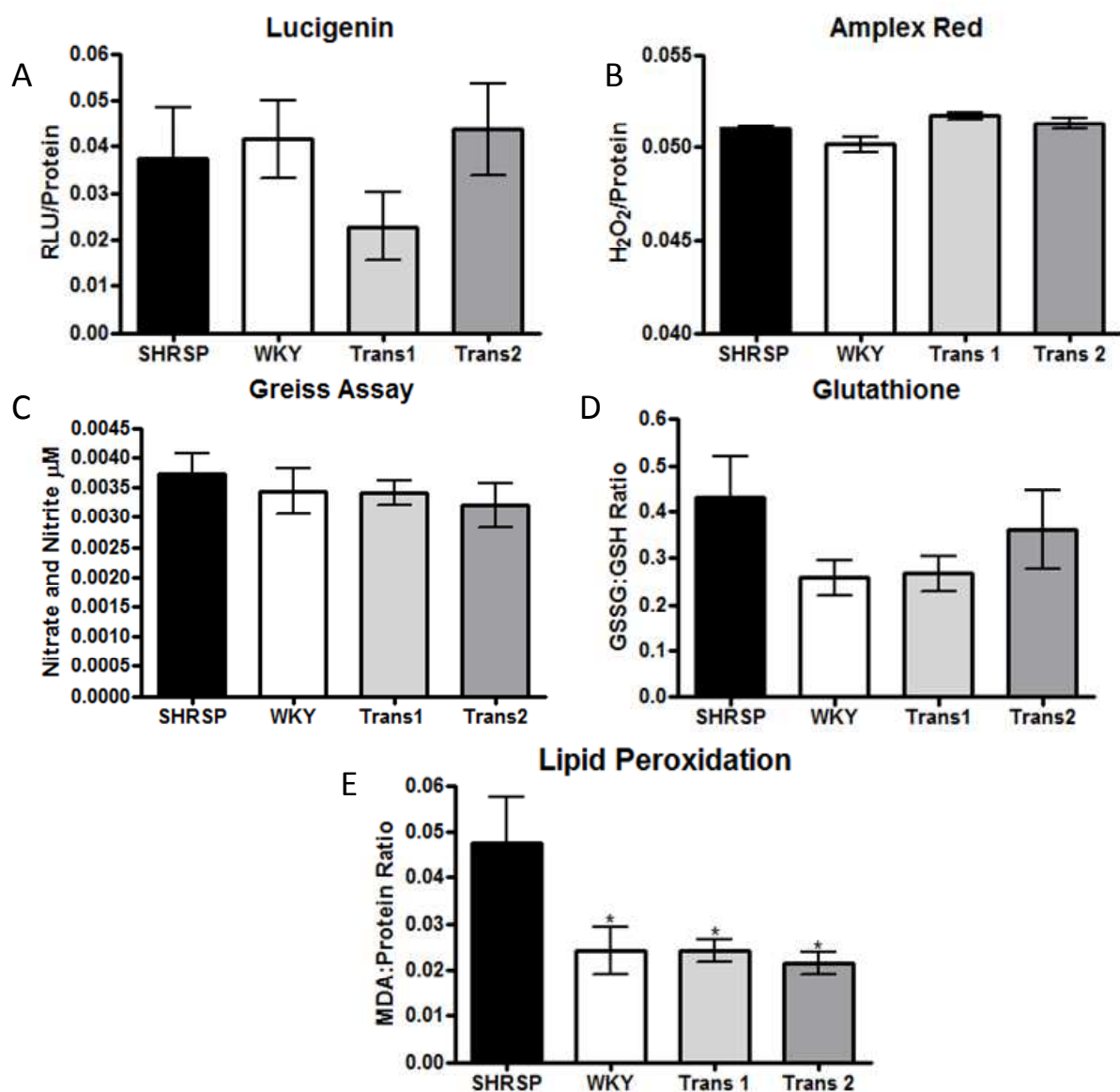


Figure 5-1: Renal Oxidative Stress Measurements in SHRSP, WKY and Transgenic lines at 21 weeks of age.

Measurements of various steps in the oxidative stress pathway in kidneys from SHRSP (n=8), WKY (n=8), Trans1 (n=8) and Trans2 (n=6) rats. There was no significant difference in oxidative stress in superoxide (lucigenin chemiluminescence), hydrogen peroxide (Amplex Red), Nitrate and Nitrite (Greiss Assay) and glutathione between all four strains ($p>0.05$). Lipid peroxidation (MDA) measurements showed a significant decrease in oxidative stress in the WKY, Trans1 and Trans2 rats when compared to the SHRSP ($p<0.05$).

Table 5-1 Renal Oxidative stress Measurements in SHRSP, WKY, and Transgenic lines at 5 wks of age

	GSSG:GSH ratio (μ M)		Lipid peroxidation (MDA:Protein Ratio)	
	5 wks	21 wks	5 wks	21 wks
SHRSP	0.0396 \pm 0.004	0.4291 \pm 0.08	0.00736 \pm 0.002	0.0476 \pm 0.01
WKY	0.0769 \pm 0.013	0.2572 \pm 0.04	0.005332 \pm 0.001	*0.0241 \pm 0.005
Trans1	0.0475 \pm 0.010	0.2666 \pm 0.04	0.01258 \pm 0.004	*0.0241 \pm 0.002
Trans2	0.0553 \pm 0.016	0.3607 \pm 0.08	0.00776 \pm 0.0003	*0.0214 \pm 0.002

The table provides oxidative stress data at 5 and 21 weeks of age for two stages in the oxidative stress pathway for comparison between ages. n=6-8 for SHRSP, WKY, and Trans1 and n=3-6 for Trans2 at 5 weeks. WKY, Trans1 and Trans2 rats are significantly different at 21 weeks of age when compared to the SHRSP *($p<0.05$).

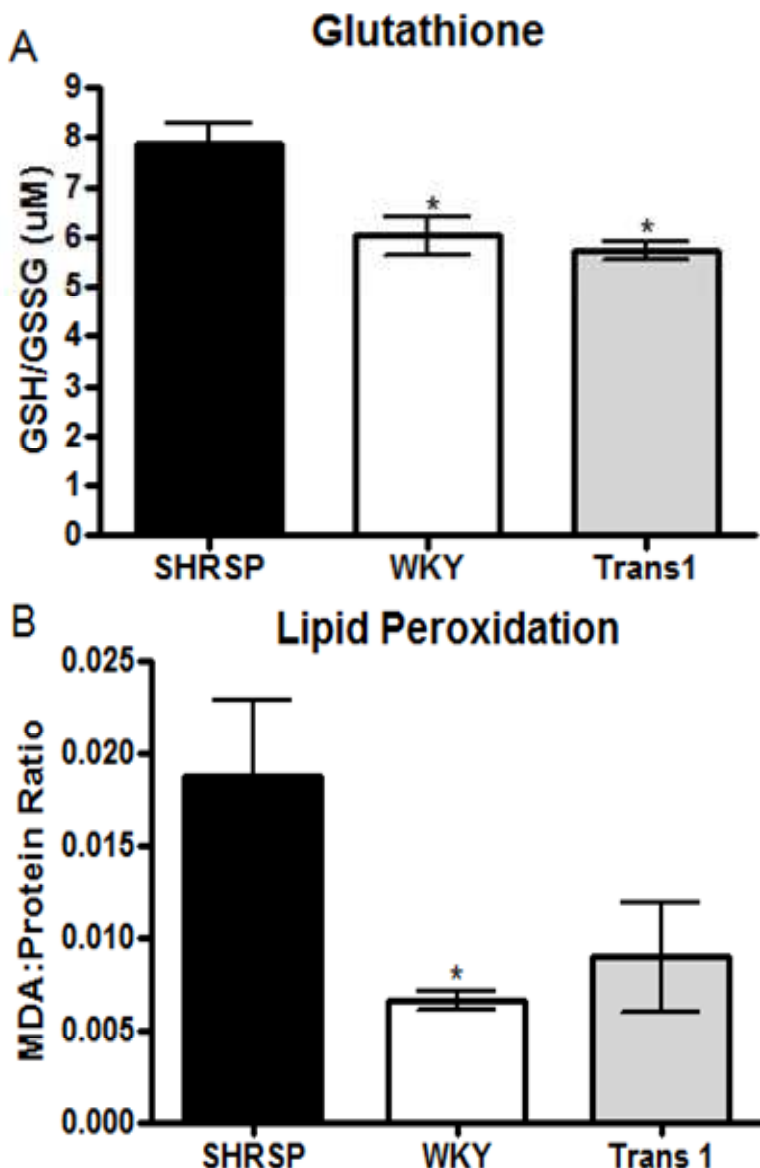


Figure 5-2: Renal Oxidative Stress Measurements in SHRSP, WKY and Transgenic lines at 21 weeks of age for Salt loaded Animals

Measurements of oxidative stress pathway parameters in SHRSP (n=8), WKY (n=8), and Trans1 (n=8) rats. (A) Glutathione measurements in WKY and Trans1 rats were significantly reduced when compared to SHRSP ($p<0.05$). (B) WKY lipid peroxidation measurements were significantly reduced when compared to SHRSP ($p<0.05$).

5.3.1.2 *Vasculation*

Intracellular GSSG: GSH ratio levels were measured in the aorta at 21 weeks age. While there was no significant difference in GSSG: GSH ratios between WKY (n=8), SHRSP (n=8), Trans1 (n=8) rats ($p>0.05$), GSH: GSSG ratios levels for Trans2 rats (n=8) were significantly increased compared to that of the SHRSP and WKY ($p<0.001$ and $p<0.01$, respectively) (Figure 5-4).

Measurement of lipid peroxidation using a malondialdehyde assay showed no significant change in aortic MDA production in the WKY (n=8), Trans1 (n=8) and Trans2 rats (n=6) when compared to the SHRSP (n=8) at 21 weeks of age ($p>0.05$) (Figure 5-4).

5.3.1.3 *Other Tissues*

Intracellular GSSG: GSH ratio levels were measured in the liver at 21 weeks age. GSSG: GSH ratios in the WKY (n=8), SHRSP (n=8), Trans1 (n=8) and Trans2 (n=8) rats were not significantly different from each other (Figure 5-5). Measurement of lipid peroxidation using a malondialdehyde assay in the heart, brain and liver were not significantly different between any of the strains ($p> 0.05$) and were all within a normal range (Figure 5-5).

5.3.2 Effects of *Gstm1* on Renal Function

5.3.2.1 Estimated GFR

Creatinine clearance, as measured by estimated (indirect) glomerular filtration rate (GFR), was measured at 21 weeks immediately prior to sacrifice. While there was a trend towards increased GFR in Trans1 rats, there was no significance difference between all four strains (Figure 5-6) ($p>0.05$) at baseline.

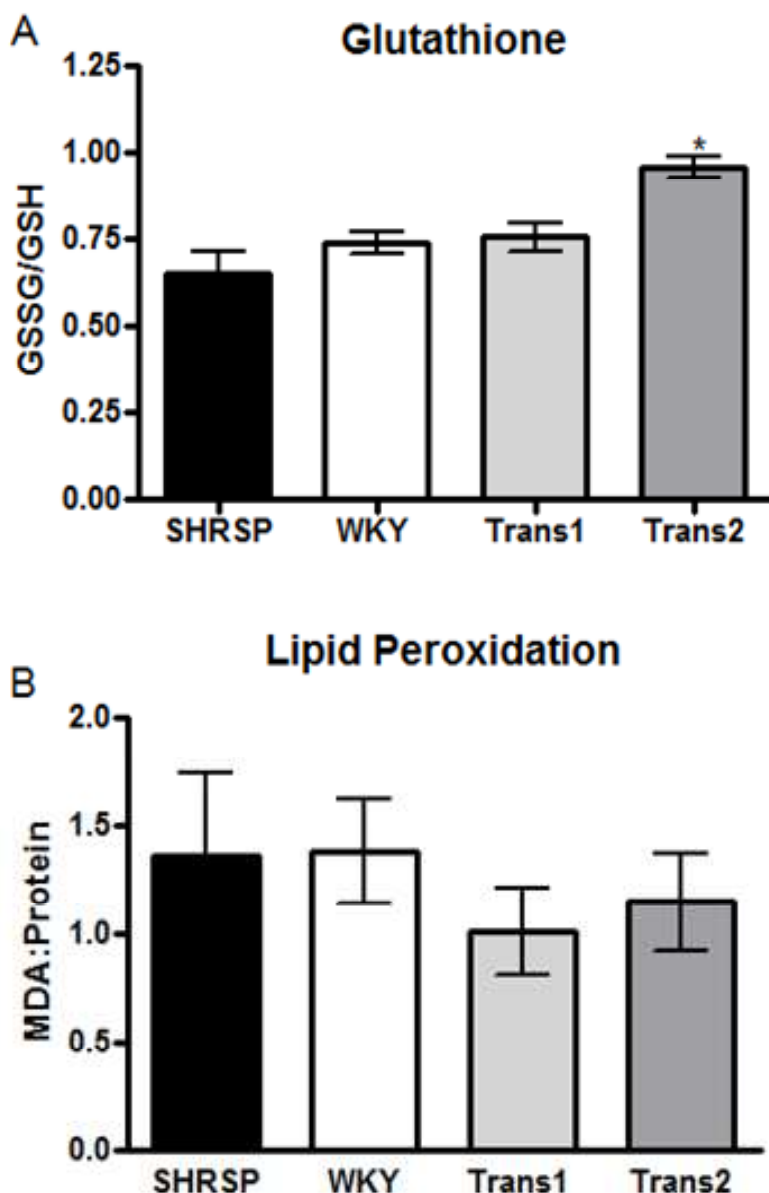


Figure 5-3: Vascular Oxidative Stress Measurements in SHRSP, WKY and Transgenic lines at 21 weeks of age

Measurements of oxidative stress parameters in the thoracic aorta for SHRSP (n=8), WKY (n=8), Trans1 (n=8) and Trans2 (n=6) rats. (A) While there was no significant difference in glutathione measurements between WKY, Trans1 and SHRSP ($p<0.05$), glutathione measurement in Trans2 rats was significantly increased when compared to the SHRSP and WKY ($p<0.001$ and $p<0.01$, respectively). (B) There was no significant difference in lipid peroxidation between WKY, Trans1, Trans2 and SHRSP rats.

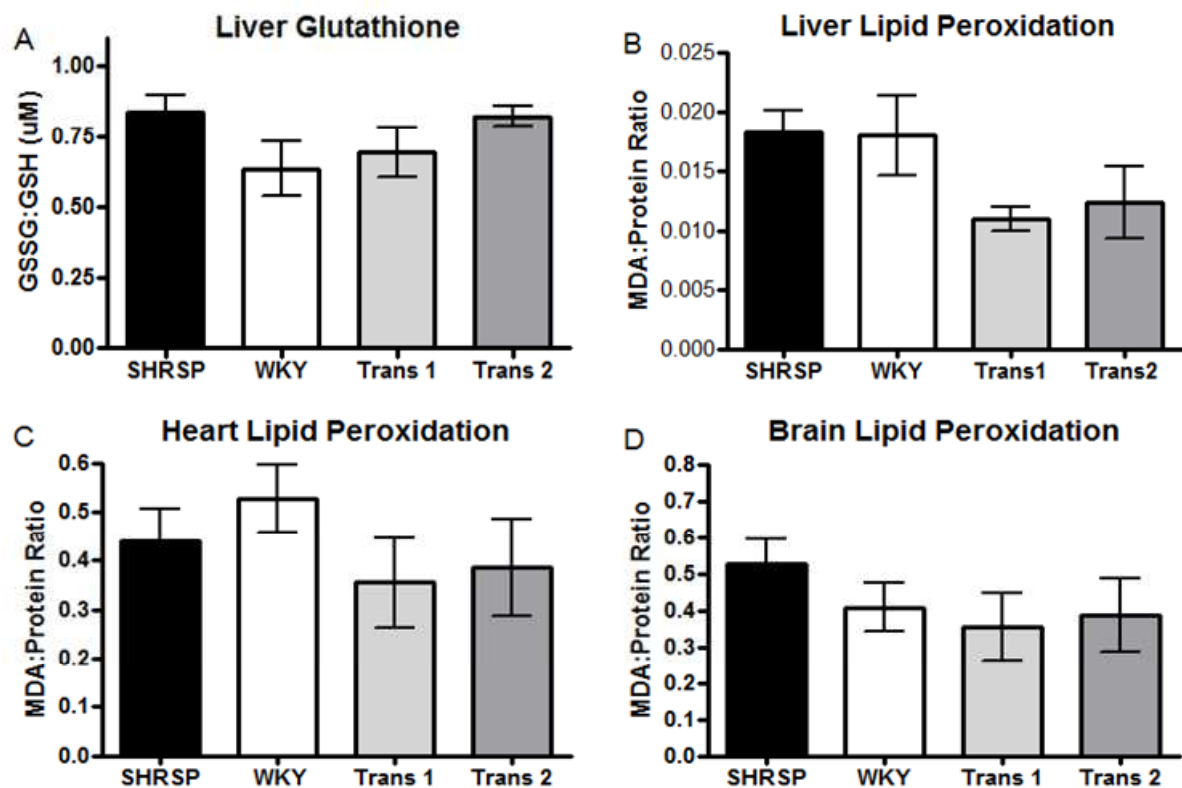


Figure 5-4: Oxidative Stress Measurements in SHRSP, WKY and Transgenic lines at 21 weeks of age in Cardiovascular Tissues

Measurements of various steps in the oxidative stress pathway in SHRSP (n=8), WKY (n=8), Trans1 (n=8) and Trans2 (n=6) rats. There was no significant difference in hepatic glutathione and lipid peroxidation measurements between all four strains ($p<0.05$). Cardiac and brain lipid peroxidation measurements were not significantly different between all four strains ($p>0.05$).

5.3.2.2 Biochemical analysis of Urine

Sodium, potassium and chloride excretion was measured at 21 wks in WKY (n=8), SHRSP (n=8), Trans1 (n=8) and Trans2 (n=8) rats. There was no significant difference between all four strains at baseline for sodium, potassium and chloride (Figure 5-7)

5.3.2.3 Renal Hypertrophy

At 21 weeks of age, kidney mass, normalized to body weight, was significantly lower in WKY (n=8) when compared to SHRSP (n=8) during both baseline conditions and after salt loading conditions ($p<0.0001$). Renal mass index for Trans1 rats (n=8) was not significantly different when compare to SHRSP at baseline or during salt-loading, and Trans2 (n=6) was not significantly different from the SHRSP at baseline (Figure 5-7). Due to breeding difficulties, salt-loading data could not be assessed for Trans2 rats.

5.3.2.4 Proteinuria

At 21 weeks of age during baseline measurements, levels of proteinuria in the WKY (n=6), Trans1 (n=6) and Trans2 (n=6) rats were significantly less than that of the SHRSP (n=12) ($p<0.05$) (Figure 5-8). During salt-loading, this significant difference between the parental strains was exaggerated, with WKY (n=8) salt-loaded animals having a significantly reduced proteinuria compared to that of the SHRSP (n=8) ($p<0.05$). After salt-loading proteinuria in Trans1 (n=8) animals was no longer significantly reduced compared to that of the SHRSP, however, it was not significantly different from that of the WKY either (Figure 5-8) ($p>0.05$).

Table 5- 2 Renal Parameters in 21 week old Animals

	SHRSP	WKY	Trans1	Trans2	SHRSP Salt	WKY Salt	Trans Salt
GFR	1.565 ± 0.206	1.642 ± 0.137	2.369 ± 0.309	1.605 ± 0.265	3.284 ± 0.56	5.296 ± 0.51	1.862 ± 0.33
NA²⁺	83.98 ± 11.13	78.24 ± 8.433	59.29 ± 7.533	76.27 ± 20.70	ND	ND	ND
K⁺	116.2 ± 14.02	149.1 ± 14.09	153.0 ± 23.60	115.1 ± 30.08	ND	ND	ND
Cl⁻	100.1 ± 10.84	148.7 ± 30.58	99.93 ± 15.76	110.6 ± 30.99	ND	ND	ND
RMI	4.242 ± 0.044	3.389 ± 0.049*	4.355 ± 0.366	4.115 ± 0.142	4.115 ± 0.11	2.91 ± 0.06*	4.44 ± 0.17

The table illustrates measurements of creatine clearance, sodium, chloride, potassium in order to determine kidney function. n=6-8 per group; *(p<0.05) denotes a significant difference between from the corresponding (Salt or Baseline treatment) SHRSP strain.

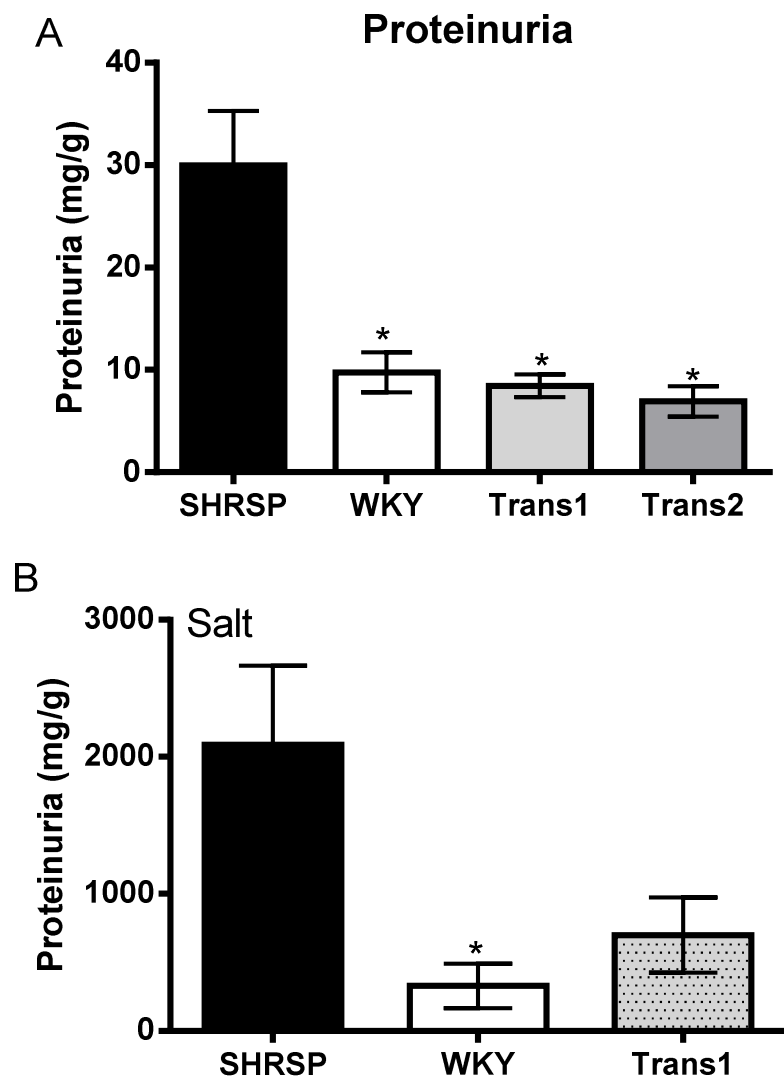


Figure 5-5: Proteinuria Measurement in Urine in 21 week old animals.

(A) Measurements of urine proteinuria at baseline in WKY (n=8), SHRSP (n=8), Trans1 (n=8) and Trans2 (n=6) rats. Proteinuria in WKY, Trans1 and Trans2 rats was significantly reduced when compared to the SHRSP ($p<0.05$). (B) Measurements of urine proteinuria after salt-loading in WKY (n=8), SHRSP (n=8), Trans1 (n=8). WKY proteinuria was significantly reduced when compared to the SHRSP ($p<0.05$).

5.3.2.5 Renal Fibrosis and Morphology

Histological evaluation of renal fibrosis was carried out in kidney sections from SHRSP (n=4), WKY (n=4), Trans1 (n=4) and Trans2 (n=4) rats at 21 weeks of age. Quantification of picrosirius red staining by % of integrated optical density (%IOD) showed no interstitial fibrosis in any of the four strains (Figure 5-10).

Renal morphology at 21 weeks of age, using haematoxylin staining, showed normal arterioles in the WKY and transgenic animals. Renal arterioles in the SHRSP were beginning to show evidence of hyperplasia, which is a sign of accelerated hypertension (Figure 5-11).

5.3.3 Effects of *Gstm1* expression on the Vasculature

5.3.3.1 Aortic Function

Alpha-adrenergic vasoconstrictor mechanisms were tested in thoracic aortae from WKY (n=7), SHRSP (n=8), Trans1 (n=6), and Trans2 (n=4) animals at 21 weeks of age. Experiments were conducted using dose-responses to phenylephrine (PE), and were normalized to 0.1M KCL. There was no significant difference in maximum PE-induced contraction in aortas between the WKY (AUC 9.012 ± 2.6), SHRSP (AUC 7.77 ± 0.75), Trans1 (AUC 6.59 ± 1.9), and Trans2 rats (AUC 6.39 ± 1.6) (Figure 5-12).

Additionally, aortas were incubated with the NOS inhibitor L-NAME for 30 mins prior to constriction of phenylephrine dose-response curves (Figure 5-12). Inhibition of NO-mediated vasodilator responses in the vessel resulted in a great contractility in aortae of WKY (AUC 11.32 ± 2.6), SHRSP (AUC 12.17 ± 1.89), Trans1 (AUC 10.45 ± 3.39), and Trans2 (AUC 11.10 ± 2.2) lines (Figure 5-12). However, there was a much larger response in the WKY animals than the SHRSP, Trans1 or Trans2 rats (Figure 5-12).

The difference in forces generated in response to PE stimulation before and after NOS inhibition was used to measure the bioavailability of NO in aortae. PE induced vasoconstriction was only significantly increased in WKY aortic rings when compared to SHRSP ($p<0.05$) (Figure 5-13). The AUC was calculated for NO bioavailability

curves and illustrated in Figure 5-13 panel B. There was no change in NO bioavailability in the transgenic lines when compared to the SHRSP.

In order to assess stimulated NO release, carbachol response curves were constructed and relaxation of vessels reached a maximum of 42% for WKY, 34% for SHRSP, 19% for Trans1, and 65% for Trans2 (Figure 5-14). While there were no significant differences in relaxation between the parental stains, Trans2 relaxation appears more pronounced than the other three strains but variability is so large that more n numbers are needed (Figure 5-x). Additionally, Trans1 appears to have very little or no relaxation in response to carbachol. The corresponding AUC for each of the strains were SHRSP (420 ± 45.56), WKY (551.6 ± 31.21), Trans1 (644.5 ± 19.98) and Trans2 (329.5 ± 139.4) showed that the only significant difference between the four strains was between SHRSP and Trans1 ($p < 0.05$)

5.3.3.2 Mesenteric resistance artery function

Alpha-adrenergic vasoconstrictor mechanisms were assessed in mesenteric resistance arteries (MRA) from WKY (n=7), SHRSP (n=6), Trans1 (n=7), and Trans2 (n=5) animals using the agonist noradrenalin. Concentration response curves before and after NOS inhibition with L-NAME were assessed (Figure 5-15 Panels A and B). Vascular reactivity was similar in all groups with noradrenalin-induced contraction. The slight left-ward shift suggests enhanced contractility after blocking NO synthase (Figure 5-15 Panel B). AUC calculations indicated that there was no significant difference between MRA function at a basal response level to noradrenalin and following NOS inhibition when comparing responses within and between relevant groups (Figure 5-15, Panel C).

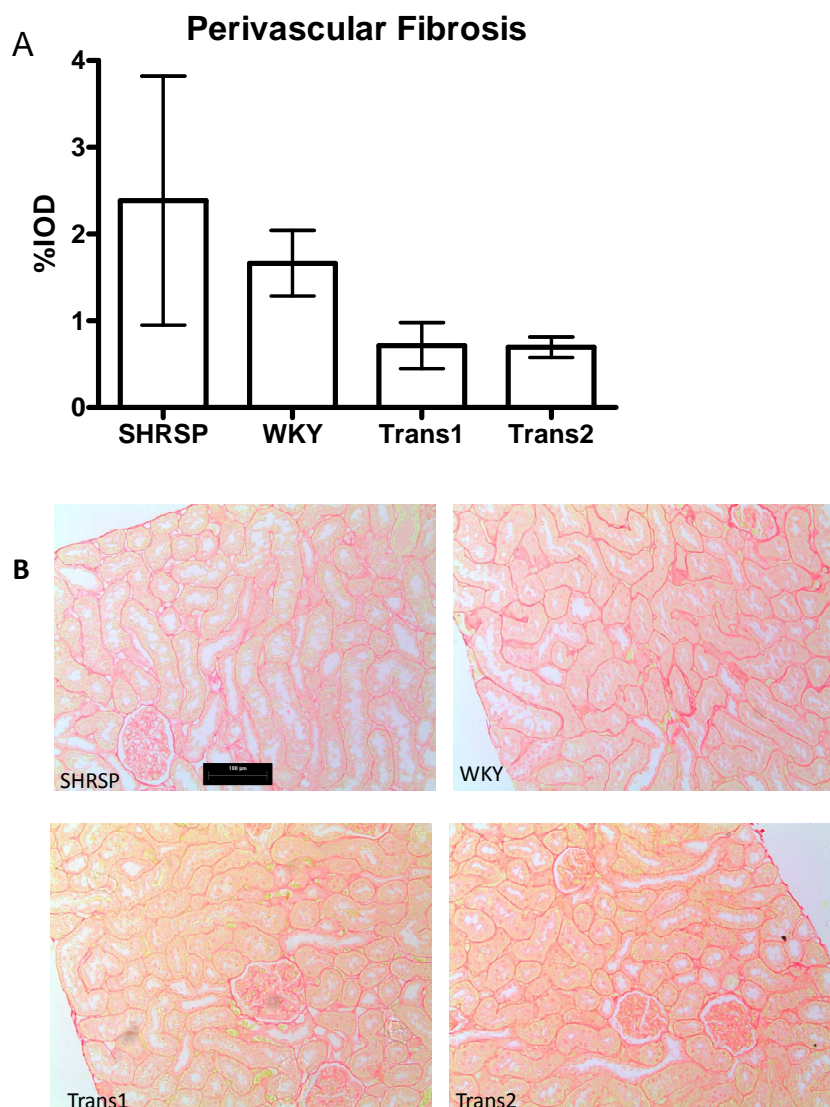


Figure 5-6: Assessment of Renal Fibrosis by Picosirius Red in 21 week old animals
Kidney sections were stained with picosirius red and intensities measured by ImageProPlus 4.1 (Media Cybernetics, US). Bar = $100\mu\text{M}$. N=4-6 per group.

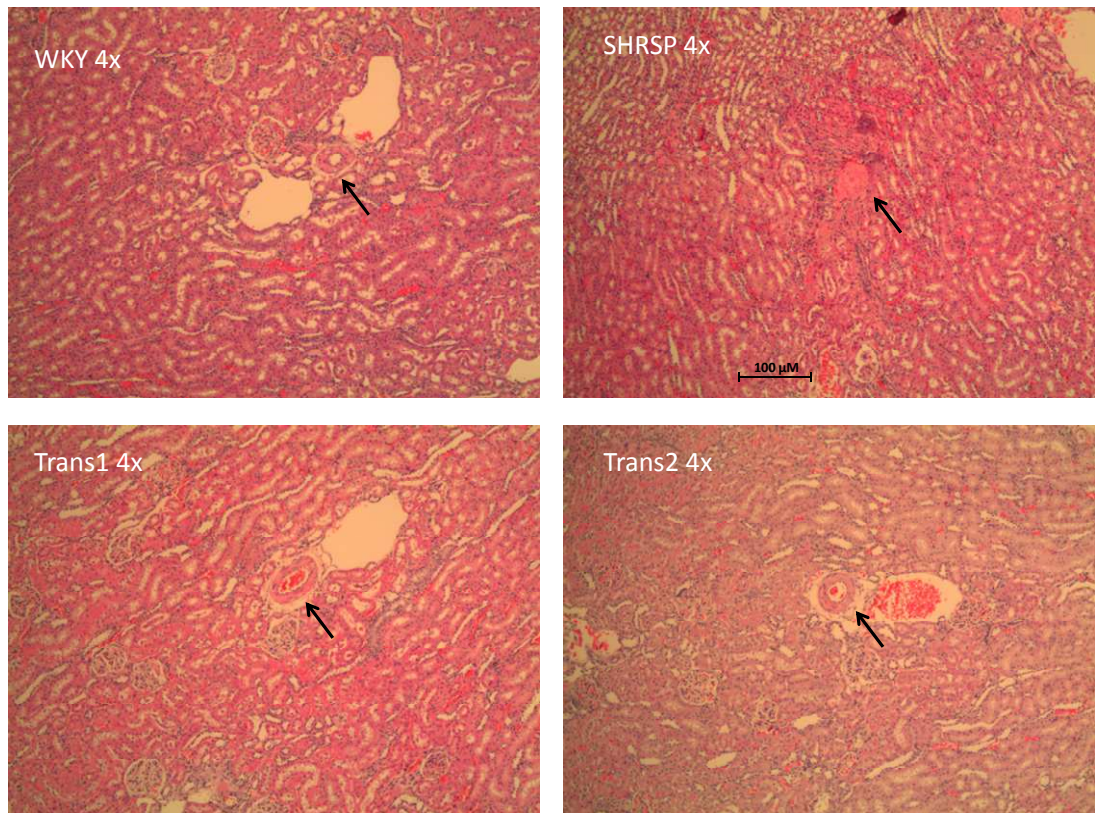


Figure 5-7: Haematoxylin and Eosin staining in kidney sections from transgenic and parental strains at 21 weeks of age.

Kidney sections from rats were stained with haematoxylin and eosin staining and show no evidence of vascular pathology in WKY, Trans1 and Trans2 rats, but evidence of vascular hyperplasia in SHRSP. Bar = $100\mu\text{M}$. N=4-6 per group.

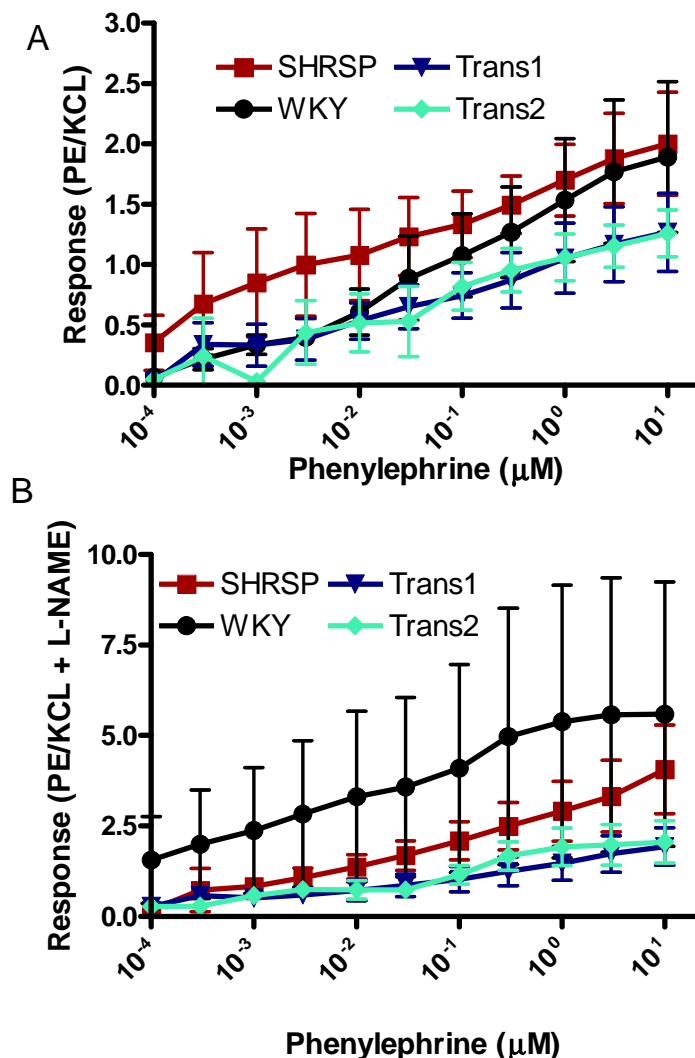


Figure 5-8: Concentration Response Curves in the presence and absence of the NOS inhibitor L-NAME in Aorta
 SHRSP (n=7), WKY (n=7), Trans1 (n=6) and Trans2 (n=5) rat aortic rings were measured for contractile response from stimulation with increasing concentrations of phenylephrine (PE) normalized to contraction with KCL. Responses (A) in the presence of PE, and (B) in the presence of PE plus L-NAME where PE-induced contractility was greatest in WKY animals in the presence of L-NAME.

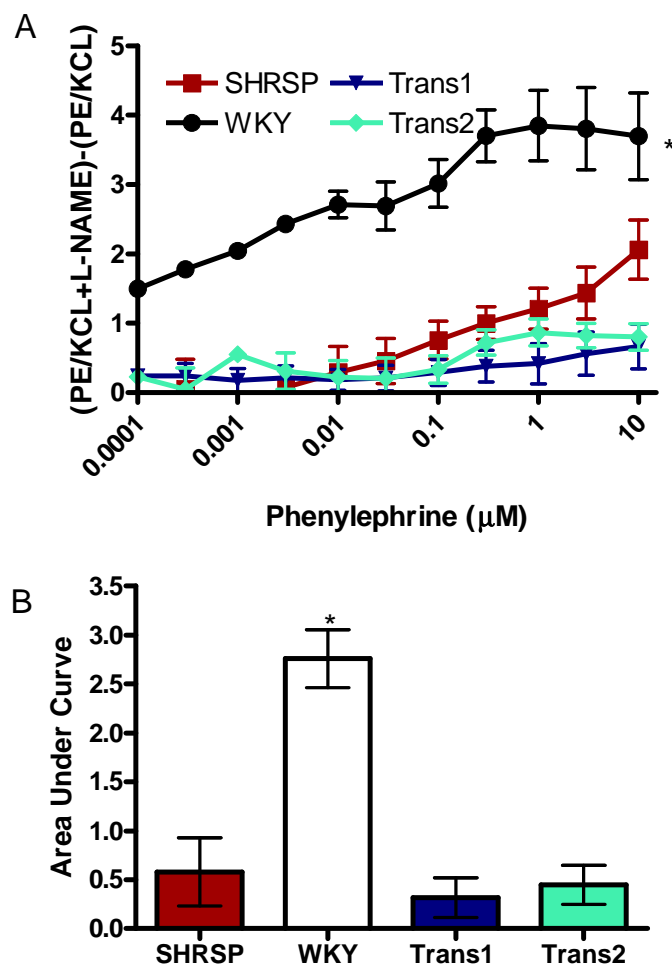


Figure 5-9: Nitric oxide bioavailability in 21 week aorta

(A) 21 week old SHRSP, WKY, Trans1 and Trans2 rat aortic nitric oxide bioavailability measured as the difference in the ability of aortae to respond to PE stimulation in the presence and absence of NOS inhibitor L-NAME (normalized to contraction with KCl). (B) NO bioavailability calculated as area under the curve. Data show a significant increase in NO bioavailability in the WKY when compared to the SHRSP *($p<0.05$). There was no significance difference in NO availability in Trans1 and Trans2 rats when compared to SHRSP ($p>0.05$)

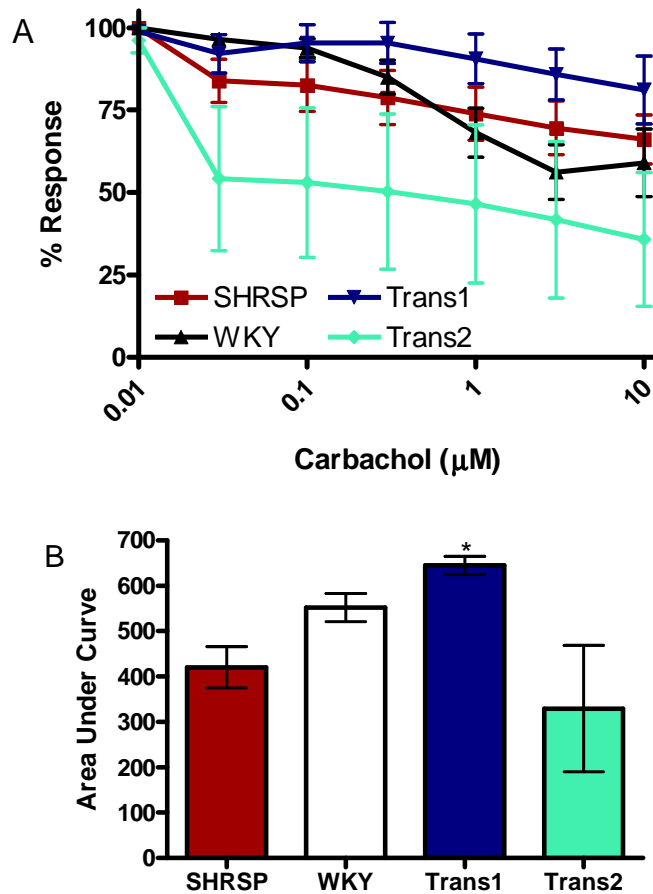


Figure 5-10: Effects on Carbachol-induced Vasorelaxation of Aortae

Pre-contracted aortas from SHRSP, WKY, Trans1 and Trans2 rats were subjected to increasing concentrations of carbachol for stimulated NO release which resulted in a reduction of tension in all groups. (B) Calculated area under the curve showed no significant difference between the parental strains, however Trans1 AUC was significantly increased compared to SHRSP ($p<0.05$).

The function of MRA's were also assessed by the vasodilatory response to carbachol-stimulated NO release (Figure 5-15 Panel A). Carbachol dose response curves in pre-contracted arteries were not modified between any of the four strains as the vessels relaxed to similar extents in response to the addition of carbachol. AUC was calculated for each group and although the highest vasodilator responses were observed with the SHRSP and WKY (AUC SHRSP: 130 ± 19.53 ; WKY: 135.5 ± 14.19) there was no significant differences between the groups (Figure 5-15 Panel B).

5.3.3.3 Mesenteric resistance artery structure and mechanics

Structural differences of MRA from SHRSP, WKY, Trans1 and Trans2 rats were assessed through pressure myography where internal diameter representing the lumen width and external diameter representing total lumen and medial width of the MRA's (Figure 5-16). While internal diameter was not significantly different, there were trends suggesting a larger increase in diameter in response to increased pressure in the WKY, Trans1 and Trans2 rats (Figure 5-16 panel A). External diameter exhibited similar trends for Tran1 and Trans2 animals and was significantly increased in the WKY when compared to the SHRSP ($p<0.01$) (Figure 5-16 panel C). Cross sectional area (CSA) was significantly increased in WKY, Trans1 and Trans2 rats when compared to SHRSP ($p<0.01$) (Figure 5-16 panel C). There were no significant differences in wall to lumen ratio (Figure 5-16 panel D) between strains.

The pressure-circumferential wall strain curves of MRA's from SHRSP ($n=5$), WKY ($n=7$), Trans1 ($n=7$) and Trans2 ($n=5$) rats are illustrated in Figure 5-16. Values were calculated from internal diameter measures (as intraluminal pressure increases) in comparison to the initial lumen diameter measurements at 10 mmHg and, therefore, indirectly the artery's ability to stretch. SHRSP had the smallest circumferential wall strain (AUC 1.167 ± 0.31) which was increased in both transgenic lines (Trans1: 1.25 ± 0.33 and Trans 2 1.85 ± 0.55) and WKY has the largest circumferential wall strain (3.83 ± 1.69), however, this did not reach significance. Circumferential wall stress, which takes into account intraluminal pressure, lumen diameter and wall thickness, was not significantly different between all four strains (Figure 5- 16).

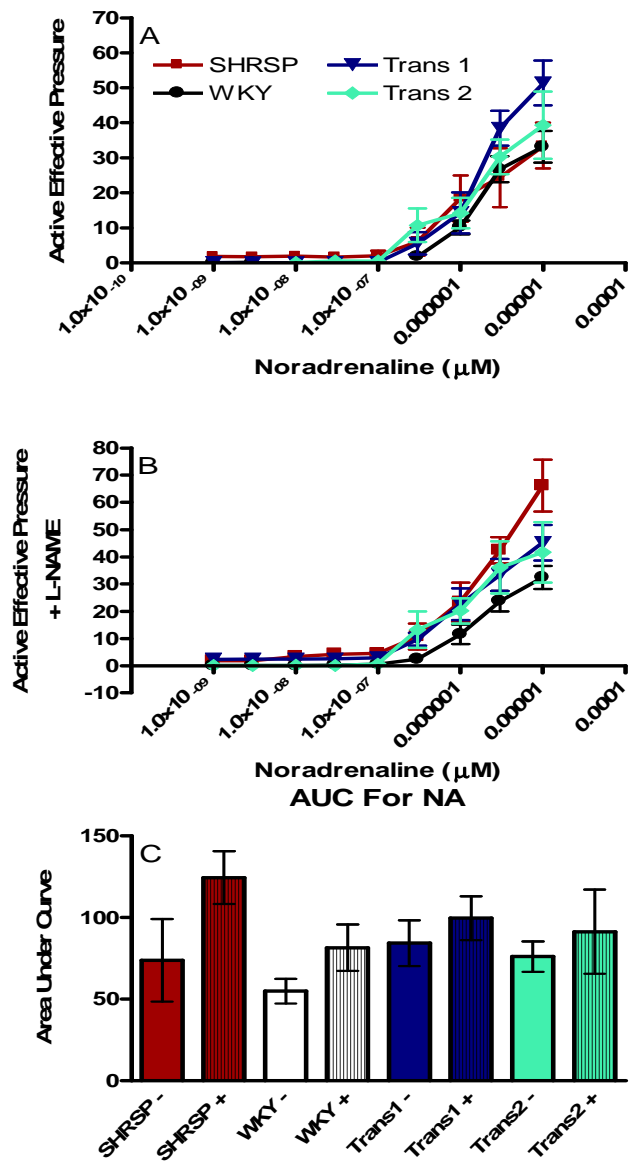


Figure 5-11: Mesenteric resistance arteries contractile response to noradrenalin
 Vasoconstriction of MRA from SHRSP (n=7), WKY (n=7), Trans1 (n=8) and Trans2 (n=5) rats using wire myography, (A) measured as a percent of their maximum response to 30 μM noradrenalin, and (B) following NOS inhibition with L-NAME. (C) AUC calculated from noradrenalin dose response curves shows similar MRA contractility in the absence (-) and presence (+) of L-NAME. Elisabeth Beattie contributed to wire myography experiments.

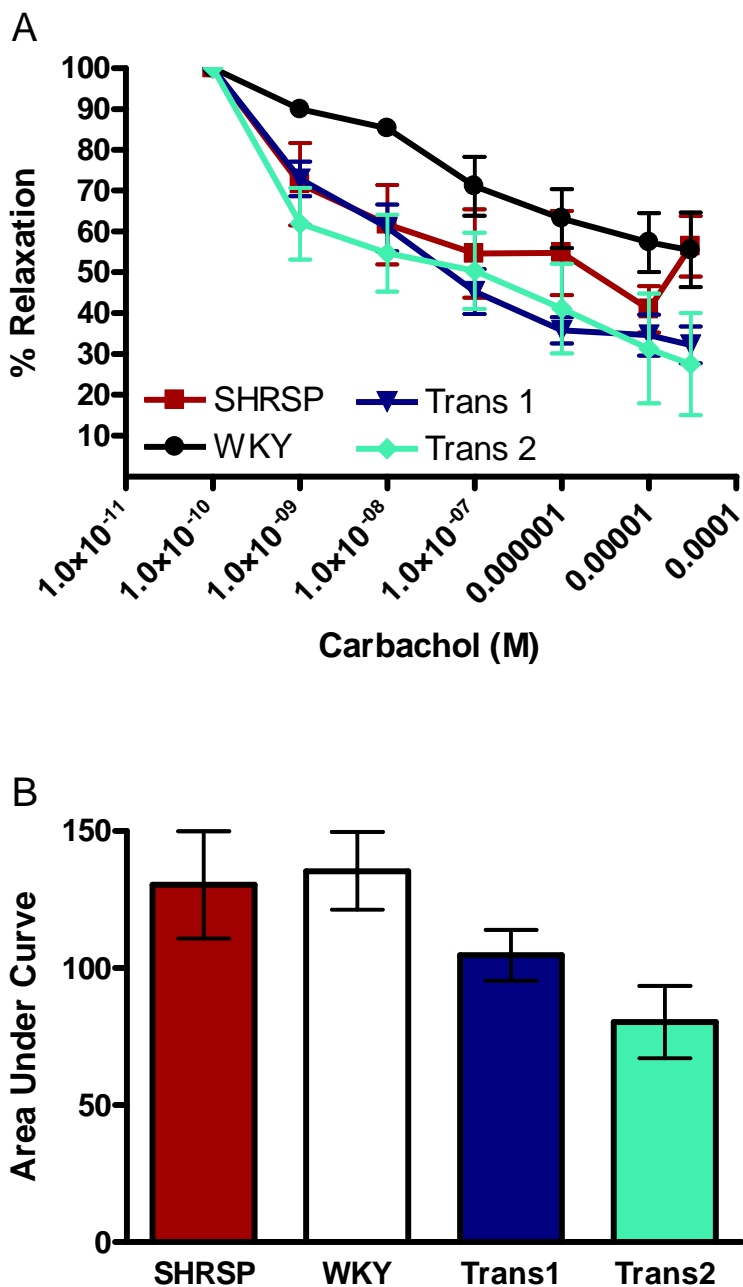


Figure 5-12: Mesenteric resistance artery function in response to carbachol-stimulated nitric oxide release.

(A) Pre-contracted MRAs from SHRSP, WKY, Trans1 and Trans2 rats were stimulated with increasing concentrations of carbachol to cause NO-mediated relaxation. (B) Corresponding area under the curve calculations do not show significant differences between SHRSP ($n=7$), WKY ($n=7$), Trans1 ($n=8$) and Trans2 ($n=5$) rats.

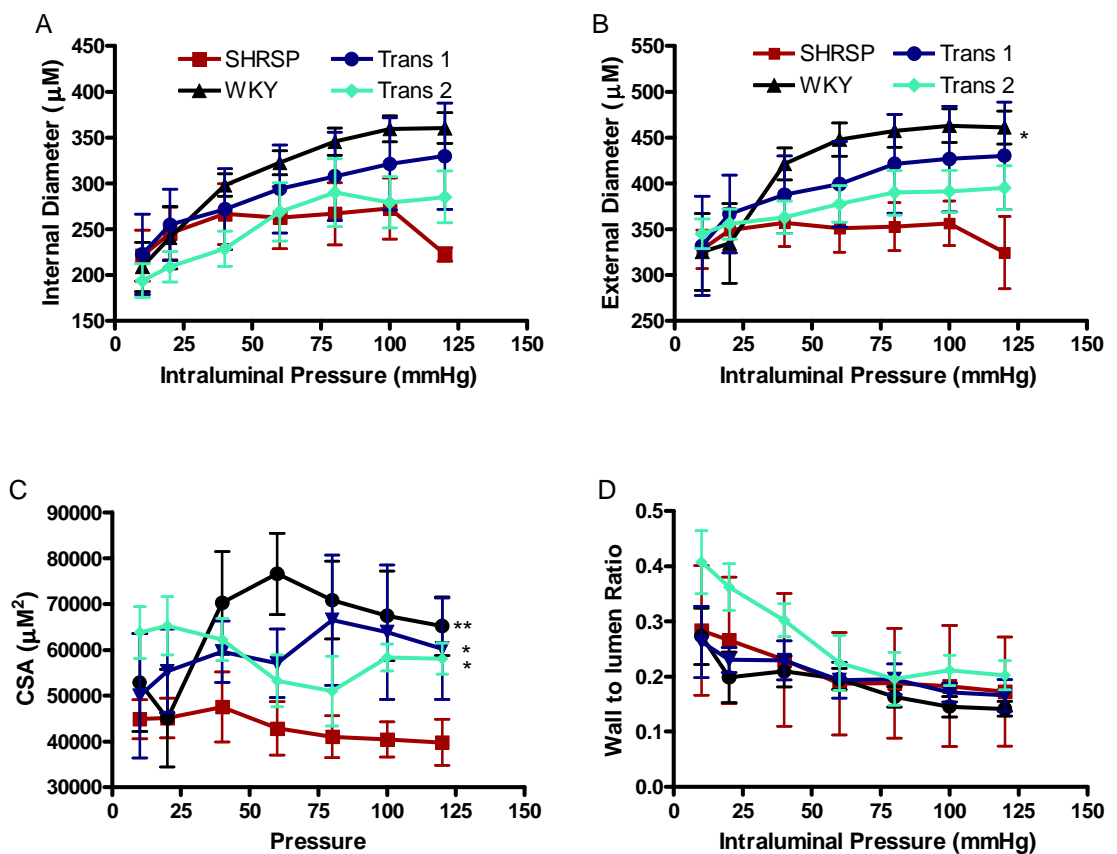


Figure 5-13: Comparison of structural parameters of mesenteric resistance arteries over a range of intraluminal pressures
 21 week old SHRSP, WKY, Trans1 and Trans2 animals. (A) Internal diameter (B) external diameter (C) cross-sectional area (CSA), and (D) wall:lumen ratio in MRAs by pressure myography. WKY, Trans1 and Trans2 rats had significantly increased CSA when compared to the SHRSP. External diameter intraluminal pressure was also significantly increased in WKY when compared to SHRSP *($p<0.01$).

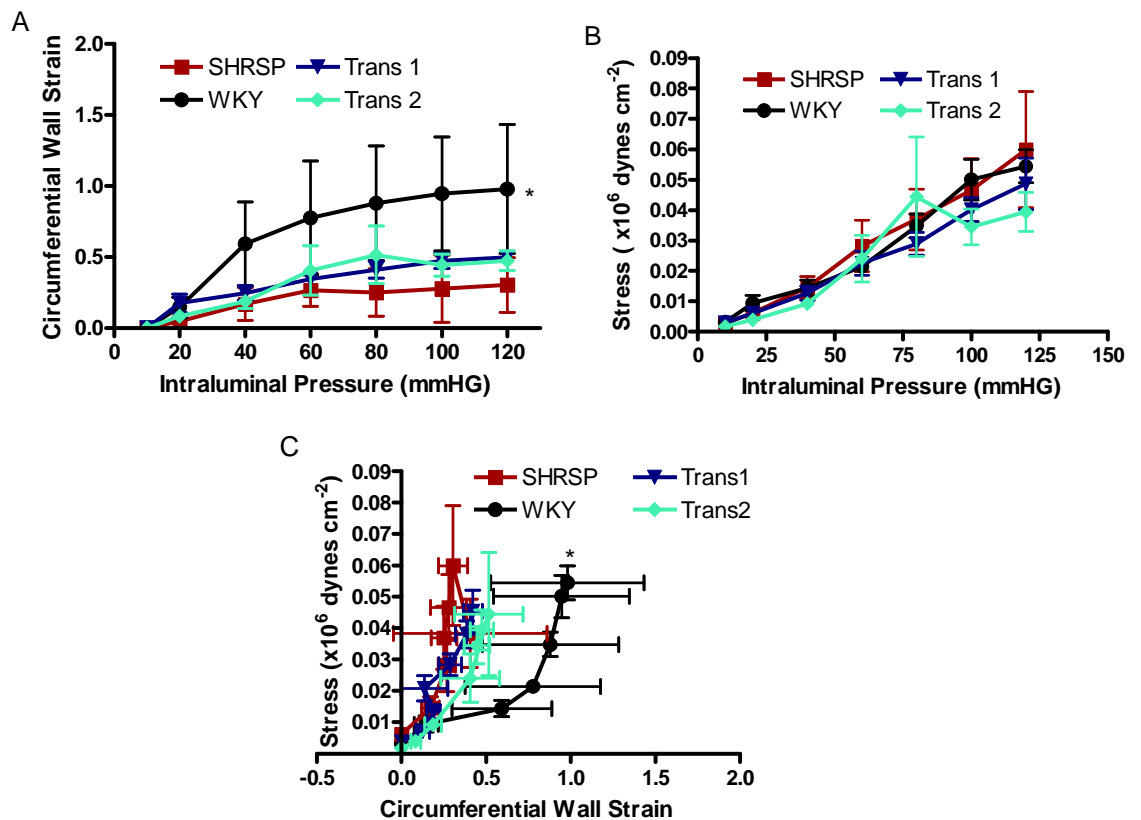


Figure 5-14: Comparison of mechanical parameters of mesenteric resistance arteries
 Pressure myography analysis in SHRSP (n=5), WKY (n=6), Trans1 (n=7) and Trans2 (n=5) rats. (A) circumferential wall strain, (B) stress-pressure relationship, and (C) stress-strain relationship curves in mesenteric arteries. SHRSP have the lowest circumferential wall strain compared to the WKY with the highest. Similarly with the right-ward shift in the stress-strain relationship indicative that WKY has reduced vessel stiffness when compared to the SHRSP.

Cross sectional-intraluminal pressure was significantly increased in WKY, Trans2 and Trans2 rats when compared to SHRSP ($p<0.01$) (Figure 5-16 Panel C). Assessment of arterial stiffness between the four strains revealed a right ward shift for WKY animals, but was not statistically significant between the groups (Figure 5-16).

5.4 Discussion

The data presented in this chapter clearly shows a reduction in renal oxidative stress in both transgenic lines (Figures 5-1). Furthermore, we saw evidence of reduced renal pathology as indicated by the absence of renal vessel hyperplasia and reduced proteinuria in the WKY, Trans1, and Trans2 rats at 21 weeks of age (Figure 5-7). These improvements in oxidative stress status and renal pathology were also apparent in salt-loaded Trans1 rats (Figure 5-2). In addition to the blood pressure reductions identified in the previous chapters and the reduced renal pathophysiology of the transgenic lines, H&E staining showed a more similar morphology to the WKY in the transgenic lines with no signs of accelerated hypertension. Aortic and mesenteric wire myography data showed that there was no significant difference between SHRSP and transgenic lines for vascular function (Figure 5-8). Mesenteric structure and function in the transgenic lines were only significantly different from the SHRSP in terms of increased vessel cross sectional area (CSA) (Figure 5-14 Panel c), but did show trends of improved structure and function (Figure 5-14).

Since previous studies have shown that the SHRSP is deficient in renal *Gstm1* expression (96), we hypothesised that production of transgenic lines in which *Gstm1* expression has been rescued would improve oxidative status and cardiovascular function. Our *ex vivo* studies have confirmed this, and although the reduction in GSH:GSSG ratio levels do not quite reach significance for Trans1 and Trans2 rats; there is a trend towards significance in the kidneys at 21 weeks. This reduction is further verified by lipid peroxidation measurements which were significantly reduced in Trans1, Trans2 and WKY rats when compared to SHRSP (Figure 5-1). This improvement of oxidative status at several steps of the oxidative stress pathway further validates the role of glutathione in the defence against oxidative stress (96).

(Figure 5-1). Given that both glutathione (*Gstm1*) and lipid peroxidation are components that occur later within the oxidative stress cascade, other earlier components of the oxidative stress pathway were investigated in order to more fully understand the mechanisms underlying the improved oxidative stress profile in these transgenic rats. Superoxide (O_2^-) and hydrogen peroxide (H_2O_2) were measured at 21 weeks of age and data showed that there were no significant differences between the strains (Figure 5-14). In contrast, previous studies in 20 week old SHRSP have demonstrated significantly increased O_2^- levels in basal and NADH stimulated renal cortex compared to WKY. There are several factors that may be responsible for this difference. Firstly, it is well recognised that measurement of reactive oxygen molecules in biological environments is inherently challenging due to their short life span and limited selectivity of detection systems (give references here). Secondly, there are differences in the methods of measurement between this and the previous study, including the use of whole kidney as opposed to renal cortex. However, similar to the current findings, there was no significant difference observed in renal H_2O_2 levels between SHRSP and WKY rats at 20 weeks of age. From the point at which glutathione acts in the ROS cascade, we observe differences in renal oxidative stress between the SHRSP and WKY, and significant improvements in the transgenic lines. Therefore, the current novel data from Trans1 and Trans2 rats, together with previous evidence in the literature convey that several components of the oxidative stress pathway are reduced in animals expressing the WKY form of *Gstm1* in the kidney (96).

To better understand the association between increased *Gstm1* expression and reduced ROS levels, renal oxidative stress was also measured at an early time point (5 weeks of age) where *Gstm1* expression is shown to be increased in both transgenic lines (Table 1). Data showed that at this early time point oxidative stress was low in all four strains when compared to kidneys from 21 week old rats. These low values at 5 weeks of age allow us to conclude that while there is an increase in *Gstm1* expression in the WKY and transgenic lines compared to the SHRSP, there is no elevation of oxidative stress in any of the four strains before the onset of hypertension. Oxidative stress measurements in other cardiovascular tissues at 21 weeks of age, i.e. the brain, show similar results to that described in the literature.

For example, Kishi *et al.* demonstrated that lipid peroxidation, (indicated by TBARS) in whole brain was significantly greater in the SHRSP than that of the WKY at 18 weeks of age (297). Results from the current study showed a trend towards a decrease in lipid peroxidation in the WKY, Trans1 and Trans2 rats when compared to the SHRSP in the whole brain at 21 weeks of age (Figure 5-4). From this data it can be concluded that increased (WKY) *Gstm1* expression at an early age not only leads to significantly decreased blood pressure levels at maturity but also improves oxidative stress levels in several organs. In addition to oxidative stress parameters, other predictors of renal pathology were measured at 21 weeks of age in order to further investigate the effects of increased *Gstm1* expression. While estimated glomerular filtration rate was within a normal range for all four strains (normal range 1.2-3.0 mls/min (298)) (Table 2), increased proteinuria levels in the SHRSP are predictive of renal damage (299). Moreover, previous studies have shown that an increased left-ventricular mass index is correlated with early signs of renal failure (300), and the SHRSP strain demonstrates both of these risk factors while our transgenic lines do not. H&E staining further supports this reduced renal pathology in our transgenic animals by showing normal WKY like arterioles throughout the kidney (Figure 5-7), whereas the SHRSP strain, at 21 weeks of age, shows signs of accelerated hypertension with the development of arteriolar hyperplasia (240). Renal fibrosis was also investigated, however, the SHRSP and WKY did not display renal fibrosis at the 21 week time point (240).

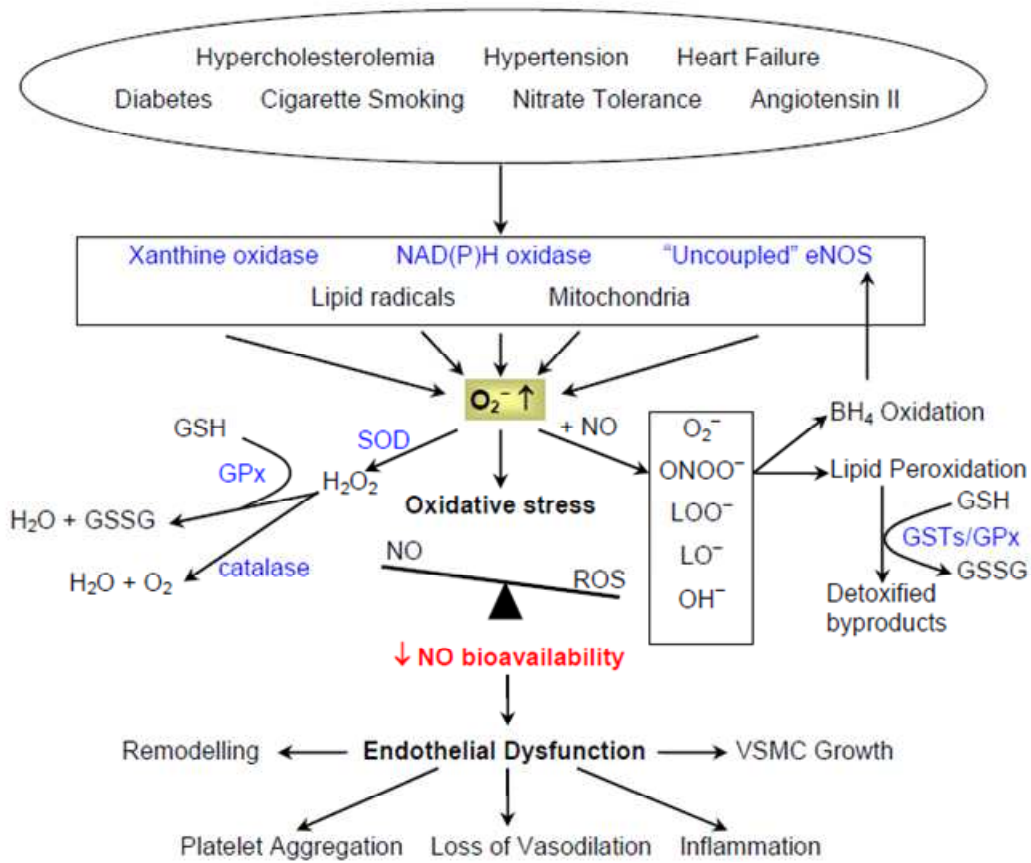


Figure 5-19: The roles of glutathione and other enzymes in the oxidative stress pathway
BH₄ = tetrahydrobiopterin; **eNOS** = endothelial nitric oxide synthase; **H₂O** = water;
H₂O₂ = hydrogen peroxide; **GPx** = glutathione peroxidase; **GSH** = glutathione; **GSSG** =
oxidized glutathione; **GSTs** = glutathione s-transferases; **LO⁻** or **LOO⁻** = lipid radicals;
NAD(P)H =nicotinamide adenine dinucleotide (phosphate); **NO** = nitric oxide; **O₂** =
molecular oxygen; **O₂⁻** = superoxide anion; **ONOO⁻** = peroxynitrite; **ROS** = reactive
oxygen species; **SOD** = superoxide dismutase; **VSMC** = vascular smooth muscle cell.
Adapted from Ref. (146)

Despite significant improvements in oxidative stress status and proteinuria, transgenic rats display similar levels of renal mass index (renal hypertrophy) to the SHRSP (Figure 5-8). This may reflect that while blood pressure is reduced in the transgenic animals, it is not equivalent to WKY levels and still display a degree of hypertension. This possibly suggests that blood pressure levels above a certain threshold (i.e. hypertensive levels) play a more significant role in renal mass index than oxidative stress (279). Furthermore, while studies consistently show a correlation between renal function and hypertension (4;284;285;301;302), this data suggests some dissociation between renal mass index and other renal pathology measurements (i.e. proteinuria and renal vascular hyperplasia), however further investigation is needed.

So far the majority of the investigations in Trans1 and Trans2 rats have focussed on the kidney. This is because the original finding of reduced *Gstm1* expression in the SHRSP was observed in the kidney. However, other organs may be contributing to the significant reduction in hypertension in Trans1 and Trans2 rats. In particular, altered contractility of the vasculature may be a contributing factor. Previous studies conducted by Kerr *et al.* have shown that the SHRSP has increased oxidative stress levels and decreased endothelial function in the aorta (234). Therefore it was important to investigate whether the increased vascular *Gstm1* expression in the transgenic animals plays a role in reducing vascular oxidative stress and improving endothelial function. Furthermore, results from a study by Yang *et al.* (303) using mice with differing susceptibility to renal injury, suggested that *Gstm1* is a novel regulator of VSMC proliferation and migration through its role in handling reactive oxygen species (303). In this study by Yang *et al.*, mice that were susceptible to vascular injury (C57BL/6) demonstrated reduced endogenous *Gstm1* expression when compared to injury resistant SV129 mice. Given that both transgenic rat lines demonstrated an increased level of expression of aortic *Gstm1* compared to the SHRSP, it was anticipated that vascular parameters and function would be similarly improved in line with the study by Yang *et al.* However, the current study failed to

show a significant change in aortic GSSG: GSH ratios and lipid peroxidation in our transgenic lines. Moreover, aortic vascular responses to phenylephrine +/- L-NAME were not significantly different between the SHRSP and transgenic animals (Figure 5-8). While these differences between the two studies can be attributed to species and background differences (i.e. mouse vs. rat, endogenous expression verses transgene), it would have been interesting to investigate if transgenic expression of *Gstm1* impacts differently on VSMC proliferation when compared to rats with endogenous expression and to further examine other down-stream effects of *Gstm1* in our transgenic lines.

Investigation of vascular function was performed through measurement of nitric oxide bioavailability in the aorta where an increase in contraction after NOS inhibition provides a measurement of basal nitric oxide available for vasodilation. In previous studies (96;240), vascular endothelial function in the SHRSP was significantly reduced when compared to the WKY (4;87;237). The data generated in this study confirms these findings in the aorta where WKY animals had significantly increased levels of basal nitric oxide bioavailability (Figure 5-12). Evaluation of endothelial function in the *Gstm1* transgenic lines however showed that there was no significant difference for either Trans1 or Trans2 animals when compared to the SHRSP. The lack of change in endothelial response in the transgenic lines, despite the increases in vascular *Gstm1* expression and reduced blood pressure (Figures 4-2), supports previous evidence suggesting that there are many factors that contribute to vascular function, especially in the SHRSP (291;304-306). Studies published by McBride *et al.*, have shown that increased vascular oxidative stress has a negative impact on vascular function (96;307). One possibility for lack of a significant endothelial response in the transgenic lines is the low sample size, especially in the Trans2 line where breeding difficulties limited the number of males available for investigation. Relaxation to carbachol was not significantly between the parental SHRSP and WKY strains, which is in direct contrast to previous studies by Koh-Tan *et al.* and McIntyre *et al.* where SHRSP rats showed an attenuated relaxation to carbachol when compare to WKY rats (240;289). The lack of significant difference in relaxation to carbachol between the parental strains and the wide variability observed in the Trans2 response could be due to damage of the

endothelial layer during experimental set up. This risk is generally greater with less experienced operators, and since sample size was limited for each strain these could be important contributing factors. In order to rectify this it would important to increase both the sample size and skill at vessel dissection and preparation, however, that was not possible within the time frame of this thesis.

Vascular remodelling in the parental and transgenic strains was assessed in MRA's. With the exception of wall to lumen ratio, basic measurements of lumen size and cross sectional areas were either significantly increased in the WKY, Trans1 and Trans2 rat MRAs (Figure 5-16) or showed trends towards significance when compared to the SHRSP. The proportional increase of diameter and cross-sectional area to increased pressure whilst maintaining similar wall to lumen ratio indicates that WKY and transgenic rats tend to have larger luminal diameter than SHRSP (despite all vessels from each of the strains being 3rd order vessels)(296;308). Mechanical properties of MRAs in the normotensive WKY animals have an improved MRA circumferential wall stain and stress-strain relationship when compared to the SHRSP which is in agreement with previously published data (308;309), Mechanical properties were not improved in the transgenic MRAs.

As mentioned previously, that while we have observed multiple significant differences between the SHRSP and the transgenic lines in terms of blood pressure, gene expression and oxidative stress, the *Gstm1* transgenic rats still remain a model of hypertension (Figure 3-1) since blood pressure is not reduced to levels equivalent to the WKY. Therefore, it is not unexpected that many of the vascular parameters measured in this study are similar between SHRSP and the transgenic lines. However, the significant impact on blood pressure levels, improved renal oxidative stress and reduced renal injury do provide strong evidence for an important role of *Gstm1* in the defence against the development of hypertension and underlying pathophysiological changes. Our findings in the rat provide strong evidence to examine the role of the *GSTM* family in a human population.

6 Characterization of the *GSTM* family in a human cohort

6.1 Introduction

Essential hypertension is a complex multifactorial disease, resulting from the combined effects of a large number of genes, each of which explain only a small fraction of blood pressure variance (280;310;311). The use of traditional methods to discover contributing genes such as genetic linkage and candidate gene approaches have proven difficult and generally failed to discover reproducible associations with hypertension (8;311). More recently, GWAS studies have had greater success identifying 43 loci associated with phenotypic variance for systolic and diastolic blood pressure (59;311;312). However, in order to understand the functional roles of these genetic loci on blood pressure regulation it is essential to interrogate the impact of these loci in suitable rodent models. This translational approach will improve our knowledge and understanding of pathways, networks and gene-environment interaction underlying essential hypertension. An equally important, alternative translational strategy is to examine robust candidate genes originally identified in rodent models, within human hypertensive and normotensive cohorts. However a major limiting factor of these studies is often poor access to suitable human tissues. In previous chapters where the *Gstm1* transgenic rat has undergone comprehensive phenotypic and molecular characterisation, it has been shown that increased renal expression of *Gstm1* plays an important role in blood pressure regulation, cardiac and renal function the SHRSP. *Gstm1* therefore represents an excellent candidate to be taken forward in a translational approach of human essential hypertension.

In humans, the glutathione-s transferases with their closely related GST isoforms and their overlapping substrate specificities have presented a particular challenge for investigators when it comes to investigating each individual enzyme. While there are many variants within the *GST* family, the majority of these studies have been focused on the *GSTM1* and *GSTT1* deletion (null) alleles and the *GSTP1* valine allele (Val/Val) (313). The significance of *GSTM1* polymorphism in human was first recognized in cancer studies demonstrating that individuals carrying the *GSTM1* deletion allele were at increased risk for colon and lung cancers (314;315). Other consequences of the genetic polymorphisms include potential differences in

tolerance to toxic agents. To date, *GSTM1* is the most comprehensively studied among all human GSTs, and has been shown to play an important role in the response to oxidative stress (196). Furthermore, many studies have linked *GSTM1* and *GSTT1* deletions to susceptibility to a number of cancers, including colorectal, lung, skin, bladder and breast cancers (211;316); in addition to being associated with increased cardiovascular risks (301;317).

Multiple studies have proposed the possible involvement of GST gene variants in human essential hypertension (8;318-320). Specifically in the study by Delles *et al.* in 2008, where they showed a significant association of the rs11807 SNP in the 3' region of *GSTM5* with hypertension in the MRC BRIGHT TDT cohort, with the T-allele being over-transmitted to hypertensive offspring. They also showed that *GSTM5* mRNA expression in renal tissue was significantly reduced in subjects homozygous for the T-allele compared with C-allele carriers (8), although they were unable to replicate the association of rs11807 SNP and hypertension in the MRC BRIGHT Study case-control cohort (involving n=1675 hypertensive and n=1654 normotensive subjects) (8).

To date, there is uncertainty as to which human glutathione S-transferase m (*GSTM*) is the direct orthologue of *Gstm1* in the rat. Although there are possibly eight members in the rat *GSTM* gene family, there are only five known members in the human *GSTM* gene family. The potential existence of several human homologues of the rat *Gstm1* and their functional involvement in cellular antioxidant defences warrant further clinical investigation. Taken together, this suggests that the entire human *GSTM* gene family should be investigated as a putative candidate gene family for cardiovascular phenotypes. In addition to investigating the *GSTM* family, in order to more fully understand the role of oxidative stress in hypertension, it will be important to examine other glutathione enzymes such as the *GPx* family. *GPx-1* and *GPx-3* considered good candidates for this due the fact that *GPx-1* is considered as an enzyme that protects the most against oxidative damage (185), while *GPx-3* is found to be predominately expressed in the kidney (189).

Human kidney tissues from a Silesian cohort of normotensive and hypertensive subjects were made available through collaboration with Dr Maciej Tomaszewski, at the University of Leicester (321). This provided an ideal opportunity to assess the human *GSTM* family and translate our findings from a rodent model of hypertension to humans. The aims of this Chapter were to (1) characterize human renal *GSTM2*, *GSTM3*, *GSTM5*, *GPx-1* and *GPx-3* expression profiles in the Silesian Renal Tissue Bank samples from both hypertensive and normotensive patients, (2) genotype the rs11807 SNP and assess correlation it with human *GSTM5* expression.

6.2 Materials and Methods

6.2.1 Ethics and Demographics

The Silesian Renal Tissue Bank is a collection of tissue from over 150 patients with nonmetastatic renal cancer. Each patient received an elective unilateral nephrectomy at the reference centre of Urology (Medical University of Silesia, Silesia Poland). Phenotyping was performed in the Department of Internal Medicine, Dialectology and Nephrology (Medical University of Silesia, Silesia Poland) which included taking a clinical history (Standard coded questionnaires), physical examinations, weight, height and blood pressure measurements according to the protocol outline in (321). Samples of approximately 1cm³ of tissue were obtained from the healthy (unaffected by cancer) pole of the kidney immediately after surgery and transferred into containers with RNAlater (Ambion, Austin, Texas, USA) and preserved at -70C before mRNA extraction and expression analysis.

Table 6-1

Demographics	Hypertensive	Normotensive
Sex (male/female)	55/37	25/20
Age (Years)	63.5 ± 9.34	55.6 ± 11.1
BMI (Kg/m ²)	28.7 ± 4.19	25.7 ± 4.0
Waist Circumference (cm)	97.95 ± 15.23	86.9 ± 12.9
SBP (mmHG)	142.98 ± 12.5	125.2 ± 7.6
DBP (mmHG)	86.4 ± 7.4	78.1 ± 6.6

DBP, diastolic blood pressure; SBP, systolic blood pressure. Data are given as mean±SD.

6.2.1.1 Ethical Approval

All subjects provided written informed consent and the study was approved by the local Ethical Committee for clinical research of the University of Leicester hospital.

6.2.2 RNA Extraction

RNA extraction from kidney tissue was conducted using RNeasy mini kits (Qiagen, USA). RNeasy kits isolate RNA based on the selective binding properties of a silica-based membrane. All steps were followed according to manufacturer's instructions; however, the extraction went as follow. The homogenation apparatus and hood

were thoroughly cleaned using RNAase (Ambion, USA) and the experiments were completed on ice to prevent RNA degradation. A maximum of 20 µg of starting tissue was used providing a yield of ~30 µg of RNA. Tissue was suspended in lysis buffer (700 µl of β-mercaptoethanol [Sigma-Aldrich, UK] in 70 ml of RTL buffer) and homogenised using a rotor-stator homogeniser. The lysate was then centrifuged for 3 min at full speed, removed and used in all future steps as illustrated in the handbook. The spin column was placed in a 1.5 ml collection tube and 40 µl of RNase-free water was added to the spin column membrane. After incubation for 1 min (room temperature), the column was centrifuged for 1 min at 8,000g room temperature. The resultant RNA-containing liquid was stored at -80°C.

6.2.2.1 Measurement of RNA quality and quantity

RNA quality and quantity was assessed using NanoDrop (Labtech) spectrophotometer in a manner identical to that described in section 2.2.1.2. The 260 nm wavelength is absorbed by RNA while the 280 nm wavelength is absorbed by sample contamination (in particular proteins). A ratio of around 2.1 (260:280 nm) indicated a pure RNA sample.

6.2.3 Reverse Transcriptase

Reverse Transcription was performed using the Applied Biostystems Reverse transcription Kit (Applied Biosystems). All steps were performed according to manufacturer's instructions. 1 µg of DNase treated RNA samples were reverse transcribed into cDNA in a 20 µL reaction containing a final concentration of 1X RT buffer, 5mM MgCL₂, 1mM dNTP mixture, 1u/µL RNAsin (RNase inhibitor), 0.5 µg of random heximers, 15 u of AMV reverse transcriptase (Multiscribe) on a 96-well plate. For negative controls, additional reactions without reverse transcriptase were included. The reaction was then placed on a thermocycler and underwent the following conditions 25°C for 10 min, 48°C for 30 mins, 95°C for 5 mins. The samples were then diluted to 100µL and stored at -20°C until use.

6.2.4 Relative real-time PCR

Relative real-time PCR was used for quantitation of mRNA expression using the ViiA™ 7 Real-Time PCR System (Applied Biosystems, USA). Sample expression was determined by a two-step RT-PCR assay using the Taqman Gene Expression Assays from Applied Biosystems/life technologies in a multiplex reaction (if the gene of interest and housekeeper reacts with the same efficiency). Each reaction consisted of 2.5 µL Taqman Expression Fast PCR Master Mix, 1x VIC labelled β-microglobulin (B2M) endogenous housekeeping probe, 1X FAM-labelled probe for the gene of interest, and 2 µL of cDNA in a final volume of 5 µL in a 384-well plate. The comparative $\Delta\Delta CT$ method was used for relative quantification of expression, normalized to B2M in each sample. While there are other common choices of control genes (including ribosomal protein, beta actin, peptidylpropyl isomerase and glucuronidase β), B2M is widely accepted to have good expression levels in a number of tissues, including those used here

Probes of interest were assessed for correct functioning using a serial dilution of cDNA input. 11 µl of TaqMan gene expression master-mix (Applied Biosystems, USA) was added to 1 µl probe of interest or control gene and 9 µl of cDNA (one reaction at each concentration of the cDNA serial dilution; 80 ng/µl, 40 ng/µl, 20 ng/µl, 10 ng/µl, 5 ng/µl). This was incubated following the protocol: denaturing at 50° C for 2 min, further denaturing at 95° C for 10 min, 50 cycles of 95° C for 15 sec each and 60° C for 1 min.

6.2.5 DNA Extraction

Peripheral blood was obtained from all participants by venipuncture. In all cases, DNA was isolated from peripheral blood mononuclear cells. 4.5 ml of red blood cell lysis solution (Qiagen, USA) was added to 4.5 ml of whole blood and inverted ten times before being incubated at room temperature for 10 min. The lysate was then centrifuged at 2000g for 10 min at room temperature. All but 5µl of the supernatant was discarded and the same volume of lysis solution (Qiagen, USA) was added and the pellet dislodged using a pipette tip. This mixture was incubated at 37°C for 1 hr, during which the tube was inverted at 10 min intervals. The solution was allowed to

homogenise for between 12 hrs and 72 hrs. 1 ml of protein precipitation solution (Qiagen, USA) was added and vortexed for 20 sec, before being centrifuged at 2000g for 10 min at room temperature. The supernatant was subsequently poured into a tube containing 3 ml of isopropranol (Qiagen, USA), inverted ~50 times and centrifuged at 2000g for 3 min at room temperature. The supernatant was poured away and the tubes left to drain for 10 min. Once dry, 3 ml of 70% (v/v) ethanol was added and tubes were inverted ten times before centrifugation at 2000g for 1 min at room temperature. Again, the supernatant was discarded and the tubes left to drain for 10 min. 250 µl of DNA hydration solution (Gentra Systems, USA) was added once dry, and incubated for 1 hr (65°C) during which the tubes were agitated at 20 min intervals. Finally, the DNA solution was left to cool overnight before being centrifuged at 2000g for 1 min at room temperature and stored at -20° C.

6.2.5.1 Measurement of DNA quantity and quality

DNA quality and quantity was assessed using a Nanodrop 8-sample spectrophotometer ND-8000 (Fisher Scientific, UK). This technology measures DNA concentration between 5 and 2000 ng/µl using different wavelengths of light projected through the sample (depending on the absorbance of DNA compared to contaminants). A 260/280 ratio of 1.8 and a 260/230 ratio of 1.8-2.2 indicates a pure sample. The Nanodrop was blanked using 2 µl of DNA hydration solution before 1 µl of each sample was loaded for analysis. The concentration and purity of each DNA sample was measured. Those with DNA concentrations <20ng/µl, a 260/280 ratio <1.6 or >2.0, or a 260/230 ratio outside of the 1.7-2.3 range were discarded. The remaining samples were diluted to 15 ng/µl using DNA hydration solution before storage at -80°C.

6.2.6 Genotyping

The Taqman genotyping assay is used to differentiate between different allelic states of SNPs through the use of coloured fluorophores. Commercially designed Taqman probe mixes (such as those used here) contain two probes, with one probe designed to anneal to each allelic state of a given SNP (e.g. one probe [VIC labelled] may anneal to the A state and one [FAM labelled] to the G state of a bi-allelic SNP).

Each probe is initially attached to a quencher in order to prevent its fluorescence. Once the probe has annealed to the DNA (SNP state allows the binding of one or both probes to DNA; homozygous major allele, heterozygous, homozygous minor allele), polymerisation and DNA amplification takes place using forward and reverse PCR primers provided with the probes. The process of polymerisation removes the quencher from the probe allowing the probes to emit fluorescence that can be detected. For this particular experiment, a human *GSTM5*-specific TaqMan gene expression assay (rs11807) was obtained from Applied Biosystems. A master-mix containing 1,200 µl of Taqman genotyping master-mix (Quanta Biosciences, USA), 800 µl of deionised water and 10 µl of specific probe mix (Applied Biosystems, USA) was vortexed for 1 min. 5 µl of this master-mix was added to 1 µl of each DNA sample placed on a 384-well plate (one DNA sample per well). At least four negative controls (containing no DNA) and two positive controls (where the allelic state was known) were placed onto each 384-well plate. The plate was then covered with a film slip and centrifuged at 2000g for 1 min at room temperature. The assay reaction was completed on a GeneAmp PCR System 9700 (Applied Biosystems, USA) using the following program: 95°C 10 min then 45 cycles of 92°C for 15 sec each, and 60°C for 1 min, 72°C for 10 min. Depending on the SNP analysed, optimisation of the reaction consisted of either the alteration of the cycle number or annealing temperature. Fluorescence was detected using a ViiA™ 7 Real-Time PCR System (Applied Biosystems, USA), where genotype calls were automatically called and checked by two independent, experienced scientists. Figure 6-1 illustrates an example of a cluster plot showing differentiation between SNP states by genotyping.

6.2.7 Statistical Analysis

Initial SNP quality checking included estimation of allele frequencies using the Hardy-Weinberg equilibrium. Gene expression was analyzed using Prism graph pad using student's t-test or 1-way ANOVA as appropriate.

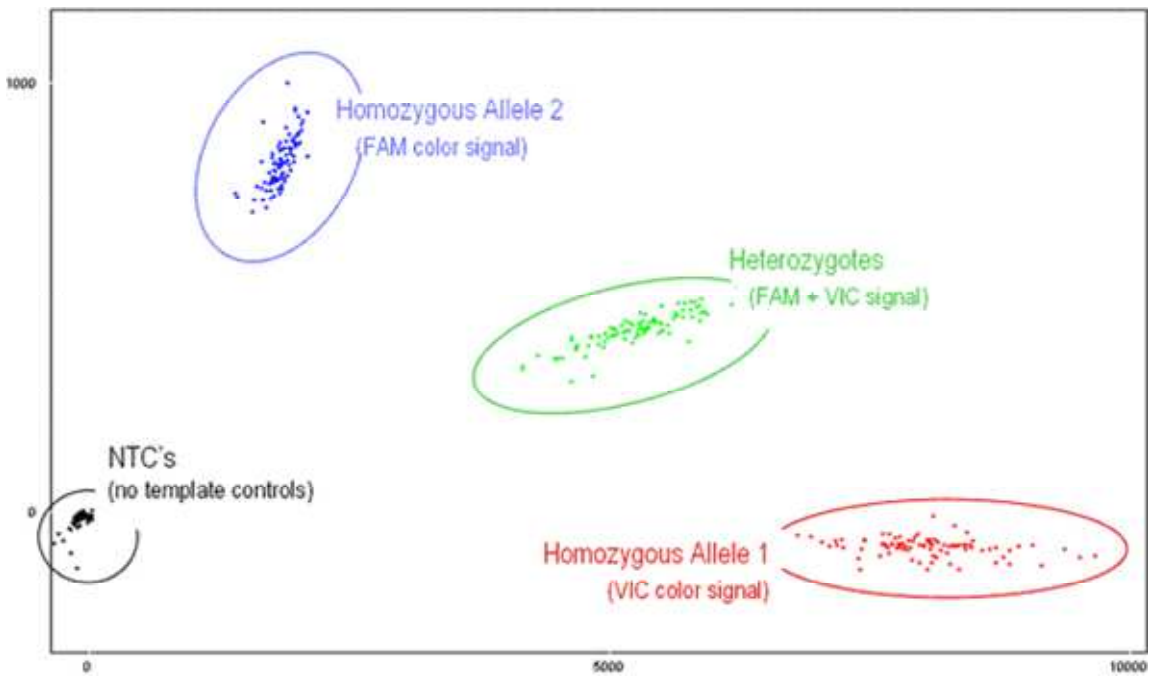


Figure 6-1: Allelic discrimination of SNPs.

SNP detection is achieved with 5' nuclease chemistry by means of exonuclease cleavage of an allele-specific 5' dye label, which generates the permanent assay signal. The Applied Biosystems SDS software uses an advanced multicomponent algorithm to calculate the distinct signal contribution of each allele of a marker from the fluorescence measurements of each sample well during the assay plate. Figure is modified from Applied Biosystems website (www.lifetechnologies.com).

6.3 Results

6.3.1.1 Genotyping

We investigated SNP rs11807, in the full Silesian Renal Tissue Bank (~200 samples). When genotyped for rs11807 ~3% (7 of 131) of the sample was homozygous for TT, 28% (54 of 131) was heterozygote for CT, and 53% (70 of 131) was homozygote for CC (Figure 6-2) (8). In the subgroup of hypertensive patients (n=56), the rs11807 SNP showed a borderline significance with increased blood pressure ($p=0.054$).

6.3.1.2 Gene Expression

Renal expression levels of *GSTM2*, *GSTM3*, and *GSTM5* were measured in renal tissue samples from both hypertensive and normotensive subjects. *GSTM5* and *GSTM3* expression was not significantly different between renal tissues from normotensive and hypertensive subjects. Renal *GSTM2* expression was significantly increased in hypertensive subjects when compared to normotensive samples ($p<0.05$) (Figure 6-3 Panel A). In addition to the glutathione s-transferases, renal glutathione peroxidises (*GPx*) were measured. There were no significant differences in *GPx-1* and *GPx-3* expression between normotensive and hypertensive patients (Figure 6-3 Panel B).

6.3.1.3 Genotype-Phenotype Association

In order to assess a genotype phenotype association, we examined how the rs11807 genotype affects *GSTM5* expression in the kidney. Renal *GSTM5* expression showed borderline significance, with lower expression in subjects homozygous for the T allele compared to subjects carrying the C allele (CC, n=47; CT n=63; TT, n=5) ($p=0.054$) (Figure 6-4).

6.3.1.4 Gene expression correlations

To determine whether gene expression patterns exists that describe or predict the differences between blood pressure, the expression patterns of the *GSTM* and *GPx* families were analyzed. Correlation between gene expression patterns were

significant between *GSTM5* and *GPx-1* ($p>0.001$) and *GSTM5* and *GPx-3* ($p>0.01$) (Figure 6-5).

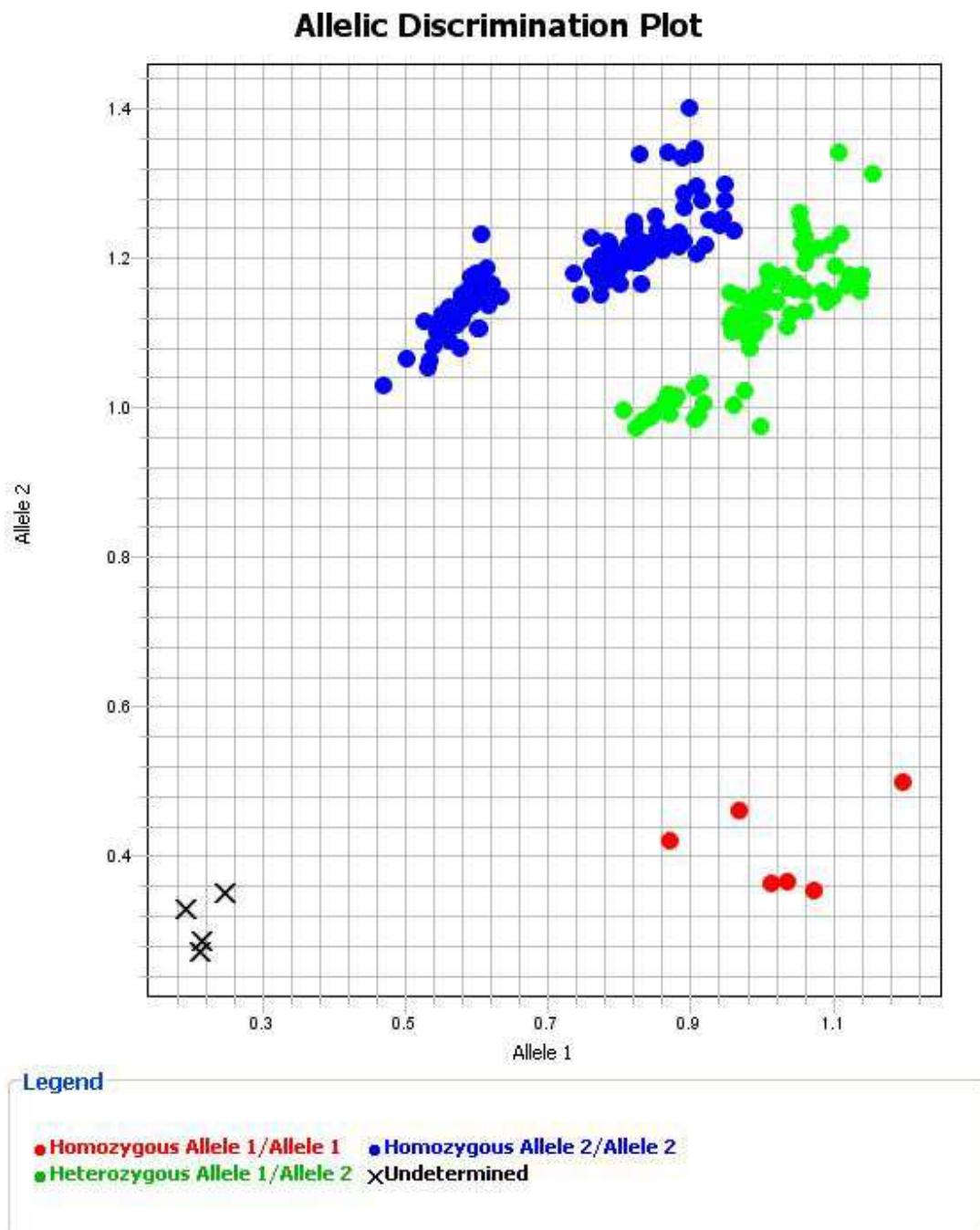


Figure 6-2: Cluster Plot of the rs11807 gene

An allelic discrimination plot showing the amplification of Allele 1 (T) on the X axis and the amplification of Allele 2 (C) on the Y axis. Samples homozygous for the T allele are identified by the red circle, and samples homozygous for the C nucleotide are identified by the blue circle. Heterozygous samples are identified by the green circles. The no template controls are indicated by the cross

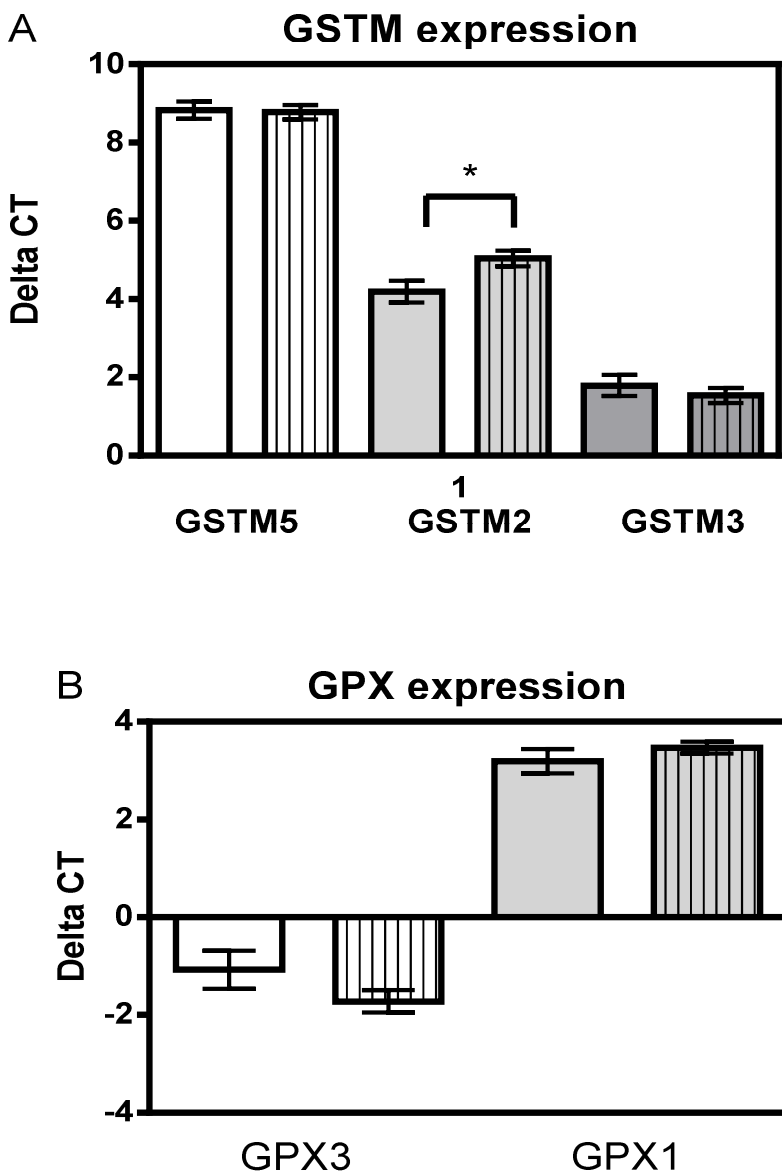


Figure 6-3: Human Glutathione s-transferase and Glutathione peroxidise expression
GSTM family renal mRNA expression was assessed in 105 subjects. Data are displayed as delta CT values. Expression of (A) *GSTM* family members, and (B) *GPx* family members. *GSTM2* expression was significantly different between normotensive (NT) and hypertensive (HT) subjects *($p<0.05$). There was no significant difference in expression of *GSTM3*, *GSTM5*, *GPx-1* or *GPx-3* ($p>0.05$) between hypertensive and normotensive subjects. Data represented as mean \pm SEM.

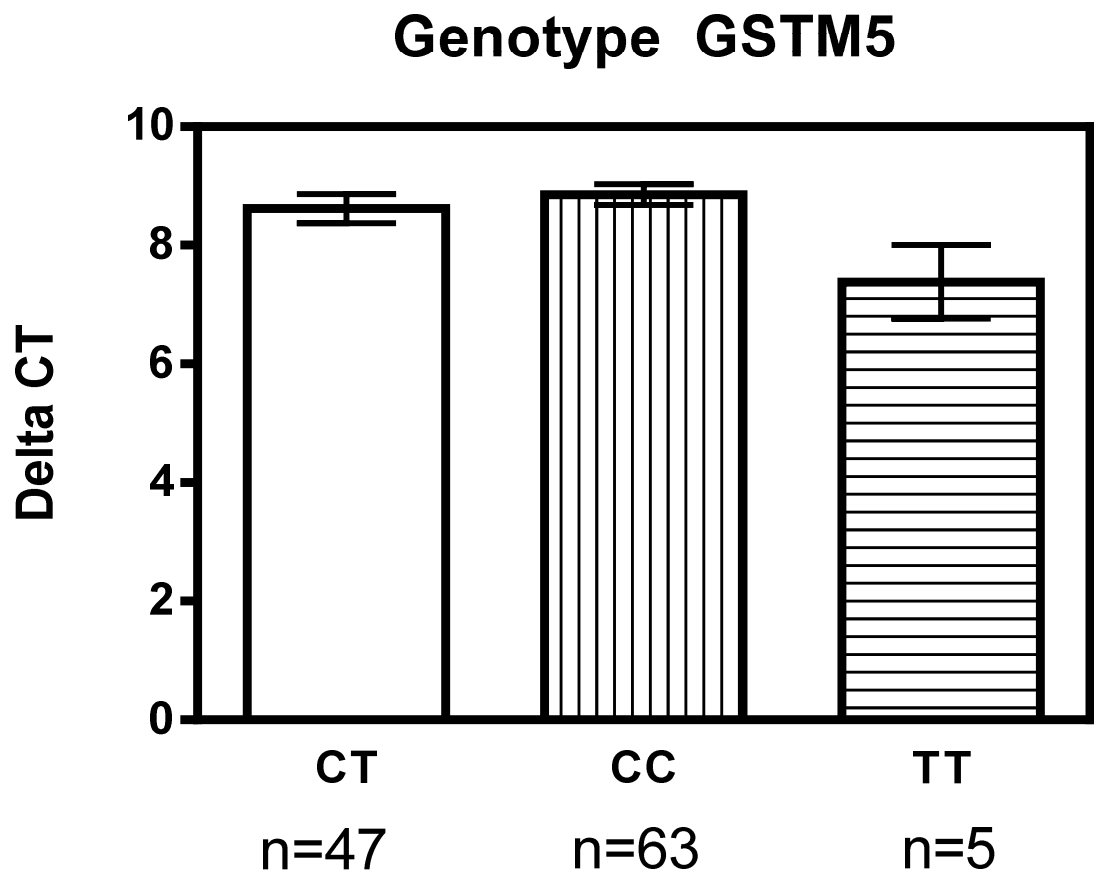


Figure 6-4: Genotype-phenotype association between *GSTM5* and rs11807.
GSTM5 renal mRNA expression was assessed in 105 subjects. Subjects were genotyped for the rs11807 polymorphism in the 3' region of *GSTM5*. Data are displayed as Delta CT values. Reduced expression in subjects homozygous for the T allele demonstrated borderline significance. Data represented as mean \pm SEM.

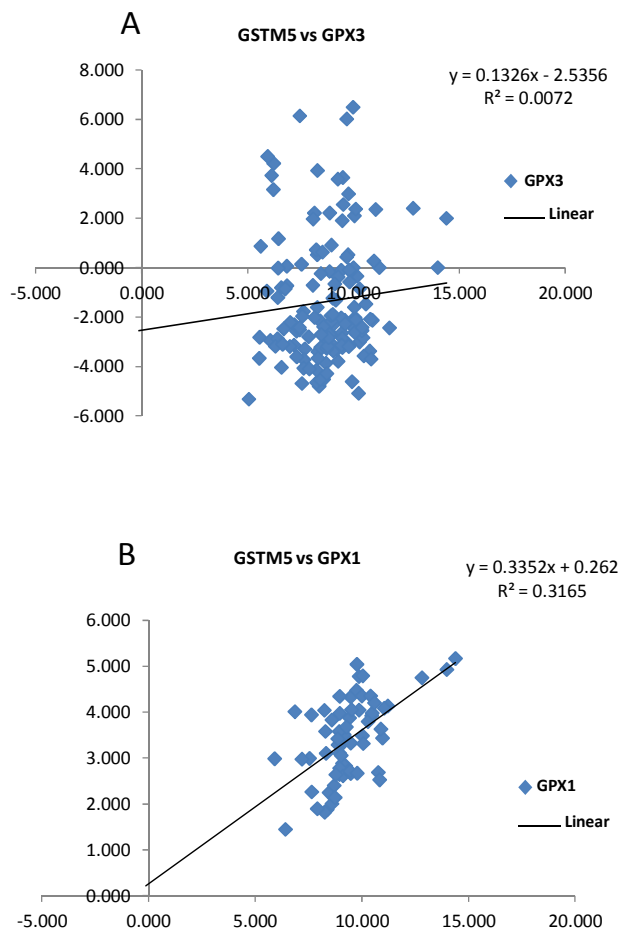


Figure 6-5: Gene expression correlation as depicted by scatter plots

The relative change of gene expression (RQ) from qRT-PCR of (A) *GSTM5* and *GPx-3* and (B) *GSTM5* and *GPx-1* were correlated. The correlations between *GSTM5/GPx-3* and *GSTM5/GPx-1* were significant at $p<0.01$ and $p<0.001$, respectively.

6.4 Discussion

The aim of this chapter was to translate findings from a rodent model of hypertension into humans and expand on the study carried out previously by Delles *et al.* (8). Expanding this investigation to include a larger number of subjects and assessment of several other members of the *GSTM* gene family has provided additional evidence to confirm a relationship between the *GSTM* family and hypertension. While there was no significant difference in renal expression in *GSTM5*, *GSTM3*, *GPx-1* and *GPx-3* between normotensive and hypertensive patients (Figure 6-3), *GSTM2* expression was significantly increased in hypertensive subjects when compared to normotensive subjects (Figure 6-3). Moreover, we identified a borderline significance ($p=0.054$) between the rs11802 SNP genotype and *GSTM5* expression. Further investigation between gene expression correlations showed there was a significant linear correlation between *GSTM5* and *GPx-1* expression levels (Figure 6-5).

The previous study carried out by Delles *et al.* used a small cohort of 45 subjects, and only examined *GSTM5* expression, as a potential ortholog of rat *Gstm1*. In this previous study it was concluded that although *Gstm1* was a robust candidate gene for hypertension in the SHRSP, it did not successfully translate to human hypertension (8). However, since a direct human ortholog of rat *Gstm1* is not apparent, in the present study the decision was made to broaden the investigation to incorporate multiple members of the *GSTM* family and also to include *GPxs*. Significant correlation between *GPx-1* and *GSTM5* was not unexpected because *GSTM5* and *GPx-1* both play a role against oxidative stress. In plants, synchronized increases in expression have been shown to routinely appear between *GSTMs* and *GPxs* (183;186). The *GPxs* have been shown to have correlated expression patterns to the *GSTM* family, and more specifically, *GPx-1* is known for its reduction of oxidative stress and *GPx-3* is found predominately in the kidney (186). Determination of unique expression profiles of the *GSTM* and *GPx* families in hypertensive patients would help to elucidate their potential role in blood pressure control and hypertension.

In humans, it is known that the *GSTM*s share a high sequence homology, because of this we hypothesized that since there is no individual ortholog, the *GSTM* family may possibly function as a combined homologue to the rat *Gstm1* gene.

Unfortunately, the expression analysis carried out in this study does not support this hypothesis so far. However, there are additional *GSTM* family members (*GSMT1* and *GSTM4*) in the human genome that need to be examined, but this was not possible in the timeframe of the visit to the University of Leicester. In contrast, another possible reason why there were no firm expression profile conclusions is that, as a family, the GST enzymes are highly redundant and to some degree other members of this family are able to compensate for the absence and or polymorphism of one isoenzyme. This has been evidenced by the recent meta-analysis of Benhamou *et al.* showed the *GSTM1* deletion carries only a small risk of lung cancer (322).

Furthermore, a recent study done by Bhattacharjee *et al.* have shown that in the absence of *GSTM1*, *GSTM2* is shown to be over expressed as a compensatory mechanism in humans (323). While our study did not have the means to incorporate *GSTM1* expression patterns and compare them to *GSTM2* expression patterns within our cohort, it is interesting to know that there are compensatory mechanism in place within the *GSTM* family. This explains part of the difficulty of trying to correlate expression patterns of the *GSTM*s within a diseased state.

We were able to show a borderline significant association of rs11807 with *GSTM5* ($p=0.054$) in the Silesian cohort; *GSTM5* mRNA expression in renal tissue was reduced in subjects homozygous for the T-allele compared with C-allele carriers, which is in concordance to the findings of Delles *et al.* (8) . Nevertheless, this does not provide strong evidence to indicate that rs11807 is the functional SNP associated with hypertension. There are a number of promotor variants that have been shown to affect *GSTM5* transcription (324). Given the strong linkage disequilibrium between markers within *GSTM5*, Delles *et al.* states that it is possible that rs11807 is in linkage disequilibrium with a functional variant upstream of this SNP regulating *GSTM5* transcription (8).

Delles *et al.* has shown through detailed synthany, that human *GSTM2* and *GSTM5* are genetically related to rat *GSTM1* (8), and thus possibly play similar roles in the

reduction of oxidative stress and blood pressure. Data from the current study supports a role for both *GSTM2* and *GSTM5*, however despite these significant relationships the results should be viewed with a certain degree of caution. Firstly, while the subjects within the Silesian cohort are considered hypertensive, each patient has been undergoing hypertension management through drug and lifestyle therapy so it is difficult to ascertain if any potential effects of *GSTM* are being confounded or masked by this treatment. Secondly, due to time and sample limitations we were unable to fully investigate oxidative stress parameters within the human cohort.

In conclusion, the translation of rat *Gstm1* findings into a human cohort demonstrated limited success. While *Gstm1* is known as a functional candidate gene for hypertension in the SHRSP, it is difficult to directly translate this into humans. This study re-confirmed the relationship between *GSTM5* mRNA expression and the T allele, and showed a correlation between *GSTM2* and hypertension. These findings should be taken forward in future studies to better identify the role *GSTM2* plays in hypertension in humans.

7 General Discussion

The aims of this study were to establish definitive proof through a transgenic rat model that reduced *Gstm1* expression in the SHRSP plays a causative role in the development of hypertension and oxidative stress. Here we provide evidence to confirm that reduced *Gstm1* expression affects blood pressure regulation and oxidative stress utilizing two independent transgenic rat lines. *Gstm1* deficiency was rescued in the SHRSP by incorporation of a normal (or WKY type) *Gstm1* gene into the SHRSP genome and this led to a significant reduction in SBP, DPB, and pulse pressure. Furthermore, oxidative stress as indicated by MDA:protein ratio and GSH:GSSG levels were significantly reduced in both transgenic lines when compared to SHRSP. Renal pathology was also reduced in both transgenic lines.

While genetic modification by random transgene insertion has proved to be a reliable and effective method to examine gene causality (7;121) recently much effort has been invested into improving techniques for gene knock out or incorporation of new genes into the rat genome. These novel advanced technologies include zinc-finger nucleases and transcription activator-like effector nucleases (TALENs) that allow for gene knockout or knock in by targeted genome editing (130;141;325). At the time of the production of our Trans1 and Trans2 rat lines, ZFN and TALEN technologies were still at a very early stage of development and were considerably more expensive e.g. around \$35,000 (£18,000) per transgenic rat in 2009, and were therefore not viable options for our transgenic rescue study. Although now considerably cheaper (approximately £5,000 per transgenic rat) it is still not possible to knockout or knock in certain genes on particular genetic backgrounds with ZFN or TALEN technology. Another recently developed genome engineering technology based on the CRISPR-Cas system (**C**lustered **R**egularly **I**nterspaced **S**hort **P**alindromic **R**epeats) developed from *Streptococcus pyogenes* is a relatively easy, and inexpensive alternative method for genome modification. The system consists of two components, namely a Cas9 endonuclease and gRNAs. The target specificity of the system relies on a 20-nucleotide variable region at the 5 prime end of the gRNAs and thus rapid, multiplexed construction of gRNA expression vectors targeting various genomic sites is possible (326). In a study by Mashimo *et al.*, CRISPR technology has been applied to the rat genome in embryos where the CRISPR method, in tandem with single strand DNA oligonucleotides as

donor templates, efficiently generated knock in mutation in rats (327). There are many advantages to this new method of transgenic production, such as a generation time of 4-6 months with a >20% efficiency and gene targeting nucleases are not strain dependent and can be used on any rodent strain (328). Furthermore, artificial nuclease can be used to induce a variety of allelic change, which was previously only available in mouse due to ES cell lines restrictions. Also, through these methods it may be possible to adapt this to other mammalian species, which would aid in the translational aspects from rodent models to humans.

When using random transgene insertion to generate transgenic rodent models, researchers can face several theoretical and technical challenges (130;141;194;329;330) some of which were faced with the *Gstm1* transgenic SHRSP rat lines. For example although both Trans1 and Trans2 lines demonstrated overall reductions in oxidative stress, BP and end organ damage, each line showed some unique molecular and phenotypic expression patterns. However, phenotypic variability within independently generated lines (despite the use of the same transgene construct and promoter) is not unique to our study. Variability has been observed by Pravenec *et al.* in the development of CD-36 transgenic rat lines in an analogous ‘transgenic rescue’ study using the ef1- α promoter (7;121). In 2001, two transgenic lines were generated, SHR-TG10, which carried 6-8 transgenic copies of CD-36 but did not show kidney transgene expression, and SHR-TG19, which carried a single transgene which was expressed at low levels in the kidney and a blood pressure reduction (121). In 2003, more transgenic lines were produced (SHR-TG93 and SHR-TG106) which showed variability regarding glucose tolerance and insulin sensitivity (7). Other limitations of gene knock-in or knockdown studies in rodent models include the intrinsic complexity of living organisms and/or the redundancy of some metabolic pathways, which prevents definitive conclusions to be made regarding the direct impact of gene modification (121;130). While transgenic animals have proven to be a powerful tool when assessing the complex mechanisms of gene-gene interaction (327), it is clear that transgenes often do not behave as independent units, but rather are significantly and variably influenced by factors such as the site of integration, the number of transgene copies in an array, expression during development and many other factors (242;260). These influences

sometimes lead to marked variations in expression patterns between different transgenic lines carrying the same construct, which appears to be the case with the *Gstm1* transgenic SHRSP. However, despite the unique characteristics of each of the transgenic lines, when investigating the role of *Gstm1* in the transgenic rat as a whole, we can conclude that increased *Gstm1* expression during developmental periods plays a role in blood pressure regulation in the SHRSP at later stages of the animal's life.

If additional time had been available, it would have been important to more fully analyze the molecular aspects of the differences in gene expression and the subsequent changes that occurred after maturation by generating additional animals from the second transgenic line (Trans2). There are many potential factors that could impact on the level of transgene expression. One of these factors could be age-related increases in DNA-methylation (275). For example two early studies in rodents, one in mouse tissues and another in rat germline competent ES and liver cells, revealed consistent age-related increases in DNA-methylation of ribosomal genes that correlated with inhibition of gene expression (241;331). A second factor that could potentially lead to variation in expression levels exhibited by insertion of identical transgenes is position effect. Often differences in expression are due to enhancers that regulate neighbouring genes (332). Future studies would be important to investigate if any of these factors play a role in the unique expression profiles between the two transgenic lines.

Furthermore, the creation of a third transgenic line would prove invaluable in clarifying the role of the WKY *Gstm1* plays in the defence against oxidative stress and the prevention of hypertension. The use of Zinc Finger Nuclease, TALEN or CRISPR technology would provide distinct benefits such as being less susceptible to transcriptional effects from the genome, an increased likelihood of physiologically faithful gene expression patterns in the transgenic lines, and a >20% efficiency (333). The production of a WKY transgenic rat in which *Gstm1* expression is knocked out or reduced could provide important confirmatory evidence for a role of *Gstm1* in the defence against the development of hypertension, if it was to show elevated blood pressure, oxidative stress and end-organ damage. Alternatively, the use of cre-lox technology (334) to produce a conditional knock-in in the SHRSP strain would

provide opportunity for more in-depth investigation. The ability to switch a gene on or off at defined times during development and maturity would allow a much clearer assessment of the roles of *Gstm1* in the development of oxidative stress in this model. Moreover, cre-lox technology could be used to generate a tissue (e.g. kidney) specific model that would further elucidate how renal oxidative stress affects blood pressure regulation. Broadening the research scope by the generation of various types of transgenic lines, would provide further evidence of the role oxidative stress plays in the development of hypertension and cardiovascular disease.

The kidney is highly vulnerable to the damage caused by ROS, and as such it is of interest to researchers due to the role it plays in blood pressure regulation (335). In this study, we have shown that in addition to the beneficial reduction of blood pressure, increased renal *Gstm1* expression during early stages of development also plays an important role in the reduction of oxidative stress and retention of optimal renal function throughout the life of the animal. Specifically, *Gstm1* transgenic rats show reduced renal pathology as indicated by the absence of renal vessel hyperplasia and reduced proteinuria when compared to the SHRSP. Furthermore, we have seen a reduction of renal oxidative stress in the transgenic lines. In certain pathological conditions, the increased generation of oxidative stress and/or the decrease in the antioxidant system leads to tissue damage (335). Moreover, lipid peroxidation is one of the many mechanisms in the oxidative stress pathway that can cause tissue damage, including within the kidney (335). These processes have been implicated in the pathogenesis of several systemic diseases such as hypertension, diabetes mellitus and hypercholesterolemia. In line with these previous findings, our study of the *Gstm1* transgenic rat has shown a significantly reduced renal lipid peroxidation and reduced blood pressure. Thus providing evidence that increasing *Gstm1* expression in SHRSP rats plays a role in the prevention of hypertension and renal pathology.

In terms of translation of our *Gstm1* findings in the rat, we were fortunate to gain access to the Silesian Renal Tissue bank, which has more than quadrupled in size since previously studied by Delles *et al.* (2008), which allowed for a more comprehensive investigation of human kidney samples from normotensive and

hypertensive subjects (8). Detailed syntenic analysis has shown that both *GSTM5* and *GSTM2* are functionally and genetically related to rat *Gstm1* and therefore worthy of further investigation. We found a borderline significant ($p=0.054$) association between the rs11802 SNP genotype and *GSTM5* expression and significantly increased *GSTM2* expression in hypertensive patients when compared to normotensive patients. Although the importance of *GSTMs* in human hypertension is still speculative, our results do indicate a potential link which requires further investigation.

While time and budget limitations in the present study prevented a more in-depth investigation of protein expression within the Silesian Renal tissue bank, our group as part of the Glasgow Biobank, has started collecting kidney biopsy tissue from normotensive and hypertensive subjects in Glasgow. These renal tissue samples are taken from the healthy pole of kidneys removed during nephrectomy due to non-metastatic renal tumor. The collection of these human samples would allow us to assess *GSTM* protein levels in the kidney along with analysis of renal oxidative stress levels in order to investigate the correlation between oxidative stress, kidney pathology and *GSTM* genotypes. It is anticipated that these studies will provide a better understanding of the role that the *GSTM* gene family plays in the defence against oxidative stress in the kidneys.

Numerous studies have shown that antioxidant and reactive oxygen species scavengers are effective in animal models for protecting against cardiovascular disease but it has been difficult to translate these findings to humans (335;336). Chronic treatment of individuals at a high risk for cardiovascular disease with varying doses of antioxidants such as vitamin C, E and β-carotene either alone or in combination have failed to reduce blood pressure, improve cardiovascular risk or reduce mortality rates(337;337-339). One example of this was shown in a study by Shao *et al.* where dietary supplementation of nitrate, in amounts resembling a rich intake of vegetables in humans, prevented the development of hypertension in young SHR rats (340). However, it is known that prolonged exposure to organic nitrates induces tolerance and endothelial dysfunction in patients with cardiovascular disease (341). It is suggested that these difficulties in translation could be due to a multiplicity of reasons, such as short duration of animal studies

(compared to a lifetime of exposure to risk factors in humans), therapeutic dose differences between animals and humans, and different pathophysiologic processes between animals and humans (335). Other reasons for antioxidant therapy failure in humans include cellular compartmentalization of antioxidants, such that potential therapeutics, do not reach appropriate targets (e.g. mitochondria). In addition, recruited patients may have advanced cardiovascular disease which is not amenable to intervention (342). Therefore, despite studies showing that patients with hypertension and oxidative damaged have an excess of ROS biomarkers, indicating the importance of oxidative stress molecular mechanisms and cardiovascular disease (336), large scale antioxidant trials have had limited success. It is possible that a stratified medicine approach, whereby the individual genetic basis of disease is taken into consideration in order to deliver personalized therapy (343), may be a more appropriate strategy for combating disease resulting from oxidative stress injury. The use of resources such as Generation Scotland (344), which is an ethically sound family- and population based biobank set up to identify the genetic basis of common complex diseases, could prove to be extremely useful in the investigation of novel prevention or therapeutic strategies, including stratified medicine approaches. Generation Scotland provides a unique opportunity to carry out health research with a highly stratified patient population could significantly improve therapeutic effectiveness or allow preventative measures before the full onset of oxidative stress injury and disease. Importantly these studies will improve our understanding of how sources of ROS and NOS are regulated, how they specifically interact with their targets, and how they modulate cardiovascular pathophysiology.

Finally, in order to more fully understand the molecular mechanisms and pathways underlying altered *Gstm1* activity and oxidative stress within the SHRSP, renal tubular epithelial cells derived from transgenic and parental rat strains could be investigated. Assessment of *Gstm1* catalytic activity could be carried out by using total GST activity assays and the proposed *GSTM1*-specific substrate 1,2-dichloro-4-nitrobenzene (DCNB) (345). This could be further investigated by analysis of the changes in renal cell oxidative stress levels and various intracellular interactions (such as cell proliferation and migration) as shown in Yang *et al.* (303). It would also

be interesting to investigate the effects of increased or decreased *Gstm1* expression in SHRSP and WKY specific vascular smooth muscle cells and the subsequent effects on oxidative stress levels within these cells in order to better understand the role of *Gstm1* on the vasculature.

In summary, multiple *in vivo*, *ex vivo* and molecular techniques have been applied in the characterisation of the *Gstm1* transgenic SHRSP rat. This model demonstrates significantly reduced blood pressure, reduced oxidative stress and improved levels of renal *Gstm1* expression. This data supports the hypothesis that reduced renal *Gstm1* plays a causative role in the development of hypertension in the SHRSP rat. Furthermore, because of these novel findings, we can apply this knowledge of the oxidative stress pathway, specifically the GSTs, to a better understanding of the cardiovascular system.

Reference List

- (1) Wolf-Maier K, Cooper RS, Kramer H, Banegas JR, Giampaoli S, Joffres MR, Poulter N, Primatesta P, Stegmayr B, Thamm M. Hypertension treatment and control in five European countries, Canada, and the United States. *Hypertension* 2004; 43(1):10-17.
- (2) He J, Ogden LG, Bazzano LA, Vupputuri S, Loria C, Whelton PK. Dietary sodium intake and incidence of congestive heart failure in overweight US men and women: first National Health and Nutrition Examination Survey Epidemiologic Follow-up Study. *Arch Intern Med* 2002; 162(14):1619-1624.
- (3) McBride MW, Carr FJ, Graham D, Anderson NH, Clark JS, Lee WK, Charchar FJ, Brosnan MJ, Dominiczak AF. Microarray analysis of rat chromosome 2 congenic strains. *Hypertension* 2003; 41(3 Pt 2):847-853.
- (4) McBride MW, Brosnan MJ, Mathers J, McLellan LI, Miller WH, Graham D, Hanlon N, Hamilton CA, Polke JM, Lee WK, Dominiczak AF. Reduction of Gstm1 expression in the stroke-prone spontaneously hypertension rat contributes to increased oxidative stress. *Hypertension* 2005; 45(4):786-792.
- (5) Polke JM, McBride MM, NS, Baker AB, Graham D, Dominiczak AF. Promoter polymorphisms implicated in reduced expression of Gstm1 in the SHRSP. 2006.
- (6) Polke JM, McBride MM, NS, Baker AB, Graham D, Dominiczak AF. Interactions between multiple promoter polymorphisms are required for reduced expression of Gstm1 in the SHRSP. 2006.
- (7) Pravenec M, Landa V, Zidek V, Musilova A, Kazdova L, Qi N, Wang J, St LE, Kurtz TW. Transgenic expression of CD36 in the spontaneously hypertensive rat is associated with amelioration of metabolic disturbances but has no effect on hypertension. *Physiol Res* 2003; 52(6):681-688.
- (8) Delles C, Padmanabhan S, Lee WK, Miller WH, McBride MW, McClure JD, Brain NJ, Wallace C, Marcano AC, Schmieder RE, Brown MJ, Caulfield MJ, Munroe PB, Farrall M, Webster J, Connell JM, Dominiczak AF. Glutathione S-transferase variants and hypertension. *J Hypertens* 2008; 26(7):1343-1352.
- (9) Lloyd-Jones D, Adams RJ, Brown TM, Carnethon M, Dai S, De SG, Ferguson TB, Ford E, Furie K, Gillespie C, Go A, Greenlund K, Haase N, Hailpern S, Ho PM, Howard V, Kissela B, Kittner S, Lackland D, Lisabeth L, Marelli A, McDermott MM, Meigs J, Mozaffarian D, Mussolino M, Nichol G, Roger VL, Rosamond W, Sacco R, Sorlie P, Roger VL, Thom T, Wasserthiel-Smoller S, Wong ND, Wylie-Rosett J. Heart disease and stroke statistics--2010 update:

a report from the American Heart Association. *Circulation* 2010; 121(7):e46-e215.

- (10) Walt G. WHO's World Health Report 2003. *BMJ* 2004; 328(7430):6.
- (11) Lloyd-Jones D, Adams RJ, Brown TM, Carnethon M, Dai S, De SG, Ferguson TB, Ford E, Furie K, Gillespie C, Go A, Greenlund K, Haase N, Hailpern S, Ho PM, Howard V, Kissela B, Kittner S, Lackland D, Lisabeth L, Marelli A, McDermott MM, Meigs J, Mozaffarian D, Mussolino M, Nichol G, Roger VL, Rosamond W, Sacco R, Sorlie P, Roger VL, Thom T, Wasserthiel-Smoller S, Wong ND, Wylie-Rosett J. Heart disease and stroke statistics--2010 update: a report from the American Heart Association. *Circulation* 2010; 121(7):e46-e215.
- (12) Lloyd-Jones D, Adams R, Carnethon M, De SG, Ferguson TB, Flegal K, Ford E, Furie K, Go A, Greenlund K, Haase N, Hailpern S, Ho M, Howard V, Kissela B, Kittner S, Lackland D, Lisabeth L, Marelli A, McDermott M, Meigs J, Mozaffarian D, Nichol G, O'Donnell C, Roger V, Rosamond W, Sacco R, Sorlie P, Stafford R, Steinberger J, Thom T, Wasserthiel-Smoller S, Wong N, Wylie-Rosett J, Hong Y. Heart disease and stroke statistics--2009 update: a report from the American Heart Association Statistics Committee and Stroke Statistics Subcommittee. *Circulation* 2009; 119(3):480-486.
- (13) Lawes CM, Vander HS, Rodgers A. The value of risk assessment and burden of disease analyses. *J Hypertens* 2006; 24(4):783-784.
- (14) Lawes CM, Vander HS, Rodgers A. The value of risk assessment and burden of disease analyses. *J Hypertens* 2006; 24(4):783-784.
- (15) European Cardiovascular Disease Statistics 2012. Available at www.BHF.co.uk, 2012. British Heart Foundation. Ref Type: Online Source
- (16) National Institute of Clinical Excellence. National Institute of Clinical Excellence. Hypertension:management of hypertension in adults in primary care. Management of Hypertension in Adults in Primary Care. Available at: www.nice.org.uk/CG034, 2014. Ref Type: Online Source
- (17) Guyton AC, Coleman TG, Fourcade JC, Navar LG. Physiologic control of arterial pressure. *Bull N Y Acad Med* 1969; 45(9):811-830.
- (18) Jeremy Booth. A Short History of Blood Pressure Measurement. Royal Society of Medicine 1977; 70.
- (19) Dieterle T. Blood pressure measurement--an overview. *Swiss Med Wkly* 2012; 142:w13517.
- (20) Akbartabartoori M, Lean ME, Hankey CR. Smoking combined with overweight or obesity markedly elevates cardiovascular risk factors. *Eur J Cardiovasc Prev Rehabil* 2006; 13(6):938-946.

- (21) Stanton JL, Braitman LE, Riley AM, Jr., Khoo CS, Smith JL. Demographic, dietary, life style, and anthropometric correlates of blood pressure. *Hypertension* 1982; 4(5 Pt 2):III135-III142.
- (22) Gradman AH, Basile JN, Carter BL, Bakris GL, Materson BJ, Black HR, Izzo JL, Jr., Oparil S, Weber MA. Combination therapy in hypertension. *J Am Soc Hypertens* 2010; 4(2):90-98.
- (23) Bianchi G, Fox U, Di Francesco GF, Giovanetti AM, Pagetti D. Blood pressure changes produced by kidney cross-transplantation between spontaneously hypertensive rats and normotensive rats. *Clin Sci Mol Med* 1974; 47(5):435-448.
- (24) Kobori H, Nangaku M, Navar LG, Nishiyama A. The intrarenal renin-angiotensin system: from physiology to the pathobiology of hypertension and kidney disease. *Pharmacol Rev* 2007; 59(3):251-287.
- (25) Harrison-Bernard LM. The renal renin-angiotensin system. *Adv Physiol Educ* 2009; 33(4):270-274.
- (26) Hall JE, Mizelle HL, Hildebrandt DA, Brands MW. Abnormal pressure natriuresis. A cause or a consequence of hypertension? *Hypertension* 1990; 15(6 Pt 1):547-559.
- (27) Head GA, Saigusa T, Mayorov DN. Angiotensin and baroreflex control of the circulation. *Braz J Med Biol Res* 2002; 35(9):1047-1059.
- (28) Bader M. Molecular interactions of vasoactive systems in cardiovascular damage. *J Cardiovasc Pharmacol* 2001; 38 Suppl 2:S7-S9.
- (29) Julius S. Corcoran Lecture. Sympathetic hyperactivity and coronary risk in hypertension. *Hypertension* 1993; 21(6 Pt 2):886-893.
- (30) WHO Global Health Risk Report 2009. Available at http://www.who.int/healthinfo/global_burden_disease/global_health_risks/en/, 2009. Ref Type: Online Source
- (31) Global Atlas on cardiovascular disease prevention and control, editors: Shanthi. World Health Organization in collaboration with the World Heart Federation and the World Stroke Organization, 2011.
- (32) Tomson J, Lip GY. Blood pressure demographics: nature or nurture genes or environment? *BMC Med* 2005; 3:3.
- (33) Oparil S, Zaman MA, Calhoun DA. Pathogenesis of hypertension. *Ann Intern Med* 2003; 139(9):761-776.
- (34) Carretero OA, Oparil S. Essential hypertension. Part I: definition and etiology. *Circulation* 2000; 101(3):329-335.

- (35) Kyrou I, Chrousos GP, Tsigos C. Stress, visceral obesity, and metabolic complications. *Ann N Y Acad Sci* 2006; 1083:77-110.
- (36) Young DB. Potassium depletion and diastolic dysfunction. *Hypertension* 2006; 48(2):201-202.
- (37) Lackland DT, Egan BM. Dietary salt restriction and blood pressure in clinical trials. *Curr Hypertens Rep* 2007; 9(4):314-319.
- (38) Rahmouni K, Correia ML, Haynes WG, Mark AL. Obesity-associated hypertension: new insights into mechanisms. *Hypertension* 2005; 45(1):9-14.
- (39) Haslam DW, James WP. Obesity. *Lancet* 2005; 366(9492):1197-1209.
- (40) Kosugi T, Nakagawa T, Kamath D, Johnson RJ. Uric acid and hypertension: an age-related relationship? *J Hum Hypertens* 2009; 23(2):75-76.
- (41) Gong M, Hubner N. Molecular genetics of human hypertension. *Clin Sci (Lond)* 2006; 110(3):315-326.
- (42) Marteau JB, Zaiou M, Siest G, Visvikis-Siest S. Genetic determinants of blood pressure regulation. *J Hypertens* 2005; 23(12):2127-2143.
- (43) Bhatnagar A. Environmental cardiology: studying mechanistic links between pollution and heart disease. *Circ Res* 2006; 99(7):692-705.
- (44) Pope CA, III. Epidemiology of fine particulate air pollution and human health: biologic mechanisms and who's at risk? *Environ Health Perspect* 2000; 108 Suppl 4:713-723.
- (45) Wald DS, Law M, Morris JK, Bestwick JP, Wald NJ. Combination therapy versus monotherapy in reducing blood pressure: meta-analysis on 11,000 participants from 42 trials. *Am J Med* 2009; 122(3):290-300.
- (46) Frisoli TM, Schmieder RE, Grodzicki T, Messerli FH. Beyond salt: lifestyle modifications and blood pressure. *Eur Heart J* 2011; 32(24):3081-3087.
- (47) Lucas DL, Brown RA, Wassef M, Giles TD. Alcohol and the cardiovascular system: research challenges and opportunities. *J Am Coll Cardiol* 2005; 45(12):1916-1924.
- (48) Norman Kaplan. Smoking and Hypertension. George Bakris, James Stoller, editors. 2-5-2014, Available at <http://www.uptodate.com/contents/smoking-and-hypertension4>. Ref Type: Online Source
- (49) Ogunbode AM, Ladipo M, Ajayi IO, Fatiregun AA. Obesity: an emerging disease. *Niger J Clin Pract* 2011; 14(4):390-394.

- (50) Palmer LG, Frindt G. Aldosterone and potassium secretion by the cortical collecting duct. *Kidney Int* 2000; 57(4):1324-1328.
- (51) Bhatnagar A. Cardiovascular pathophysiology of environmental pollutants. *Am J Physiol Heart Circ Physiol* 2004; 286(2):H479-H485.
- (52) Brook RD, Franklin B, Cascio W, Hong Y, Howard G, Lipsett M, Luepker R, Mittleman M, Samet J, Smith SC, Jr., Tager I. Air pollution and cardiovascular disease: a statement for healthcare professionals from the Expert Panel on Population and Prevention Science of the American Heart Association. *Circulation* 2004; 109(21):2655-2671.
- (53) Kunes J, Kadlecova M, Vaneckova I, Zicha J. Critical developmental periods in the pathogenesis of hypertension. *Physiol Res* 2012; 61 Suppl 1:S9-17.
- (54) Feinleib M, Garrison RJ, Fabsitz R, Christian JC, Hrubec Z, Borhani NO, Kannel WB, Rosenman R, Schwartz JT, Wagner JO. The NHLBI twin study of cardiovascular disease risk factors: methodology and summary of results. *Am J Epidemiol* 1977; 106(4):284-285.
- (55) Longini IM, Jr., Higgins MW, Hinton PC, Moll PP, Keller JB. Environmental and genetic sources of familial aggregation of blood pressure in Tecumseh, Michigan. *Am J Epidemiol* 1984; 120(1):131-144.
- (56) Biron P, Mongeau JG, Bertrand D. Familial aggregation of blood pressure in 558 adopted children. *Can Med Assoc J* 1976; 115(8):773-774.
- (57) Lifton RP. Molecular genetics of human blood pressure variation. *Science* 1996; 272(5262):676-680.
- (58) Lifton RP, Gharavi AG, Geller DS. Molecular mechanisms of human hypertension. *Cell* 2001; 104(4):545-556.
- (59) Ehret GB, Caulfield MJ. Genes for blood pressure: an opportunity to understand hypertension. *Eur Heart J* 2013; 34(13):951-961.
- (60) Ehret GB. The Contribution of the Framingham Heart Study to Gene Identification for Cardiovascular Risk Factors and Coronary Heart Disease. *Glob Heart* 2013; 8(1):59-65.
- (61) Jeunemaitre X, Soubrier F, Kotelevtsev YV, Lifton RP, Williams CS, Charru A, Hunt SC, Hopkins PN, Williams RR, Lalouel JM, . Molecular basis of human hypertension: role of angiotensinogen. *Cell* 1992; 71(1):169-180.
- (62) Staessen JA, Kuznetsova T, Wang JG, Emelianov D, Vlietinck R, Fagard R. M235T angiotensinogen gene polymorphism and cardiovascular renal risk. *J Hypertens* 1999; 17(1):9-17.

- (63) Corvol P, Persu A, Gimenez-Roqueplo AP, Jeunemaitre X. Seven lessons from two candidate genes in human essential hypertension: angiotensinogen and epithelial sodium channel. *Hypertension* 1999; 33(6):1324-1331.
- (64) Fornage M, Amos CI, Kardia S, Sing CF, Turner ST, Boerwinkle E. Variation in the region of the angiotensin-converting enzyme gene influences interindividual differences in blood pressure levels in young white males. *Circulation* 1998; 97(18):1773-1779.
- (65) O'Donnell CJ, Lindpaintner K, Larson MG, Rao VS, Ordovas JM, Schaefer EJ, Myers RH, Levy D. Evidence for association and genetic linkage of the angiotensin-converting enzyme locus with hypertension and blood pressure in men but not women in the Framingham Heart Study. *Circulation* 1998; 97(18):1766-1772.
- (66) Hunt SC, Ellison RC, Atwood LD, Pankow JS, Province MA, Leppert MF. Genome scans for blood pressure and hypertension: the National Heart, Lung, and Blood Institute Family Heart Study. *Hypertension* 2002; 40(1):1-6.
- (67) Levy D, Ehret GB, Rice K, Verwoert GC, Launer LJ, Dehghan A, Glazer NL, Morrison AC, Johnson AD, Aspelund T, Aulchenko Y, Lumley T, Kottgen A, Vasan RS, Rivadeneira F, Eiriksdottir G, Guo X, Arking DE, Mitchell GF, Mattace-Raso FU, Smith AV, Taylor K, Scharpf RB, Hwang SJ, Sijbrands EJ, Bis J, Harris TB, Ganesh SK, O'Donnell CJ, Hofman A, Rotter JI, Coresh J, Benjamin EJ, Uitterlinden AG, Heiss G, Fox CS, Witteman JC, Boerwinkle E, Wang TJ, Gudnason V, Larson MG, Chakravarti A, Psaty BM, van Duijn CM. Genome-wide association study of blood pressure and hypertension. *Nat Genet* 2009; 41(6):677-687.
- (68) Newton-Cheh C, Johnson T, Gateva V, Tobin MD, Bochud M, Coin L, Najjar SS, Zhao JH, Heath SC, Eyheramendy S, Papadakis K, Voight BF, Scott LJ, Zhang F, Farrall M, Tanaka T, Wallace C, Chambers JC, Khaw KT, Nilsson P, van der Harst P, Polidoro S, Grobbee DE, Onland-Moret NC, Bots ML, Wain LV, Elliott KS, Teumer A, Luan J, Lucas G, Kuusisto J, Burton PR, Hadley D, McArdle WL, Brown M, Dominiczak A, Newhouse SJ, Samani NJ, Webster J, Zeggini E, Beckmann JS, Bergmann S, Lim N, Song K, Vollenweider P, Waeber G, Waterworth DM, Yuan X, Groop L, Orho-Melander M, Allione A, Di GA, Guerrera S, Panico S, Ricceri F, Romanazzi V, Sacerdote C, Vineis P, Barroso I, Sandhu MS, Luben RN, Crawford GJ, Jousilahti P, Perola M, Boehnke M, Bonnycastle LL, Collins FS, Jackson AU, Mohlke KL, Stringham HM, Valle TT, Willer CJ, Bergman RN, Morken MA, Doring A, Gieger C, Illig T, Meitinger T, Org E, Pfeufer A, Wichmann HE, Kathiresan S, Marrugat J, O'Donnell CJ, Schwartz SM, Siscovick DS, Subirana I, Freimer NB, Hartikainen AL, McCarthy MI, O'Reilly PF, Peltonen L, Pouta A, de Jong PE, Snieder H, van Gilst WH, Clarke R, Goel A, Hamsten A, Peden JF, Seedorf U, Syvanen AC, Tognoni G, Lakatta EG, Sanna S, Scheet P, Schlessinger D, Scuteri A, Dorr M, Ernst F, Felix SB, Homuth G, Lorbeer R, Reffelmann T, Rettig R, Volker U, Galan P, Gut IG, Hercberg S, Lathrop GM, Zelenika D, Deloukas P, Soranzo N, Williams FM, Zhai G, Salomaa V, Laakso M, Elosua R,

- Forouhi NG, Volzke H, Uiterwaal CS, van der Schouw YT, Numans ME, Matullo G, Navis G, Berglund G, Bingham SA, Kooner JS, Connell JM, Bandinelli S, Ferrucci L, Watkins H, Spector TD, Tuomilehto J, Altshuler D, Strachan DP, Laan M, Meneton P, Wareham NJ, Uda M, Jarvelin MR, Mooser V, Melander O, Loos RJ, Elliott P, Abecasis GR, Caulfield M, Munroe PB. Genome-wide association study identifies eight loci associated with blood pressure. *Nat Genet* 2009; 41(6):666-676.
- (69) Niu T, Yang J, Wang B, Chen W, Wang Z, Laird N, Wei E, Fang Z, Lindpaintner K, Rogus JJ, Xu X. Angiotensinogen gene polymorphisms M235T/T174M: no excess transmission to hypertensive Chinese. *Hypertension* 1999; 33(2):698-702.
 - (70) Luft FC. Molecular genetics of human hypertension. *Curr Opin Nephrol Hypertens* 2000; 9(3):259-266.
 - (71) Lawes CM, Vander HS, Law MR, Elliott P, MacMahon S, Rodgers A. Blood pressure and the global burden of disease 2000. Part II: estimates of attributable burden. *J Hypertens* 2006; 24(3):423-430.
 - (72) Gaziano T, Reddy KS, Paccaud F, Horton S, Chaturvedi V. *Cardiovascular Disease*. 2006.
 - (73) Chobanian AV, Bakris GL, Black HR, Cushman WC, Green LA, Izzo JL, Jr., Jones DW, Materson BJ, Oparil S, Wright JT, Jr., Roccella EJ. Seventh report of the Joint National Committee on Prevention, Detection, Evaluation, and Treatment of High Blood Pressure. *Hypertension* 2003; 42(6):1206-1252.
 - (74) Gupta R, Guptha S. Strategies for initial management of hypertension. *Indian J Med Res* 2010; 132:531-542.
 - (75) Harrap SB. Where are all the blood-pressure genes? *Lancet* 2003; 361(9375):2149-2151.
 - (76) Gupta R. Defining hypertension in the Indian population. *Natl Med J India* 1997; 10(3):139-143.
 - (77) Appel LJ, Moore TJ, Obarzanek E, Vollmer WM, Svetkey LP, Sacks FM, Bray GA, Vogt TM, Cutler JA, Windhauser MM, Lin PH, Karanja N. A clinical trial of the effects of dietary patterns on blood pressure. DASH Collaborative Research Group. *N Engl J Med* 1997; 336(16):1117-1124.
 - (78) McBride MW, Carr FJ, Graham D, Anderson NH, Clark JS, Lee WK, Charchar FJ, Brosnan MJ, Dominiczak AF. Microarray analysis of rat chromosome 2 congenic strains. *Hypertension* 2003; 41(3 Pt 2):847-853.
 - (79) Jeffs B, Negrin CD, Graham D, Clark JS, Anderson NH, Gauguier D, Dominiczak AF. Applicability of a "speed" congenic strategy to dissect blood

- pressure quantitative trait loci on rat chromosome 2. *Hypertension* 2000; 35(1 Pt 2):179-187.
- (80) Clark JS, Jeffs B, Davidson AO, Lee WK, Anderson NH, Bihoreau MT, Brosnan MJ, Devlin AM, Kelman AW, Lindpaintner K, Dominiczak AF. Quantitative trait loci in genetically hypertensive rats. Possible sex specificity. *Hypertension* 1996; 28(5):898-906.
- (81) Lerman LO, Chade AR, Sica V, Napoli C. Animal models of hypertension: an overview. *J Lab Clin Med* 2005; 146(3):160-173.
- (82) Sun ZJ, Zhang ZE. Historic perspectives and recent advances in major animal models of hypertension. *Acta Pharmacol Sin* 2005; 26(3):295-301.
- (83) OKAMOTO K, AOKI K. Development of a strain of spontaneously hypertensive rats. *Jpn Circ J* 1963; 27:282-293.
- (84) Yamori Y, Horie R, Akiguchi I, Kihara M, Nara Y, Lovenberg W. Symptomatological classification in the development of stroke in stroke-prone spontaneously hypertensive rats. *Jpn Circ J* 1982; 46(3):274-283.
- (85) Conrad CH, Brooks WW, Robinson KG, Bing OH. Impaired myocardial function in spontaneously hypertensive rats with heart failure. *Am J Physiol* 1991; 260(1 Pt 2):H136-H145.
- (86) Yamori Y, Mori C, Nishio T, Ooshima A, Horie R, Ohtaka M, Soeda T, Saito M, Abe K, Nara Y, Nakao Y, Kihara M. Cardiac hypertrophy in early hypertension. *Am J Cardiol* 1979; 44(5):964-969.
- (87) Koh-Tan HH, Graham D, Hamilton CA, Nicoll G, Fields L, McBride MW, Young B, Dominiczak AF. Renal and vascular glutathione S-transferase mu is not affected by pharmacological intervention to reduce systolic blood pressure. *J Hypertens* 2009; 27(8):1575-1584.
- (88) Hainsworth AH, Markus HS. Do in vivo experimental models reflect human cerebral small vessel disease? A systematic review. *J Cereb Blood Flow Metab* 2008; 28(12):1877-1891.
- (89) Yamori Y, Tomimoto K, Ooshima A, Hazama F, OKAMOTO K. Proceedings: Developmental course of hypertension in the SHR-substrains susceptible to hypertensive cerebrovascular lesions. *Jpn Heart J* 1974; 15(2):209-210.
- (90) Hilbert P, Lindpaintner K, Beckmann JS, Serikawa T, Soubrier F, Dubay C, Cartwright P, De GB, Julier C, Takahasi S, . Chromosomal mapping of two genetic loci associated with blood-pressure regulation in hereditary hypertensive rats. *Nature* 1991; 353(6344):521-529.
- (91) Nabika T, Ohara H, Kato N, Isomura M. The stroke-prone spontaneously hypertensive rat: still a useful model for post-GWAS genetic studies? *Hypertens Res* 2012; 35(5):477-484.

- (92) OKAMOTO K, Hazama F, Yamori Y, Haebara H, Nagaoka A. Pathogenesis and prevention of stroke in spontaneously hypertensive rats. *Clin Sci Mol Med Suppl* 1975; 2:161s-163s.
- (93) Gupta PK, Rustgi S. Molecular markers from the transcribed/expressed region of the genome in higher plants. *Funct Integr Genomics* 2004; 4(3):139-162.
- (94) Mackay TF. The genetic architecture of quantitative traits: lessons from *Drosophila*. *Curr Opin Genet Dev* 2004; 14(3):253-257.
- (95) Roff DA. A centennial celebration for quantitative genetics. *Evolution* 2007; 61(5):1017-1032.
- (96) McBride MW, Brosnan MJ, Mathers J, McLellan LI, Miller WH, Graham D, Hanlon N, Hamilton CA, Polke JM, Lee WK, Dominiczak AF. Reduction of *Gstm1* expression in the stroke-prone spontaneously hypertension rat contributes to increased oxidative stress. *Hypertension* 2005; 45(4):786-792.
- (97) Frantz SA, Kaiser M, Gardiner SM, Gauguier D, Vincent M, Thompson JR, Bennett T, Samani NJ. Successful isolation of a rat chromosome 1 blood pressure quantitative trait locus in reciprocal congenic strains. *Hypertension* 1998; 32(4):639-646.
- (98) Garrett MR, Rapp JP. Two closely linked interactive blood pressure QTL on rat chromosome 5 defined using congenic Dahl rats. *Physiol Genomics* 2002; 8(2):81-86.
- (99) Cormier RT, Hong KH, Halberg RB, Hawkins TL, Richardson P, Mulherkar R, Dove WF, Lander ES. Secretory phospholipase *Pla2g2a* confers resistance to intestinal tumorigenesis. *Nat Genet* 1997; 17(1):88-91.
- (100) Fridman E, Pleban T, Zamir D. A recombination hotspot delimits a wild-species quantitative trait locus for tomato sugar content to 484 bp within an invertase gene. *Proc Natl Acad Sci U S A* 2000; 97(9):4718-4723.
- (101) Nadeau JH, Frankel WN. The roads from phenotypic variation to gene discovery: mutagenesis versus QTLs. *Nat Genet* 2000; 25(4):381-384.
- (102) Singer JB, Hill AE, Nadeau JH, Lander ES. Mapping quantitative trait loci for anxiety in chromosome substitution strains of mice. *Genetics* 2005; 169(2):855-862.
- (103) Lipshutz RJ, Fodor SP, Gingeras TR, Lockhart DJ. High density synthetic oligonucleotide arrays. *Nat Genet* 1999; 21(1 Suppl):20-24.
- (104) Bibikova M, Yeakley JM, Wang-Rodriguez J, Fan JB. Quantitative expression profiling of RNA from formalin-fixed, paraffin-embedded tissues using randomly assembled bead arrays. *Methods Mol Biol* 2008; 439:159-177.

- (105) Fan JB, Yeakley JM, Bibikova M, Chudin E, Wickham E, Chen J, Doucet D, Rigault P, Zhang B, Shen R, McBride C, Li HR, Fu XD, Oliphant A, Barker DL, Chee MS. A versatile assay for high-throughput gene expression profiling on universal array matrices. *Genome Res* 2004; 14(5):878-885.
- (106) Seki M, Ishida J, Narusaka M, Fujita M, Nanjo T, Umezawa T, Kamiya A, Nakajima M, Enju A, Sakurai T, Satou M, Akiyama K, Yamaguchi-Shinozaki K, Carninci P, Kawai J, Hayashizaki Y, Shinozaki K. Monitoring the expression pattern of around 7,000 *Arabidopsis* genes under ABA treatments using a full-length cDNA microarray. *Funct Integr Genomics* 2002; 2(6):282-291.
- (107) McCarthy MI, Abecasis GR, Cardon LR, Goldstein DB, Little J, Ioannidis JP, Hirschhorn JN. Genome-wide association studies for complex traits: consensus, uncertainty and challenges. *Nat Rev Genet* 2008; 9(5):356-369.
- (108) Eaves IA, Wicker LS, Ghandour G, Lyons PA, Peterson LB, Todd JA, Glynne RJ. Combining mouse congenic strains and microarray gene expression analyses to study a complex trait: the NOD model of type 1 diabetes. *Genome Res* 2002; 12(2):232-243.
- (109) Flint J, Valdar W, Shifman S, Mott R. Strategies for mapping and cloning quantitative trait genes in rodents. *Nat Rev Genet* 2005; 6(4):271-286.
- (110) Copland JA, Davies PJ, Shipley GL, Wood CG, Luxon BA, Urban RJ. The use of DNA microarrays to assess clinical samples: the transition from bedside to bench to bedside. *Recent Prog Horm Res* 2003; 58:25-53.
- (111) Muller U. Ten years of gene targeting: targeted mouse mutants, from vector design to phenotype analysis. *Mech Dev* 1999; 82(1-2):3-21.
- (112) Li P, Tong C, Mehrian-Shai R, Jia L, Wu N, Yan Y, Maxson RE, Schulze EN, Song H, Hsieh CL, Pera MF, Ying QL. Germline competent embryonic stem cells derived from rat blastocysts. *Cell* 2008; 135(7):1299-1310.
- (113) Buehr M, Meek S, Blair K, Yang J, Ure J, Silva J, McLay R, Hall J, Ying QL, Smith A. Capture of authentic embryonic stem cells from rat blastocysts. *Cell* 2008; 135(7):1287-1298.
- (114) Voigt B, Serikawa T. Pluripotent stem cells and other technologies will eventually open the door for straightforward gene targeting in the rat. *Dis Model Mech* 2009; 2(7-8):341-343.
- (115) Ryu BY, Kubota H, Avarbock MR, Brinster RL. Conservation of spermatogonial stem cell self-renewal signaling between mouse and rat. *Proc Natl Acad Sci U S A* 2005; 102(40):14302-14307.
- (116) Shinohara T, Kato M, Takehashi M, Lee J, Chuma S, Nakatsuji N, Kanatsu-Shinohara M, Hirabayashi M. Rats produced by interspecies spermatogonial transplantation in mice and in vitro microinsemination. *Proc Natl Acad Sci U S A* 2006; 103(37):13624-13628.

- (117) Kitada K, Ishishita S, Tosaka K, Takahashi R, Ueda M, Keng VW, Horie K, Takeda J. Transposon-tagged mutagenesis in the rat. *Nat Methods* 2007; 4(2):131-133.
- (118) Zan Y, Haag JD, Chen KS, Shepel LA, Wigington D, Wang YR, Hu R, Lopez-Guajardo CC, Brose HL, Porter KI, Leonard RA, Hitt AA, Schommer SL, Elegbede AF, Gould MN. Production of knockout rats using ENU mutagenesis and a yeast-based screening assay. *Nat Biotechnol* 2003; 21(6):645-651.
- (119) Smits BM, Mudde JB, van de Belt J, Verheul M, Olivier J, Homberg J, Guryev V, Cools AR, Ellenbroek BA, Plasterk RH, Cuppen E. Generation of gene knockouts and mutant models in the laboratory rat by ENU-driven target-selected mutagenesis. *Pharmacogenet Genomics* 2006; 16(3):159-169.
- (120) Aitman TJ, Critser JK, Cuppen E, Dominiczak A, Fernandez-Suarez XM, Flint J, Gauguier D, Geurts AM, Gould M, Harris PC, Holmdahl R, Hubner N, Izsvak Z, Jacob HJ, Kuramoto T, Kwitek AE, Marrone A, Mashimo T, Moreno C, Mullins J, Mullins L, Olsson T, Pravenec M, Riley L, Saar K, Serikawa T, Shull JD, Szpirer C, Twigger SN, Voigt B, Worley K. Progress and prospects in rat genetics: a community view. *Nat Genet* 2008; 40(5):516-522.
- (121) Pravenec M, Landa V, Zidek V, Musilova A, Kren V, Kazdova L, Aitman TJ, Glazier AM, Ibrahimi A, Abumrad NA, Qi N, Wang JM, St Lezin EM, Kurtz TW. Transgenic rescue of defective Cd36 ameliorates insulin resistance in spontaneously hypertensive rats. *Nat Genet* 2001; 27(2):156-158.
- (122) Li X, Li Z, Jouneau A, Zhou Q, Renard JP. Nuclear transfer: progress and quandaries. *Reprod Biol Endocrinol* 2003; 1:84.
- (123) Thomas KR, Capecchi MR. Site-directed mutagenesis by gene targeting in mouse embryo-derived stem cells. *Cell* 1987; 51(3):503-512.
- (124) Chung S, Andersson T, Sonntag KC, Bjorklund L, Isacson O, Kim KS. Analysis of different promoter systems for efficient transgene expression in mouse embryonic stem cell lines. *Stem Cells* 2002; 20(2):139-145.
- (125) Londrigan SL, Brady JL, Sutherland RM, Hawthorne WJ, Thomas HE, Jhala G, Cowan PJ, Kay TW, O'Connell PJ, Lew AM. Evaluation of promoters for driving efficient transgene expression in neonatal porcine islets. *Xenotransplantation* 2007; 14(2):119-125.
- (126) Qin L, Ding Y, Pahud DR, Chang E, Imperiale MJ, Bromberg JS. Promoter attenuation in gene therapy: interferon-gamma and tumor necrosis factor-alpha inhibit transgene expression. *Hum Gene Ther* 1997; 8(17):2019-2029.
- (127) Dai Y, Roman M, Naviaux RK, Verma IM. Gene therapy via primary myoblasts: long-term expression of factor IX protein following transplantation in vivo. *Proc Natl Acad Sci U S A* 1992; 89(22):10892-10895.

- (128) Kay MA, Li Q, Liu TJ, Leland F, Toman C, Finegold M, Woo SL. Hepatic gene therapy: persistent expression of human alpha 1-antitrypsin in mice after direct gene delivery in vivo. *Hum Gene Ther* 1992; 3(6):641-647.
- (129) Geurts AM, Cost GJ, Freyvert Y, Zeitler B, Miller JC, Choi VM, Jenkins SS, Wood A, Cui X, Meng X, Vincent A, Lam S, Michalkiewicz M, Schilling R, Foeckler J, Kalloway S, Weiler H, Menoret S, Anegon I, Davis GD, Zhang L, Rebar EJ, Gregory PD, Urnov FD, Jacob HJ, Buelow R. Knockout rats via embryo microinjection of zinc-finger nucleases. *Science* 2009; 325(5939):433.
- (130) Klug A. The discovery of zinc fingers and their development for practical applications in gene regulation and genome manipulation. *Q Rev Biophys* 2010; 43(1):1-21.
- (131) Choo Y, Klug A. Toward a code for the interactions of zinc fingers with DNA: selection of randomized fingers displayed on phage. *Proc Natl Acad Sci U S A* 1994; 91(23):11163-11167.
- (132) Bogdanove AJ, Schornack S, Lahaye T. TAL effectors: finding plant genes for disease and defense. *Curr Opin Plant Biol* 2010; 13(4):394-401.
- (133) Boch J, Bonas U. *Xanthomonas AvrBs3* family-type III effectors: discovery and function. *Annu Rev Phytopathol* 2010; 48:419-436.
- (134) Boch J, Scholze H, Schornack S, Landgraf A, Hahn S, Kay S, Lahaye T, Nickstadt A, Bonas U. Breaking the code of DNA binding specificity of TAL-type III effectors. *Science* 2009; 326(5959):1509-1512.
- (135) Moscou MJ, Bogdanove AJ. A simple cipher governs DNA recognition by TAL effectors. *Science* 2009; 326(5959):1501.
- (136) Mussolino C, Cathomen T. TALE nucleases: tailored genome engineering made easy. *Curr Opin Biotechnol* 2012; 23(5):644-650.
- (137) Mussolino C, Morbitzer R, Lutge F, Dannemann N, Lahaye T, Cathomen T. A novel TALE nuclease scaffold enables high genome editing activity in combination with low toxicity. *Nucleic Acids Res* 2011; 39(21):9283-9293.
- (138) Miller JC, Tan S, Qiao G, Barlow KA, Wang J, Xia DF, Meng X, Paschon DE, Leung E, Hinkley SJ, Dulay GP, Hua KL, Ankoudinova I, Cost GJ, Urnov FD, Zhang HS, Holmes MC, Zhang L, Gregory PD, Rebar EJ. A TALE nuclease architecture for efficient genome editing. *Nat Biotechnol* 2011; 29(2):143-148.
- (139) Capecchi MR. Altering the genome by homologous recombination. *Science* 1989; 244(4910):1288-1292.
- (140) Wood AJ, Lo TW, Zeitler B, Pickle CS, Ralston EJ, Lee AH, Amora R, Miller JC, Leung E, Meng X, Zhang L, Rebar EJ, Gregory PD, Urnov FD, Meyer BJ.

Targeted genome editing across species using ZFNs and TALENs. *Science* 2011; 333(6040):307.

- (141) Tesson L, Usal C, Menoret S, Leung E, Niles BJ, Remy S, Santiago Y, Vincent AI, Meng X, Zhang L, Gregory PD, Anegon I, Cost GJ. Knockout rats generated by embryo microinjection of TALENs. *Nat Biotechnol* 2011; 29(8):695-696.
- (142) Antoniades C, Tousoulis D, Tentolouris C, Toutouzas P, Stefanadis C. Oxidative stress, antioxidant vitamins, and atherosclerosis. From basic research to clinical practice. *Herz* 2003; 28(7):628-638.
- (143) Sanderson KJ, van Rij AM, Wade CR, Sutherland WH. Lipid peroxidation of circulating low density lipoproteins with age, smoking and in peripheral vascular disease. *Atherosclerosis* 1995; 118(1):45-51.
- (144) Redon J, Oliva MR, Tormos C, Giner V, Chaves J, Iradi A, Saez GT. Antioxidant activities and oxidative stress byproducts in human hypertension. *Hypertension* 2003; 41(5):1096-1101.
- (145) Chen K, Keaney JF, Jr. Evolving concepts of oxidative stress and reactive oxygen species in cardiovascular disease. *Curr Atheroscler Rep* 2012; 14(5):476-483.
- (146) Cai H, Harrison DG. Endothelial dysfunction in cardiovascular diseases: the role of oxidant stress. *Circ Res* 2000; 87(10):840-844.
- (147) Touyz RM, Schiffrin EL. Reactive oxygen species in vascular biology: implications in hypertension. *Histochem Cell Biol* 2004; 122(4):339-352.
- (148) Griendling KK, FitzGerald GA. Oxidative stress and cardiovascular injury: Part I: basic mechanisms and in vivo monitoring of ROS. *Circulation* 2003; 108(16):1912-1916.
- (149) Griendling KK, Sorescu D, Lassegue B, Ushio-Fukai M. Modulation of protein kinase activity and gene expression by reactive oxygen species and their role in vascular physiology and pathophysiology. *Arterioscler Thromb Vasc Biol* 2000; 20(10):2175-2183.
- (150) Touyz RM. Reactive oxygen species, vascular oxidative stress, and redox signaling in hypertension: what is the clinical significance? *Hypertension* 2004; 44(3):248-252.
- (151) Epstein BJ, Smith SM, Choksi R. Recent changes in the landscape of combination RAS blockade. *Expert Rev Cardiovasc Ther* 2009; 7(11):1373-1384.
- (152) Matsuno K, Yamada H, Iwata K, Jin D, Katsuyama M, Matsuki M, Takai S, Yamanishi K, Miyazaki M, Matsubara H, Yabe-Nishimura C. Nox1 is involved

- in angiotensin II-mediated hypertension: a study in Nox1-deficient mice. *Circulation* 2005; 112(17):2677-2685.
- (153) Zhang A, Jia Z, Wang N, Tidwell TJ, Yang T. Relative contributions of mitochondria and NADPH oxidase to deoxycorticosterone acetate-salt hypertension in mice. *Kidney Int* 2011; 80(1):51-60.
- (154) Dikalova AE, Bikineyeva AT, Budzyn K, Nazarewicz RR, McCann L, Lewis W, Harrison DG, Dikalov SI. Therapeutic targeting of mitochondrial superoxide in hypertension. *Circ Res* 2010; 107(1):106-116.
- (155) Widder JD, Fraccarollo D, Galuppo P, Hansen JM, Jones DP, Ertl G, Bauersachs J. Attenuation of angiotensin II-induced vascular dysfunction and hypertension by overexpression of Thioredoxin 2. *Hypertension* 2009; 54(2):338-344.
- (156) Ignarro LJ, Buga GM, Wood KS, Byrns RE, Chaudhuri G. Endothelium-derived relaxing factor produced and released from artery and vein is nitric oxide. *Proc Natl Acad Sci U S A* 1987; 84(24):9265-9269.
- (157) Forstermann U, Nakane M, Tracey WR, Pollock JS. Isoforms of nitric oxide synthase: functions in the cardiovascular system. *Eur Heart J* 1993; 14 Suppl I:10-15.
- (158) Forstermann U. Oxidative stress in vascular disease: causes, defense mechanisms and potential therapies. *Nat Clin Pract Cardiovasc Med* 2008; 5(6):338-349.
- (159) Forstermann U, Munzel T. Endothelial nitric oxide synthase in vascular disease: from marvel to menace. *Circulation* 2006; 113(13):1708-1714.
- (160) Vaziri ND, Wang XQ, Oveis F, Rad B. Induction of oxidative stress by glutathione depletion causes severe hypertension in normal rats. *Hypertension* 2000; 36(1):142-146.
- (161) Wu D, Cederbaum AI. Alcohol, oxidative stress, and free radical damage. *Alcohol Res Health* 2003; 27(4):277-284.
- (162) Irani K. Oxidant signaling in vascular cell growth, death, and survival : a review of the roles of reactive oxygen species in smooth muscle and endothelial cell mitogenic and apoptotic signaling. *Circ Res* 2000; 87(3):179-183.
- (163) Griendling KK, Fitzgerald GA. Oxidative stress and cardiovascular injury: Part I: basic mechanisms and in vivo monitoring of ROS. *Circulation* 2003; 108(16):1912-1916.
- (164) Wolin MS, Gupte SA, Oeckler RA. Superoxide in the vascular system. *J Vasc Res* 2002; 39(3):191-207.

- (165) Meister A. On the discovery of glutathione. *Trends Biochem Sci* 1988; 13(5):185-188.
- (166) Yuan L, Kaplowitz N. Glutathione in liver diseases and hepatotoxicity. *Mol Aspects Med* 2009; 30(1-2):29-41.
- (167) Pallardo FV, Markovic J, Garcia JL, Vina J. Role of nuclear glutathione as a key regulator of cell proliferation. *Mol Aspects Med* 2009; 30(1-2):77-85.
- (168) Huang CS, Anderson ME, Meister A. Amino acid sequence and function of the light subunit of rat kidney gamma-glutamylcysteine synthetase. *J Biol Chem* 1993; 268(27):20578-20583.
- (169) Meister A. Glutathione, metabolism and function via the gamma-glutamyl cycle. *Life Sci* 1974; 15(2):177-190.
- (170) Monostori P, Wittmann G, Karg E, Turi S. Determination of glutathione and glutathione disulfide in biological samples: an in-depth review. *J Chromatogr B Analyt Technol Biomed Life Sci* 2009; 877(28):3331-3346.
- (171) Dalle-Donne I, Rossi R, Colombo R, Giustarini D, Milzani A. Biomarkers of oxidative damage in human disease. *Clin Chem* 2006; 52(4):601-623.
- (172) Meister A, Anderson ME. Glutathione. *Annu Rev Biochem* 1983; 52:711-760.
- (173) Anderson ME, Luo JL. Glutathione therapy: from prodrugs to genes. *Semin Liver Dis* 1998; 18(4):415-424.
- (174) Briviba K, Klotz LO, Sies H. Defenses against peroxynitrite. *Methods Enzymol* 1999; 301:301-311.
- (175) Valko M, Leibfritz D, Moncol J, Cronin MT, Mazur M, Telser J. Free radicals and antioxidants in normal physiological functions and human disease. *Int J Biochem Cell Biol* 2007; 39(1):44-84.
- (176) Meister A. Glutathione, ascorbate, and cellular protection. *Cancer Res* 1994; 54(7 Suppl):1969s-1975s.
- (177) Meister A. Glutathione-ascorbic acid antioxidant system in animals. *J Biol Chem* 1994; 269(13):9397-9400.
- (178) Flohe L, Gunzler WA, Schock HH. Glutathione peroxidase: a selenoenzyme. *FEBS Lett* 1973; 32(1):132-134.
- (179) Fang YZ, Yang S, Wu G. Free radicals, antioxidants, and nutrition. *Nutrition* 2002; 18(10):872-879.
- (180) Arthur JR. The glutathione peroxidases. *Cell Mol Life Sci* 2000; 57(13-14):1825-1835.

- (181) Saito Y, Sato N, Hirashima M, Takebe G, Nagasawa S, Takahashi K. Domain structure of bi-functional selenoprotein P. *Biochem J* 2004; 381(Pt 3):841-846.
- (182) Schremmer B, Manevich Y, Feinstein SI, Fisher AB. Peroxiredoxins in the lung with emphasis on peroxiredoxin VI. *Subcell Biochem* 2007; 44:317-344.
- (183) Toppo S, Flohe L, Ursini F, Vanin S, Maiorino M. Catalytic mechanisms and specificities of glutathione peroxidases: variations of a basic scheme. *Biochim Biophys Acta* 2009; 1790(11):1486-1500.
- (184) Flohe L, Schlegel W. [Glutathione peroxidase. IV. Intracellular distribution of the glutathione peroxidase system in the rat liver]. *Hoppe Seylers Z Physiol Chem* 1971; 352(10):1401-1410.
- (185) MILLS GC. Hemoglobin catabolism. I. Glutathione peroxidase, an erythrocyte enzyme which protects hemoglobin from oxidative breakdown. *J Biol Chem* 1957; 229(1):189-197.
- (186) Flohe L. Glutathione peroxidase. *Basic Life Sci* 1988; 49:663-668.
- (187) Chu FF, Doroshow JH, Esworthy RS. Expression, characterization, and tissue distribution of a new cellular selenium-dependent glutathione peroxidase, GSHPx-GI. *J Biol Chem* 1993; 268(4):2571-2576.
- (188) Takahashi K, Avissar N, Whitin J, Cohen H. Purification and characterization of human plasma glutathione peroxidase: a selenoglycoprotein distinct from the known cellular enzyme. *Arch Biochem Biophys* 1987; 256(2):677-686.
- (189) Avissar N, Ornt DB, Yagil Y, Horowitz S, Watkins RH, Kerl EA, Takahashi K, Palmer IS, Cohen HJ. Human kidney proximal tubules are the main source of plasma glutathione peroxidase. *Am J Physiol* 1994; 266(2 Pt 1):C367-C375.
- (190) Yamasaki T, Tahara K, Takano S, Inoue-Murayama M, Rose MT, Minashima T, Aso H, Ito S. Mechanism of plasma glutathione peroxidase production in bovine adipocytes. *Cell Tissue Res* 2006; 326(1):139-147.
- (191) Comhair SA, Bhathena PR, Farver C, Thunnissen FB, Erzurum SC. Extracellular glutathione peroxidase induction in asthmatic lungs: evidence for redox regulation of expression in human airway epithelial cells. *FASEB J* 2001; 15(1):70-78.
- (192) Esworthy RS, Chu FF, Geiger P, Girotti AW, Doroshow JH. Reactivity of plasma glutathione peroxidase with hydroperoxide substrates and glutathione. *Arch Biochem Biophys* 1993; 307(1):29-34.
- (193) Winterbourn CC, Metodiewa D. Reactivity of biologically important thiol compounds with superoxide and hydrogen peroxide. *Free Radic Biol Med* 1999; 27(3-4):322-328.

- (194) Fu Y, Porres JM, Lei XG. Comparative impacts of glutathione peroxidase-1 gene knockout on oxidative stress induced by reactive oxygen and nitrogen species in mouse hepatocytes. *Biochem J* 2001; 359(Pt 3):687-695.
- (195) Weiss N, Zhang YY, Heydrick S, Bierl C, Loscalzo J. Overexpression of cellular glutathione peroxidase rescues homocyst(e)ine-induced endothelial dysfunction. *Proc Natl Acad Sci U S A* 2001; 98(22):12503-12508.
- (196) Hayes JD, McLellan LI. Glutathione and glutathione-dependent enzymes represent a co-ordinately regulated defence against oxidative stress. *Free Radic Res* 1999; 31(4):273-300.
- (197) Sheehan D, Meade G, Foley VM, Dowd CA. Structure, function and evolution of glutathione transferases: implications for classification of non-mammalian members of an ancient enzyme superfamily. *Biochem J* 2001; 360(Pt 1):1-16.
- (198) Kabesch M, Hoefler C, Carr D, Leupold W, Weiland SK, von ME. Glutathione S transferase deficiency and passive smoking increase childhood asthma. *Thorax* 2004; 59(7):569-573.
- (199) Yang P, Bamlet WR, Ebbert JO, Taylor WR, de AM. Glutathione pathway genes and lung cancer risk in young and old populations. *Carcinogenesis* 2004; 25(10):1935-1944.
- (200) Hayes JD, Pulford DJ. The glutathione S-transferase supergene family: regulation of GST and the contribution of the isoenzymes to cancer chemoprotection and drug resistance. *Crit Rev Biochem Mol Biol* 1995; 30(6):445-600.
- (201) Danielson UH, Esterbauer H, Mannervik B. Structure-activity relationships of 4-hydroxyalkenals in the conjugation catalysed by mammalian glutathione transferases. *Biochem J* 1987; 247(3):707-713.
- (202) Hubatsch I, Ridderstrom M, Mannervik B. Human glutathione transferase A4-4: an alpha class enzyme with high catalytic efficiency in the conjugation of 4-hydroxynonenal and other genotoxic products of lipid peroxidation. *Biochem J* 1998; 330 (Pt 1):175-179.
- (203) Esterbauer H, Schaur RJ, Zollner H. Chemistry and biochemistry of 4-hydroxynonenal, malonaldehyde and related aldehydes. *Free Radic Biol Med* 1991; 11(1):81-128.
- (204) Berhane K, Widersten M, Engstrom A, Kozarich JW, Mannervik B. Detoxication of base propenals and other alpha, beta-unsaturated aldehyde products of radical reactions and lipid peroxidation by human glutathione transferases. *Proc Natl Acad Sci U S A* 1994; 91(4):1480-1484.

- (205) Hayes JD, Strange RC. Potential contribution of the glutathione S-transferase supergene family to resistance to oxidative stress. *Free Radic Res* 1995; 22(3):193-207.
- (206) Jakobsson PJ, Morgenstern R, Mancini J, Ford-Hutchinson A, Persson B. Common structural features of MAPEG -- a widespread superfamily of membrane associated proteins with highly divergent functions in eicosanoid and glutathione metabolism. *Protein Sci* 1999; 8(3):689-692.
- (207) Pemble SE, Wardle AF, Taylor JB. Glutathione S-transferase class Kappa: characterization by the cloning of rat mitochondrial GST and identification of a human homologue. *Biochem J* 1996; 319 (Pt 3):749-754.
- (208) Nebert DW, Vasiliou V. Analysis of the glutathione S-transferase (GST) gene family. *Hum Genomics* 2004; 1(6):460-464.
- (209) Listowsky I, Abramovitz M, Homma H, Niitsu Y. Intracellular binding and transport of hormones and xenobiotics by glutathione-S-transferases. *Drug Metab Rev* 1988; 19(3-4):305-318.
- (210) Abramovitz M, Wong E, Cox ME, Richardson CD, Li C, Vickers PJ. 5-lipoxygenase-activating protein stimulates the utilization of arachidonic acid by 5-lipoxygenase. *Eur J Biochem* 1993; 215(1):105-111.
- (211) Hayes JD, Flanagan JU, Jowsey IR. Glutathione transferases. *Annu Rev Pharmacol Toxicol* 2005; 45:51-88.
- (212) van Bladeren PJ. Glutathione conjugation as a bioactivation reaction. *Chem Biol Interact* 2000; 129(1-2):61-76.
- (213) Frova C. Glutathione transferases in the genomics era: new insights and perspectives. *Biomol Eng* 2006; 23(4):149-169.
- (214) Okuda T, Sumiya T, Mizutani K, Tago N, Miyata T, Tanabe T, Kato H, Katsuya T, Higaki J, Ogihara T, Tsujita Y, Iwai N. Analyses of differential gene expression in genetic hypertensive rats by microarray. *Hypertens Res* 2002; 25(2):249-255.
- (215) Okuda T, Sumiya T, Iwai N, Miyata T. Difference of gene expression profiles in spontaneous hypertensive rats and Wistar-Kyoto rats from two sources. *Biochem Biophys Res Commun* 2002; 296(3):537-543.
- (216) Mannervik B, Awasthi YC, Board PG, Hayes JD, Di IC, Ketterer B, Listowsky I, Morgenstern R, Muramatsu M, Pearson WR, . Nomenclature for human glutathione transferases. *Biochem J* 1992; 282 (Pt 1):305-306.
- (217) Xu S, Wang Y, Roe B, Pearson WR. Characterization of the human class Mu glutathione S-transferase gene cluster and the GSTM1 deletion. *J Biol Chem* 1998; 273(6):3517-3527.

- (218) McLellan RA, Oscarson M, Alexandrie AK, Seidegard J, Evans DA, Rannug A, Ingelman-Sundberg M. Characterization of a human glutathione S-transferase mu cluster containing a duplicated GSTM1 gene that causes ultrarapid enzyme activity. *Mol Pharmacol* 1997; 52(6):958-965.
- (219) Board PG. Gene deletion and partial deficiency of the glutathione S-transferase (ligandin) system in man. *FEBS Lett* 1981; 135(1):12-14.
- (220) Seidegard J, Vorachek WR, Pero RW, Pearson WR. Hereditary differences in the expression of the human glutathione transferase active on trans-stilbene oxide are due to a gene deletion. *Proc Natl Acad Sci U S A* 1988; 85(19):7293-7297.
- (221) Tetlow N, Robinson A, Mantle T, Board P. Polymorphism of human mu class glutathione transferases. *Pharmacogenetics* 2004; 14(6):359-368.
- (222) Koh-Tan HH. Cardiovascular Candidate Gene within the Oxidative Stress Pathways: Rat and Human Studies. 2007.
- (223) Polke JM, McBride MM, NS, Baker AB, Graham D, Dominiczak AF. Promoter polymorphisms implicated in reduced expression of Gstm1 in the SHRSP. 2006.
- (224) Evans AL, Brown W, Kenyon CJ, Maxted KJ, Smith DC. Improved system for measuring systolic blood pressure in the conscious rat. *Med Biol Eng Comput* 1994; 32(1):101-102.
- (225) Graham D, Huynh NN, Hamilton CA, Beattie E, Smith RA, Cocheme HM, Murphy MP, Dominiczak AF. Mitochondria-targeted antioxidant MitoQ10 improves endothelial function and attenuates cardiac hypertrophy. *Hypertension* 2009; 54(2):322-328.
- (226) Jeffs B, Negrin CD, Graham D, Clark JS, Anderson NH, Gauguier D, Dominiczak AF. Applicability of a "speed" congenic strategy to dissect blood pressure quantitative trait loci on rat chromosome 2. *Hypertension* 2000; 35(1 Pt 2):179-187.
- (227) Davidson AO, Schork N, Jaques BC, Kelman AW, Sutcliffe RG, Reid JL, Dominiczak AF. Blood pressure in genetically hypertensive rats. Influence of the Y chromosome. *Hypertension* 1995; 26(3):452-459.
- (228) Masson R, Nicklin SA, Craig MA, McBride M, Gilday K, Gregorevic P, Allen JM, Chamberlain JS, Smith G, Graham D, Dominiczak AF, Napoli C, Baker AH. Onset of experimental severe cardiac fibrosis is mediated by overexpression of Angiotensin-converting enzyme 2. *Hypertension* 2009; 53(4):694-700.
- (229) Graham D, Hamilton C, Beattie E, Spiers A, Dominiczak AF. Comparison of the effects of omapatrilat and irbesartan/hydrochlorothiazide on endothelial function and cardiac hypertrophy in the stroke-prone

- spontaneously hypertensive rat: sex differences. *J Hypertens* 2004; 22(2):329-337.
- (230) Vargas F, Rodriguez-Gomez I, Perez-Abud R, Vargas TP, Baca Y, Wangensteen R. Cardiovascular and renal manifestations of glutathione depletion induced by buthionine sulfoximine. *Am J Hypertens* 2012; 25(6):629-635.
- (231) Tian N, Moore RS, Braddy S, Rose RA, Gu JW, Hughson MD, Manning RD, Jr. Interactions between oxidative stress and inflammation in salt-sensitive hypertension. *Am J Physiol Heart Circ Physiol* 2007; 293(6):H3388-H3395.
- (232) XIN J.ZHOU, XIU Q.WANG, FRED G.SILVA, and ZOLTAN LASZIK. Nitric Oxide Synthase Expression in Hypertension Induced by Inhibition of Glutathione Synthase. 300. 2002.
- (233) Mukaddam-Daher S, Menaouar A, Paquette PA, Jankowski M, Gutkowska J, Gillis MA, Shi YF, Calderone A, Tardif JC. Hemodynamic and cardiac effects of chronic eprosartan and moxonidine therapy in stroke-prone spontaneously hypertensive rats. *Hypertension* 2009; 53(5):775-781.
- (234) Kerr S, Brosnan MJ, McIntyre M, Reid JL, Dominiczak AF, Hamilton CA. Superoxide anion production is increased in a model of genetic hypertension: role of the endothelium. *Hypertension* 1999; 33(6):1353-1358.
- (235) Grunfeld S, Hamilton CA, Mesaros S, McClain SW, Dominiczak AF, Bohr DF, Malinski T. Role of superoxide in the depressed nitric oxide production by the endothelium of genetically hypertensive rats. *Hypertension* 1995; 26(6 Pt 1):854-857.
- (236) Giordano FJ. Oxygen, oxidative stress, hypoxia, and heart failure. *J Clin Invest* 2005; 115(3):500-508.
- (237) Hamilton CA, Miller WH, Al Benna S, Brosnan MJ, Drummond RD, McBride MW, Dominiczak AF. Strategies to reduce oxidative stress in cardiovascular disease. *Clin Sci (Lond)* 2004; 106(3):219-234.
- (238) Polke JM, McBride MM, NS, Baker AB, Graham D, Dominiczak AF. Interactions between multiple promoter polymorphisms are required for reduced expression of Gstm1 in the SHRSP. 2006.
- (239) Graham D, Hamilton C, Beattie E, Spiers A, Dominiczak AF. Comparison of the effects of omapatrilat and irbesartan/hydrochlorothiazide on endothelial function and cardiac hypertrophy in the stroke-prone spontaneously hypertensive rat: sex differences. *J Hypertens* 2004; 22(2):329-337.
- (240) Koh-Tan HH, McBride MW, McClure JD, Beattie E, Young B, Dominiczak AF, Graham D. Interaction between chromosome 2 and 3 regulates pulse

- pressure in the stroke-prone spontaneously hypertensive rat. *Hypertension* 2013; 62(1):33-40.
- (241) Kong Q, Wu M, Huan Y, Zhang L, Liu H, Bou G, Luo Y, Mu Y, Liu Z. Transgene expression is associated with copy number and cytomegalovirus promoter methylation in transgenic pigs. *PLoS One* 2009; 4(8):e6679.
- (242) Perez VI, Cortez LA, Lew CM, Rodriguez M, Webb CR, Van RH, Chaudhuri A, Qi W, Lee S, Bokov A, Fok W, Jones D, Richardson A, Yodoi J, Zhang Y, Tominaga K, Hubbard GB, Ikeno Y. Thioredoxin 1 overexpression extends mainly the earlier part of life span in mice. *J Gerontol A Biol Sci Med Sci* 2011; 66(12):1286-1299.
- (243) Verdecchia P, Schillaci G, Borgioni C, Ciucci A, Pede S, Porcellati C. Ambulatory pulse pressure: a potent predictor of total cardiovascular risk in hypertension. *Hypertension* 1998; 32(6):983-988.
- (244) Vaccarino V, Berger AK, Abramson J, Black HR, Setaro JF, Davey JA, Krumholz HM. Pulse pressure and risk of cardiovascular events in the systolic hypertension in the elderly program. *Am J Cardiol* 2001; 88(9):980-986.
- (245) Franklin SS, Gustin W, Wong ND, Larson MG, Weber MA, Kannel WB, Levy D. Hemodynamic patterns of age-related changes in blood pressure. The Framingham Heart Study. *Circulation* 1997; 96(1):308-315.
- (246) Safar ME. Pulse pressure in essential hypertension: clinical and therapeutical implications. *J Hypertens* 1989; 7(10):769-776.
- (247) Safar ME, Nilsson PM, Blacher J, Mimran A. Pulse pressure, arterial stiffness, and end-organ damage. *Curr Hypertens Rep* 2012; 14(4):339-344.
- (248) Parati G, Ochoa JE, Bilo G. Blood pressure variability, cardiovascular risk, and risk for renal disease progression. *Curr Hypertens Rep* 2012; 14(5):421-431.
- (249) Flores-Munoz M, Work LM, Douglas K, Denby L, Dominiczak AF, Graham D, Nicklin SA. Angiotensin-(1-9) attenuates cardiac fibrosis in the stroke-prone spontaneously hypertensive rat via the angiotensin type 2 receptor. *Hypertension* 2012; 59(2):300-307.
- (250) McLachlan J, Beattie E, Murphy MP, Koh-Tan CH, Olson E, Beattie W, Dominiczak AF, Nicklin SA, Graham D. Combined therapeutic benefit of mitochondria-targeted antioxidant, MitoQ10, and angiotensin receptor blocker, losartan, on cardiovascular function. *J Hypertens* 2014; 32(3):555-564.
- (251) Conklin DJ, Bhatnagar A. Are glutathione S-transferase null genotypes "null and void" of risk for ischemic vascular disease? *Circ Cardiovasc Genet* 2011; 4(4):339-341.

- (252) Polke JM, McBride MM, NS, Baker AB, Graham D, Dominiczak AF. Interactions between multiple promoter polymorphisms are required for reduced expression of Gstm1 in the SHRSP. 2006.
- (253) Seubert JM, Xu F, Graves JP, Collins JB, Sieber SO, Paules RS, Kroetz DL, Zeldin DC. Differential renal gene expression in prehypertensive and hypertensive spontaneously hypertensive rats. *Am J Physiol Renal Physiol* 2005; 289(3):F552-F561.
- (254) Polke JM, McBride MM, NS, Baker AB, Graham D, Dominiczak AF Promoter polymorphisms implicated in reduced expression of Gstm1 in the SHRSP. 2006.
- (255) Polke JM, McBride MM, NS, Baker AB, Graham D, Dominiczak AF. Interactions between multiple promoter polymorphisms are required for reduced expression of Gstm1 in the SHRSP. 2006.
- (256) Aitman TJ, Gotoda T, Evans AL, Imrie H, Heath KE, Trembling PM, Truman H, Wallace CA, Rahman A, Dore C, Flint J, Kren V, Zidek V, Kurtz TW, Pravenec M, Scott J. Quantitative trait loci for cellular defects in glucose and fatty acid metabolism in hypertensive rats. *Nat Genet* 1997; 16(2):197-201.
- (257) Matsumoto I, Leah J, Shanley B, Wilce P. Immediate Early Gene Expression in the Rat Brain during Ethanol Withdrawal. *Mol Cell Neurosci* 1993; 4(6):485-491.
- (258) Flavell DM, Wells T, Wells SE, Carmignac DF, Thomas GB, Robinson IC. Dominant dwarfism in transgenic rats by targeting human growth hormone (GH) expression to hypothalamic GH-releasing factor neurons. *EMBO J* 1996; 15(15):3871-3879.
- (259) Hasuwa H, Kaseda K, Einarsdottir T, Okabe M. Small interfering RNA and gene silencing in transgenic mice and rats. *FEBS Lett* 2002; 532(1-2):227-230.
- (260) Pravenec M, Churchill PC, Churchill MC, Viklicky O, Kazdova L, Aitman TJ, Petretto E, Hubner N, Wallace CA, Zimdahl H, Zidek V, Landa V, Dunbar J, Bidani A, Griffin K, Qi N, Maxova M, Kren V, Mlejnek P, Wang J, Kurtz TW. Identification of renal Cd36 as a determinant of blood pressure and risk for hypertension. *Nat Genet* 2008; 40(8):952-954.
- (261) Santos RA, Ferreira AJ, Nadu AP, Braga AN, de Almeida AP, Campagnole-Santos MJ, Baltatu O, Iliescu R, Reudelhuber TL, Bader M. Expression of an angiotensin-(1-7)-producing fusion protein produces cardioprotective effects in rats. *Physiol Genomics* 2004; 17(3):292-299.
- (262) Nagasaki H, Yokoi H, Arima H, Hirabayashi M, Ishizaki S, Tachikawa K, Murase T, Miura Y, Oiso Y. Overexpression of vasopressin in the rat

- transgenic for the metallothionein-vasopressin fusion gene. *J Endocrinol* 2002; 173(1):35-44.
- (263) Brinster RL, Chen HY, Trumbauer ME, Yagle MK, Palmiter RD. Factors affecting the efficiency of introducing foreign DNA into mice by microinjecting eggs. *Proc Natl Acad Sci U S A* 1985; 82(13):4438-4442.
- (264) Charreau B, Tesson L, Soulillou JP, Pourcel C, Anegon I. Transgenesis in rats: technical aspects and models. *Transgenic Res* 1996; 5(4):223-234.
- (265) Goldman LA, Cutrone EC, Kotenko SV, Krause CD, Langer JA. Modifications of vectors pEF-BOS, pcDNA1 and pcDNA3 result in improved convenience and expression. *Biotechniques* 1996; 21(6):1013-1015.
- (266) Wakabayashi-Ito N, Nagata S. Characterization of the regulatory elements in the promoter of the human elongation factor-1 alpha gene. *J Biol Chem* 1994; 269(47):29831-29837.
- (267) Salpea P, Russanova VR, Hirai TH, Sourlingas TG, Sekeri-Pataryas KE, Romero R, Epstein J, Howard BH. Postnatal development- and age-related changes in DNA-methylation patterns in the human genome. *Nucleic Acids Res* 2012; 40(14):6477-6494.
- (268) Baup D, Fraga L, Pernot E, Van AA, Vanherck AS, Breckpot K, Thielemans K, Schurmans S, Moser M, Leo O. Variegation and silencing in a lentiviral-based murine transgenic model. *Transgenic Res* 2010; 19(3):399-414.
- (269) Garrick D, Fiering S, Martin DI, Whitelaw E. Repeat-induced gene silencing in mammals. *Nat Genet* 1998; 18(1):56-59.
- (270) Mutskov V, Felsenfeld G. Silencing of transgene transcription precedes methylation of promoter DNA and histone H3 lysine 9. *EMBO J* 2004; 23(1):138-149.
- (271) Bessereau JL. Transposons in *C. elegans*. *WormBook* 2006;1-13.
- (272) Ueda Y, Mizuno N, Araki M. Transgenic *Xenopus laevis* with the ef1-alpha promoter as an experimental tool for amphibian retinal regeneration study. *Genesis* 2012; 50(8):642-650.
- (273) Gross JB, Hanken J, Oglesby E, Marsh-Armstrong N. Use of a ROSA26:GFP transgenic line for long-term *Xenopus* fate-mapping studies. *J Anat* 2006; 209(3):401-413.
- (274) Kinoshita M, Tanaka M, Yamashita M. [Development of transgenic fish strain and promoter analysis]. *Tanpakushitsu Kakusan Koso* 2000; 45(17 Suppl):2954-2961.

- (275) Thummel R, Burkett CT, Hyde DR. Two different transgenes to study gene silencing and re-expression during zebrafish caudal fin and retinal regeneration. *ScientificWorldJournal* 2006; 6 Suppl 1:65-81.
- (276) Clark AJ, Bissinger P, Bullock DW, Damak S, Wallace R, Whitelaw CB, Yull F. Chromosomal position effects and the modulation of transgene expression. *Reprod Fertil Dev* 1994; 6(5):589-598.
- (277) Johnson AD, Krieg PA. pXeX, a vector for efficient expression of cloned sequences in *Xenopus* embryos. *Gene* 1994; 147(2):223-226.
- (278) Ogino H, McConnell WB, Grainger RM. High-throughput transgenesis in *Xenopus* using I-SceI meganuclease. *Nat Protoc* 2006; 1(4):1703-1710.
- (279) Locatelli F, Canaud B, Eckardt KU, Stenvinkel P, Wanner C, Zoccali C. Oxidative stress in end-stage renal disease: an emerging threat to patient outcome. *Nephrol Dial Transplant* 2003; 18(7):1272-1280.
- (280) Dominiczak AF, Graham D, McBride MW, Brain NJ, Lee WK, Charchar FJ, Tomaszewski M, Delles C, Hamilton CA. Corcoran Lecture. Cardiovascular genomics and oxidative stress. *Hypertension* 2005; 45(4):636-642.
- (281) Abu-Amarah I, Bidani AK, Hacioglu R, Williamson GA, Griffin KA. Differential effects of salt on renal hemodynamics and potential pressure transmission in stroke-prone and stroke-resistant spontaneously hypertensive rats. *Am J Physiol Renal Physiol* 2005; 289(2):F305-F313.
- (282) Stitt-Cavanagh E, MacLeod L, Kennedy C. The podocyte in diabetic kidney disease. *ScientificWorldJournal* 2009; 9:1127-1139.
- (283) Matsumoto K, Morishita R, Moriguchi A, Tomita N, Yo Y, Nishii T, Nakamura T, Higaki J, Ogihara T. Prevention of renal damage by angiotensin II blockade, accompanied by increased renal hepatocyte growth factor in experimental hypertensive rats. *Hypertension* 1999; 34(2):279-284.
- (284) Wu XC, Johns EJ. Interactions between nitric oxide and superoxide on the neural regulation of proximal fluid reabsorption in hypertensive rats. *Exp Physiol* 2004; 89(3):255-261.
- (285) Yi W, Fu P, Fan Z, Aso H, Tian C, Meng Y, Liu J, Yamori Y, Nara Y, Ying C. Mitochondrial HMG-CoA synthase partially contributes to antioxidant protection in the kidney of stroke-prone spontaneously hypertensive rats. *Nutrition* 2010; 26(11-12):1176-1180.
- (286) Stitt-Cavanagh E, MacLeod L, Kennedy C. The podocyte in diabetic kidney disease. *ScientificWorldJournal* 2009; 9:1127-1139.
- (287) Potenza MA, Marasciulo FL, Chieppa DM, Brigiani GS, Formoso G, Quon MJ, Montagnani M. Insulin resistance in spontaneously hypertensive rats is associated with endothelial dysfunction characterized by imbalance

- between NO and ET-1 production. *Am J Physiol Heart Circ Physiol* 2005; 289(2):H813-H822.
- (288) Vaziri ND, Ding Y, Ni Z, Gonick HC. Altered nitric oxide metabolism and increased oxygen free radical activity in lead-induced hypertension: effect of lazaroid therapy. *Kidney Int* 1997; 52(4):1042-1046.
- (289) McIntyre M, Dominiczak AF. Nitric oxide and cardiovascular disease. *Postgrad Med J* 1997; 73(864):630-634.
- (290) Ma XL, Gao F, Nelson AH, Lopez BL, Christopher TA, Yue TL, Barone FC. Oxidative inactivation of nitric oxide and endothelial dysfunction in stroke-prone spontaneous hypertensive rats. *J Pharmacol Exp Ther* 2001; 298(3):879-885.
- (291) Tschudi MR, Mesaros S, Luscher TF, Malinski T. Direct *in situ* measurement of nitric oxide in mesenteric resistance arteries. Increased decomposition by superoxide in hypertension. *Hypertension* 1996; 27(1):32-35.
- (292) Schiffrin EL. Vascular stiffening and arterial compliance. Implications for systolic blood pressure. *Am J Hypertens* 2004; 17(12 Pt 2):39S-48S.
- (293) Pu Q, Brassard P, Javeshghani DM, Iglarz M, Webb RL, Amiri F, Schiffrin EL. Effects of combined AT1 receptor antagonist/NEP inhibitor on vascular remodeling and cardiac fibrosis in SHRSP. *J Hypertens* 2008; 26(2):322-333.
- (294) Briones AM, Gonzalez JM, Somoza B, Giraldo J, Daly CJ, Vila E, Gonzalez MC, McGrath JC, Arribas SM. Role of elastin in spontaneously hypertensive rat small mesenteric artery remodelling. *J Physiol* 2003; 552(Pt 1):185-195.
- (295) Briones AM, Rodriguez-Criado N, Hernanz R, Garcia-Redondo AB, Rodrigues-Diez RR, Alonso MJ, Egido J, Ruiz-Ortega M, Salaices M. Atorvastatin prevents angiotensin II-induced vascular remodeling and oxidative stress. *Hypertension* 2009; 54(1):142-149.
- (296) Mulvany MJ. Biophysical aspects of resistance vessels studied in spontaneous and renal hypertensive rats. *Acta Physiol Scand Suppl* 1988; 571:129-137.
- (297) Kishi T, Hirooka Y, Kimura Y, Ito K, Shimokawa H, Takeshita A. Increased reactive oxygen species in rostral ventrolateral medulla contribute to neural mechanisms of hypertension in stroke-prone spontaneously hypertensive rats. *Circulation* 2004; 109(19):2357-2362.
- (298) Rhodin MM, Anderson BJ, Peters AM, Coulthard MG, Wilkins B, Cole M, Chatelut E, Grubb A, Veal GJ, Keir MJ, Holford NH. Human renal function maturation: a quantitative description using weight and postmenstrual age. *Pediatr Nephrol* 2009; 24(1):67-76.
- (299) Burton C, Harris KP. The role of proteinuria in the progression of chronic renal failure. *Am J Kidney Dis* 1996; 27(6):765-775.

- (300) Levin A, Thompson CR, Ethier J, Carlisle EJ, Tobe S, Mendelsohn D, Burgess E, Jindal K, Barrett B, Singer J, Djurdjev O. Left ventricular mass index increase in early renal disease: impact of decline in hemoglobin. *Am J Kidney Dis* 1999; 34(1):125-134.
- (301) Wang XL, Greco M, Sim AS, Duarte N, Wang J, Wilcken DE. Glutathione S-transferase mu1 deficiency, cigarette smoking and coronary artery disease. *J Cardiovasc Risk* 2002; 9(1):25-31.
- (302) Bianchi G, Niutta E, Ferrari P, Salvati P, Salardi S, Cusi D, Colombo R, Cesana B, Tripodi G, Pati P, . A possible primary role for the kidney in essential hypertension. *Am J Hypertens* 1989; 2(2 Pt 2):2S-6S.
- (303) Yang Y, Parsons KK, Chi L, Malakauskas SM, Le TH. Glutathione S-transferase-micro1 regulates vascular smooth muscle cell proliferation, migration, and oxidative stress. *Hypertension* 2009; 54(6):1360-1368.
- (304) Grunfeld S, Hamilton CA, Mesaros S, McClain SW, Dominiczak AF, Bohr DF, Malinski T. Role of superoxide in the depressed nitric oxide production by the endothelium of genetically hypertensive rats. *Hypertension* 1995; 26(6 Pt 1):854-857.
- (305) Hamilton CA, Brosnan MJ, Al Benna S, Berg G, Dominiczak AF. NAD(P)H oxidase inhibition improves endothelial function in rat and human blood vessels. *Hypertension* 2002; 40(5):755-762.
- (306) Takai S, Krimura K, Jin D, Muramatsu M, Yoshikawa K, Mino Y, Miyazaki M. Significance of angiotensin II receptor blocker lipophilicities and their protective effect against vascular remodeling. *Hypertens Res* 2005; 28(7):593-600.
- (307) Graham D, McBride MW, Gaasenbeek M, Gilday K, Beattie E, Miller WH, McClure JD, Polke JM, Montezano A, Touyz RM, Dominiczak AF. Candidate genes that determine response to salt in the stroke-prone spontaneously hypertensive rat: congenic analysis. *Hypertension* 2007; 50(6):1134-1141.
- (308) Mulvany MJ, Korsgaard N. Correlations and otherwise between blood pressure, cardiac mass and resistance vessel characteristics in hypertensive, normotensive and hypertensive/normotensive hybrid rats. *J Hypertens* 1983; 1(3):235-244.
- (309) Intengan HD, Thibault G, Li JS, Schiffrin EL. Resistance artery mechanics, structure, and extracellular components in spontaneously hypertensive rats : effects of angiotensin receptor antagonism and converting enzyme inhibition. *Circulation* 1999; 100(22):2267-2275.
- (310) Delles C, McBride MW, Padmanabhan S, Dominiczak AF. The genetics of cardiovascular disease. *Trends Endocrinol Metab* 2008; 19(9):309-316.

- (311) Padmanabhan S, Melander O, Hastie C, Menni C, Delles C, Connell JM, Dominiczak AF. Hypertension and genome-wide association studies: combining high fidelity phenotyping and hypercontrols. *J Hypertens* 2008; 26(7):1275-1281.
- (312) He J, Kelly TN, Zhao Q, Li H, Huang J, Wang L, Jaquish CE, Sung YJ, Shimmin LC, Lu F, Mu J, Hu D, Ji X, Shen C, Guo D, Ma J, Wang R, Shen J, Li S, Chen J, Mei H, Chen CS, Chen S, Chen J, Li J, Cao J, Lu X, Wu X, Rice TK, Gu CC, Schwander K, Hamm LL, Liu D, Rao DC, Hixson JE, Gu D. Genome-Wide Association Study Identifies Eight Novel Loci Associated with Blood Pressure Responses to Interventions in Han Chinese. *Circ Cardiovasc Genet* 2013.
- (313) Ali-Osman F, Akande O, Antoun G, Mao JX, Buolamwini J. Molecular cloning, characterization, and expression in *Escherichia coli* of full-length cDNAs of three human glutathione S-transferase Pi gene variants. Evidence for differential catalytic activity of the encoded proteins. *J Biol Chem* 1997; 272(15):10004-10012.
- (314) Cotton SC, Sharp L, Little J, Brockton N. Glutathione S-transferase polymorphisms and colorectal cancer: a HuGE review. *Am J Epidemiol* 2000; 151(1):7-32.
- (315) Hou SM, Ryberg D, Falt S, Deverill A, Tefre T, Borresen AL, Haugen A, Lambert B. GSTM1 and NAT2 polymorphisms in operable and non-operable lung cancer patients. *Carcinogenesis* 2000; 21(1):49-54.
- (316) Hayes JD, Flanagan JU, Jowsey IR. Glutathione transferases. *Annu Rev Pharmacol Toxicol* 2005; 45:51-88.
- (317) Abu-Amro KK, Al-Boudari OM, Mohamed GH, Dzimiri N. T null and M null genotypes of the glutathione S-transferase gene are risk factor for CAD independent of smoking. *BMC Med Genet* 2006; 7:38.
- (318) Polimanti R, Piacentini S, Lazzarin N, Re MA, Manfellotto D, Fuciarelli M. Lack of association between essential hypertension and GSTO1 uncommon genetic variants in Italian patients. *Genet Test Mol Biomarkers* 2012; 16(6):615-620.
- (319) Polimanti R, Piacentini S, Lazzarin N, Re MA, Manfellotto D, Fuciarelli M. Glutathione S-transferase variants as risk factor for essential hypertension in Italian patients. *Mol Cell Biochem* 2011; 357(1-2):227-233.
- (320) Bessa SS, Ali EM, Hamdy SM. The role of glutathione S- transferase M1 and T1 gene polymorphisms and oxidative stress-related parameters in Egyptian patients with essential hypertension. *Eur J Intern Med* 2009; 20(6):625-630.
- (321) Tomaszewski M, Brain NJ, Charchar FJ, Wang WY, Lacka B, Padmanabahn S, Clark JS, Anderson NH, Edwards HV, Zukowska-Szczechowska E, Grzeszczak

- W, Dominiczak AF. Essential hypertension and beta2-adrenergic receptor gene: linkage and association analysis. *Hypertension* 2002; 40(3):286-291.
- (322) Benhamou S, Lee WJ, Alexandrie AK, Boffetta P, Bouchardy C, Butkiewicz D, Brockmoller J, Clapper ML, Daly A, Dolzan V, Ford J, Gaspari L, Haugen A, Hirvonen A, Husgafvel-Pursiainen K, Ingelman-Sundberg M, Kalina I, Kihara M, Kremers P, Le ML, London SJ, Nazar-Stewart V, Onon-Kihara M, Rannug A, Romkes M, Ryberg D, Seidegard J, Shields P, Strange RC, Stucker I, To-Figueras J, Brennan P, Taioli E. Meta- and pooled analyses of the effects of glutathione S-transferase M1 polymorphisms and smoking on lung cancer risk. *Carcinogenesis* 2002; 23(8):1343-1350.
- (323) Bhattacharjee P, Paul S, Banerjee M, Patra D, Banerjee P, Ghoshal N, Bandyopadhyay A, Giri AK. Functional compensation of glutathione S-transferase M1 (GSTM1) null by another GST superfamily member, GSTM2. *Sci Rep* 2013; 3:2704.
- (324) Guy CA, Hoogendoorn B, Smith SK, Coleman S, O'Donovan MC, Buckland PR. Promoter polymorphisms in glutathione-S-transferase genes affect transcription. *Pharmacogenetics* 2004; 14(1):45-51.
- (325) Cermak T, Doyle EL, Christian M, Wang L, Zhang Y, Schmidt C, Baller JA, Somia NV, Bogdanove AJ, Voytas DF. Efficient design and assembly of custom TALEN and other TAL effector-based constructs for DNA targeting. *Nucleic Acids Res* 2011; 39(12):e82.
- (326) Li W, Teng F, Li T, Zhou Q. Simultaneous generation and germline transmission of multiple gene mutations in rat using CRISPR-Cas systems. *Nat Biotechnol* 2013; 31(8):684-686.
- (327) Mashimo T. Gene targeting technologies in rats: Zinc finger nucleases, transcription activator-like effector nucleases, and clustered regularly interspaced short palindromic repeats. *Dev Growth Differ* 2014; 56(1):46-52.
- (328) Mashimo T, Takizawa A, Voigt B, Yoshimi K, Hiai H, Kuramoto T, Serikawa T. Generation of knockout rats with X-linked severe combined immunodeficiency (X-SCID) using zinc-finger nucleases. *PLoS One* 2010; 5(1):e8870.
- (329) Fu Y, Foden JA, Khayter C, Maeder ML, Reyne D, Joung JK, Sander JD. High-frequency off-target mutagenesis induced by CRISPR-Cas nucleases in human cells. *Nat Biotechnol* 2013; 31(9):822-826.
- (330) Radecke S, Radecke F, Cathomen T, Schwarz K. Zinc-finger nuclease-induced gene repair with oligodeoxynucleotides: wanted and unwanted target locus modifications. *Mol Ther* 2010; 18(4):743-753.

- (331) Calero-Nieto FJ, Bert AG, Cockerill PN. Transcription-dependent silencing of inducible convergent transgenes in transgenic mice. *Epigenetics Chromatin* 2010; 3(1):3.
- (332) Williams A, Harker N, Ktistaki E, Veiga-Fernandes H, Roderick K, Tolaini M, Norton T, Williams K, Kioussis D. Position effect variegation and imprinting of transgenes in lymphocytes. *Nucleic Acids Res* 2008; 36(7):2320-2329.
- (333) Giraldo P, Montoliu L. Size matters: use of YACs, BACs and PACs in transgenic animals. *Transgenic Res* 2001; 10(2):83-103.
- (334) Kilic G, Alvarez-Mercado AI, Zarrouki B, Opland D, Liew CW, Alonso LC, Myers MG, Jr., Jonas JC, Poitout V, Kulkarni RN, Mauvais-Jarvis F. The Islet Estrogen Receptor-alpha Is Induced by Hyperglycemia and Protects Against Oxidative Stress-Induced Insulin-Deficient Diabetes. *PLoS One* 2014; 9(2):e87941.
- (335) Ozbek E. Induction of oxidative stress in kidney. *Int J Nephrol* 2012; 2012:465897.
- (336) Montezano AC, Touyz RM. Molecular mechanisms of hypertension--reactive oxygen species and antioxidants: a basic science update for the clinician. *Can J Cardiol* 2012; 28(3):288-295.
- (337) O'Connor PM, Guterman DD. Resurrecting hope for antioxidant treatment of cardiovascular disease: focus on mitochondria. *Circ Res* 2010; 107(1):9-11.
- (338) Xu H, Perez-Cuevas R, Xiong X, Reyes H, Roy C, Julien P, Smith G, von DP, Leduc L, Audibert F, Moutquin JM, Piedboeuf B, Shatenstein B, Parra-Cabrera S, Choquette P, Winsor S, Wood S, Benjamin A, Walker M, Helewa M, Dube J, Tawagi G, Seaward G, Ohlsson A, Magee LA, Olatunbosun F, Gratton R, Shear R, Demianczuk N, Collet JP, Wei S, Fraser WD. An international trial of antioxidants in the prevention of preeclampsia (INTAPP). *Am J Obstet Gynecol* 2010; 202(3):239.
- (339) Chen J, He J, Hamm L, Batuman V, Whelton PK. Serum antioxidant vitamins and blood pressure in the United States population. *Hypertension* 2002; 40(6):810-816.
- (340) Chien SJ, Lin KM, Kuo HC, Huang CF, Lin YJ, Huang LT, Tain YL. Two different approaches to restore renal nitric oxide and prevent hypertension in young spontaneously hypertensive rats: l-citrulline and nitrate. *Transl Res* 2014; 163(1):43-52.
- (341) Gori T, Burstein JM, Ahmed S, Miner SE, Al-Hesayen A, Kelly S, Parker JD. Folic acid prevents nitroglycerin-induced nitric oxide synthase dysfunction and nitrate tolerance: a human in vivo study. *Circulation* 2001; 104(10):1119-1123.

- (342) Schiffрин EL. Antioxidants in hypertension and cardiovascular disease. *Mol Interv* 2010; 10(6):354-362.
- (343) Medical Research Council. Stratified Medicine. Available at www.MRC.ac.uk 2014. Ref Type: Online Source
- (344) Generation Scotland. Availabl at <http://www.generationscotland.org/> 2014. Ref Type: Online Source
- (345) Fujimoto K, Arakawa S, Shibaya Y, Miida H, Ando Y, Yasumo H, Hara A, Uchiyama M, Iwabuchi H, Takasaki W, Manabe S, Yamoto T. Characterization of phenotypes in Gstm1-null mice by cytosolic and in vivo metabolic studies using 1,2-dichloro-4-nitrobenzene. *Drug Metab Dispos* 2006; 34(9):1495-1501.

Appendices

Microsatellite Markers

D2Rat18

D2Wox13

D2Wox5

D2Mit3

D2Rat14

D2Wox3

D2Mit5

D2Mit6

D2Rat167

D2Wox15

D2Rat28

D2Mit18

D2Wox9

D2Wox19

D2Mit21

D2Mit14

D2Rat49

D2Arb18

D2Mgh12

D2Rat58

Transgene Sequence

>pEF1/Myc-His A

AATATTATTGAAGCATTATCAGGGTTATTGTCTCATGAGCGGATACATATTGAATGTATT
 AGAAAAATAACAAATAGGGTTCCCGCGCACATTCCCCGAAAAGTGCACCT**GACGTC** GACG
 GATCGGGAGATCTCCGATCCCCTATGGTCACTCTCAGTACAATCTGCTCTGATGCCGCATA
 GTTAAGCCAGTATCTGCTCCCTGCTTGTGTGGAGGTCGCTGAGTAGTGCAGCAGCAAAT
 TTAAGCTACAACAAGGCAAGGCTTGACCGACAATTGCATGAAGAATCTGCTTAGGGTTAGGCG
 TTTGCGCTGCTTCGCGATGTACGGGCCAGATATAACGCGTTGACATTGATTATTGACTAGGCT
 TTTGCAAAAAGCTTGCAAAGATGGATAAAGTTAACAGAGAGGAATCTTGCAGCTAATG
 GACCTTCTAGGTCTGAAAGGAGTGGGAATT**GGCTCCGGTGCCCGTCAGTGGCAGAGCGCAG**
ATCGCCCACAGTCCCCGAGAAGTTGGGGGGAGGGTCGGAATTGAACCGGTGCCTAGAGAAG
GTGGCGCGGGTAAACTGGAAAAGTGATGTCGTGTACTGGCTCCGCCTTTTCCGAGGGTGG
GGGAGAACCGTATAAAGTCAGTAGTCGCCGTGAACGTTCTTTTCGCAACGGTTTGCCGC
CAGAACACACAGGTAAGTGCCGTGTGGCTGCAGTACGTGATTCTGATCCGAGCCTCGGGT
TTGCGTGCCTTGAATTACTCCACCTGGCTGCAGTACGTGATTCTGATCCGAGCCTCGGGT
TGGAAGTGGTGGGAGAGTTCGAGGCCTTGCCTTAAGGAGCCCCTTCGCCTCGTGTGAGT
TGAGGCCTGGCCTGGCGCTGGGCCGGCGTGCAGTCTGGTGGCACCTCGCCGTGTCT
CGCTGCTTCGATAAGTCTCTAGCCATTAAAATTGATGACCTGCTGCAGCCTTTT
CTGGCAAGATAGTCTTGTAAATGCCGGCAAGATCTGCACACTGGTATTCGGTTTGGGC
CGCGGGCGCGACGGGCCCGTGCCTCCAGCGCACATGTCGGCGAGGGGGCGCTGCGAGC
GCGGCCACCGAGAACCGACGGGGTAGTCTCAAGCTGGCCGCCTGCTCTGGTGCCTGGCCT
CGCGCCGCCGTGTATGCCCGCCCTGGCGGCAAGGCTGGCCGGTGGCACCGAGTGCCTG
ACCGGAAAGATGCCGCTTCCGCCCTGCTGCAGGGAGCTAAAATGGAGGACGCCGCGCTC
GGGAGAGCGGGCGGGTAGTCACCCACACAAAGGAAAAGGGCTTCCGTCCTCAGCCGTCGC
TTCATGTGACTCCACGGAGTACCGGGCGCCGTCCAGGCACCTCGATTAGTTCTGAGCTTTG
GAGTACGTCGTCTTAGGTTGGGGAGGGTTTATGCGATGGAGTTCCCACACTGAGTG
GGTGGAGACTGAAGTTAGGCCAGTTGGCACTTGATGTAATTCTCCTTGAATTGCCCTTT
TGAGTTGGATCTGGTTCATTCTCAAGCCTCAGACAGTGGTCAAAGTTTTCTTCCATT
TCAGGTGTCGTGAGGAATTAGCTGGTACTAATACGACTCACTATAGGG**AGACCCAAAGCTGGC**
TAGGTAAGCTTGGTACCGTTAAACTCGAGGTGACGGTATCGATAAGCTTCAAATTGAGAAG****

ACCACAGCGCCAGAACCATGCCCTATGATACTGGGATACTGGAACGTCCGGGCTGACACACC
CGATCCGCTGCTCTGGAATACACAGACTCAAGCTATGAGGAGAACGAGATACGCCATGGCG
ACGCTCCGACTATGACAGAACGCCAGTGGCTGAATGAGAACGTTCAAACGGCCTGGACTTCC
CCAATCTGCCCTACTTAATTGATGGATCGCGCAAGATTACCCAGAGCAATGCCATAATGCGCT
ACCTTGCCTGCCAGAACACCACCTGTGGAGAGACAGAGGAGGAGCGGATTGTCAGACATTG
TGGAGAACCGAGTCATGGACAACCGCATGCACTCATGCTTGTGTTACAACCCGACTTTG
AGAACGAGAACGCCAGAGTTCTGAAGACCATCCCTGAGAACGATGAAGAGCTACTCTGAGTTCC
TGGGCAAGCGACCAGGTTGCAGGGGACAAGGTACCTATGTGGATTCTGCTTATGACA
TTCTTGACCACTTGTGAGGCCAAGTGCCTGGACGCCCTCCAAACCTGAAGGACT
TCCTGGCCGCTTCGAGGGCCTGAAGAACGATCTCTGCCTACATGAAGAGCAGCCACTACCTCT****

CAACACCTATATTCGAAGTTGGCCAATGGAGTAACAAGTAGGCCCTGCTACACTGGCAC
TCACAGGAGGACCTATCCACATTGGATCCTGCAGGTTCTAGGAGGCCCTTCGAACAAAAACTC****

ATCTCAGAACGAGGATCTGAATATGCATACCGGTACATCACCACCATGAGTTAAACC
CGCTGATCAGCCTCGACTGTGCCTCTAGTTGCCAGCCATCTGTTGCCCCTCCCCGTG****

CCTTCCCTGACCCCTGGAGGTGCCACTCCCACTGTCCTTCTAATAAAATGAGGAATTGCA
TCGCATTGTCTGAGTAGGTGTCATTCTATTCTGGGGGTGGGCAAGGACAGCAAGGGG
GAGGATTGGGAAGACAATAGCAGGCATGCTGGGATGCCGTGGCTATGGCTTGTGAGGCG

GAAAGAAC**CAGCTG**GGGCTCTAGGGGTATCCC**ACGCGCCCTGTAGCGGC**GCATTAAGCGCG
 GCGGGTGTGGTGGTTACGCGCAGCGTAGCGCTACACTGCCAGCGCCCTAGCGCCGCTCCT
 TTCGCTTCTCCCTTCCTCGCACGTTGCCGGCTTCCCCGTCAAGCTCTAAATCGG
 GGGCTCCCTTAGGGTCCGATTAGTGCTTACGGCACCTCGACCCCCAAAAACTGATTAG
 GGTGATGGTCACGTAGTGGCCATGCCCTGATAGACGGTTTTCGCCCTTGACGTTGGAG
 TCCACGTTCTTAATAGTGGACTCTGTTCCAAACTGGAACAACACTCAACCCTATCTGGTC
 TATTCTTTGATTATAAGGGATTGCGATTCTGGAATGTGTGTCAGTTAGGGTGTGAAAGTCCC
 CAGGCTCCCCAGCAGGCAGAAGTATGCAAAGCATGCACTCAATTAGTCAGCAACCAGGTGTG
 GAAAGTCCCCAGGCTCCCCAGCAGGCAGAAGTATGCAAAGCATGCACTCAATTAGTCAGCAA
 CCATAGTCCCAGGCTTAACCCGCCATCCGCCCTAACTCCGCCAGTCCGCCATTCTC
 CGCCCCATGGCTGACTAATTTTTATTGAGAGGCCGAGGCCCTGCCTCTGAGC
 TATTCCAGAAGTAGTGAGGAGGCTTTTGAGGCCTAGGCTTGCAAAAGCTCCGGAG
 CTTGTATATCCATTTCGGATCTGATCAAGAGACAGGATGAGGATCGTTCGATGATTGAAC
 AAGATGGATTGCAAGCAGGCTCCGGCTGGTGGAGAGGCTATTGGCTATGACTGGG
 CACAACAGACAATCGGCTGCTGATGCCGCCGTGTCAGCGCAGGGCGCCGG
 TTCTTTTGTCAGAAGACCGACCTGTCGGTGCCTGAATGAACCTGCAAGGAGGCG
 TATCGTGGCTGGCACGACGGCGTTCTGCG**CAGCTG**TGCTCGACGTTGCACTGAAGCGG
 GAAGGGACTGGCTGCTATTGGCGAAGTGCCGGGCAGGATCTCTGTCACTCACCTGCTC
 CTGCCGAGAAAGTATCCATCATGGCTGATGCAATGCCGGCTGCATACGCTTGCATCCGGCTA
 CCTGCCATTGACCAACCGAACATCGCAGCGAGCACGTAACCGATGGAAGCCG
 GTCTTGTGATCAGGATGATCTGGACGAAGAGCATCAGGGCTCGCGCAGCCGAACCTGTC
 CCAGGCTCAAGGCGCGATGCCGACGGCGAGGATCTCGTGCACCCATGGCGATGCCTGCT
 TGCGAATATCATGGTGGAAAATGGCGCTTCTGATTGACTCGACTGTGGCCGGCTGGTG
 TGGCGGACCGCTATCAGGACATAGCGTTGGCTACCGTGATATTGCTGAAGAGCTGGCG
 AATGGGCTGACCGCTTCCTCGTGTACGGTATGCCGCTCCGATTGCAAGCGCATGCC
 TCTATGCCCTCTGACGAGTTCTGAGCAGCTCTGAGCGGGACTCTGGGTTCGCAAATGACCG
 GCGACGCCAACCTGCCATCACGAGATTGCAACCGCCCTATGAAAGGTTGGG
 TTCGGAATCGTTCCGGACGCCGGCTGGATGATCCTCCAGCGCGGGATCTCATGCTGGAG
 TTCTCGCCCACCCAACTTGTATTGAGCTTACAAATAAGCAATAGCATC
 ACAAAATTTCACAAATAAGCATTTCACTGCATTCTAGTTGTGGTTGTCAAACCATC
 AATGTATCTTATCATGTGTACCGTCGACCTCTAGCTAGAGCTTGGCGTAATCATGGTCA
 TAGCTGTTCTGTGAAATTGTTATCCGCTCACAATTCCACACAATACGAGCCGGAAGC
 ATAAAGTGTAAAGCCTGGGTGCCTAATGAGTGAGCTAACATTAATTGCGTGCCTCA
 CTGCCCGCTTCACTCGGGAAACCTGCG**CAGCTG**CATTAAATGAATCGGCCACGCG
 GGGAGAGCGGTTGCGTATTGGCGCTCTCCGCTCTCGCTCACTGACTCGCTCGCTCG
 GTCGTTCGCTCGCGAGCGGTATCAGCTACTCAAAGGCGGTAAACCGTTATCCACAGAA
 TCAGGGATAACGCAAGGAAAGAACATGTGAGCAAAGGCCAGGAACCGTAAAAGGCCG
 GCTGGCGTTCCATAGGCTCCGCCCTGACGAGCATCACAAAATCGACGCTCAAGTCA
 GAGGTGGCGAAACCCGACAGGACTATAAGATACCAGGGTTCCCGCTTCTCCCTCGGAAAG
 CGTGGCGCTTCTCATAGCTACGCTGTAGGTATCTCAGTTGGTAGGTCGTTCGCTCAA
 GCTGGGCTGTGTCACGAACCCCCGTTCAGCCGACCGCTGCCCTATCCGTAACATCG
 TCTTGAGTCCAACCCGGTAAGACACGACTATGCCACTGGCAGCAGCCACTGGTAACAGGAT
 TAGCAGAGCGAGGTATGTAGGCGGTCTACAGAGTTCTGAAGTGGTGGCCTAACTACGGCTA
 CACTAGAAGAACAGTATTGGTATCTGCGCTCTGCTGAAGCCAGTTACCTCGGAAAAGAGT
 TGGTAGCTTGTGATCCGGCAAACAAACCACCGCTGGTAGCGGTGGTTTTGCAAGCA
 GCAGATTACGCGCAGAAAAAAAGGATCTCAAGAAGATCCTTGATCTTCTACGGGCTG
 CGCTCAGTGGAACGAAACTCACGTTAAGGGATTGGTCATGAGATTATCAAAAAGGATCTT
 CACCTAGATCCTTAAATAAAAATGAAGTTAAATCAATCTAAAGTATATGAGTAAAC

TTGGTCTGACAGTTACCAATGCTTAATCAGTGAGGCACCTATCTCAGCGATCTGTCTATTCG
 TTCATCCATAGTTGCCCTGACTCCCCGTCGTAGATAACTACGATACGGGAGGGCTTACCATC
 TGGCCCCAGTGCCTGCAATGATAACCGCGAGACCACCGCTCACCGGCTCCAGATTATCAGCAAT
 AAACCAGCCAGCCGAAGGGCCGAGCGCAGAAGTGGTCCTGCAACTTATCCGCCTCCATCCA
 GTCTATTAATTGTCGGGGAAAGCTAGAGTAAGTAGTTCGCCAGTTAATAGTTGCGAACGT
 TGTTGCCATTGCTACAGGCATCGTGGTGCACGCTCGTCTGGTATGGCTTCATTAGCTC
 CGGTTCCCAACGATCAAGGCGAGTTACATGATCCCCATGTTGCAAAAAGCGGTTAGCTC
 CTTCGGTCTCCGATCGTTGTCAGAAGTAAGTTGGCCGCAGTGTATCAGTTATGGC
 AGCACTGCATAATTCTCTTACTGTATGCCATCCGTAAGATGCTTTCTGTGACTGGTGAGTA
 CTCAACCAAGTCATTCTGAGAAATAGTGTATGCCGCACCGAGTTGCTCTGCCGGCGTCAAT
 ACGGGATAATACCGGCCACATAGCAGAACTTAAAAGTGCTCATGGAAAACGTTCTTC
 GGGGCGAAAACCTCTAAGGATCTTACCGCTGTTGAGATCCAGTTGATGTAACCCACTCGTGC
 ACCCAACTGATCTTCAGCATCTTACTTACCGCTGGGTGAGCAAAACAGGAAG
 GCAAAATGCCGCAAAAAGGGAATAAGGGCGACACGGAAATGTTGAATACTCATACTCTCCT
 TTTTC

GREEN = EF1 promoter

UNDERLINED = polyA HisA

YELLOW = polyA Myc-His

BOLD ITALIC = *PvuII* site

BOLD = Start of f1 Ori

GREY = Sequence quoted in Goodwin EC, Rottman FM. The 3'-flanking sequence of the bovine growth hormone gene contains novel elements required for efficient and accurate polyadenylation. J Biol Chem. 1992 Aug 15;267(23):16330-4. PMID: 1644817

BGH RVS PRIMER: TAGAAGGCACAGTCGAGG

Binding sequence: **CCTCGACTGTGCCTCTA**

T7 Primer: **TAATACGACTCACTATAGGG**

AatII: **GACGTC** - One Cut Site: 6872bp

PvuII: **CAGCTG** - 3 sites. Fragments: 1096bp; 1071bp; 4705bp

AatII/PvuII fragment: 2725bp

Cut with PvuII 1st, extract 4705bp fragment. Cut with AatII, extract 2725bp fragment (leaving 1980bp fragment).

KpnI: **GGTAC/C**

Xhol: **T/CTAGA**

SLUDGE = *GSTM1+GSTM4a* primers

BOLD UNDERLINED = MCS of pAD5 K-NpA

UNDERLINED = 5' and 3' UTR (NB - not entire UTR sequences, only those bound by *GSTM1* and *GSTM4* primers.

RED = SNPs found between SP and WKY sequences

BLUE = Confirmed BGH polyA reference sequence from Invitrogen

